FACULDADE DE ENGENHARIA DA UNIVERSIDADE DO PORTO

MACHINING OF HYBRID COMPOSITES

Luís Miguel Pereira Durão

Mechanical Engineer
Faculty of Engineering – University of Porto

PhD. Thesis

Dissertation supervisor
Professor Doutor António Torres Marques
Department of Mechanical Engineering and Industrial Management
Faculty of Engineering – University of Porto

Porto, June 2005

Our material history has traversed the *stone*, the *bronze* and the *iron* ages. Today we are in the "*composite* age".

In International Encyclopaedia of Composites – 2nd Edition

FOREWORD

For the past decades fibre reinforced plastics – FRP's – are increasing their importance as one of the most interesting group of materials, because of their unique properties. Advantages are related with their low weight, high strength and stiffness. Although the development of these materials has been related with the aerospace and aeronautical usage, recent years have seen the spread of their use in many other industries like automotive, sport, railway, naval and many others.

Earlier concerns related to high cost and marginal manufacturability have been satisfactorily addressed through high volume and innovative design and manufacturing. However, their use is limited by the difficulties found during machining and joining of parts. The high cost associated with machining and finishing has been a barrier to their widespread use. Machining operations, such as drilling, milling and others usually cause damage to parts, like delamination, fibre pull-out, cracks, thermal damage and high rate of tool wear. Irregular surface roughness resulting in a poor aesthetic look of machined parts, when compared with metal machined parts, also results as a negative factor for the use of machined FRP's parts.

Good hole drilling processes are essential to join composite parts with other composite or metal parts. To obtain holes of good quality it is important to identify the type of material and ply stacking sequence together with fibre orientation. Afterwards techniques and tools as well as parameters are selected. Required hole tolerance and available equipment also influence hole drilling process selection.

FRP's show some difficulties in their study due to their non-homogeneity and properties dependence on fibre and matrix materials, fibre volume fraction, ply lay-up, fibre orientation and others. As a result, conclusions that are valid for a certain type of FRP with some fibre orientation may not be valid if fibre orientation is changed. A strong point for the use of composite parts is the possibility of parts manufacturing with 'taylored' mechanical properties related with the stress expected when in service.

Recent years have shown a considerable increase in the use of FRP's. Confidence in using composite materials has improved substantially. Besides the advantages mentioned above, composites are corrosion resistant, have long fatigue lives and the ability to form complex shapes. Broad advances can be expected in the near future. A good example is the use of composites for major primary structures in both new Boeing 787 and Airbus A380, now in build.

ACKNOWLEDGMENTS

This work was fulfilled in FEUP – Faculdade de Engenharia da Universidade do Porto – and in INEGI – CEMACOM, under the supervision of Prof. Dr. António Torres Marques to whom I wish to express my gratitude for his advices and support during the accomplishment of this thesis.

In second place, I wish to sincerely thank to PRODEP III for the financial support given, as well as to the Scientific Council and Mechanical Department of my institution – ISEP – Instituto Superior de Engenharia do Porto, who had believed in my capacities of successful achievement.

I also thank to my colleague António Magalhães, from ISEP, for his guidance, availability and for revising this work.

A special gratitude to Eng. Afonso Fernandes, from ISEP, for his initial recommendations and information about non-destructive techniques.

To INEGI-CEMACOM team, Célia Novo, Paulo Nóvoa, João Ferreira, Miguel Sousa, Pedro Vieira, José Esteves, António Ferreira, Elisabete and Fernanda for their assistance and knowledge given in plates manufacturing and tests performed.

A special reference to Rui Oliveira, for his cooperation in acoustic emission tests.

To FEUP-DEMEGI, Prof. Dr. A. Monteiro Baptista, Miguel Figueiredo, Aguiar Vieira, Mário Pinto, workshop team and Rui Silva for their help in the fulfilment of the experiments, namely by their trust in allowing the use of drilling equipment, dynamometer and profilometer.

To João Tavares for his teamwork in the use of Computational Vision techniques, that was essential, as well as to Mário Vaz for the ESPI tests done.

To my colleague Marcelo Moura, whose assistance was crucial for the development of the Finite Element Model here presented.

To Prof. Dr. Manuel Freitas and Mr. Sá Mões from DEM-IST (Lisbon) and to Jorge Justo from ISEP for their help and care during the realization of the ultrasonic tests.

To Prof. Dr. Pedro Camanho and Cassilda Tavares for their instruction about the bearing test.

To Arnaldo Pinto, to Jorge Almeida and to the team of INEGI-CETECOP for spending some of their time when I needed.

For all those that even though are not referred, have in one way or the other helped during this period, just by some detail or a simple conversation. To all of them, my appreciation.

Finally to my family for being there, for their care and understanding. Part of the time I spent during the completion of this work was taken to them.

TABLE OF CONTENTS

2. STATE-OF-THE-ART

3. EXPERIMENTAL WORK

LIST OF FIGURES

LIST OF TABLES

LIST OF SYMBOLS

d ; D	tool diameter
f	feed rate per revolution
f_r	feed rate per minute
k_c	specific cutting pressure
v_c	cutting speed
D_{RAT}	damage ratio
E	modulus of elasticity
F_c	cutting force in orthogonal cutting
F_{crit}	critical thrust force for delamination onset
F_d	delamination factor
F_t	thrust force in orthogonal cutting
F_x	thrust force during drilling
G	shear modulus
G_{Ic}	interlaminar fracture toughness in mode I
G_{IIc}	interlaminar fracture toughness in mode II
G_{IIIc}	interlaminar fracture toughness in mode III
M_t	torque during drilling
N	rotational speed of the drill
R''	resultant tool force in orthogonal cutting
R_a	average surface roughness
R_m	maximum individual peak-to-valley height
R_z	ten-point average height
S/N	signal-to-noise ratio
T_g	glass transition temperature
V_f	fibre volume fraction
α	relief angle
β	edge angle
γ	rake angle
ν	Poisson ratio
σ	tensile strength
σ_{bear}	bearing strength
τ	shear stress

LIST OF ABBREVIATIONS

AE	acoustic emission
ANOVA	analysis of variance
CFRP	carbon fibre reinforced plastic
CT	computerized tomography
DCB	double cantilever beam
DMTA	dynamic mechanical thermal analysis
DOC	depth of cut
ESPI	electronic speckle pattern interferometry
FE	finite element
FEM	finite element model
FRP	fibre reinforced plastic
GFRP	glass fibre reinforced plastic
HM	high modulus
HS	high strength
HSS	high speed steel
ILSS	interlaminar shear strength
IM	intermediate modulus
LEFM	linear elastic fracture mechanics
LVDT	linear vertical displacement transducer
PCD	synthetic polycrystalline diamond
RTM	resin transfer moulding
UHM	ultra high modulus
WC	tungsten carbide

ABSTRACT

Composites are one of the most interesting groups of materials in our technological society. Their light weight and high strength characteristics make them suitable in applications where a high stiffness and strength-to-weight ratio are desired.

Although composites components are produced to near-net shape, machining is often needed, as it turns out necessary to fulfil requirements related with tolerances or assembly needs. Among the several machining processes, drilling is one of the most frequently used for the production of holes for screws, rivets and bolts. Machining operations in composites can be carried out in conventional machinery normally used to metallic parts. However, it is necessary to bear in mind the need to adapt the processes and/or tooling. When composites parts are subjected to drilling operations, the defects that are likely to appear differ from metallic parts, making evaluation of hole quality more difficult. Besides process related problems in composites fabrication, drilling can cause several defects like, delamination, intralaminar cracks, fibre pull out and thermal damage. These problems can affect the mechanical properties of the produced parts, hence, lower reliability. Some of these defects are not visible in a visual inspection, and so the trend is very cautious when using FRPs in critical parts. This has caused a barrier to the widespread of composites usage in other applications, namely in primary structural components. On the other hand, composites are highly abrasive, causing a high rate of tool wear. Finally, the direct adoption of quality standards used for metallic parts may not be the more convenient as specific characteristics of composites are different from those of metals. In spite of all these aspects, confidence in the use of composite materials is increasing rapidly.

Production of higher quality holes, with damage minimization, is a challenge to everyone related with composites industry. However, the amount of research papers reported in open literature is yet limited. So, it means that extensive experimental analysis and modelling must be carried out until composites machining reach the same level of knowledge and confidence that one can find now when searching for information related with metal machining. Another difficulty in getting that level of knowledge may be related with the composites nature itself, as their inhomogeneity results in properties dependence on fibre and matrix materials, fibre volume fraction, ply lay-up sequence, orientation and other factors. Hence, conclusions that are valid for a certain type of FRP with some fibre orientation may not be valid if changed from unidirectional to cross-ply or other, just to quote an example.

In this work, drilling of three types of fibre reinforced plastics, glass fibre, carbon fibre and hybrid - carbon and glass - fibre, in an epoxy matrix, is studied. All the parts in this study are quasi-isotropic, considering ply lay-up and fibre orientation. The tools considered in this work were, in the beginning, those normally available in tool manufacturer's catalogues, namely in high-speed steel, carbide and coated carbide. Diamond tools were not considered as, despite their superior quality, they are normally not competitive economically.

Hole damage extension is related with drilling parameters, cutting speed and feed rate and with data from monitoring performed during drilling, i. e. thrust forces and torque. Hole surface superficial roughness was measured. Non-destructive tests, radiography and ultrasonic scanning were performed on drilled parts. Images were analyzed using Computational Vision techniques and employed to establish evaluation results based on existing criteria for damage assessment. Thrust forces are compared with models available for the determination of critical thrust force for the onset of delamination on composite materials that includes properties like Young's modulus and interlaminar fracture toughness in Mode I. Mechanical tests, like Double Cantilever Beam and Bearing were performed to compare materials or hole drilling techniques.

Finally, a new tool design with the intention to minimize damage around the hole is proposed and experimented. Results from the tests, including thrust force, torque, delamination, surface roughness and bearing are presented and compared with those previously gathered with market available tools.

A finite element model – FEM - was developed for the simulation of drilling of composite parts. Part was modelled with a quasi-isotropic stacking sequence, although the model can accept any other sequence. Composite properties are considered and the model is sensible to different values of Young's modulus, ultimate strength and interlaminar fracture toughness in mode I. For FEM development, only carbon/ epoxy composites were considered. Tool was modelled as a 'rigid body' and several tool geometries were compared in order to assess the values for the onset of delamination, as well as maximum forces during drilling.

Three objectives are intended in this work. The first is to explore and optimize different machining strategies, based in available damage models that enable composites machining to be regarded as a competitive and reliable technique.

The second is the proposal of a drill design that accounts for the specificity of composites machining.

The final one is the presentation of a FEM that assist composites drilling study.

RESUMO

Os compósitos constituem um dos mais interessantes grupos de materiais da nossa actual sociedade tecnológica. O seu baixo peso e elevada resistência tornam-nos ideais em aplicações onde elevadas rigidez e resistência específica são desejadas.

Embora as peças em compósitos sejam produzidas em forma quase-final, a maquinagem torna-se por vezes necessária sempre que se verifica a necessidade de cumprir com tolerâncias apertadas ou por questões de montagem. Entre os vários processos de maquinagem normalmente utilizados, a furação é um dos mais frequentes na produção de furos para a montagem de rebites, cavilhas ou parafusos. A realização de operações de maquinagem em compósitos pode ser executada por máquinas-ferramenta convencionais habitualmente utilizadas no trabalho de metais. O processo deverá, no entanto, ser convenientemente adaptado, quer a nível de parâmetros quer a nível das ferramentas a utilizar. Quando uma peça compósita é sujeita a uma operação de furação, os defeitos que se podem encontrar são diversos dos referidos para peças metálicas, dificultando a avaliação da qualidade do furo. Para além de problemas inerentes ao seu processo de fabrico, as peças em materiais compósitos podem, após furação, apresentar defeitos tais como delaminação, fissuras intralaminares, arrancamento de fibras ou danos por sobreaquecimento. Tais danos causam o abaixamento das propriedades mecânicas dos componentes e, consequentemente, da sua fiabilidade em serviço. Alguns destes danos não são detectáveis por intermédio de uma inspecção visual, fazendo com que o uso de plásticos reforçados com fibras – PRFs - em componentes considerados críticos seja alvo das maiores cautelas. Tal facto tem constituído um obstáculo ao mais rápido alargamento no uso de tais materiais, nomeadamente em componentes estruturais. Por outro lado, os compósitos são extremamente abrasivos provocando um rápido desgaste nas ferramentas de corte. Acresce, ainda, que a adopção directa dos critérios de qualidade utilizados para as peças metálicas não são os mais convenientes para avaliar estas peças devido às suas especificidades. Apesar de tudo, a confiança no uso de materiais compósitos tem vindo a aumentar rapidamente.

A obtenção de furos de qualidade adequada, com minimização do dano, é um desafio que se coloca actualmente à indústria dos compósitos. No entanto, verifica-se que a quantidade de estudos publicados sobre este assunto é ainda limitada. Isto significa que será necessário realizar um extenso trabalho experimental até que a

maquinagem de compósitos atinja o mesmo nível de conhecimento e confiança que actualmente se reconhece à maquinagem de metais e ligas metálicas. Uma outra dificuldade em atingir tal grau de confiança relaciona-se com a natureza dos próprios compósitos cuja não-homogeneidade resulta em propriedades dependentes das matérias usadas como reforço e como matriz, da fracção volúmica de fibras, da sequência de empilhamento, da orientação das fibras e outros factores. Em consequência, resultados válidos para um determinado PRF podem não ser válidos se a orientação das fibras é alterada, por exemplo, de unidireccional para camadas cruzadas a 90º.

Nesta tese é estudada a furação de três tipos de plásticos reforçados com fibras - vidro, carbono e híbridos com vidro e carbono – numa matriz epóxida. Todas as peças ensaiadas têm uma sequência e orientação das camadas de modo a conferir-lhes propriedades quasi-isotrópicas. As ferramentas utilizadas são brocas disponíveis nos catálogos dos fornecedores, em materiais como o aço rápido e o carboneto de tungsténio sem e com revestimento. As ferramentas em diamante não foram tomadas em consideração pois, apesar da sua superior qualidade, tornam-se pouco atractivas numa perspectiva de custo/ benefício.

A extensão do dano provocado pela furação é relacionada com os parâmetros de corte, tais como a velocidade e o avanço e com os dados da monitorização recolhidos durante a maquinagem – força axial e binário. A rugosidade superficial das paredes do furo é medida. São realizados diversos ensaios não-destrutivos de radiografia e varrimento com ultra-sons às peças furadas. As imagens assim obtidas são analisadas recorrendo a técnicas de Visão Computacional, servindo para calcular os resultados através da utilização de critérios estabelecidos para a avaliação do dano. Os valores de força axial são comparados com modelos conhecidos para a determinação da força crítica para o início da delaminação em placas compósitas, que incluem na sua formulação propriedades dos materiais como o módulo de elasticidade e a taxa crítica de libertação de energia em modo I. São igualmente realizados ensaios mecânicos, como o DCB (Double Cantilever Beam) e o de esmagamento com a finalidade de comparar materiais ou técnicas de furação.

Finalmente, um novo desenho de ferramenta com o intuito de minimizar o dano em volta do furo, é proposta e experimentada. Os resultados dos diversos testes realizados, incluindo força axial, binário, delaminação, rugosidade superficial e tensão de esmagamento são apresentados e comparados com os obtidos com as ferramentas existentes no mercado.

É apresentado o desenvolvimento de um modelo de elementos finitos – MEF – para simular a furação de placas compósitas. As placas são modeladas com uma sequência de empilhamento quasi-isotrópica, embora o modelo possa aceitar qualquer outra. As propriedades dos materiais compósitos são consideradas no modelo e este é sensível à alteração dos valores do módulo de elasticidade, tensão de rotura e da taxa crítica de libertação de energia em modo I. Na fase de desenvolvimento apresentada, só foram consideradas as placas em carbono/epóxido. A ferramenta – broca - é modelada como um "corpo rígido" e são comparados os resultados da força necessária para o início da delaminação, bem como da força máxima atingida, para as diversas geometrias de ferramenta seleccionadas.

São três os objectivos propostos neste trabalho.

O primeiro é o estudo e optimização de diversas estratégias de maquinagem, baseado em modelos de dano conhecidos, possibilitando que a maquinagem de compósitos possa ser vista como uma técnica fiável e competitiva.

O segundo é a apresentação de uma proposta para um desenho de ferramenta que tenha em consideração a especificidade da maquinagem de materiais compósitos.

O último é a definição de um MEF que auxilie o estudo da furação de materiais compósitos.

RÉSUMÉ

Les composites constituent un des groupes de matériaux les plus intéressantes de notre actuelle société technologique. Leurs caractéristiques de bas poids et grande résistance rendent ces matériaux appropriés aux applications où une résistance spécifique ou une rigidité élevée est souhaitée.

Bien que les pièces en composites soient produites proches de leur forme finale, des opérations supplémentaires d'usinage sont normalement nécessaires afin d'obtenir des tolérances spécifiées ou bien pour besoins d'assemblage. Parmi les différents procédés d'usinage, le perçage est l'un des plus utilisés pour faire des trous pour vis, rivets et boulons. Les opérations d'usinage en composites peuvent être exécutées par des machines-outils conventionnelles habituellement employées pour les métaux. Le procédé doit, toutefois, être convenablement adapté tant au niveau de paramètres qu'au niveau des outils à utiliser. Quand on fait un trou dans une plaque composite, les défauts probables sont différents de ceux rencontrés dans le cas des métaux ou alliages métalliques, ce qui constitue une difficulté additionnelle dans la évaluation de la qualité d'une pièce usinée. Outre les problèmes inhérents au processus de fabrication, les pièces en matériau composite peuvent après perçage présenter des défauts tel que délaminage, fissuration intralaminaires, arrachement des fibres et endommagement thermiques. Tous ces problèmes causent une dégradation des propriétés mécaniques des composants et, par conséquence, une perte de leur fiabilité. Certains de ces mécanismes d'endommagements ne sont pas visibles par inspection visuelle, ce qui fait que l'utilisation des plastiques à renfort de fibre - PRFs - dans des éléments considérés critiques soit sujet à une grande prudence. Ceci constitue un obstacle à une utilisation plus répandu des composites dans éléments structurels. D'un autre coté, les composites sont extrêmement abrasifs provoquant une diminution de la durée de vie d'un outil. Finalement, l'adoption directe des critères de qualité utilisées pour les pièces métalliques ne sont pas les plus appropriés pour évaluer ces pièces à cause des caractéristiques spécifiques des composites, autres que des métaux. Malgré tout, la confiance dans l'utilisation des matériaux composites connaît une croissance rapide.

L'obtention de trous de qualité appropriée, avec minimisation d'endommagement, est un défi pour l'industrie des matériaux composites. Toutefois, il apparaît que la quantité d'études publiées sur le sujet est encore limitée. Cela signifie qu'il sera nécessaire de réaliser un travail expérimental extensif jusqu'à ce que l'usinage des

composites atteigne le même niveau de connaissance et de confiance qu'est actuellement reconnu à l'usinage des métaux. Une autre difficulté pour atteindre un tel degré de confiance est due à la propre nature des composites dont l'inhomogénéité résulte en propriétés dépendantes de la nature des fibres et de la matrice, de la fraction volumique des fibres, de la séquence d'empilement, de l'orientation et d'autres facteurs. Par conséquence, des résultats valides pour un PRF déterminé peuvent ne pas être valides si l'orientation des fibres est changée, par exemple, d'unidirectionnel par plis croisés à 90°.

Dans cette dissertation est étudiée l'usinage de trois types de plastiques renforcés par fibres de verre, de carbone et hybrides avec fibres de verre et carbone alternées dans une matrice en résine époxy. Toutes les plaques ont une séquence de empilement et orientation de mode à leur conférer des propriétés quasi-isotropiques. Les forêts utilisés sont ceux disponibles dans les catalogues des fournisseurs. Elles sont faites de matériaux tel que l'acier rapide et le carbure de tungstène. Les forêts en diamant n'ont pas été considérés, car malgré leur qualité supérieure, ils s'avèrent peux attractifs dans une perspective rapport prix/bénéfice.

L'étendue de l'endommagement provoqué par le perçage est relationné avec les paramètres de perçage, tels que la vitesse et l'avancement, et avec les données du suivi obtenus au cours pendant l'usinage - force axiale et binaire. La rugosité de la surface des forêts a été mesurée. Des essais non destructifs de radiographie et d'inspection ultrasonore ont été réalisés dans les plaques percées. Les images ont été analysées par Vision Numérique, servant comme base pour l'évaluation de l'endommage en utilisant des critères établis. Les efforts axiales sont comparés avec les modèles existant pour la détermination de l'effort critique de l'initiation du délaminage des plaques en matériaux composites, comprenant des propriétés comme le module de Young et la taux de restitution d'énergie critique en mode I. Sont également réalisés des essais mécaniques – DCB et écrasement – afin d'établir une comparaison entre les matériaux ou les techniques de perçage utilisées.

Enfin, un nouveau dessin d'un outil ayant pour finalité la minimisation de l'endommage autour du trou est proposé et essayé. Les résultats des différents tests réalisés, comprenant l'effort axial, binaire, délaminage, rugosité superficielle et écrasement sont présentés et comparés avec ceux précédemment obtenus avec les outils disponibles dans le marché.

Un modèle de éléments finis – MEF – a été développé pour faire la simulation du perçage des plaques composites. La plaque a été modélisée avec une séquence

d’empilement quasi-isotropique, bien que le modèle puisse accepter quelque autre séquence. Les propriétés des composites sont considérées dans le modèle et celui-ci est sensible aux changement des valeurs du module de Young, de la charge à rupture et du taux de restitution d’énergie critique en Mode I. Pendant le développement, seules les plaques carbone/époxy ont été considérées. L’outil – forêt - est modélisé comme un "corps rigide" et sont comparées les valeurs de la force nécessaire pour l’initiation délaminage, ainsi que la force maximale pendant le perçage pour différentes géométries de l’outil.

Trois objectifs sont proposés dans ce travail:

Le premier est l’étude et l’optimisation des différentes stratégies d’usinage, basée sur des models d’endommagement connus, permettant que l’usinage des plaques composites puisse être regardée comme une technique fiable et compétitive.

Le deuxième est la proposition d’un dessin d’outil qui ait en considération la spécificité de l’usinage des matériaux composites.

Le dernier est l’établissement d’un MEF pour faciliter l’étude du perçage des composites.

CHAPTER 1 - INTRODUCTION

1.1 SCOPE AND OBJECTIVES

1.1.1 SCOPE

The major aim of this work is the study of composite materials machining and to establish conditions that allow the modelling of machining strategies with damage minimization, including a proposal for a tool geometry model. That is intended to be done using well-established damage models.

As composite materials refer to a large variety of materials, a more specific selection of the type of materials has to be made. So, it was decided to study fibre reinforced thermoplastics. The author had some previous professional experience with thermoplastics, mainly in industrial injection processes. On the other side, conditions for the development of fibre reinforced plastics machining were also one of the aims in INEGI. Finally, the availability of raw materials makes it easy to decide what kind of materials should be studied. Pre-impregnated materials are easy to deal with and they can be layered according to different angles to obtain specific properties in the materials.

Among the machining processes the main focus was on drilling. Several informal conversations with some engineers in industrial areas that work with reinforced plastics highlighted the evidence that turning is not very desirable in these materials, as the final appearance is never pleasant or extra operations are needed, making the product more expensive. On the other side, drilling is a widely used technique as it is always needed to assemble components in more complex structures. It can also be reminded that, in the aircraft industry, about 60% of part rejections come from drilling-associated delamination [1]. There is a long way to follow until reach compatible performance that is standard in metallic construction.

In the beginning glass reinforced plastic was used as there were plates available because of some ongoing work. Subsequently, there was an evolution for carbon reinforced plastics, as they represent a more promising material in terms of performances, mainly stiffness and specific strength. The only problem with carbon fibres is their price, but perspective of reaching more competitive prices is getting bigger, as installed production capacity all over the world has been increasing. In a third phase there was the will to combine the two materials previously studied, obtaining an hybrid material with glass and carbon fibres in an epoxy matrix, and try to compare the behaviour of this material when subjected to drilling with results from glass/epoxy and carbon/epoxy plates. Although it is normal to produce plates with a fibre orientation according to the solicitation that the parts are expected to be subjected when in service, here this need was not felt. As there was not a main direction to take into account, all the parts produced had an quasi-isotropic distribution, giving the material a behaviour more close to the metallic materials, as mechanical characteristics can be considered as independent of orientation.

On the evaluation of damage and conditions during machining, the focuses were on the use of existing techniques and evaluation of their feasibility on the study and characterization of damage caused by machining. During machining there was a dynamometer available allowing to monitor forces and torque. This technique was used in almost all the plates that were machined along this work. That data make it possible to correlate damage with forces developed during drilling or turning of the plates. Also during machining, acoustic emission was monitored in order to try to establish a correlation between damage and acoustic emissions generated during drilling. There were some tries performed both with glass/epoxy and carbon/epoxy plates, but as results were not satisfactory, this technique was not extensively used.

After machining, several evaluation techniques were used, some with better results than others. Apart from the visual evaluation, by naked eye or with the help of a microscope with graduated scale, imaging techniques were also used. The one more used was enhanced X-ray as it turned out to be of simple use. So, a great number of drilled plates were radiographed in order to be able to compare different conditions. Another imaging technique is the scanning of the parts. Although being also a simple and useful technique, the results concerning damaged area were not as accurate as those of radiography. Another technique that was also tried is ESPI – Electronic Speckle Pattern Interferometry -, but results were not satisfactory. The measurement accuracy of damaged areas is also important. For that purpose, Computational Vision

based in an existing processing and image analysis platform was used, turning possible to accomplish the measurement of damaged areas around the hole.

In metallic parts, surface roughness of machined parts is considered a quality parameter. In composite parts it has been pointed out that roughness may not have that importance. However, surface profilometry was carried through and roughness results of machined parts obtained according to the standards used for metallic parts.

Other techniques are also possible, but for insufficient know-how or lack of availability, were not thoroughly tried. The most interesting of them is an imaging technique normally used in hospitals, CT – computerized tomography. There was one experience done with a carbon plate and the results seem promising. However, due to the primary use of the equipment for hospital purposes, it was not possible to adapt the device to specific composite regulations. Electron microscopy was also an alternative evaluated but not really tried. Another view of drilling could be related with temperature development during drilling or chip shape. Due to absence of evidence of thermal damages, this aspect was not detailed.

In order to have reference properties of the materials used, a certain amount of mechanical test was done. So, materials were subjected to tensile and bending tests, as well as DMTA analysis. With these tests, tensile strength, elasticity modulus, Poisson ratio, flexure modulus and glass transition temperature T_g were determined. Fibre volume fraction was also evaluated. It was also needed to carry double cantilever beam tests (DCB) to the determination of interlaminar fracture toughness G_{Ic} of the materials used. This parameter is used in every known model that determines the critical thrust force for delamination during drilling.

Machined specimens were subjected to bearing tests, in order to establish comparison between different drilling conditions. Open hole tension test was not performed as it was referred as to be not influenced by machining conditions, on the contrary of bearing test. Nevertheless the results did not appear to be very dependent of drilling conditions but more on the material itself.

Finally, as finite element modelling progresses there was the need to apply the determined interlaminar fracture toughness in Mode I, G_{Ic}. Although the tests were performed for the three types of interfaces involved in this work, glass-glass, carbon-carbon and carbon-glass, only the value determined for carbon-carbon interface was used in the finite element model.

As there was a considerable quantity of experimental data, a finite element model was developed in order to easily estimate the influence of different drill geometry. In that model, only the four last plies of the composite plate are 'drilled' as it was necessary to reduce computational time. Results from the model are compared with experimental results and good agreement is achieved.

1.1.2 OBJECTIVES

The main objectives of this work are:

- characterize the cutting conditions in fibre reinforced materials, namely glass fibre reinforced plastics (GFRP), carbon fibre reinforced plastics (CFRP), and hybrids reinforced plastics using these two reinforcement fibres;

- definition of a tool profile that is able to drill holes using existing machines and capable of optimize the objective of damage minimization;

- development of a finite element model, based in existing interface elements, that is able to simulate the conditions experimentally obtained in terms of thrust forces and damages and capable of giving results about the drill geometry.

Other objectives are:

- characterization of the typical damages caused by drilling;

- development of non-destructive analysis procedures to evaluate the damage caused by the drilling process;

- acquaintance of the existing models based in linear elastic fracture mechanics (LEFM);

- definition of a range of best parameters in order to minimize damage, considering the results from force and non-destructive analysis, as well as existing damage models;

1.1.3 ORGANIZATION OF THE DISSERTATION

This dissertation is organized in six chapters.

Chapter 1 gives a brief description of basic knowledge about polymeric composite materials which are to be studied. It also gives a short overview of material removal processes, namely the orthogonal cutting model, normally used in machining theory.

Finally, a small description of the known work published about finite element method applied to composites drilling is presented.

Chapter 2 is dedicated to the state-of-art of current knowledge in machining of fibre reinforced composites, both for conventional and non-traditional techniques. Special attention is paid to drilling. Included in this chapter is also the present knowledge about machining related damage, published damage models based in LEFM and available techniques for the monitoring and damage analysis.

In chapter 3 the experimental work is described, as well as the results and respective discussion. The materials used are described and characterized. A discussion about tool selection is presented. Results comprise force and torque, delamination measurements, machined surface roughness and mechanical tests.

Chapter 4 is dedicated to the presentation of the new models developed as a result of the research work. First, the new tool geometry model is explained and experimental results of the holes drilled using this new tool are given. A prototype was produced in order to have such results, including thrust force and torque, delamination, surface roughness and bearing test. After, a finite element model – FEM - based on and developed according to the experimental work is described. In that FEM the drilling process is simulated and model results consist of delamination onset force, progress of thrust force with tool movement and identification of delaminated regions.

The conclusions of the work and some recommendations for future studies are presented in chapter 5.

Finally, references and bibliography are presented.

1.1.4 ORIGINAL CONTRIBUTIONS

The original contributions intended to result from this work are:

- definition of a specific tool to the drilling of fibre reinforced polymeric composites;
- development of a finite element model that can increase knowledge about the delamination mechanism;
- a study on the possibilities of the several non-destructive techniques available for the analysis of these materials;
- application of Computational Vision techniques in damage evaluation of drilled plates.

1.2 COMPOSITE MATERIALS

Composite materials are a mixture or a combination of two or more macro constituents differing in form and/or material composition and that are essentially insoluble in each other [2]. Both constituents maintain their identity as they do not solve or melt in each other, and act in such a way that a new material results whose properties are better than the sum of their constituents. Generally, the components can be physically identified and an interface between them is possible to be identified.

Even though composites seem like modern materials, examples of their use can be observed in early civilized cultures.

In early Egypt, bricks were made from clay reinforced with straw and baked at the sun or in ovens. Moulds used for shaping the bricks were also made in a kind of ceramic material reinforced with plant fibres.

It is also possible to find testimony of employment of straw reinforcement in the bricks used to build the watchtowers of the Great Wall of China (approx. 200 BC).

The ancestor of paper, Egyptian papyrus (2000-3000 BC), is referred as made with the use of fibres that were laid parallel to each other with alternate layers with perpendicular orientation. These fibres were consolidated with the help of natural resin binders. Paper invention in China, circa 100 AC, is the result of the separation of fibres from numerous woods and grasses that were after reconsolidated under pressure [3].

Even in the manufacturing of weapons, examples of composite materials can be found. Arches used by Mongol warriors were built in horn in the parts subjected to compression and in wood, bound silks or ox tendons in the parts subjected to tension. Japanese sabres have their blade in steel and a soft iron in their nucleus, making them more resistant to flexure and impacts.

In the present days several examples of composites can be observed in daily usage:

- concrete, a mixture of cement, sand and grains, in building construction;
- tyres, made of rubber, canvas and steel;
- paper and cardboard, from resins, fillers and cellulose fibres;
- woodwork for furniture, made from wood particles and resin binder.

Usually a composite has two constituents, the matrix and the reinforcement. The matrix is the continuous phase and gives to the manufactured part its bulk form. It also

keeps constant the geometrical distribution of the reinforcement and transfers the stress to the fibres. The other phase is the reinforcement that gives to composite its internal structure. The mechanical properties of the reinforcement are superior to those of the matrix, resulting in an increase of the mechanical strength and stiffness. In some cases, this phase may be itself the result of the use of more than one phase with different characteristics, receiving then the composite the designation of hybrid.

A known exception to this rule is the case of polymeric materials modified with elastomers, in which a rigid polymeric matrix is charged with elastomeric particles. In this case, the objective is not to increase mechanical properties, but to give better resistance to impacts.

When describing a composite material it is necessary to define their constituents and respective properties, the reinforcement distribution, including orientation, shape, length and concentration, and the interface matrix/reinforcement. Reinforcement volume content is an important parameter when determining some properties of a composite. It can be measured as a fraction in volume or in weight. When considering composites with the same volume content, one must account for the reinforcement distribution. If it is uniform, it enables the composite some proportion of homogeneous properties and the measure of their properties can be considered independent of the measuring point. Non-uniform reinforcement distribution can cause early failures, localized in poor reinforced areas. In fibre reinforced composites, their anisotropy is determined by fibre orientation. Composite materials are anisotropic, that is to say, when subjected to a certain amount of stress, their reaction differs according to the stress direction. This property is one of the most important of composite materials: the possibility to manipulate the finished product anisotropy adapting the design and manufacture of the material to the desired properties.

Reinforcement materials used in composites are fibres, particles, laminates, flakes or fillers. Fibres can be organic – cellulose, polypropylene, graphite (graphite is considered as organic because they are manufactured from organic precursors) whose characteristics properties are their lightweight, flexibility, elasticity and heat sensitive or inorganic – glass, tungsten, ceramic – with high mechanical strength, good heat resistance, stiffness, good damping properties and good behaviour under fatigue.

According to their constituents' nature, composites can be divided in three main groups:

- **Organic matrix composites**, such as resins and charges, reinforced with mineral fibres, organic fibres or metallic fibres. These are the most used ones, yet they are not able to withstand temperatures above 200 to 300ºC.

- **Metallic matrix composites**, using aluminium, magnesium or titanium light and ultra-light alloys. Mineral fibres like carbon or silicon carbide, metallic fibres like boron and metallic-mineral fibres (boron with silicon carbide coating) are used as reinforcement. Their use is widespread, mainly in automotive industry. They can be used with temperatures up to 600 ºC.

- **Mineral or ceramic matrix composites** reinforced with metallic fibres (boron), metallic particles (cermet) or mineral particles (carbides, nitrides, etc). They are particularly adequate to high temperature environments.

Composite materials can be classified according to the shape of their constituents as reinforced with fibres or particles. If the reinforcement has one dimension that is clearly predominant to the others, it is designed as fibre. Fibres can be continuous or discontinuous and they can be oriented in a way that allows the composite to have their properties modelled according to project characteristics. Particles are reinforcements that do not have a dimension clearly greater that the others, and are used to improve certain properties in composites such as stiffness, heat or abrasion resistance and others.

1.2.1 MATRICES

Matrices can be thermoplastic or thermosetting resins, minerals and metallic. Usual resins are polyesters, phenolic, melamine, silicone, polyurethane and epoxy. Mineral matrices, like silicon, carbide or carbon, are capable to withstand high temperatures. Aluminium alloys and oriented eutectics are examples of metallic matrices. Their main function is to bear the mechanical stress to the fibres and protect them from the working environment. They shall be deformable, have good compatibility with fibres and a good environment resistance. Their specific weight shall be low, in order to give high specific properties to the composite.

In this work, we will concentrate in polymeric matrix composites, whose matrix receives the general designation of resins. We can observe that there are thermoplastic and thermosetting resins. The main and most used thermosetting resins

are unsaturated polyester, condensation resins (phenolic, etc) and epoxy. Due to their low production cost, their diversity and good adaptability to simple construction processes, polyester resins are the most used. As advantages they present a good stiffness explained by their high modulus, good dimensional stability, good fibre and tissue wetting, easy to work, good chemical stability and resistance to hydrocarbons. Their disadvantages are the maximum service temperature under 120ºC, sensitivity to cracks, high retraction, degradation under UV radiation and flammability.

Condensation resins are divided in phenolic, amino plastics and furan. Phenolic are the oldest ones and a well known example is Baquelite®. They have good dimensional stability, good resistance to heat and chemical agents, low retraction, fair mechanical characteristics and low cost. However, they do not allow big production output, are limited in available colours and are not compatible with food. Amino plastics resins, similar to phenolic, are food compatible and can be coloured. Furan resins are the most expensive, they have shorter cure time and high resistance to corrosive chemical agents.

Epoxy resins are the most used just after polyesters, their price being the only limit to their usage. They have better mechanical characteristics in tension, compression, impact and others when compared with polyester resins, and so they are preferred in the manufacturing of high performance parts like those used in aeronautics and others. Besides they present good heat resistance up to 150 to 190 ºC, have good chemical resistance, low retraction, good reinforcement wetting and an excellent adhesion to metallic materials. As disadvantages, their cost is high, polymerization time is long, there is the need to protect the workers that deal with it and they are sensible to cracks.

Thermoplastic resins, or plastics in a shorter term, are a huge product family that can be divided in general use plastics and technical plastics. General use plastics are those like polypropylene, polyethylene, polyvinyl chloride (PVC), polystyrene, polyamide, polycarbonate and others. Parts are manufactured by injection or extrusion, cost is low, but mechanical properties are weak. These resins can be reinforced with fibres and became a composite material. Their use is not frequent.

Resins can incorporate charges and additives with the purpose of giving certain characteristics, mechanical or others. The use of charges has the main objective of increasing the mechanical properties of the resin. According to their shape they can be classified as spherical or non-spherical. Spherical charges can be solid or hollow, with diameters between 10 and 150 μm. They can be in glass, carbon or in organic

materials like epoxy, phenolic or others. Among the non-spherical charges the most used one is mica.

Non reinforcing charges are used to lower resin cost or to raise some properties. Most used charges are chalks, silicates to reduce resin cost, aluminium hydrate to give fire-extinguish properties, electrical conducting or anti-static.

Additives are used in low percentage and act as lubricating or mould removing agents, as colouring agents, anti-ageing or ultraviolet protection.

1.2.2 REINFORCEMENTS

The role of a reinforcement in a composite is to increase mechanical properties of neat resin, like stiffness, tensile strength, hardness or others. They can equally improve physical, chemical or electrical properties. Reinforcement materials shall have high mechanical properties, low density, good resin compatibility, be easy to manufacture and low cost, among others.

Reinforcements can be distributed in the following ways:

- one-dimensional, when fibres are oriented towards one direction;
- bi-dimensional, or according to a plan, in tissue or non-tissue surfaces;
- tri-dimensional, in pre-shaped volumes or not, if fibres are oriented according to more than two dimensions in space.

The mechanical strength of a composite is determined by fibre orientation as well as the direction that presents higher properties. We can say that there is a relation between the amount of fibres aligned in one particular direction and the mechanical properties along the same direction.

Reinforcements more common are in fibre or tissue shape, but one can also find it in whiskers, that are short fibres with higher mechanical properties, but more difficult to elaborate.

Materials more used as reinforcement are glass fibres, aramid (Kevlar®), carbon, boron and silicon carbide.

Glass is a material known as fragile. However, when in filament shape of some tens micrometers of diameter, it looses its fragile nature and presents good mechanical

properties. Due to the simplicity of their fabrication and low cost they are the most used fibres and among them E-glass. This fibre has good tensile and compression strength, good electrical properties but low impact resistance. They have the lower cost of all glass fibres. Other glass fibres are D-type with good dielectric properties, C-type with good chemical resistance and R, S or T-type, equivalent to E-glass, but having higher strength or modulus than it.

Aramid fibre is a man-made polymer (aromatic polyamide). It is more commonly known under trade name 'Kevlar®', from Dupont de Nemours (USA), although there are other suppliers of this fibre. This fibre has high specific strength, low density, and good resistance to impact, reason why lower modulus grades are used in ballistic applications (bullet proof jackets). Compressive strength is lower, as well as flexure and bending and they are sensitive to interlaminar shearing.

Carbon fibre is elaborated from coal or oil distillation by adequate processes. Graphite hexagonal closed-packed crystal structure gives to this fibres good thermal and electrical conductive properties, as well as high mechanical properties in the direction of crystallographic plans. Its price is high, but has been lowering, as the production capacity installed has been increasing. These fibres are classified according to their elastic modulus range. So there are the high strength (HS), intermediate modulus (IM), high modulus (HM) and ultra high modulus (UHM). The filament diameter of most types is about 5 to 7 μm. Carbon fibre has the highest specific stiffness of any fibre commercially available, very high strength both in tension and in compression and a high resistance to corrosion creep and fatigue. However, their impact strength is low, being HM and UHM fibres particularly brittle.

Another type of fibres that are similar to carbon, are graphite fibres. Although both designations tend to be used indistinctly, there are differences, even though they both have carbon in their composition. Carbon fibres have a carbon percentage between 93 and 95%, and graphite fibres have a higher degree of purity with carbon percentages higher than 99%. In their fabrication process, graphite fibres can reach 1900ºC to 3000ºC and carbon fibres reach lower temperatures, around 1300ºC.

In this work, it will only be studied composites with glass and carbon fibre as reinforcement.

The following table shows some properties of some of the fibres mentioned, like E-glass, HS and HM carbon and aramid Kevlar49® [4].

Table 1.1 – Characteristics of some fibres used as reinforcement.

Characteristic	Unit	E-glass	HS Carbon	HM Carbon	Kevlar® 49
Density	kg/m^3	2600	1750	1800	1450
Diameter	µm	10 to 20	5 to 7	5 to 7	12
Modulus of elasticity in tension	GPa	74	230	390	130
Shear modulus	GPa	30	50	20	12
Poisson ratio	---	0,25	0,3	0,35	0,4
Tensile strength	MPa	2500	3200	2500	2900
Elongation		3,5	1,3	0,6	2,3
Coefficient of thermal expansion	K^{-1}	0.5×10^{-5}	0.02×10^{-5}	0.08×10^{-5}	-0.2×10^{-5}
Thermal conductivity	W/m K	1	200	200	0.03
Maximum operating temperature	ºC	700	> 1500	> 1500	

Ceramic fibres are another group including boron fibres elaborated from the reaction of boron chloride and hydrogen, boron-boron carbide fibres, silicon carbide fibres, BorSiC fibres (boron – silicon carbide), alumina fibres (Al_2O_3), aluminium silicate fibres (Al_2O_3,Si O_2) and boron aluminium silicate fibres (Al_2O_3,Si O_2,B_2O_3).

Other fibres can be mentioned like polyester, polyethylene, quartz and natural fibres, from fibrous plans like jute and sisal that can be used when desired mechanical properties are not so high.

All fibres are treated at the surface in order to lower their abrasiveness and ensure better adhesion to matrix.

1.2.3 HYBRIDS

The term hybrid refers to a composite that has more than one type of matrix or fibre in its construction. The use of hybrid composites can expand the range of achievable properties when using composite materials, and can be more cost-effective than conventional or advanced composites. One of the main attractive when using hybrids is their synergy effect also called as ‘hybrid effect’. The most common effect is to obtain a composite property, like tensile strength, whose value is higher than would be predicted from a simple application of the rule of mixtures. This would be a positive hybrid effect. In some cases, a negative effect may also occur [5].

The term hybrid applies to advanced composites using various combinations of graphite, boron, Kevlar® or glass filaments in a thermosetting or thermoplastic matrix. Hybrids have unique features that can be used to meet design requirements in a more cost-effective way than advanced or conventional composites. Some of those advantages are the balanced strength and stiffness, balanced thermal distortion, reduced weight and/or cost, improved fatigue resistance, reduced notch sensitivity, improved fracture toughness and impact resistance [2].

According to M. M. Schwartz [2], there are four basic types of hybrid composites:

- *interply hybrids*, that consists of plies from two or more different unidirectional composites stacked in a specific sequence;
- *intraply hybrids*, consisting in two or more different fibres mixed in the same ply;
- *interply-intraply hybrids*, in which interply and intraply hybrids are stacked in a specific sequence;
- *superhybrids*, that are resin-matrix composite plies stacked in a specific sequence.

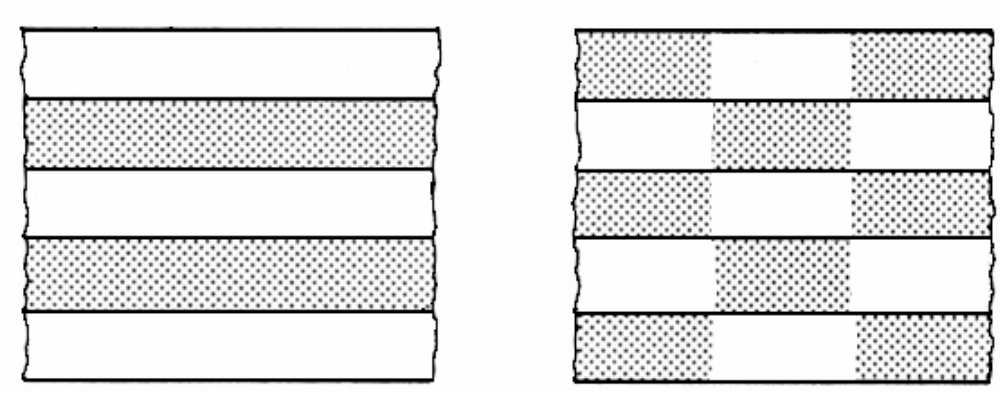

a) interply hybrid b) intraply hybrid

Figure 1.1 – Interply a) and intraply b) hybrids [5].

The first two types of hybrids generally have the same matrix. Although thermosetting and thermoplastic resins can be used for hybrid composites, epoxies remain the most used. Thermosetting polyester resins are already used in a large number of applications in automotive and aeronautic industry. Fibres most currently found in hybrids are carbon, boron, glass and Kevlar®. The potential for the number of fibre-resin combination for hybrids is vast. Using only two resins – epoxy or polyester –

and three types of fibre – carbon, glass or aramid – a large number of hybrid composites can be produced, combining fibre content and orientation in the matrix.

Here we will only regard to the interply hybrids using two types of reinforcement, with adjacent layers having different fibres. When considering such hybrids, the most referred combinations are:

- **carbon/ aramid** – this hybrid combines the high impact resistance and tensile strength of aramid fibre with the stiffness and high compressive and tensile strength of carbon fibre. It is expensive. As the coefficients of thermal expansion of these two fibres are similar, the internal thermal stresses are minimized.
- **aramid/ glass** – the low density, high impact resistance and tensile strength of aramid fibre combine with the good compressive and tensile strength of glass, with low costs.
- **carbon/ glass** – carbon fibre contributes with high tensile and compressive strength and stiffness and reduces density while glass reduces final cost. This combination is an excellent mix, as price and mechanical properties can be balanced according to designer needs. A hybrid carbon/ glass with only 25% of carbon can increase the elasticity and flexure modulus by 60% with a cost increase of approximately 5%.

Even though not mentioned here, many other combinations of fibres and resins are possible, so multiplying the variety of hybrids that can be produced.

1.2.4. LAMINATES

From the several types of normally used composites, laminates are the ancient ones. Their main and more distinctive characteristic is the existence of layers that are easily detected in a simple naked eye observation. In a laminate two of its dimensions are clearly superior to the third. Laminates are a kind of material particularly attractive to engineers for its presentation in film or sheets makes design, production specification and control easier. Among the most usual utilisations we can identify sandwich materials. Another advantage is the possibility of combining the alignment of different layers in order to achieve mechanical properties that are previously defined.

When all the layers in a composite have their fibres oriented according to one direction only, laminate is designed as unidirectional. Different orientation can be

defined for different layers, usually defined as an angle to a reference direction, named as 0º. In that case, it becomes necessary to have a symmetry plan in order to avoid coupling between bending and extension. Layers with angles of 90º and 45º to the reference direction are more usual, but other angles like 30º and 60º can also be found. Normally the reference direction (0º) is the direction of the main efforts that the part is expected to be subjected when in service. If the stacking sequence of the laminate has alternated layers with 0º, +45º, 90º, -45 º orientation, the laminate is designed as quasi-isotropic. In that case, their properties are approximately identical in any direction considered in laminate plan. One must note that this general assumption is more real for elastic properties than for mechanical strength of the part [6]. Using Lamb waves, Otterloo et al. [7] have determined that elastic modulus and Poisson ratio show a 30% variation according to the direction considered in a quasi-isotropic laminate.

When the stacking sequence is another, the laminate is anisotropic, and so the reaction to a given strain depends and changes with its direction.

1.2.5 PROPERTIES OF POLYMERIC MATRIX COMPOSITES

In the precedent pages we have referred composite constituents and their properties. In a composite material, properties are the result of matrix/ reinforcement association and depend of several factors, such as:

- amount of fibre in the composite (‘Fibre Volume Fraction’)
- size, shape and orientation of fibres;
- manufacturing process.

Generally, in a composite, the following properties can be mentioned:

- tensile strength is dependent of reinforcement volume fraction and orientation;
- composites do not deform plastically, their yield strength is equal to tensile strength;
- composites have good resistance to fatigue;
- ageing of composites happens by moisture (absorbed) and heat actions;
- composites are not sensible to corrosion, except when there is contact between aluminium and carbon fibres that cause a galvanic corrosion;
- composites do not react with chemical products currently used in mechanical construction;

- composites are less resistant to impacts and shocks than most of metallic materials;
- for the same (small) thickness, composites have better resistance to fire than light alloys, but smoke from their combustion that can be hazardous.

Table 1.2 compares composites with 60% fibre volume fraction with steel normally used in metallic construction.

Table 1.2 - Example of composite properties with 60% volume fibre and epoxy matrix, compared with steel– indicative values [4].

Property	Unit	Glass	Kevlar®	Carbon	Steel
Nominal density	kg/m^3	2 080	1 350	1 530	7 800
Tensile strength, fibre direction *l*	MPa	1 250	1 410	1 270	400 to 1600
Compress. strength, fibre direction *l*	MPa	600	280	1 130	
Tensile strength, perpendicular direction *t*	MPa	35	28	42	
Compress. strength, perpendicular direction *t*	MPa	141	141	141	
Shear strength in plan *l,t*	MPa	63	45	63	
Interlaminar shear strength	MPa	80	60	90	
Modulus of elasticity fibre direction *l*	MPa	45 000	85 000	134 000	205 000
Modulus of elasticity perpendicular direction *t*	MPa	12 000	5 600	7 000	
Shear modulus	MPa	4 500	2 100	4 200	79 000
Poisson ratio	---	0.3	0.34	0.25	0.3
Coefficient of thermal expansion, fibre direction *l*	K^{-1}	$0.4 - 0.7 \times 10^{-5}$	-0.4×10^{-5}	-0.12×10^{-5}	1.3×10^{-5}
Coefficient of thermal expansion, perpendicular direction *t*	K^{-1}	$1.6 - 2 \times 10^{-5}$	5.8×10^{-5}	3.4×10^{-5}	

1.2.6 MANUFACTURING PROCESSES

Manufacturing process is an influencing factor in composite final properties. There are several production methods to be used. A small reference is now made to the processes that are going to be mentioned further on in this work.

- **Hand lay-up and cure**

This is the more simple process and maybe the first to be used in composites manufacturing. Resins are impregnated by hand into fibres, usually in form of woven, knitted, stitched or bonded fabrics. Fibres are laid on a plate or inside a mould and excess air is removed with the help of rollers. Successive layers of fibre can be laid until desired thickness is achieved. Laminates are left to cure under standard atmospheric conditions, but heat can be used to accelerate the curing process. The use of a gel-coat in the mould allows the improvement of surface finish, if necessary.

- **Resin Transfer Moulding (RTM)**

This is a closed mould process. A low viscosity resin is injected at low pressure in a mould where previously the dry reinforcement was laid. Vacuum can be applied to mould cavity to assist resin in being drawn into the reinforcement material. Mould must be tightly closed and an air exit is necessary. Once the mould is filled with resin, resin inlets and air exhaust are closed and the laminate is allowed to cure inside the mould.

- **Hot plate moulding**

This process is used with prepregs or other laminates. Prepregs are supplied by a material manufacturer and have a determined percentage of fibres already impregnated with a resin. Plies of prepreg are stacked in a pre-determined sequence and orientation. The plate is bagged (or vacuum bagged) and heated to 120-180ºC, typically, and pressure (up to 5 daN/cm^2) applied. The temperature reduces resin viscosity and eases fibre wetting and exit of entrapped air. Excess resins flows out, and an empty space to receive it must exist in the bag. Laminate cure is inside the mould and the part is taken out only when ambient temperature is reached.

Other processes used to bring fibre reinforced parts to the desired form are braiding, filament winding, pultrusion, sandwich construction and adhesive bonding. Some of these processes need cure in vacuum bag, oven, autoclave, heated platen press or thermoforming, where pressure and/or temperature are combined to ensure

that matrix will be intact and able to maintain the fibres adequately positioned to carry the loads that will be applied to the part.

Braiding is a textile process where two or more strands, yarns or ropes are intertwined in the bias direction to form an integrated structure. Filament winding is used for hollow, generally circular or oval sectioned components, like pipes and tanks. In pultrusion, fibres are pulled from a creel through a resin bath and then through a die where its final shape is given. A sandwich construction consists, in its simplest form, of a structural panel with two thin, parallel sheets of structural material bonded to, and separated by, a relatively thick, light-weight core. Adhesive bonding is an assembly technique where one surface adheres to one other, using an adhesive as bonding agent.

1.3 MATERIAL REMOVAL PROCESSES

1.3.1. OVERVIEW OF MACHINING THEORY

Composite machining began with the use of machines, tools and processes already existent and well established in the machining of metals and metallic alloys. In the last decades, due to the rising interest in composites, research on its machining has increased, with the purpose of optimizing processes developed to metal machining.

Machining is a manufacturing process in which a cutting tool is used to remove excess material from a workpiece. This process is classified as orthogonal or bi-dimensional, or as oblique or tri-dimensional. The latter is a more generic model that considers an inclination angle not equal to 90º between the cutting edge and the direction of cutting speed. This geometric model, closer to real machining operation, is somewhat complex. In orthogonal cutting model, the cutting edge is perpendicular to the direction of the cutting speed. This enables the process to be represented in a bi-dimensional way, which reduces geometric complexity and allows establishing simple geometric relations, force and speed vectorial analysis (fig.1.2). The orthogonal cutting model, by its simplicity, has been used for the development of theoretical and practical work. In this work this model will be used.

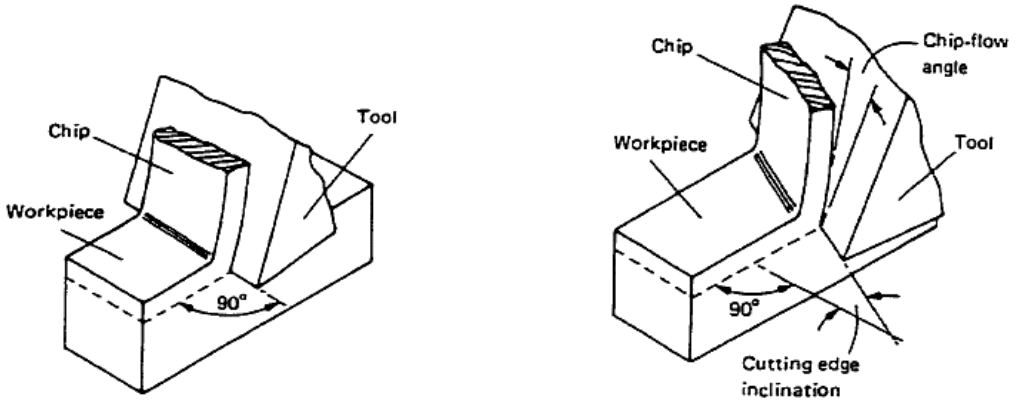

a) b)

Figure 1.2 – Orthogonal –a) – and oblique – b) – cutting models [8].

When orthogonal cutting model is used, a certain number of simplifications are accepted, although they are not real. So, material is considered homogeneous,

isotropic and plastic deformation is negligible. Chip formation is seen as a stationary phenomena and it deforms according to a plane. Material cutting resistance is reduced to plastic chip deformation along cutting plan and friction along rake plan. Cutting tool action on material is reduced to a force applied in cutting edge.

In order to form a chip, relative motion between the tool and part is required, and a small portion of the part, called chip, is removed from it. The cutting tool shape is an edge, formed by the intersection of two tool surfaces – rake face and tool flank -, usually designed as cutting edge, whose function is to separate the chip from the parent part. The rake face, which directs the flow of the chip, is oriented at a certain angle called the *rake angle* γ. The flank of the tool is the surface that is facing the material to be cut and provides a clearance between the tool and the generated work surface, protecting it from abrasion. This surface is oriented at an angle called the *relief angle* α.

The penetration of the cutting tool below the original working surface, depth of cut, is equal to chip nominal width, and is considered as constant for model simplification, although it is not true. The angles above mentioned, defining the rake and flank inclinations relative to the work surface, are important parameters when tool characterization is concerned. As shown in fig. 1.3, rake angle is measured in relation to a plane perpendicular to the work surface, and it can be positive, zero or negative. Relief angle is measured between the tool flank surface and work generated surface and its value has influence on tool wear. There is a third angle, the *edge angle* β, related with the other two by equation $\alpha + \beta + \gamma$ = 90º.

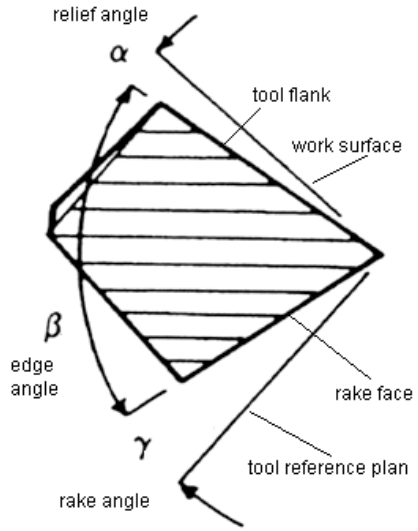

Figure 1.3 – Cutting edge geometry [8].

These angles can be of two types: tool angles, referring to tool construction or sharpening angles and working or effective angles, referring to tool in machine tool. The two types are related trigonometrically.

Theory of material removal processes is based in chip formation under a quick plastic deformation under a compressive action. Chip shape and size depends from machined material and cutting conditions. For ductile materials, like mild steels or aluminium, chip is normally continuous. When machining fragile materials like cast irons, chip is discontinuous. This kind of chip can also be obtained in the machining of ductile materials under specific cutting conditions – high feed and low speed.

During orthogonal cutting, forces acting against the tool can be classified as cutting force - F_c - that is in the direction of cutting, and a perpendicular one called thrust force - F_t (fig.1.4). Measurements of these forces are possible by dynamometers and they have been object of extensive work. A third force should also be considered, the penetration force, perpendicular to the surface defined by the first two forces. Resultant tool force – R'' - is the sum of the cutting and thrust forces and the sum of tool force with penetration force is called total machining force. Its value depends on material to be machined, cutting section area, cutting speed, tool geometry and material. The product of cutting force and cutting speed gives the power (energy per unit time) required to perform a machining operation.

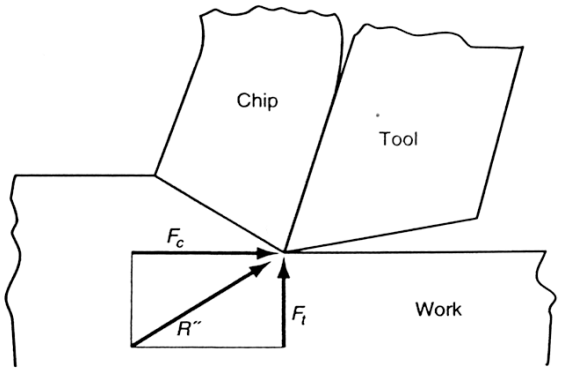

Figure 1.4 – Forces acting in orthogonal cutting [9].

Power consumption and material removal rate are proportional to cutting speed. Another parameter can be defined, specific cutting energy k_c – also known as specific

cutting pressure or specific cutting force –, which give information about process efficiency independently of cutting speed

$$k_c = \frac{P_m}{Z_w} = \frac{F_c}{A_c} \quad (1.1),$$

where P_m is machining power, Z_w is the material removal rate, F_c is the cutting force and A_c is the chip nominal sectional area. Specific cutting energy is first of all a function of working material. However, it can be affected by cutting speed, feed, relief angle and others.

1.3.2 DRILLING

Drilling is, usually, performed with a rotating cylindrical tool that has two cutting edges on its working end. The tool is called a *drill* or *drill bit* [9]. The rotating drill feeds, parallel to machine axis, into the stationary work part to form a hole whose diameter is determined by the drill diameter. Vertical movement rate is called feed *f* and is specified in mm/rev. Feed can be converted to feed rate, f_r, expressed in mm/min, using equation

$$f_r = f \times N \quad (1.2).$$

Rotational speed of the drill *N* is given in rpm (revolutions per minute). Knowing this speed and the drill diameter D in mm, it is possible to determine the cutting speed v_c, which is the surface speed at the outside diameter of the drill in m/min by equation:

$$v_c = \frac{\pi * D * N}{1000} \quad (1.3).$$

One should not forget that in drilling, as the centre of the drill is approached, cutting speed reduces linearly until zero. In drilling, depth of cut is equal to drill radius.

The standard twist drill geometry is illustrated in figure 1.5. The body of the drill has two spiral flutes, whose angle is called the helix angle, typically around 30º or 35º. One of its functions is to evacuate the chips. The web provides support for the drill over its length. The point of the drill can be briefly described as having the general shape of a cone, which most common design is the *chisel edge*, as the one in figure 1.5 and a typical value of point angle is 118º. This angle has a decisive influence in the way drill penetrates into the material until maximum diameter is reached. Connected to the chisel edge are two cutting edges – lips – that lead into the flutes. The portion of each flute adjacent to the cutting edge acts as the rake face of the drill.

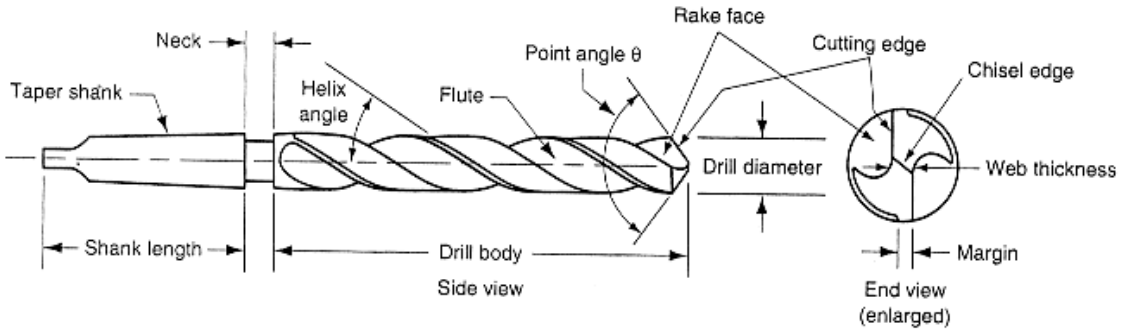

Figure 1.5 – Standard geometry of a drill [9].

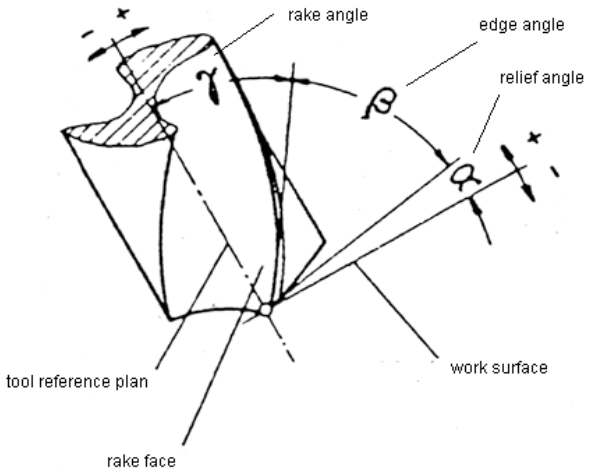

Figure 1.6 – Tool angles in a twist drill [10].

The main tool system angles of a twist drill – rake, clearance and edge angles – are shown in figure 1.6. During work an increase in feed causes a variation in tool angles, increasing rake angle and diminishing relief angle.

There are two measurable components to be considered during drilling: thrust force and torque. Thrust force is the necessary force to maintain a given feed rate into the material. Torque is the amount of tangential force necessary to maintain drill rotational speed. These two forces are affected by cutting parameters like speed, feed, drill geometry and work piece material.

From the torque value M_t, in Nm, it is possible to derive the specific cutting energy in N/mm^2 by equation

$$k_c = \frac{4000 \times M_t}{\pi \times f \times D^2} \qquad (1.4).$$

where f is the feed rate in mm/rev and D the drill diameter in mm.

When feed increases, the chip thickness also increase, the specific cutting energy is lower and tangential force and chip section are greater, causing a torque increase. Chip thickness can also be increased by the use of greater point angles, reducing torque and specific cutting energy.

The cutting action of a twist drill is complex. As the cutting speed varies as function of the distance from its axis, so does the cutting efficiency, being less efficient in the centre. Chip removal mechanism is similar to oblique cutting, but more complicated as the cutting speed and rake angle change continuously. The relative velocity of the drill point is zero and so no cutting takes place, except on the external edges. The chisel edge of the drill pushes aside the material as it penetrates into the hole, requiring a large thrust force to drive the twist drill forward [9]. On the other side, contribution to torque is minimum. When drilling, chisel edge action is more similar to an extrusion.

Other problems in drilling are chip removal and temperature rise. A ‘pecking’ procedure can be an alternative for drilling operations, when fluids cannot be used. In this procedure, the drill is periodically withdrawn from the hole, allowing cooling and chip exit.

In summary, drilling is a very complicated process that depends on a large diversity of factors.

1.4 FINITE ELEMENT METHOD

Fundamental to all finite element analysis is the replacement of a continuum, in which problems variables may be determined exactly, by an assembly of finite elements in which they are only determined at a set number of points, called the nodes of the elements. Values of the variables, or any derived quantity, between the nodes are determined by interpolation. Nodes are the vertices of the elements and an element is divided in a certain number of nodes according to its geometric complexity.

As machining is a material removal process, criteria must be included to deal with chip formation, that is to say, the separation of a certain amount of elements from the body to effectively simulate machining conditions. The real issue for a criteria definition is when a connection between elements breaks, by a strain, energy or displacement condition.

Finite element method offers an economical and alternative approach to the experimental study of machining processes, that can be expensive and time consuming. In finite element studies, the objective is to derive a computational model predicting the deformations, stresses and strains in the workpiece, as well as the loads on the tool working under specific cutting parameters [11].

Mackerle [11] completed a bibliographic review of published articles about the application of FEM in machining, where it can be seen that several aspects about machining have been studied. Material removal is based on orthogonal and oblique models, the former being easier to simulate, but also the effect of geometric and process parameters e.g., thermal aspects, residual stresses, tool wear or chip formation mechanism. However, the majority of them are related to metal machining, leading to a situation that is totally similar to the one already referred in precedent chapter about material removal processes. There are only few articles about composites machining, at least to the author knowledge. The most relevant of them are referred below.

Mahdi and Zhang [12] proposed an adaptive finite element algorithm for the simulation of orthogonal cutting of composite materials. Their first objective was to establish a criterion for local remeshing. They have found that maximum stress criterion is appropriate for cutting simulations. During simulation they have found, as expected, that cutting force increases when the tool start to interact with the workpiece and decreases when elements at the cutting zone start to be removed. They compared

three different meshes observing that a finer mesh results in better agreement with measurements.

In [13], the same authors used the Tsai-Hill criteria for chip production and compared their results with the experimental ones obtained by Wang and Zhang. They concluded that there was good agreement between the model predictions and experimental measurements. The piece is taken as stationary and the cutting tool has a predefined movement (displacement boundary conditions) in the negative *x*-direction. In this work, two different meshes were used – fine and coarse – in order to predict the effect of mesh size on the cutting force - figure 1.7. Finer mesh smoothened variation of cutting force but also lowered its magnitude. That is an expected consequence as stresses depend on the mesh used.

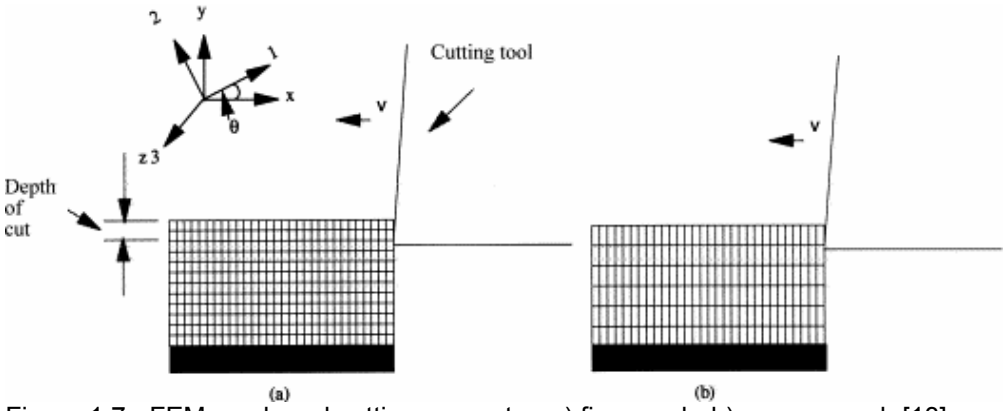

Figure 1.7 - FEM mesh and cutting geometry: a) fine mesh; b) coarse mesh [13].

Ramesh et al. [14] used finite elements to analyse FRP's machining. In their work, anisotropic theory of plasticity was used. The model for analysis was similar to the one shown in figure 1.7 – orthogonal cutting -, but has the interest of considering four different FRP materials as well as four different fibre orientation angles. Materials were boron/epoxy, two kinds of glass/polyester and a graphite/epoxy. Orientation angles were 0º, 45º, 90º and -45º. The objective was to find out the minimum load required to remove the first chip. With the model they were able to trace lines of minimum and maximum principal stresses for the four materials. As conclusions they pointed that plastic strains during FRP's machining are very small and the orientation angle -45º minimize the load required to achieve first crack, which was also observed in experiments.

Arola et al. [15] developed a finite element model to simulate chip formation in the edge trimming of unidirectional Graphite/Epoxy with orthogonal cutting tools. Seven models were considered with fibre orientations of 0º, 15º, 30º, 45º, 60º, 75º, and 90º. The models were configured with a secondary shear plane that was located at a certain distance ahead of the cutting tool. Mesh density near tool contact zone was higher, but only in a small portion, in order to minimize computation time. Tool was modelled as a rigid body and also as a deformable body in independent analyses. Different geometries of cutting edges were also considered. For each fibre orientation, four rake angles (γ) - 0º, 5º, 10º and 15º - and two clearance angles (α) - 7º and 17º - were modelled. For all tools an edge radius of 15 μm and a flank wear land of 30 μm were used. The results showed that the model was able to predict the principal and thrust cutting forces for the orthogonal cutting of unidirectional graphite/epoxy. Principal cutting forces agreed well with experimental results, but thrust forces don't. Tool rake angle that minimizes cutting forces was found to be 15º. However, this result is valid only for this material, as it depends on particular process needs.

Zitoune et al. [16] adopt a simplified model with orthogonal cutting with the aim to model damage during drilling of carbon/epoxy unidirectional laminates. In their simulation, fibres are aligned with the tool cutting direction.

Budan and Vijayarangan [17] conducted drilling experiments on bidirectional glass-fibre reinforced plastics using high speed steel drills. Then they performed a finite element analysis to predict the influence of drill speed, feed rate and fibre concentration on surface finish, hole quality, dimensional variations and thrust forces causing delamination. The model proposed is shown in figure 1.8.

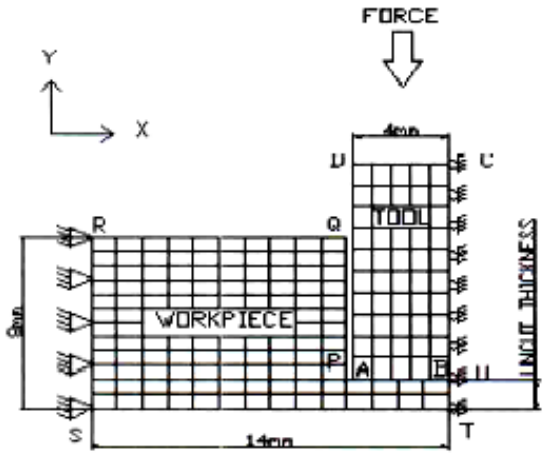

Figure 1.8 - FEM model [17].

Sicot at al. [18] used incremental hole-drilling method for the determination of residual stresses caused by different cure cycles in composites. A non-through hole was made incrementally by removing elements from the hole, as showed in figure 1.9. Results were compared with experimental procedure and showed good agreement.

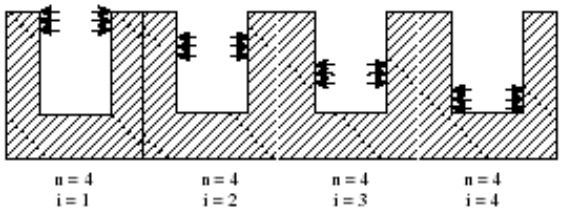

Figure 1.9 – Incremental hole-drilling method [18].

A final note to a paper from Strenkowski et al. [19] where an analytical finite element technique for predicting thrust force and torque in drilling of AISI 1020 steel was developed. The authors' approach was based on representing the cutting forces along the cutting lips as a series of oblique sections. Chisel region cutting was treated as orthogonal cutting. The model described is three-dimensional and is applicable to general drill geometries.

1.4.1 OTHER APPLICATIONS OF FINITE ELEMENTS

Finite elements are used to predict composites properties in a large variety of situations, some of them are here referred. Camanho and Matthews [20, 21] used three-dimensional finite elements to study the onset of delamination and damage model for fastened joints in composite laminates. In these works, it was shown that the use of laminates with less adjacent layers of the same fibre orientation have higher delamination onset and smaller initial delaminated surfaces. The progressive damage model was able to predict accurately failure modes in joints as well as stiffness and strength.

C. V. Nori et al. [22] modelled composite hybrid specimens with several combinations of glass/epoxy and carbon/epoxy subjected to axial and flexural vibration. The aim of this work was the research of hybridization effects on dynamic mechanical

properties. Although there were some differences noted between experimental and model results, the trends of the results from the model were the same as obtained in experimental results.

A.B. de Morais et al. [23] use finite elements to analyse crack propagation during double cantilever beam (DCB) of multidirectional laminates. In another paper [24] the interlaminar fracture of cross-ply carbon/epoxy composites is analysed. In both papers, the DCB test for the determination of critical strain energy release rate in mode I (G_{Ic}) is the main subject. In [25], de Moura et al. analysed the influence of interlaminar cracking on the apparent interlaminar mode I fracture toughness of cross-ply laminates. Considerations about G_{Ic} test are resumed further in this work – chapter 4.

Application of the FEM to predict the onset of delamination for DCB, ENF (End Notch Flexure) and MMB (Mixed Mode Bending) tests was presented by Jiménez et al. [26]. In this paper FEM simulation was used as a part of the material characterisation process, for a carbon/epoxy unidirectional laminate. Experimental results were compared in order to successfully validate the proposed model.

CHAPTER 2 – STATE-OF-THE-ART

2.1 COMPOSITES MACHINING

Although their physical properties make composites an attractive group of materials, machining poses a certain number of specific issues, when compared with metallic materials. Generally, machined parts have poor surface appearance and tool wear is high. One of the problems of machining composites is related with the fibre reinforcement that is usually very abrasive and causes rapid tool wear and deterioration of the machined surfaces [27]. Machining can cause several damages such as delamination, fibre pull-out, thermal damages [28] and other damages that will be described in section 2.3. When considering the drilling of a composite part, good results are mainly fibre related and less dependent of the matrix material [29].

Koplev et al. [30] examined the cutting process of unidirectional carbon fibre reinforced plastics in directions perpendicular, as well as parallel to fibre orientation. A series of quick-stop experiments were carried out to examine the area near the tool tip. The author stated that machining of CFRP consists in a series of fractures, each creating a chip. When this material is machined, a large number of chips are created and the examination of these chips revealed that they are not subjected to large plastic deformation as is normally found in metal chips. Machining parallel to the fibres gives smoother surfaces than machining perpendicular to fibres, and matrix cracking is also smaller.

Composites are produced to near-net shape, minimizing machining needs of manufactured parts. However, machining operations like trimming to final shape and drilling to enable assembly of parts in complex structures, like aircrafts, are usual operations in industries that deal with these kinds of materials. Besides those techniques, turning, milling or grinding are examples of machining operations that can

be executed on composite parts, in order to obtain the final shape or fulfil specified tolerances. In this section conventional machining of composites is discussed. In next chapter, non-conventional machining techniques used in composites will be briefly described.

2.1.1 CUTTING MECHANISM

Composite materials are characterized for being non-homogeneous and, in most cases, anisotropic. Fibre orientation towards cutting direction is an influencing factor in the development of forces and stresses during machining. Definition of fibre orientation angle – θ – is shown in figure 2.1.

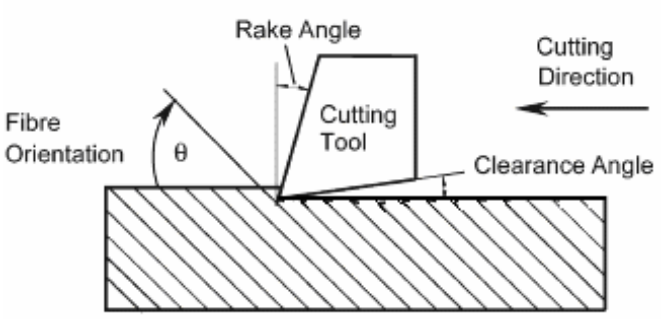

Figure 2.1 – Definition of fibre orientation angle and other cutting variables.

In an experimental research performed with a carbon/epoxy composite with unidirectional fibres, Wang and Chang [31] verified that fibre orientation has a determining influence on the forces that developed during the cut, no matter what tool rake angle – γ -. Depth of cut – DOC – can have some influence, function of fibre orientation angle. Their conclusions are summarized in table 2.1.

Table 2.1 – Effect of fibre orientation angle on cutting forces.

Fibre orientation θ	Cutting force	Notes
0 to 60º	increase	------
60 to 120º	decrease	increase if DOC great
> 120º	increase	decrease if DOC great

Fibre fracture plays an important role in the cutting mechanism which differs according to the machining angle to the fibre orientation – figure 2.2.

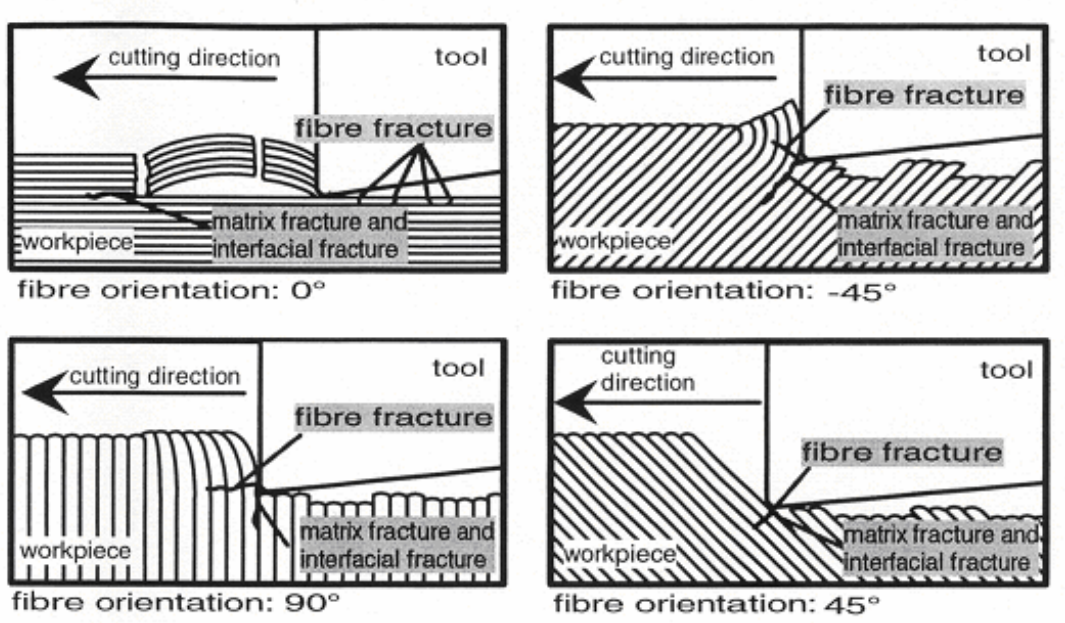

Figure 2.2 – Cutting mechanism for orthogonal cutting of FRP's [32].

Klocke et al. [32] had drawn some conclusions regarding fracture in orthogonal cutting, which are now summarized. When the angle to the fibre orientation is 0º, the laminate is subjected to compression. Material failure occurs by delamination or interfacial fibre failure. When machining at an angle of 90º, fibres are subjected to bending and are sheared off. As that angle increases to 135º, fibres are compressed and bent in the direction opposite to fibre orientation. Fibre breaking is a result of bending and compression. Angles in the interval between 120º and 150º are the least favourable, resulting in poor surface quality. An orientation of 45º is more favourable to cut. Fibres are subjected to bending and tensile stresses and break in bundles. Sometimes, individual fibres are ripped off the matrix due to insufficient adhesion.

Table 2.2 – Deformation and cutting mechanisms with fibre orientation.

Fibre orientation θ	Fibre stress	Fibre breakage	Notes
0º	compression	delamination	
0º<θ<90º	bending and tensile	breaking	45º best value
90º	bending	shear off	
>90º	bending and compression	breaking	least favourable

Wang and Chang [31] had related fibre deformation mechanisms in the cutting zone with fibre orientation angle θ. When this angle is less than 90º (fig. 2.3a) the fibre is pushed by the tool in a direction perpendicular to its axis and towards the workpiece subsurface. Fibre is supported by uncut material behind and the bending of the fibre is small. A tensile stress is created along the fibre axis and carbon fibres, brittle, fracture easily. Surface roughness and subsurface damage is small. For angles greater than 90º, they divided the mechanism according to the depth of cut. For small depths of cut (fig. 2.3b), fibre is subjected to an axial compression. As a result of that force, matrix material around the fibre is fractured. Thus a machined surface has protruded fibres resulting in greater surface roughness. When the depth of cut is great (fig 2.3c), fibres are pushed towards the external of the workpiece. As the support from surrounding material is weaker, the result is fibre bending and fibre-matrix debonding. This causes a rougher surface finish and deeper subsurface damage. Figure 2.3 gives an aid on the explanation of the above mentioned mechanisms.

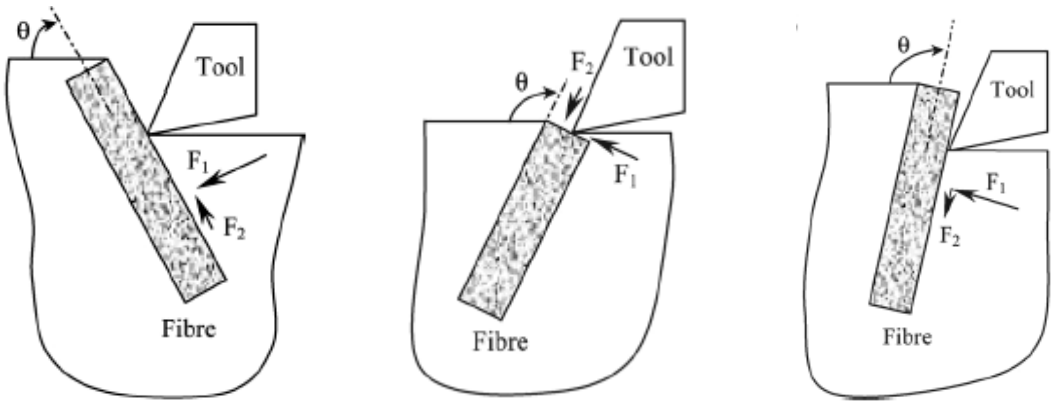

a) θ < 90º b) θ > 90º, DOC small c) θ > 90º, DOC great

Figure 2.3 – Schematic cutting mechanisms [31].

2.1.2 TURNING

Turning of fibre reinforced composite materials with HSS or carbide tools has been found to be not cost effective due to the abrasiveness and inhomogeneity of those materials. Machined parts have poor surface finish and high tool wear [33, 34]. In composites reinforced with carbon fibres the use of high speed tools is rare, due to the

great abrasiveness of these fibres. Carbide tools are more normally used. Ceramic tooling, due to its low thermal conductivity, is not adequate for this type of materials.

Recently, the use of PCD (synthetic polycrystalline diamond) has shown satisfactory results, but for the moment, there is limited scarce information on the optimum grain sizes effect and optimization of tool geometry. Ramulu [33] investigated machining by turning of graphite/epoxy composite material with the purpose of comparing different PCD grain sizes and the identification of dominant parameters in the tool edge geometry. Graphite fibre reinforced materials are extremely abrasive, leading to the need to use diamond abrasive cutters.

The finish of machined surface depends largely on fibre orientation, but roughness values show some variation according to the orientation of the fibres to the cutting edge.

PCD tools were found to have longer tool life, generating surfaces with better characteristics than carbide tools. It has a good thermal conductivity, in the range of 5.0 to 9.2 W/cm·K, allowing a rapid removal of the heat generated in the cutting edge area. They also have a very high resistance to shock and vibration. Tools made from coarser grains have greater wear resistance than a finer grade, but surface finish is worse. Although they are expensive, they can pay off in the long run due to lower operating costs [33]. When compared with carbide tooling, in continuous cut, a PCD tool can last more 120 times, approximately.

Machining experiments were performed under a cutting speed of 230 m/min and a feed of 0.18 mm/rev. The cutting conditions remain constant and the tool geometry was changed along the tests. Tool wear geometry for minimum tool wear was found to be a clearance angle of 17º, and a rake angle of 7º. Negative rakes should be avoided and greater clearance angles reduce edge angle without benefit in tool life.

Krishnamurthy et al. [35] conducted a study on the machinability of three types of composites with different reinforcement fibres – glass, carbon and aramid – using K20 carbide tools. Coated carbides, TiC and TiN, did not perform well owing to coating deformation and subsequent chipping and spalling. Tool have a rake angle of -6º, a clearance angle of 6º and an edge radius of 0.8 mm. Cutting speeds were in a large range of 12.5 to 200 m/min and feed rate between 0.025 and 0.15 mm/rev. They have observed that reinforcement fibres were a dominant factor in machinability. Depending on fibre nature, its orientation and angle to cutting edge removal mechanisms may be associated with rupture, deformation or shearing, as illustrated in fig. 2.4.

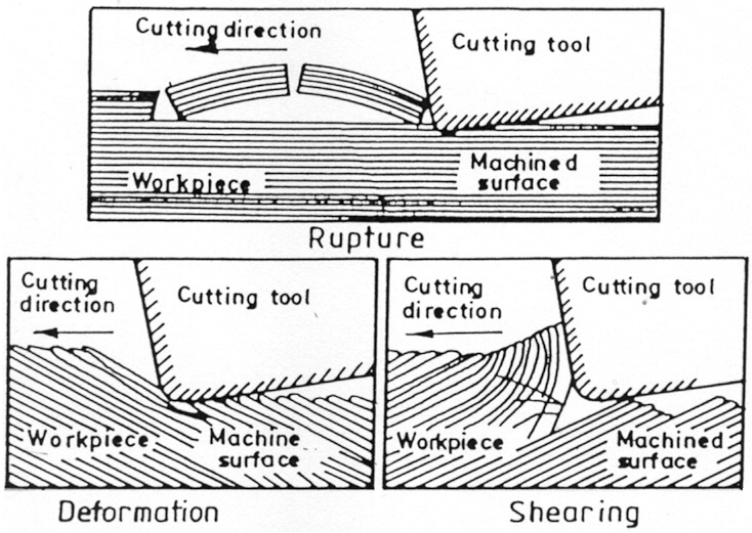

Figure 2.4 – Rupture, deformation and shearing of fibre reinforced composites during machining [35].

Referring to cutting forces, it was seen that, for the composites studied, the thrust and feed force are higher than the main cutting force. Eventually, this can be related with the high depth of cut of 1.5 mm used in all machining trials. Concerning specific cutting energy, the smallest value was obtained when machining carbon reinforced composite, so this material has shown better machinability. The values from cutting forces and specific cutting energy were minimized when a cutting speed of 100m/min was used. That speed was identified as the critical cutting speed. When cutting with speeds above or below that value, forces tend to increase.

In another study with Sreejith et al. [36], Krishnamurthy verified that the same cutting speed of 100 m/min also minimize temperature rise during turning of these materials. For higher cutting speeds, thermal rise was greater. An increase in feed rate also gives a contribution to workpiece temperature rise during machining.

2.1.3 MILLING

The main characteristic of milling operations on parts made of fibre composite plastics is a low ratio of removed volume to total part volume. Milling is used as a corrective operation in order to produce well-defined and quality surfaces. The fibre has the greater influence in the selection of tools and parameters [32].

Optimization of milling process is influenced on one side by the nature of the fibres which must be cut in and near to the top layers and on the other side by the thermal stress on the contact surface. The latter are caused by material abrasiveness and the friction between material and tool, affecting the quality of the cut surface [37]. The combination of high cutting speeds with low feeds can lead to matrix melting and stuck to laminate surface or to the chips. Under some conditions matrix could even burn. A significant reduction in cutting velocity and an increase in feed can limit this problem. However, these cutting parameters lead to the presence of inadequately cut fibres that remains attached to the surface layers [37].

Thermal stress on tools becomes critical when small diameter tooling is used. Fibre reinforced composites are characterized by their low thermal conductivity, so the tool has to absorb a considerable amount of generated heat, in opposition to what happens to steels. If the capacity of the tool to absorb the heat is also low, an increase in friction leads to higher thermal stress, more tool wear and poorer operational safety [38].

Cutting mechanisms during machining are a function of fibre orientation. When machining below 0º to the fibre orientation, failure is caused by buckling under axial load or by spalling due to interfacial fracture with a crack running ahead of the cutting edge, depending on tool angle and contact conditions. This mechanism is very favourable to a low tool wear. If milling occurs below 90º to fibre orientation, fibres are subjected to bending and compression loads. Cutting edge must cut individually each fibre, causing increased tool wear.

2.1.4 GRINDING

Grinding of carbon fibre reinforced plastics poses considerable problems such as fibre pull-out, delamination, burrs and burning [39]. Surface roughness is a function of fibre orientation, with better results when they are perpendicular to grinding direction. Greater depths of grinding cause more damage to workpiece. When compared with drilling, grinding causes less burrs and edge effect problems.

Lee and Kim [30] measured the temperature rise and surface roughness of carbon/epoxy composites, under dry and wet grinding conditions, which is not always possible. Grinding directions were parallel and perpendicular to fibre orientation. Temperature rise in dry grinding was more elevated when direction was perpendicular to fibres, reaching 280 ºC, that can certainly cause matrix degradation. To avoid it, a

wet condition is preferable. In wet grinding temperature rise is lower, no more than 60º C. When varying grinding speed and depth, no relevant effect was found in temperature rise. They concluded that wet grinding is preferable to avoid matrix degradation.

Surface roughness measurement results showed higher values when grinding was parallel to fibre direction, in agreement with results from [39].

Grinding is the preferred machining process for ceramic materials, due to their peculiar characteristics. Ceramics possess high hardness, high heat resistance, abrasiveness and fragility. Machining of ceramics puts high demands on the tools. Diamond grinding wheels are the only ones that allow stable and cost-effective machining. Diamond is the hardest known material. The diamond grains, used as abrasive material, are bonded either by metals, polymers or ceramics [40].

2.1.5 DRILLING

Drilling in composites comes from the need to assemble several parts in structures, and it is one of the most common machining operations on composite parts. Drilling is a complex process which is characterized by the existence of extrusion and cut mechanisms, the former performed by drill chisel edge that has null or very small linear speed and the latter by the existence of rotating cutting lips at a certain speed.

The most common drill is the conventional conical point drill. The cutting process is unique and can be divided in two distinct regions: chisel edge and cutting lips. In a common drill, there is a small region around the centre of the chisel edge where the tool does not cut but extrudes the material, called the indentation zone. The region outside the indentation zone, called secondary cutting edges area, the rake angle is highly negative. As fibre reinforced plastics are more brittle than metals, it is unlikely that extrusion really takes place and orthogonal cutting could be assumed for the entire chisel edge. However, model predictions based in this assumption do not agree with experimental data. Along the cutting lips, cutting action of a drill is a three-dimensional oblique cutting process. The cutting speed, rake angles and other varies along the cutting lips with the radial distance from the centre. The cutting action is more efficient at the outer regions of the cutting lips than near drill centre [41, 42].

As composites are non-homogeneous and anisotropic, drilling raises specific problems that can affect parts strength and fatigue life [43, 44, 45]. Typical damages after drilling are push-out delamination, peel-up at entrance, intralaminar cracking, fibre/matrix debonding and thermal damage. Due to their abrasiveness, composites drilling cause high tool wear, leading to the need of frequent tool changes that affect the production cycle. From all these problems, delamination is the most serious as it reduces severely the load carrying capacity of laminated composite structures and must be avoided [27]. Delamination is a defect that occurs in interlaminar regions, that is to say, in the contact plan between adjacent layers, so it depends not only on fibre nature but also on resin type and respective adhesive properties. Delamination mechanisms are divided according to the laminate region where it occur, exit or entrance, respectively called push-out and peel-up.

Peel-up is caused by the cutting force pushing the abraded and cut materials to the flute surface. Initially, the cutting edge of the drill will abrade the laminate. As drill moves forward it tends to pull the abraded material along the flute and the material spirals up before being effectively cut. This action creates a peeling force upwards that tends to separate the upper laminas of the plate (fig. 2.5). This peeling force is a function of tool geometry and friction between tool and workpiece [46].

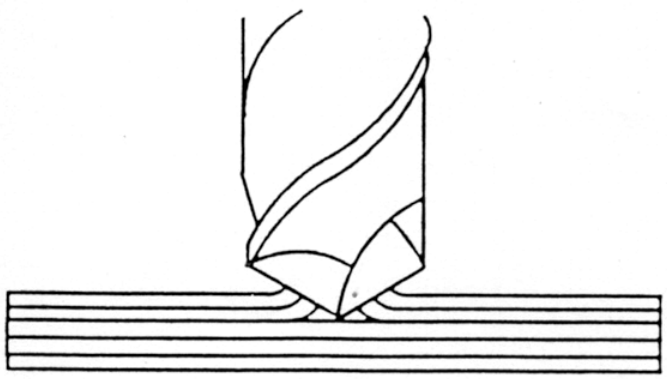

Figure 2.5 – Peel-up delamination at entrance [27].

Push-out is a consequence of the compressive thrust force that the drill always exerts on the workpiece. The laminate under the drill tends to be drawn away from the upper plies, breaking the interlaminar bond in the region around the hole. As the drill approaches the end of the laminate, the uncut thickness becomes smaller and the resistance to deformation decreases. At some point, the loading exceeds the interlaminar bond strength and delamination occurs, before the laminate is totally

penetrated by the drill (fig 2.6). A different tool geometry that lowers thrust force can reduce delamination [46].

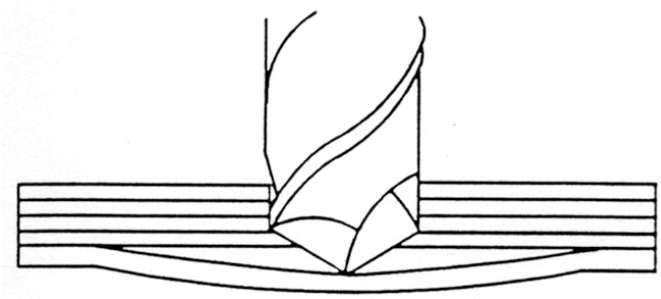

Figure 2.6 – Push-out delamination at exit [27].

Thermal stress that develops during drilling can also facilitate delamination by matrix softening.

Fibre/matrix debonding is observed along the machined hole walls and is characterized by the existence of fibres torn away by the action of drill cutting edges. Intralaminar cracks are also reported in literature as a typical damage mode occurring in a composite plate after drilling [47].

Tool wear is a consequence of composite abrasiveness and low thermal conductivity that causes tool heating superior to what is normally observed in the drilling of metallic materials. In carbon-epoxy drilling 50% of the energy is absorbed by the tool and the remainder is absorbed almost equally by the workpiece and chips. When drilling metals 75% of the thermal energy is eliminated with chips, 18% by the tool and only 7% by the workpiece [27].

After drilling is completed, circularity shall be observed, as there is a bouncing back tendency of the material that cause hole deformation. The return to its initial position causes tightening around the drill, and the drilled diameter is less than the drill diameter. This roundness error is due to the anisotropy of the material [48].

The above mentioned defects are responsible for the rejection of producing parts and contribute to the rise of fabrication costs.

2.1.5.1 DRILLING OF GLASS/EPOXY COMPOSITES

Tagliaferri et al. [49] carried out drilling tests on a glass/epoxy panel obtained from prepreg in a quasi-isotropic stacking sequence, high speed steel (HSS) drills, without backing or cutting fluid. By analyzing the variation of cutting speed and feed, they concluded that, if feed remains constant, damage reduction is accomplished by an increase in cutting speed, and if speed remains constant, lower feeds show better results in terms of damage reduction. They also said that the tensile strength of a GFRP containing a hole is not dependent on damage extent and that bearing strength only correlates with damage extent when this damage is quite large. Finally, they suggested that an optimal ratio between speed and feed seems to exist for maximum bearing strength, adopting lower drilling speeds.

Bongiorno et al. [50] drilled several glass/epoxy plates in different process conditions, generating different kinds and levels of damage, using HSS drills with 5 mm diameter. Plates were subjected to fatigue bearing tests. Results showed that the presence of defects like intralaminar cracks along the hole section deeply affects fatigue behaviour as these cracks propagate quickly into the material, while delamination played a minor role. To avoid these types of cracks a low feed should be adopted. They also verified that the presence of a support plate reduces push-out delamination only, but does not affect internal hole damage.

Khashaba [51] conducted a study to determine the effect of various values of fibre volume fractions (V_f) and drill sizes in notched and point bearing strengths of randomly oriented GFRP composites. Results showed that fibre volume fraction plays a significant role on bearing tests and stress intensity factor. He also concluded that the ratio of width to diameter must be greater than 5 for the development of full bearing strength.

More recently, the same author [52] conducted an experimental investigation about the effect of cutting speed and feed on thrust force, torque and delamination of GFRP composites. He concluded that push-out delamination is more severe than peel-up delamination. Other conclusions were the increase of delamination size with increasing feed and decreasing speed. A change in material matrix or ply orientation can affect delamination as well as thrust forces and torque. Composites with polyester matrix had higher torque and greater delamination than those with epoxy matrix. Using of variable feed and cross-plying led to delamination free holes. An investigation on the factors

that affect the machinability of glass/epoxy composites was conducted by El-Sonbaty et al. [53]. In their conclusions, the authors stated that increasing cutting speed has insignificant effect on thrust force, however torque has decreased. Both thrust force and torque increase with feed raise.

Davim et al. [54] studied the effect of cutting parameters on specific cutting energy, thrust force, damage and surface roughness using analysis of variance (ANOVA) during drilling with carbide tools. They concluded that feed rate is the cutting parameter which has greater influence on the specific cutting energy and thrust force. On the other hand, the cutting speed had higher influence on damage and surface roughness. Surface roughness increase with feed rate and decrease with cutting speed in GFRP.

Velayudham et al. [55] evaluated the drilling characteristics of high volume fraction fibre glass reinforced composite. The results indicate that thrust force and torque increase with increasing feed rate, but also with tool wear.

Lin and Shen [56] studied the effects of increasing cutting speed ranging from 9550 to 38650 rpm, or 210 to 850 m/min, on average thrust force, torque, tool wear and hole quality on glass reinforced composite. For that, they used 7 mm carbide drills with two different geometries, twist and multifaceted drill (fig. 2.7) and three levels of feeds, 0.03, 0.05 and 0.07 mm/rev. It was found that multifaceted drills worn out faster than twist drills as cutting speed increases, but for both geometries tool wear increase as speed increases. Lower feeds reduced tool wear. Thrust force was affected by number of holes drilled, feed rate, cutting speed and drill geometry, due to tool wear. Delamination was less when using multifaceted drills although thrust force was higher than the values measured with twist drills.

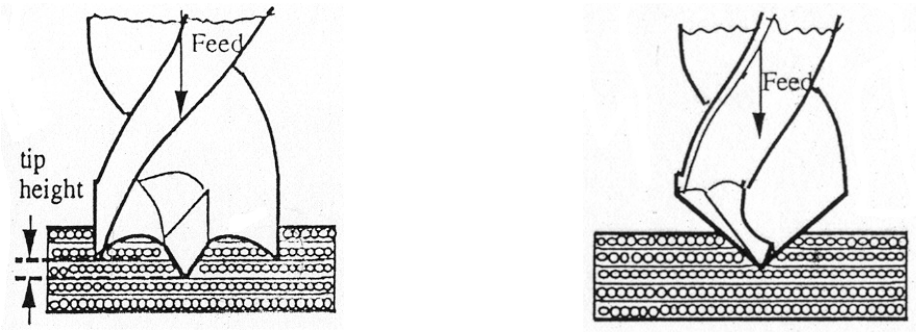

a) b)

Figure 2.7 – Different drill geometries: a) multifaceted drill; b) twist drill [56].

Ramkumar et al. [57] studied the effect of workpiece vibration on drilling of GFRP unidirectional laminates. In their work, the part was subjected to a vibration using a variable frequency generator close to the hole being drilled. Frequency used was 220 Hz and amplitude was 10-15 μm. Drill performance had increased, delamination reduced, and tool life was longer.

Aoyama et al. [58] studied the drilling of glass/epoxy, plain woven cloth, with 1 mm diameter drills, typically used for printed wiring board hole drilling. Cutting speed was 15.7 mm/min and feeds in the range of 5 to 63 μm/rev. An aluminium plate as top stiffener and a bakelite plate as bottom stiffener were used. It was clearly found that damage caused by drilling was larger at a fibre angle of 45º, and that the damage increased when feed increases.

2.1.5.2 DRILLING OF CARBON/EPOXY COMPOSITES

Piquet et al. [48] completed an experimental analysis of drilling damage in thin carbon/epoxy plates using special drills. The plates had quasi-isotropic properties. According to the authors, best drill material is tungsten carbide, based in economic considerations when compared with diamond. Peel-up delamination can be reduced with the use of a small rake angle (6º) preventing the first ply from lifting up and tearing off. A greater number of cutting edges, three to six, increase the contact length between tool and part, facilitating heat removal. Point angle of 118º is necessary for the main cutting edges and then 70º for the minor cutting edges. Chisel edge dimensions have a direct relation with the onset of delamination, so it is necessary to be as reduced as possible. Normally the non-cutting edge represents 20% of the drill diameter. Pre-drilling neutralize the chisel edge effect, having an effect similar to the non-existence of chisel edge. Machining condition can be improved by applying a variable feed rate, combining a low machining time in the initial plies using high feeds with a reduction of axial thrust force, using low feeds, to avoid delamination in the last plies of the laminate. This procedure requires the use of CNC drilling machines.

Hocheng and Puw [47] characterized the response to drilling of reinforced thermoset and thermoplastics. The specimens were epoxy – thermoset – and ABS – thermoplastic - (acrylonitrile butadiene styrene) with continuous carbon fibre reinforcement, and the volume fraction was 60 and 10%, respectively. Tool was a HSS drill of 5 mm diameter, cutting speeds were in the range of 2 to 63 m/min and feed

rates from 0.0125 to 2.4 mm/rev. Chips produced by machining were different according to the matrix material. While for carbon/ABS chips were in continuous or curling form, for carbon/epoxy the chips were discontinuous. In the authors opinion this is explained by the large elongation capability of thermoplastics under loads and by the brittle nature of thermosets causing the chips to break earlier.

For both materials, an increase in feed rate showed an increase in thrust force, although forces involved in carbon/ABS machining were always smaller than those from carbon/epoxy drilling. Specific cutting energy, that gives a good indication of the machining effort, was greater when machining carbon/epoxy, but this could be a consequence of its rich fibre content.

Surface roughness is more dependent on the material than on cutting parameters. Carbon/epoxy drilled holes have higher values of roughness. As surface integrity of parts is concerned, it is important to avoid the use of high speeds together with low feeds, because of heat build-up that can cause matrix degradation. In the particular case of carbon/epoxy, due to its fragile behaviour, machining is more difficult leading to a more accurate feed control and tool wear to avoid or minimize the occurrence of delamination.

Machining parameters are a function of the material to be machined and tool material. As a general rule, feed shall be below 0.1 mm/rev or less, if possible. Nevertheless lower feeds tend to cause a greater amount of heat that must be dissipated. The use of CNC machines, with the possibility of variable feed regulation can improve machining conditions. Cutting speeds can vary between 25 m/min with HSS drills to 150 m/min or more, using PCD drills.

Other studies have been done on carbon/epoxy drilling, trying to obtain delamination free holes, using alternative methods of conventional drilling.

Park et al. [59] applied the helical-feed method to avoid fuzzing and delamination. Tool used for the drilling experiments was a core drill made of cast iron with bonded diamond in two shapes, straight and rounded. The latter showed the best results as no delamination was observed around drilled holes. A tungsten carbide drill was used for results comparison and it was found that drilling quality degraded and fuzzing observed as the number of drilled holes increased due to the wear of cutting edge. The use of helical-feed allows the drilling operation to be completed efficiently without any limitation of drilling depth. Tensile tests performed on specimens drilled in different conditions did not show dependency of drilling methods on test results

Persson et al. [43, 44] studied the effect of hole machining defects on strength and fatigue life of carbon/epoxy composite laminates. For that purpose they have compared two traditional machining methods using a PCD drill, a Dagger drill and the orbital drilling method. This a patented method by NOVATOR®, developed by Zackrisson, Persson and Bäcklund at the Department of Aeronautics of Kungl Tekniska Högskolan (KTH) in Sweden. The hole generation method is shown in figure 2.8. The hole is machined both axially and radially by rotating the cutting tool about its own axis as well as eccentrically about a principal axis while feeding through the laminate.

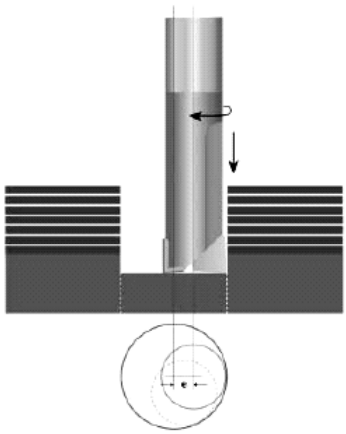

Figure 2.8 – Hole generation using NOVATOR® orbital drilling method. Source: NOVATOR AB.

Some advantages of this method are referred by the authors in [43] when compared to traditional hole machining methods. First is the elimination of a stationary tool centre, thus reducing axial force. Second is the reduction of the risk of tool clogging, as the tool diameter is smaller than hole diameter. For this reason the cutting edges are only partially and intermittently in contact with hole surface, allowing efficient removal of cut material and efficient cooling of tool and hole surface. Third advantage is the possibility of using one tool diameter to machine holes of several diameters and fourth is the precision of the hole that is determined by tool positioning and not by tool precision itself, reducing tool costs.

Quasi-isotropic carbon/epoxy plates were drilled using the three methods and the following conclusions were drawn. Radiographs showed no damage around orbital drilled specimens, damage extended to nearly a quarter of hole radius in Dagger drilled specimens and almost equal to hole radius in PCD drilled specimens. Static testing of pin load specimens gives the highest values for orbital drilled specimens with a

reduction of 2 to 3% for Dagger specimens and about 11% for PCD specimens. Fatigue testing results yielded 8 to 10% lower strengths for PCD and Dagger than orbital drilled specimens. Dagger drill, although giving fair results, has some disadvantages, in the authors' opinion. Due to its long and sharp tip it is less suitable in situations with limited space on the exit side of the laminate. Other disadvantages are related with the inability to remove chips and the relatively short tool life, around 70 holes.

Another work concerning influence of drilling on fatigue behaviour of carbon/epoxy laminates was presented by Hamdoun et al. [45]. Two kinds of specimens were produced, a 'defect-free' and another with defects intentionally introduced during drilling. The two specimens were subjected to the same compression cyclic loading. Specimens with defects showed slightly lower values of fatigue resistance. That can be explained by lower stiffness of the specimens caused by the existence of delaminations around the hole.

Murphy et al. [60] compared the performance of three different types of tungsten carbide drills, TiN (titanium nitride) and DLC (diamond like carbon) coated and an uncoated drill. Testing involved a series of consecutive holes. During these tests the thrust forces and torques were monitored, toll wear was inspected and workpiece also inspected for hole tolerance, delamination and spalling. They have verified that tool wear caused thrust force and torque to increase and unacceptable damage to the composite was found, even though the wear is small when compared with that associated to drilling conventional materials. When holes were measured it was found that only a small number of holes satisfied an H8 tolerance criterion. Finally, the use of coatings was found to be of no benefit when machining carbon-epoxy laminates, reducing neither tool wear nor composite damage.

Dharan and Won [61] conducted a series of machining experiments in order to propose an intelligent machining scheme that avoids delamination by peel-up at entrance and by push-out at exit. Study of drilling action has divided this process in three components: extrusion at chisel edge, secondary cutting at chisel edge and primary cutting at cutting lips. For metallic drilling, the portion of the thrust force acting on the chisel edge is about 50 to 60% of total thrust force. On the other hand, torque acting on chisel edge is relatively small.

The authors have divided the drilling cycle in seven steps, described herewith.

1. Approach: the drill approaches the workpiece;

2. Contact: the drill tip makes the contact;
3. Normal drilling: drilling without delamination;
4. Delamination onset: when critical thrust force is exceeded;
5. Drill breakthrough: the drill tip exits the workpiece;
6. Completion: the hole is completed;
7. Withdrawing drill: the drill must be moved backward and withdrawn from the workpiece.

An 'intelligent' system shall be able to perform steps 1 and 7 as quickly as possible and limit feed in steps 2 and 5 to avoid entry and exit delamination. During step 3, feed must be controlled to prevent delamination.

With the same objective of delamination prevention, Stone and Krishnamurthy [1] studied the implementation of a neural network thrust force controller, using Hocheng and Dharan model [46] for critical thrust force calculation. In this study, cutting forces along three axis and torque were measured with Kistler dynamometer, although only the thrust force was of interest. As there are variations of the force signal due to drill rotation, thrust force signal was averaged over one spindle revolution. Controller act to update feed rate every three spindle revolutions for allowing the system to detect the beginning and end of a revolution and carry out necessary neural network computations. The study has shown that the neural network control scheme can minimize delamination of a graphite/epoxy laminate, varying feed in order to control thrust force. For comparison, the authors also drilled some plates with constant feed and concluded that results regarding delamination were not so good.

Hocheng et al. [62] analysed the machinability of carbon reinforced plastics with different matrix material – epoxy, PEEK, ABS –. The experimental observation discusses chip characteristics and the effect of cutting speed and feed on specific cutting energy and axial thrust force. Generally, an increase in feed causes an increase in thrust force and a decrease in specific cutting energy. Cutting speed effects are less visible and for the two lay-ups used in the experiments – $[0/90]_{4s}$ e $[0/\pm45/90]_{2s}$ – it showed no influence on thrust force. Carbide drills are adequate for drilling these laminates and smaller point angles should be used when materials with less interlaminar fracture toughness are drilled, as thrust force is reduced.

In the experimental work described in [62], material with greater interlaminar fracture toughness in Mode I – G_{Ic} – was carbon/PEEK with a value of 1800 J/mm^2 and

edge quality was better when compared with carbon/epoxy edges, whose G_{Ic} value is 800 J/mm^2. They also verified that lay-up of the laminate did not make a difference on hole edge quality. As a conclusion for their work, an optimal operation domain is presented (figure 2.9). Proper parameter choice shall consider the use of conservative feed and speed. An increase in feed can cause delamination and burrs, while increasing speed raises cutting thrust force and torque as well as reduces tool life.

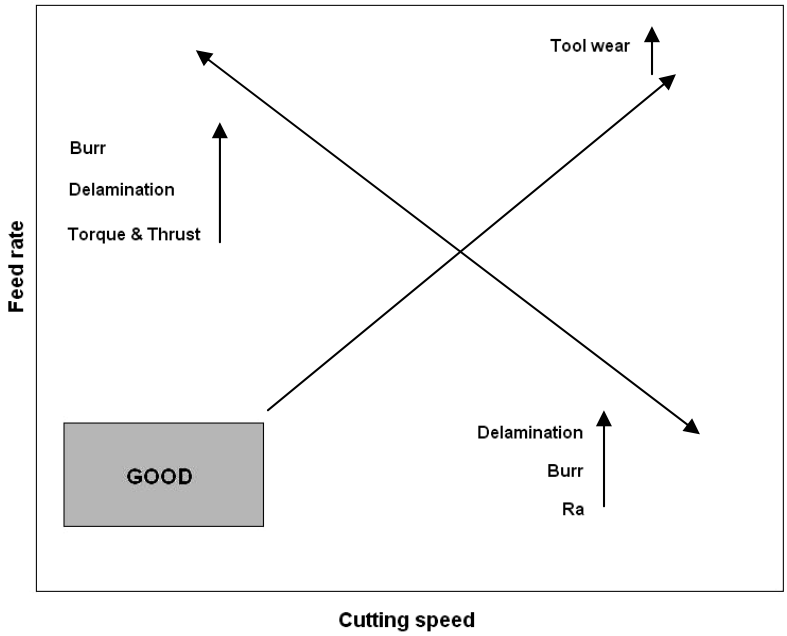

Figure 2.9 – Suggested domain of operation [62].

Won and Dharan [63] conducted drilling tests on aramid and carbon fibre-reinforced composite laminates using carbide drills. During these tests, thrust force and torque were monitored to establish the contribution of chisel edge cutting force to total thrust force at different speeds. A ratio of thrust force acting on the chisel edge to total thrust force was established drilling in one step and with a pre-drilled pilot hole, whose diameter was slightly greater than the chisel edge length of the carbide drill. Results show that independently of hole diameter, chisel edge contribution to total thrust force was between 60 and 85%, increasing at higher feed rates. They also verify that thrust force increases with feed rate.

Using Hocheng-Dharan delamination model for critical thrust force [46], a maximum feed rate of 0.145 mm/rev was found for carbon/epoxy laminates, with a 6.35 mm drill and a spindle speed of 1000 rpm. For aramid/epoxy laminates the feed would be 0.045 mm/rev for the same drill but lower spindle speed. These feed rates for drilling without

delamination were calculated with the following empirical relationships for thrust force, for a given feed rate *f* and a drill diameter *d*,

$$F_t = 40.77(fd)^{0.66} - 0.36d^2 \quad (2.1),$$

for carbon/epoxy laminates, and

$$F_t = 35.84(fd)^{0.50} - 0.09d^2 \quad (2.2),$$

for aramid/epoxy laminates.

Calculations for maximum feed without delamination at exit side are based in Hocheng-Dharan model [46], explained in section 2.4.

In another paper [64], Won and Dharan studied the effect of chisel edge on thrust force and also the effect of pre-drilling the laminate with a pilot hole on carbon fibre reinforced composites. They have observed that the effect of chisel edge on thrust force decreases with increasing drill diameter and increases significantly with increasing feed. They also stated that thrust force acting on chisel edge, being a significant component of total thrust force, may govern the occurrence of delamination. A new empirical relationship for drills with pilot holes was determined using experimental results [64],

$$F_t = 3.50(fd)^{0.66} + 0.11d^2 \quad (2.3).$$

Forces measured for specimens with pilot holes are 20 to 50% lower than those without pilot hole, with an average result of 27% reduction in data published. It is important to note that specimens drilled with pilot holes did not exhibit any delamination over the range of feed tested (0.1 to 0.7 mm/rev). A model for predicting critical thrust force for delamination onset, based on linear elastic fracture mechanics, is presented in [64]. That model can be found in section 2.4. It shows that the critical thrust force decreases slightly for specimens with pilot holes. In their study they have calculated a 9

percent reduction when the chisel edge length is approximately 0.18 of the final hole diameter.

More recently, Tsao and Hocheng [65] took the same model but with the interest in studying the effect of chisel edge length and associated pilot hole on delamination. Two chisel edge lengths of 0.15 and 0.2 of drill diameter were considered. An optimal ratio of chisel edge length to drill diameter was derived, as a function of Poisson's ratio of the laminate (section 2.4). A thrust reduction of 25 to 50% was found when comparing results of holes with and without pilot hole, using 10 mm drills, a spindle speed of 1000 rpm and feeds in the range of 0.008 to 0.012 mm/rev. In the authors' opinion, based on experimental work and models developed, the dimensionless chisel edge length should be around 0.09 to 0.2 of drill diameter. With proper settings of cutting parameters and chisel edge length or pilot hole diameter is possible to produce delamination free holes. Critical thrust force is reduced with pre-drilled hole, while axial drilling thrust is largely reduced by cancelling the chisel edge effect. Small feed rates opens a wider range of pilot hole diameters that can be used.

A two stage drilling shall have a pilot hole diameter equal to the chisel edge length of the final drill in order to reduce potential for delamination damage [64]. A pilot hole to final hole ratio of 0.18 is well inside the optimum interval of the dimensionless chisel edge length and in the range of chisel edge lengths in standard twist drills.

Enemuoh et al. [66] developed an approach for damage-free drilling of carbon fibre reinforced thermosetting resins. This approach is based on a combination of Taguchi's experimental analysis technique and a multi-objective optimization criterion. The first step is used to select an optimum parameter range where the global optimum will reside while the second step will search for the global optimum within the optimum range from step 1. This second step is accomplished by the use of a multi-objective optimization criterion with a nonlinear sequential quadratic programming algorithm. The authors describe an experiment procedure where this technique was applied. Four experimental responses were considered: thrust force, delaminations, damage width and hole surface roughness. Experimental factors were cutting speed, feed rate and tool point angle and the ANOVA was used to determine the relative significance of process factors. After an optimum range is selected, a multi-objective technique is developed. Recommendations from this work are the use of low feeds, in the range of 0.02 to 0.05 mm/rev and speed from 40 to 60 m/min, to minimize delamination and have good hole surface finish.

Linbo et al. [67] presented a new vibration drilling technology using a hybrid variation parameter method, with the purpose of limiting thrust force during drilling. In vibration drilling, a piezoelectric crystal oscillator is fixed in the spindle sleeve. The application of a high voltage across the crystal produces a vibration in axis direction. In addition, the feed motion is provided by means of a servomotor driving a harmonic gearbox, which turns the spindle sleeve. Hybrid variation parameters method is a controlling strategy on vibration drilling that enables, according to numerical simulations and experimental results in carbon/epoxy laminates, the drilling of good quality holes. The applicability of this method can be extended to other laminates.

After laminate holes are drilled, it is important to establish criteria that can easily compare the delamination degree of various processes, even though they can only be applied to composites with the same lay-up regarding orientation and number of plies.

Chen [68] proposed a comparing factor that enables the evaluation and analysis of delamination extent in laminated composites. That ratio was called the *Delamination Factor* F_d and it was defined has the quotient between the maximum delaminated diameter D_{max} and the hole nominal diameter D,

$$F_d = D_{\max} / D \tag{2.4}.$$

In the experimental work presented in [68], the author examined the effects of tool geometry and cutting parameters as well as tool wear on delamination factor. Two types of drills were used: a carbide drill and a HSS drill with 5 mm diameter. Damage zone was evaluated by using X-ray non-destructive inspection. Results showed a near-linear relationship between the delamination factor and average thrust forces for both drill materials. The author also concluded that thrust force increased when drill point angle increases and that helix angle did not have a significant effect on this force. Tool flank wear causes an increase of delamination factor, as thrust force increases with tool wear.

Although feed rate has a strong influence on thrust force, cutting speed did not show a significant effect on that force. Finally, he has noticed the absence of built up edge during carbon/epoxy machining.

Tsao and Hocheng [69] evaluated the delamination factor in the use of three different drills, computing the results with images obtained from ultrasonic C-Scan of

drilled holes. In the experimental work, Taguchi's method and analysis of variance (ANOVA) were used in order to establish the influence of the different factors involved. At the end, it was found that feed rate, as well as drill diameter, have the largest contribution on drilling performance, but the use of an adequate tool can reduce delamination.

Davim et al. [70, 71] presented several experimental studies about the effect of drilling parameters on delamination factor, based on Taguchi's method and ANOVA. The authors concluded that feed rate has the greater influence on specific cutting energy and thrust force, and when feed rate increase also the damage increases. The same effect is verified when cutting speed is higher, but is not so significant.

Mehta et al. [72] have suggested a different ratio with the same purpose, named Damage Ratio (D_{RAT}), defined as the ratio of Hole Peripheral Damage Area (D_{MAR}) to Nominal Drilled Hole Area (A_{AVG}), i.e.,

$$D_{RAT} = D_{MAR} / A_{AVG} \quad (2.5).$$

This hole damage evaluation method is based on the existence of damage images from C-Scan and pixel counting of the digitized damage area, as described in [72], or from digitized radiographs [73]. In the study referred there, the authors assessed hole quality executed with three different types of drill. Statistical analysis showed that drill type was the factor having the greatest influence on hole quality. Other conclusions from this study were that the use of a backup plate only act to reduce the push-out delamination and roughness did not appear to be a reliable parameter on hole quality measurement. Based on the results of Damage Ratio observed, a value of peripheral damage around two should not be exceeded.

2.1.5.3 DRILLING OF ARAMID/EPOXY COMPOSITES

The drilling of aramid reinforced composites is more complicated and frequently causes shredding, giving a bad surface finishing to the hole. Shredded fibres have to be manually removed, increasing operation time and associated costs. In order to obtain good geometric tolerances and no shredding it is necessary that drilling proceed

in such a way that fibres are preloaded by tensile stress and then cut by shearing motion [29]. For a rotating tool, that means that the cutting edge of the drill should be C-shaped to cut from outside to the centre (fig. 2.10).

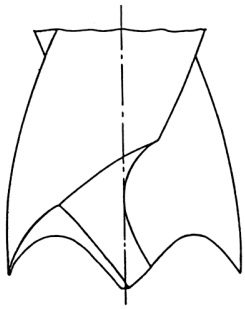

Figure 2.10 – Drill geometry for aramid fibre cutting [74].

Di Ilio et al. [74] reported the results of an experimental research on the drilling of aramid fibre reinforced plastics. For this material, parameters used were a cutting speed of 120 m/min, with feeds in the range of 0.006 to 0.07 mm/rev. The authors have detected large oscillations of the thrust force during drilling, due to the inhomogeneity of the material inside single plies and poor interlaminar strength, causing piercing effects at the interfaces. Another important aspect to be taken in account is the low thermal conductivity of aramid composites, resulting in heat build-up that must be carried away by the tool, accelerating wear processes. Temperature increase at the cutting front has the effect to cause a decrease in thrust force due to the reduction of material strength. Friction forces are high, which is evidenced by torque increase, contributing to the raise of power needed for cutting as well as causing temperature increase.

Further work by the same authors employing a variable feed rate strategy during drilling [75] showed significant improvement in hole quality. The drill used was a C-shape, already referred as most suitable for this material.

2.1.6 CONCLUDING REMARKS

Generally, composites are produced to near-net shape. Machining, when necessary, is considered a finishing process.

New problems arise during the machining of composite materials. Unlike metal machining, where there are a vast number of handbooks, there are few publications addressing composites machining [66]. Experience acquired from metal cutting cannot be directly transplanted to fibre reinforced plastics [76]. According to Caprino et al. [77] much experimental and theoretical work must be carried out before optimization of the machining conditions for composite materials can be accomplished.

A large range of cutting speeds and feeds can be found in different studies as a function of the reinforcement fibre, fibre angle to cutting edge, tool material, showing that there is still a long way to go until quality and reliability are combined with satisfactory tool life. It can be said that, at the present, machining of fibre reinforced plastics still offers a challenge.

2.2 NONTRADITIONAL COMPOSITES MACHINING

Besides conventional machining that was referred in section 2.1, it is necessary to consider the existence of alternative machining processes. There are several reasons that can lead to the use of one of those machining processes, like the poor machinability of composites due to their higher hardness, abrasiveness or lower thermal resistance. It can be also the result from the need to obtain complex shapes, avoid superficial cracks and residual stresses, high accuracy or miniaturization of parts or surfaces. These processes are already known for the machining of other materials like metallic. Some of them are limited in their use due to their high installation cost or low productivity, in terms of produced parts per hour. The alternative processes that are going to be briefly referred are laser, water jet and abrasive water jet, ultrasonic, electron beam and electrochemical machining. The applicability of these processes is related with the material properties, and not all of them are suitable to epoxy, thermosetting material, matrix composites that constitute the subject of this work.

2.2.1 LASER MACHINING

Laser beam techniques have already been used in industrial applications for some time. As it is a non-contact process, it allows the cut of fragile parts and as the force applied is low, clamping devices can be simplified. The basic principle of LASER – Light Amplification of Stimulated Emission of Radiation – is the application of a highly coherent light beam with a single wavelength and highly collimated [9]. High concentration of light in a very small spot produces energy densities up to 10^6 W/mm^2, causing localized material vaporization, with a reduced heat affected zone (HAZ). There are materials, however, that suffer thermal degradation by this localized heating, and therefore laser cannot be used on them.

In industrial composite cutting two types of LASER are available. Nd:YAG laser has a wavelength of 1.06 μm and a pulse length of 200 pulsed per second. It can be used effectively in the cutting of metallic composites without an organic resin. Those materials do not absorb the laser wavelength and can decompose [78]. The other type is CO_2 laser with a wavelength of 10.6 μm and can operate with pulse lengths of the order of 10^{-4} second. It is effectively absorbed by most organic materials [78]. This laser system was used for cutting fibreglass sheets, with a narrow HAZ and melting the

ends of the fibre, preventing fraying. However, a good exhaust system is needed, as particles resulting from vaporization create a health hazard. It is also possible the use of this laser for the cut of Kevlar®-graphite/epoxy and Kevlar®/epoxy composites. Kevlar®, known as a material difficult to cut, has good cutting behaviour by laser, leaving a small edge with burning signs that can be easily removed. Graphite showed poor cutting behaviour because of its high dissociation temperature, around 3600ºC, and thermal conductivity causing degradation at a certain distance from the cutting edge [78].

A final reference goes to the use of laser in ceramic turning. In this case, the light beam, with a diameter equal to cut width, focuses in the area that is going to be cut by the tool, causing an intense and localized heating. Material removal is the result of two effects: laser beam sublimation and softened material removal by the cutting edge of the tool.

2.2.2 WATER JET MACHINING

Water jet is an alternative method of cutting used in a wide variety of composites like reinforced polymers, metallic and non-metallic but also plywood and plastics. The jet cutting nozzle can have a diameter as small as 0.13 mm with a water pressure of 350 MPa [78].

This process can be used effectively to cut narrow slits or drill small holes. Besides other advantages, this process allows the cut to be started in any position, as long as there is care enough to avoid delamination. One possible option is to start the cut in an area that is going to be removed by the operation. Another benefit is that the cut is not affected when water jet beam suffers speed variations. The cut slit is narrow, reducing material consumption, process is easily controlled and automated with the help of an X-Y controller table and part clamping can be simplified as very low forces are imposed to the workpiece. With this method there are no burning of work surface material and no environmental pollution.

Disadvantages in this process are the high noise levels generated by air coupling into a large high-velocity volume of air/water. Because of the noise level, ear protection is needed as well as the use of noise catcher systems. Another concern is that the cutting fluid must be properly filtered and conditioned to reduce wear. The cut of

composite materials can cause layer delamination, if internal pressures are generated [78].

There is a wide variety of materials, besides composites, that can be cut by this method like metallic materials, plastics, cork, rubber, wood and plywood, stone and even frozen food. Among composite materials that can be cut are those with glass, carbon, aramid or boron fibre reinforcement.

2.2.3 ABRASIVE WATER JET

Abrasive water jet – AWJ - is a process very similar to water jet, the main difference being the use of an abrasive material that is introduced into the water jet after the primary jet is formed [79]. In spite of being more complex, due to the need to incorporate an abrasive feeding system, this process is well suited for the cut of abrasive non-homogeneous materials that cause rapid tool wear when conventional cutting tools are used, for materials that can produce hazardous fumes or dusts when cut or for materials that have high hardness or are sensitive to high temperatures. When using abrasive water jet cutting, the jet stream tends to angle away from cutting direction. This ‘trailback’ effect becomes more pronounced when workpiece thickness increases or if nozzle feed rate is increased. During water jet cutting, the kerf is generally wider at the water jet entrance than at the exit side [79], but this effect varies with feed rate and material.

This method is used for the cutting of metals and metal alloys, glass and metallic matrix composites, ceramic and reinforced plastics with glass, carbon or aramid fibres. When used to trim laminate composite materials, it does not cause delaminations or visible fibres beyond the cutting edges.

Ramulu and Arola [80] studied the micromechanical behaviour of both fibres and matrix of a unidirectional graphite/ epoxy composite under water jet and abrasive water jet cutting conditions. In their study they have concluded that AWJ machining consists of a combination of material removal mechanisms including shearing, micromachining and erosion. Machined surface quality is better than those produced by water jet, so AWJ is a more feasible process for the cut of the material studied.

More recently, Hocheng et al. [81] studied the feasibility of AWJ milling of carbon/ epoxy laminate with 64 layers. They have found that the width-to-depth ratio and lateral feed increment are two important parameters for producing acceptable surfaces. Fibre

orientation does not affect the volume removal rate and surface roughness. They have found that abrasive water jet has proved to be a satisfactory machining process.

2.2.4 ULTRASONIC MACHINING

Ultrasonic machining is a process in which abrasives contained in a slurry are driven at high velocity against the work by a vibrating tool. The tool has a low amplitude vibration – 0.05 to 0.125 mm – and high frequency – 20 to 30 kHz – oscillating in a direction perpendicular to the work surface and fed slowly, so that the shape of the tool is formed in the part [9]. The abrasive particles used for this process are aluminium oxide, silicon carbide, boron oxide and similar materials. According to Hocheng et al. [82], this method reduces the concerns with material damage as delaminations, fibre pull-out, micro cracking or burrs are not likely to happen when using ultrasonic machining. Besides, there are no thermal, chemical, electric or metallurgical effects on parts.

This process is suitable for drilling and slitting ceramics and several composites.

2.2.5 ELECTRICAL DISCHARGE MACHINING

The operation of electrical discharge machining – EDM – or spark machining is based on the eroding effect of an electrical spark that is generated between an electrode and the workpiece in the presence of a dielectric fluid. The spark generated produces a localized high temperature which melts and vaporizes the material to form a small crater on the workpiece surface [78]. Crater dimensions depend on machining parameters used. As electrical conductivity is necessary for the process, it is only suitable for materials that possess uniform and continuous electrical conductivity.

EDM is used for machining metal matrix and other composites that exhibit good electrical conductivity. One of the great challenges nowadays is the use of EDM to ceramic machining. Ceramics have poor machinability, due to their toughness, high harness and abrasive characteristics, although the use of this material is widespreading. They also have poor electrical conductivity, making EDM use a problem that may be solved if electrical conductivity is increased.

2.2.6 ELECTRON BEAM MACHINING

Electron beam machining is a thermoelectric process, generally carried out in a vacuum, in which high speed electrons impinge on the workpiece surface, and the heat generated vaporizes the material locally [78]. Vacuum is necessary to eliminate collisions of the electrons with gas molecules. This process is considered to be micromachining, but material removal rates can reach 0.01 mg/s in metals. Extremely closed tolerances can be maintained using this process, with no heat-affected zone on the workpiece.

This process is suitable for machining small holes and cutting or slitting of most composites. On the other hand, it is too expensive and the need for a vacuum chamber increases workpiece processing time.

2.2.7 ELECTROCHEMICAL MACHINING

Electrochemical machining removes material from an electrically conductive workpiece by anodic dissolution. It is the reverse of electroplating. The workpiece is the anode and the tool is the cathode. Material is deplated form the anode (positive pole) and deposited onto the cathode (negative pole) in the presence of an electrolyte bath [9]. The electrolyte is usually sodium chloride mixed with water, sodium nitrate and other fluids that can chemically react with the workpiece.

This process can be used for machining complex cavities and for slitting, drilling and cutting most composites that exhibit continuous and uniform electrical conductivity. One advantage of this process is that it does not cause any thermal damage.

2.2.8 CONCLUDING REMARKS

A wide variety of non-traditional machining methods are available for the machining of composites. These methods are promising as they are becoming cost effective. Although some of these processes are only suitable to some materials, it is important to be aware of the relative performances. Surface finish and tolerances obtainable are different for each process. The rate of material removal and cost per unit material removal rate are important considerations in the selection of the process.

2.3 MACHINING RELATED DAMAGE

Damage in composite materials can be caused by several ways. Composites can be damaged during manufacture, assembly, transport or field deployment, besides expected damages during normal use. As composites can be used in critical applications, damages that remain undetected or that are of difficult detection can turn into a serious problem [83].

One of the possible solutions is to increase the design safety factor, over designing the part, with a penalty in weight and final cost. However, this solution does not prevent damage nor considers its possible extent, which may turn out to be wider than predicted exceeding the safety factor allowance. Unexpected ruptures during service must be avoided. Therefore, the solution most often used is to implement special damage protection methods [83].

There are a variety of defects that can be caused in composite parts during machining. These operations are normally included in the assembly phase, but one should remind that some damage can be caused prior to assembly, i.e. during parts manufacturing.

2.3.1. MANUFACTURING DAMAGES

Composite parts manufacturing is a process in which fibres and resins are combined in a single product, using a certain fabrication technique. Some defects of the parts can be found after part manufacturing, like:

- uncured or not correctly cured resin;
- incorrect fibre fraction, either by excess or lack of resin;
- existence of voids;
- foreign inclusion metallic or non-metallic;
- fibre misalignment;
- ply misalignment;
- delamination;
- fibre defects;
- adhesion defects.

The possibility of occurrence of those defects is normally related with the fabrication process. Prior to be sent to the assembly phase, parts shall be conveniently inspected in order to prevent that unacceptable damaged parts are assembled. Inspection criteria shall be defined and applied either to visual inspection or non-destructive testing and defects classified in allowable, repairable and non-repairable.

In order to enable damage assessment, several types of damage have been defined (table 2.3). These definitions can be useful in field situations, to decide the amount of repair that must be done to correct damage and also to predict possible causes of damage.

Table 2.3 – Damage types and description [83].

Damage Type	Description
Delamination	Separation of adjacent composite plies
Crack	Fractures in matrix and/or fibres
Abrasion	Wearing away of a portion of the surface by either natural, mechanical or man-made means; penetrates only surface finish
Dent	A concave depression that does not rupture plies or debond the composite structure
Gouge	A special type of dent: some, but not all, composite plies are severed
Scratch	An elongated surface discontinuity due to damage that is very small in width compared to length
Impact damage	Damage from contact with foreign object
Cut	Fibres severed by sharp edge

2.3.2. MACHINING DEFECTS

Machining processes, based in the contact between a cutting edge and the part, generate stresses that are transmitted to the part. These stresses that are supported by the part cause deformation and temperature increase, that may be absorbed or not by the composite part. This is the main cause of damage existence, depending the type and amount of damage on the machining process used. In this section only drilling related damage will be referred.

Drilling is a major process used in most of the parts that are assembled in complex structures for aeronautic, aerospace, automotive, railway, wind turbines and other industries. Parts are joined either by rivets and bolts. Some parts are riveted or bolted and bonded. Bonded joints are also used, but in that case drilling is not necessary, hence bonding is not in the scope of this work. Service reliability is sensitive to machined holes quality [48].

The damages that usually can be caused by drilling composite parts are delamination, either superficial or between plies, fibre/matrix debonding, intralaminar cracks, burrs and thermal damage [31, 41, 49, 50, 66, 72, 84]. The extent of these defects is largely dependent on drilling tools and parameters selected. Attention shall be also paid to non-circularity of holes after machining.

As described in table 2.3, delamination is the separation of adjacent composite plies. If this separation occurs between laminate outer plies it is called superficial. If this separation occurs between laminate inner plies, than delamination is internal or interlaminar.

Surface delamination can occur mainly in two different occasions: one is when the tip of the drill touches the part and the other is when the tip of the drill reaches the last plies of the laminate, i.e. approaches the exit side of the part. In the moment when the drill tip starts to get in contact with the material, there is a peel-up effect of the first ply along the drill main cutting edge. This kind of defect is associated with the material, the tool and the cutting conditions or developed cutting forces. This defect has the tendency to increase when the rake angle (γ) is greater and tends towards ply detachment. The chip formed tends to turn backwards with the action of the drill flank. The resulting load pushes onto the hole edge via the fibres which connect to the chip to the rest of the ply. The only force which can resist delamination is the bonding strength applied by the matrix. If the localised peel force is greater than that resistance, delamination occurs [48] – fig. 2.11.

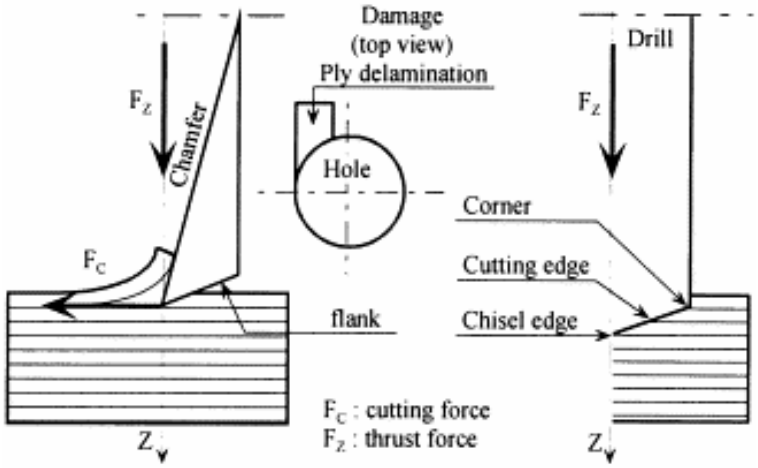

Figure 2.11 – Hole inlet defect – surface delamination [48].

Delamination at the exit side of the part is an expected consequence of the drilling itself, mainly when twist drills are used without a backing plate. The relatively large non-cutting chisel edge is its main drawback, as it has the effect of an extrusion instead of a drilling action. When the active part of the drill approaches the last laminate plies, beyond the critical thrust stress greater than the ply cohesion force, cracking forms and then spreads, in a plane perpendicular to the drill axis. Crack propagation frequently starts on a matrix-rich zone and remains on the plane. Adhesion failure in this matrix leads to bending and delamination of the remaining plies [48] – fig. 2.12.

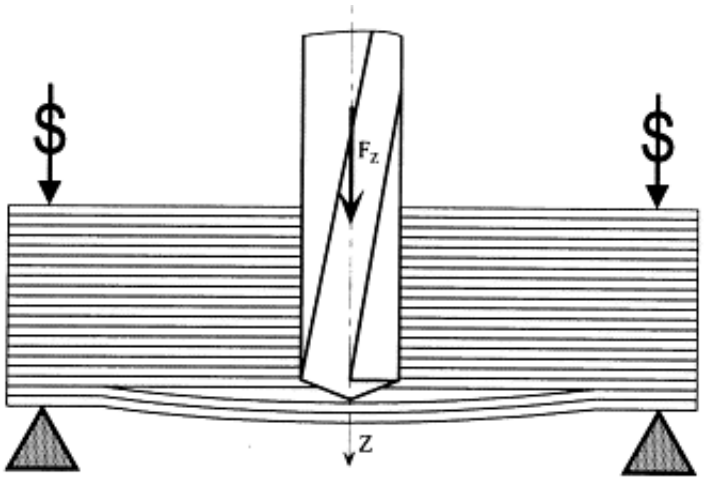

Figure 2.12 – Exit defect in a hole drilled without backing plate [48].

Fibre/matrix pull-out is evidenced by fibres pulled out of the matrix, affecting the final value of machined surfaces superficial roughness. This defect is influenced by tool material, anisotropy and the type of loading, that is to say, according to the relative

orientation between the fibres and the cutting edge. Fibres can be subjected to a compression loading as they are pushed towards the matrix, or to tensile loading or pure shear. Cutting mechanisms are different, affecting the final value of surface roughness [48].

Intralaminar cracking has its onset in the inner plies of the laminate. Normally, at the start, it has an inclination of 60º to the ply plane. The crack extends according to that direction until it reaches an interlaminar plane, turning then into a delamination, in agreement with the definition established [84].

Burrs are little portions of material broken in a corner or edged surface, but still attached to the part. Their existence is related with cutting edge roundness not allowing a clean cut. Their importance is mainly aesthetic.

Thermal damage is a consequence of friction between part and tool cutting edge, causing localised heating, which has more importance in composites cutting as cooling fluids are not recommended for these materials. An abnormally high temperature of the hole can cause local damage to the matrix, like burning or even melting, if the temperature reaches or exceeds the glass transition temperature (T_g). Low feeds increase the possibility of high temperature generation. Sometimes even fibres can be thermally affected. In a research by Caprino and Tagliaferi [84], with the aim to clarify the interactions between damage and cutting parameters, several microscopic observations showed no thermal damage in the matrix, for all feeds used from 0.0057 to 2.63 mm/rev. The authors reported a strong influence of feed in delamination, being low feeds better to reduce this damage.

If carbon reinforced composites are considered, thermal damages become more serious, due to the low thermal conductivity of carbon fibres. As some fibres are bent instead of being cut, they tend to return to the initial position, causing tightening around the drill and increasing friction. This increase in friction is responsible for added heating of the part and temperatures can reach glass transition temperature of the resin and cause matrix damage. In some cases, matrix material can stick to the drill, interrupting the drilling process and damaging the tool as well [48].

Another problem related with composites drilling is the roundness error, due to material anisotropy. During drilling the tool cutting edge orientation to the fibres varies continuously, as well as the fibre cutting mechanism. When a unidirectional laminate is considered, this orientation goes from 0º to 90º, from 90º to 180º, from 180º to 270º and from 270º to 360º, as the drill completes one revolution – fig. 2.13. When the

orientation goes from 0º to 90º, fibres are compressed and from 90º to 180º they are under tension. From 180º to 360º, the stress cycle repeats inversely. When the orientation is equal to 90º, fibres are mostly bent and so their shrinkage by elastic deformation caused by the action of the cutting edge makes the hole narrower and become elliptical. The angle between the large diameter of the ellipse and the fibre axis is 90º. This phenomenon may be supposed identical in the case of a multidirectional ply lay-up, although ellipse main axis may have different orientations depending on material thickness.

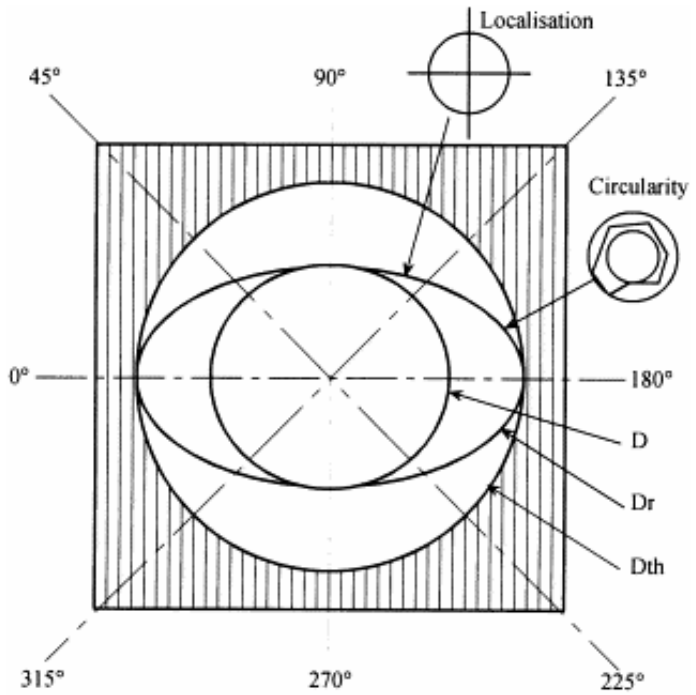

Figure 2.13 – Hole defects observed in a unidirectional plate [48].

2.4 DAMAGE MODELS

Analysis of delamination during drilling in composite materials using a fracture mechanics approach has been developed and different models presented. The models herewith referred are based in the study of carbon/epoxy laminates, although other materials, like glass/epoxy or hybrid composites are also suitable for their application. The main focus on carbon/epoxy laminates can be explained by the fragile nature of carbon fibres, when compared with glass fibres that are less troublesome in machining study.

From the known models, the one that is most referred is the Hocheng and Dharan delamination model [46]. The authors studied the onset of delamination in two different situations: push-out at exit and peel-up at entrance. The first one is the result of the compressive thrust force that the drill exerts on the uncut plies of the laminate, whose thickness is reduced as the drill advances. At some point the loading exceeds the interlaminar bond strength of the material and delamination occurs.

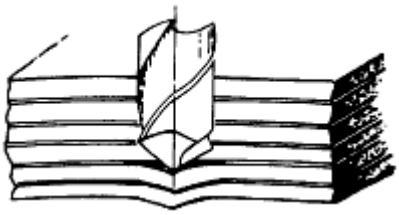

Figure 2.14 – Mechanism of push-out delamination [46].

Delamination mechanisms are assumed to be modelled by linear-elastic fracture mechanics (LEFM), considering the laminate structure of composites, its high modulus of elasticity and the failure in delamination form. According to authors, the applicability of LEFM to composite has been previously discussed and confirmed, provided that crack growth is collinear and the crack is in a plane of material symmetry.

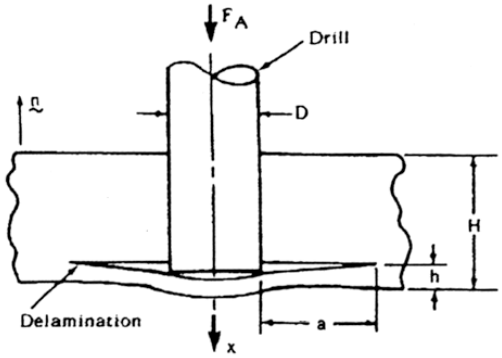

Figure 2.15 – Circular plate model for delamination analysis [46].

As shown in figure 2.15, drill has a diameter *D*, F_A is the applied thrust force, x is the displacement, *H* is the thickness of the structure, h is the uncut depth under the tool and a is the assumed size of an existing crack. The equation of energy balance, from linear elastic fracture mechanics, can be written as

$$G\pi(D+2a)da = F_A dx - dU \quad (2.6),$$

where *G* is the energy release rate per unit area and *U* is the stored strain energy. The correlation linking F_A , x and *U* together uses Timoshenko's classical plate bending theory for a circular plate with clamped ends and concentrated loads. The strain energy is given by

$$U = \frac{8\pi M x^2}{\left(a+\frac{D}{2}\right)^2} \quad (2.7),$$

where

$$M = \frac{Eh^3}{12\left(1-\upsilon^2\right)} \quad (2.8),$$

and the displacement *x* is expressed as

$$x = \frac{F_A\left(a + \frac{D}{2}\right)^2}{16\pi M} \quad (2.9).$$

Substituting (2.7) to (2.9) into (2.6), the critical load at the onset of crack propagation can be calculated

$$F_A^* = F_{crit} = \pi\left[\frac{8G_{Ic}Eh^3}{3(1-\upsilon^2)}\right]^{1/2} \quad (2.10).$$

To avoid delamination the applied thrust force should not exceed this value, which is a function of the material properties and uncut thickness. It can be said that a drill geometry that reduces axial thrust forces is able to reduce delamination during composite laminates drilling.

According to the authors, several simplifications are made in this model, considering the values of E and G_{Ic}, giving the results of the critical load on the conservative side.

The other mechanism of delamination, peel-up, is caused by the cutting force pushing the abraded and cut materials to the flute surface – fig. 2.16. The material spirals up before it is completely machined. A peeling force pointing upwards is introduced that tend to separate the upper laminas of the uncut portion held by the downward acting thrust force. Peel-up effect becomes progressively more difficult as drilling proceeds and resisting thickness becomes greater.

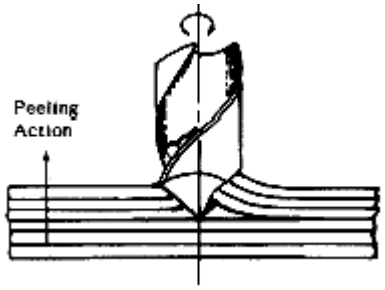

Figure 2.16 – Mechanism of peel-up delamination [46].

The authors assume that a critical peeling force, F_p*, in the axial direction is related to the horizontal critical cutting force F_c* by a *peeling factor*, k_p, defined as

$$k_p = \frac{F_C^*}{F_P^*} \tag{2.11}.$$

The peeling factor is a function of tool geometry and friction between tool and workpiece. The LEFM mechanism used for push-out delamination model is here assumed to be applicable. Substituting F_P for F_A and the uncut thickness by the cut thickness, the critical cutting force at the onset of delamination at entrance is

$$F_{Crit}^* = k_p \pi \left[\frac{8 G_{Ic} E (H-h)^3}{3(1-\upsilon^2)} \right]^{1/2} \tag{2.12}.$$

The results from these models show that the cutting at entrance should be limited in order to reduce peel-up action. They also show that the thrust at exit has to be kept to a small finite value to avoid push-out delamination. Since delamination occurs only between laminas, the minimum value of F_A^*, which occurs at exit, is not zero as it is a function of last ply thickness. This value increase when drilled material has higher E and/or G_{IC} values.

Another model is presented by Lachaud et al. [85, 86], for the drilling of carbon/epoxy composite laminates with twist drills. First of all the authors characterize the four most frequent damages in composites drilling: hole entry defect, circular defect, damage from a heat source and delamination.

Hole entry defect, leading to the tearing of the first ply of the first layer in contact with the drill, does not appear in every occasion. It is related to the fibrous character of the material and to the drill geometry.

Circular defect is linked to the presence of an angle created by the direction of the fibres of the ply concerned and by the direction of the cutting edge. Depending on the angular position of the cutting edges, and just before being cut, the fibres are subjected

to an alternating stress varying between bending and compression. When carbon fibres are used as reinforcement, their unilateral behaviour lead to an elliptical hole shape. The minor axis of the ellipse coincides with the direction of the fibres of the ply under consideration.

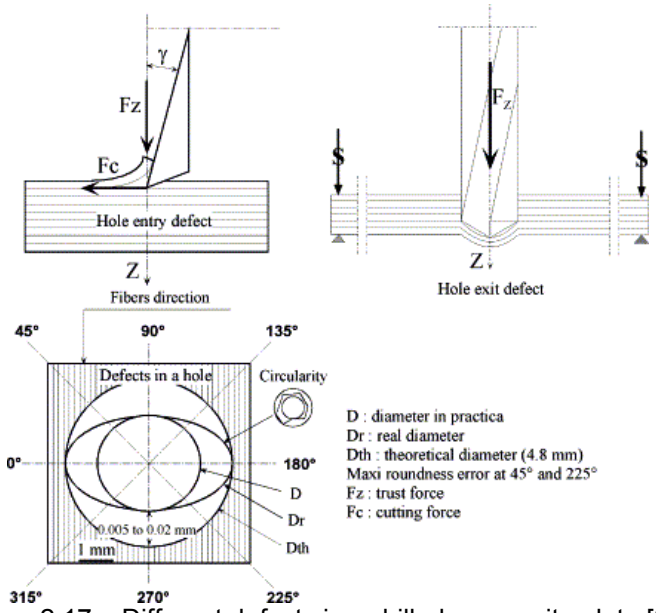

Figure 2.17 – Different defects in a drilled composite plate [85].

Damage from a heat source is due to friction between the fibres and the two minor cutting edges of the drill. It can cause damage to the matrix at the hole edge, thus increasing the likelihood of torn fibres due to the mechanical action of the minor cutting edges. Removal of the fibres leads to a roughness defect on the side wall of the hole.

Delamination at the exit hole is a consequence of the cutting conditions imposed by the fact that the chisel edge of a twist drill cannot cut through the material. The thrust force of the twist drill, function of feed rate, may cause normal stress which is likely to open the ply interface, corresponding to a crack opening in mode I. Delamination between plies spreads beyond the hole diameter and can occur at varying depths as the drill progresses.

In the proposed model, Lachaud considered the existence of a normal stress perpendicular to the ply surface. To obtain the final result, the part of the plate located beneath the drill has been modelled in terms of a thin circular orthotropic plate, with radius a equal to drill radius, and clamped on the laminate surface – fig. 2.18. This

representation does not take into account the global deflection of the plate. It is only valid for a small number of plies under the drill. Two hypotheses are considered:

- distributed load model with resultant F_z;

- point load model with the load F_z concentrated in a point.

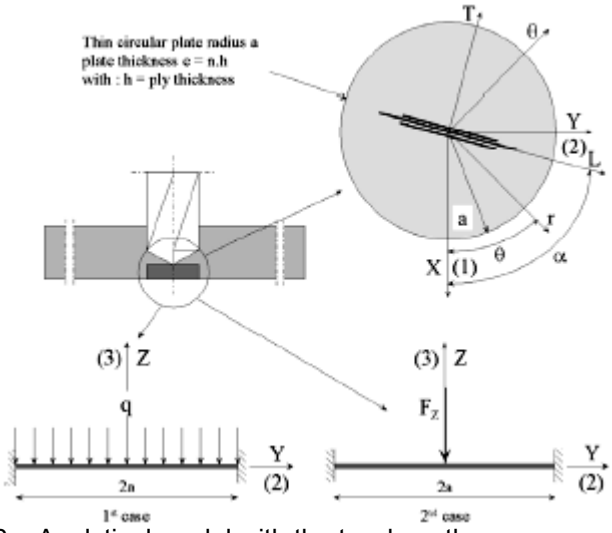

Figure 2.18 – Analytical model with the two hypotheses represented [85].

In the distributed load model, by applying the plate theory, the equilibrium equation of a plate element is

$$\frac{\partial^2 M_{xx}}{\partial x^2} + \frac{\partial^2 M_{yy}}{\partial y^2} + \frac{2\partial^2 M_{xy}}{\partial x \partial y} = -q \qquad (2.13),$$

with M_{xx}, M_{yy} e M_{xy} bending moments and

$$q = \frac{F_z}{\pi a^2} \qquad (2.14).$$

The stress/strain law for the part of the plate in contact with the drill is

$$\begin{Bmatrix} M_{xx} \\ -M_{yy} \\ -M_{xy} \end{Bmatrix} = \begin{vmatrix} D_{11} & D_{12} & D_{16} \\ D_{12} & D_{22} & D_{26} \\ D_{16} & D_{26} & D_{66} \end{vmatrix} \begin{Bmatrix} -\dfrac{\partial^2 w}{\partial x^2} \\ -\dfrac{\partial^2 w}{\partial y^2} \\ -2\dfrac{\partial^2 w}{\partial x \partial y} \end{Bmatrix} \quad (2.15).$$

The D_{ij} coefficient (bending stiffness) has been calculated by using relations of laminates theory. The terms D_{16} and D_{26} are null in the situation considered – orthotropic plate and axis-symmetrical deflection -, and the equilibrium equation (2.13) becomes

$$D_{11}\frac{\partial^4 w}{\partial x^4} + 2(D_{12} + 2D_{66})\frac{\partial^4 w}{\partial x^2 \partial y^2} + D_{22}\frac{\partial^4 w}{\partial y^4} = -q \quad (2.16).$$

The transversal displacement w of the clamped circular plate, radius a, under uniform loading which is a solution of equation (2.16) is given by Timoshenko

$$w(r) = \frac{q(a^2 - r^2)^2}{64D} \quad (2.17),$$

where

$$D = \frac{1}{8}(3D_{11} + 2D_{12} + 4D_{66} + 3D_{22}) \quad (2.18).$$

An energetic approach based on the application of the theorem of virtual work to the equilibrium of the part of the plate affected by the drill, enables the critical drilling load to be determined. The parameter which varies virtually is radius a

$$\delta W = \delta U + \delta U d, \quad (2.19),$$

δW is the work of external forces, δU is the potential energy variation and δUd is the energy absorbed by the spread of cracking.

Delamination energy Ud is derived by multiplying the critical energy release rate in mode I (G_{IC}) by the supposedly circular fracture surface

$$Ud = G_{Ic} S = G_{Ic} \pi a^2 . \quad (2.20).$$

Considering

$$D' = \frac{D_{11} + D_{12}}{2} + \frac{D_{12} + D_{66}}{3} \quad (2.21),$$

the critical value of the thrust force is

$$F_{crit} = 8\pi \left[\frac{2 G_{Ic} D}{(1/3) - (D'/8D)} \right]^{1/2} \quad (2.22).$$

In the point load model - fig. 2.18 – transversal displacement is given by

$$w(r) = \frac{F}{16\pi D} \left[2r^2 \ln \frac{r}{a} + (a^2 - r^2) \right] \quad (2.23),$$

by carrying out the same procedure as for the preceding model, the critical drilling axial thrust force is

$$F_{crit} = 8\pi \left[\frac{2 G_{Ic} D}{1 - (D'/8D)} \right]^{1/2} \quad (2.24).$$

Test plates of carbon/epoxy resin with quasi-isotropic lay-up were drilled using a twist drill made of K20 tungsten carbide. Different drilled depths were chosen and a perpendicular load was applied to the non-drilled part of the plate. The drill was then used as a punch, without rotation. Results from the experiments and the theoretical model were compared. The values of the distributed load model were closest to experimental results.

Zhang et al. [87] considered a different approach. In their model the shape of delamination is elliptical, even when multidirectional composites are drilled, as was revealed by drilling experiments. The ellipse has two principal directions, a and b, whose directions are aligned respectively with ply fibre direction and transverse direction (fig. 2.19).

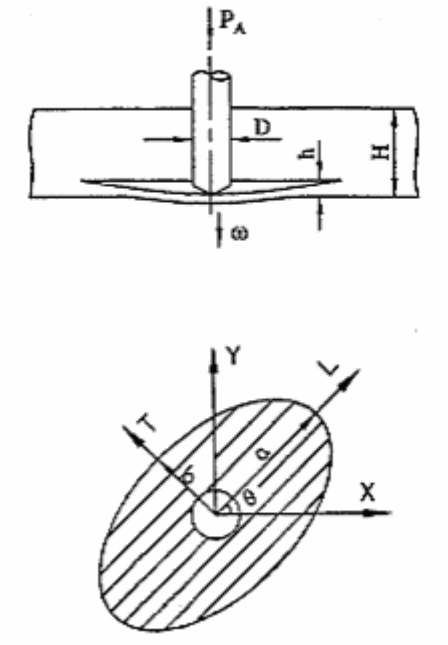

Figure 2.19 - Model and elliptical shape of delamination [87].

In this model, when delamination propagates the ellipticity ratio remains constant, i.e.,

$$a/b = \xi = \text{constant} \qquad (2.25).$$

According to LEFM theory, the energy balance equation can be written as

$$F_{Crit}\, d\omega_0 = G_{IC}\, dA + dU \quad (2.26),$$

where F_{Crit} is the critical thrust force at which delamination begins to occur, $d\omega_0$ is the drill displacement, G_{IC} is the energy release rate per unit area in mode I, dA is the area of the crack and dU is the infinitesimal strain energy.

Drill displacement is given by

$$d\omega_0 = 2F_C C_3 a\, da \quad (2.27),$$

where C_3 comes from mechanical characteristics of the laminate.

The expression of the infinitesimal strain energy is

$$dU = 2KaF_C^2\, da \quad (2.28),$$

where K comes again from mechanical characteristics of the laminate.

Substituting equations (2.28) and (2.27) into (2.26), the expression of critical thrust forces results:

$$F_{Crit} = \sqrt{\frac{\pi G_{IC}}{\xi\left(C_3 - K\right)}} \quad (2.29).$$

For unidirectional composite laminates, this equation can be simplified to

$$F_{Crit} = \frac{3\pi}{\xi}\sqrt{2G_{IC}D^*} \quad (2.30),$$

where D^* is a result of flexure properties of the laminate.

The same paper refers another case, of an unbalanced cross-plied composite laminate, where equations giving critical thrust force can also be obtained.

Tsao and Chen [88] used Hocheng and Dharan model [46] as a starting point and considering a circular shape of delamination, obtained equation (2.10). Then, differentiating this equation with respect to *h* and letting $\partial F_C / \partial h = 0$, the value of *h* corresponding to critical thrust force, $h_{isotropic}$*, can be calculated:

$$h_{isotropic}* = \left(\frac{1-\upsilon^2}{4\pi G_{IC} E} \right)^{1/2} \quad (2.31).$$

Then, the value of $h_{isotropic}$* used for the prediction of delamination may be determined theoretically by the above equation, knowing the values of v, G_{IC} and E.

The authors state that in reality, each layer of composite laminates is highly anisotropic because the bending stiffness transverse and parallel to the fibre direction are different. For this reason, a more realistic shape of delamination should be elliptical. Model development with this assumption gives more elaborated equations to critical thrust force

$$F_{Crit}* = 3\pi^4 \left(\frac{E_{11}}{E_{22}} \right)^{1/2} \left\{ \frac{G_{IC}(h*)^3}{6(1-\upsilon_{12}\upsilon_{21})} E_C^* \right\}^{1/2} \quad (2.32),$$

and the corresponding value of *h*, expressed empirically,

$$h* = 0.0000254 h_{cam} (h_{anisotropic}*) \left(\frac{E_{22}}{E_{11}} \right)^{0.62208} (G_{IC} E_C *) \quad (2.33),$$

where h_{cam} is the ply thickness, E_{11} e E_{22} are the Young's modulus in the directions parallel and transverse to fibre direction, $h_{anisotropic}$* and E_C* are given by

$$h_{anisotropic}* = \left\{ \frac{4(1-\upsilon_{12}\upsilon_{21})}{3G_{IC}\pi} \left(\frac{E_{11}}{E_{22}} \right) \frac{1}{4E_C^*} \right\}^{1/2} \quad (2.34),$$

and

$$E_C^* = 2E_{11} + \frac{2}{3} \left(\frac{E_{11}}{E_{22}} \right)^{1/2} (E_{22}\upsilon_{12} + 2G_{12}(1-\upsilon_{12}\upsilon_{21})) \quad (2.35).$$

Jain and Yang [89] developed a model starting from Hocheng and Dharan [46], where the delamination zone has an elliptical shape, and the critical thrust force for the onset of delamination is given by

$$F_{Crit} = 3\pi \left(\frac{D_{22}}{D_{11}} \sqrt{2G_{IC}D_C^*} \right)^{1/4} \quad (2.36),$$

where

$$D_C^* = 2D_{11} + \frac{2(D_{12} + 2D_{66})}{3} \sqrt{\frac{D_{11}}{D_{22}}} \quad (2.37),$$

where all *D's* are a function of sublaminate flexural rigidity.

Sadat followed the studies by Hocheng and Dharan [46] and Jain and Yang [89] to predict delamination load [90]. In this model the critical value of thrust force for delamination onset is

$$F_{Crit} = 8\pi \left[\frac{G_{IC}D}{(1/3) - (D'/8D)} \right]^{1/2}$$

(2.38),

where

$$D = \frac{1}{8}(3D_{11} + 2D_{12} + 4D_{66} + 3D_{22})$$
$$D' = \frac{D_{11} + D_{12}}{2} + \frac{D_{12} + D_{66}}{3} \quad (2.38),$$

where the D_{ij}'s are also a function of sublaminate flexural rigidity.

Jung et al. [91] proposed a new formulation for the critical thrust force at delamination propagation in multidirectional laminates. Delamination zone was considered as an elliptical shape under a concentrated load with clamped boundary conditions. The load causes bending, twisting, mid-plane extension and shear of the plate. The starting relation is the energy balance equation

$$Pdw_o = GdA + dU \quad (2.39),$$

where G, dU, dA, P and dw_o are the energy release rate per unit area, the infinitesimal strain energy, the increase in the area of the crack, the thrust force and the infinitesimal deflection at the centre of the laminate, respectively.

Deflection is obtained in the form

$$w_o = \frac{Pa^4}{6\pi abD'} \quad (2.40),$$

where a and b are the ellipse axes, and D' is a function of the coefficients of the bending stiffness matrix.

The strain energy U for the elliptical delamination zone is obtained by

$$U = \frac{\pi w_o^2}{a^2}\left(\frac{b}{a}\right)\Delta = \frac{P^2 a^4}{36\pi b^2 (D')^2}\left(\frac{b}{a}\right)\Delta \quad (2.41).$$

Finally, the critical thrust force comes from (2.39), (2.40), (2.41), considering the ellipticity ratio a/b at critical thrust, using G_{Ic} instead of G and considering D'_c as another function of the coefficients of the bending stiffness matrix

$$F_{Crit} = 6\pi D'_c \left(\frac{a}{b}\right)^{0.25} \sqrt{\frac{G_{IC}}{\left(6D'_c - \Delta\right)}} \qquad (2.42).$$

If the twisting and mid-plane extensions are ignored, the results from this model agree with previous studies.

Tsao and Hocheng [92] studied the effect of eccentricity of twist drill and candle stick drill on delamination in drilling composite materials. With that purpose, and taking the energy balance equation (2.6), the authors considered the existence of two loads. One concentrated central load, whose critical thrust force is equation (2.10) and an eccentric concentrated load, whose critical thrust force F_{Crit} is, for a twist drill:

$$F_{Crit} = \pi \sqrt{\frac{32 G_{IC} M}{\left[1 + \frac{11}{4}\xi^2 + 7\xi^4 - 5\xi^2 \ln \xi + \left(1 + \xi^2\right)\xi^2 \ln^2 \xi\right]}} \qquad (2.43),$$

where M is the stiffness per unit width of the fibre reinforced material and $\xi = e/a$, being e the chisel eccentricity of the drill and a the radius of delamination.

For candle stick drill, a similar equation is derived. Results from the model, confirmed by experience, show that the critical thrust force is reduced with increasing eccentric ratio ξ.

Kim and Lee [93] determined the critical thrust force for delamination when drilling FRP/metallic strips. In their model, the drill entry side is the metallic strip, and so the push-out delamination occurs by a mechanism similar to those previously presented. Two methods are presented. The first uses the definition of energy release rate. The equation obtained is

$$F_{crit} = b\sqrt{\frac{2G_{IC}}{\left(\frac{a^2}{8D_{11}} + \frac{1}{2} + \frac{3}{4}\right)}} \quad (2.44),$$

where a and b are respectively the tool radius and laminate width, and D_{11} comes from the bending stiffness matrix.

The second method applies the energy balance equation (2.6) and the final formulation is

$$F_{crit} = \sqrt{\frac{G_{IC}b}{\left(\frac{a^2}{2\pi bD_{11}} - \frac{16a^2}{15\pi^2 b^2 D_{11}^2}\right)}} \quad (2.45).$$

Won and Dharan [64] determined quantitatively the effect of chisel edge and pilot hole in composite laminates drilling. The results showed a large reduction in the thrust force when a pilot hole is present, removing the chisel edge contribution. From the experimental results they have formulated nonlinear relationships between drilling forces and drilling parameters.

For specimens without pilot holes this relationship is

$$F_x = 40.77(fd)^{0.66} - 0.36d^2 \quad (2.46).$$

For specimens with pilot holes it becomes

$$F_x = 3.50(fd)^{0.66} + 0.11d^2 \quad (2.47).$$

A delamination model for predicting the critical thrust force for specimens with predrilled pilot holes is then presented. The starting model is equation (2.10) and LEFM and the final expression is equivalent to (2.48).

They concluded that the potential for delamination can be reduced considerably if drilling in two stages: first with a pilot hole whose diameter is equal to the chisel edge width of the final hole; secondly with the final diameter drill. This strategy divides the total thrust force into two stages.

Tsao and Hocheng [65] also studied the effect of pre-drilling in delamination, showing that the existence of a pre-drilled pilot hole can reduce significantly the occurrence of this damage. A model based in LEFM was presented and the final result equivalent to the model presented in [65], with an exception on the consideration of a new variable – ζ – to represent the ratio between pilot hole and final hole diameter.

In this model, the pilot hole is selected equal to the chisel length of the drill, in order to eliminate the disadvantage of the chisel-induced thrust force and avoid the threat of create large delamination by large pre-drilled hole. Considering $2b$ as the diameter of pilot hole and d the drill diameter, the critical thrust force at the onset of crack propagation with pre-drilled pilot hole is

$$F_{crit} = \frac{4\pi}{1-\upsilon}\left\{\frac{G_{IC}Eh^3\left[(1-\upsilon)+2(1+\upsilon)\zeta^2\right]^2}{3(1+\upsilon)\left[2(1-\upsilon)(1+2\upsilon^2)-(12-4\upsilon+3\upsilon^2+3\upsilon^3)\zeta^2-8(1+3\upsilon)\zeta^2\ln\zeta\right]}\right\}^{1/2} \quad (2.48),$$

where $\zeta = 2b/d$. The differentiation of equation (2.48) with respect to ζ and letting the result equal to zero, gives the value of ζ^* at the minimum of the critical thrust force

$$\zeta^* = \frac{\partial F^*_{crit}}{\partial \zeta} = \zeta^2\left(-16+16\upsilon+26\upsilon^2-12\upsilon^3-6\upsilon^4-16\ln\zeta-64\upsilon\ln\zeta-48\upsilon^2\ln\zeta\right)+\ln\zeta+ \quad (2.49).$$
$$\left(24\left(8+16\upsilon-24\upsilon^2\right)-8\upsilon+3\upsilon^2-19\upsilon^4\right)=0$$

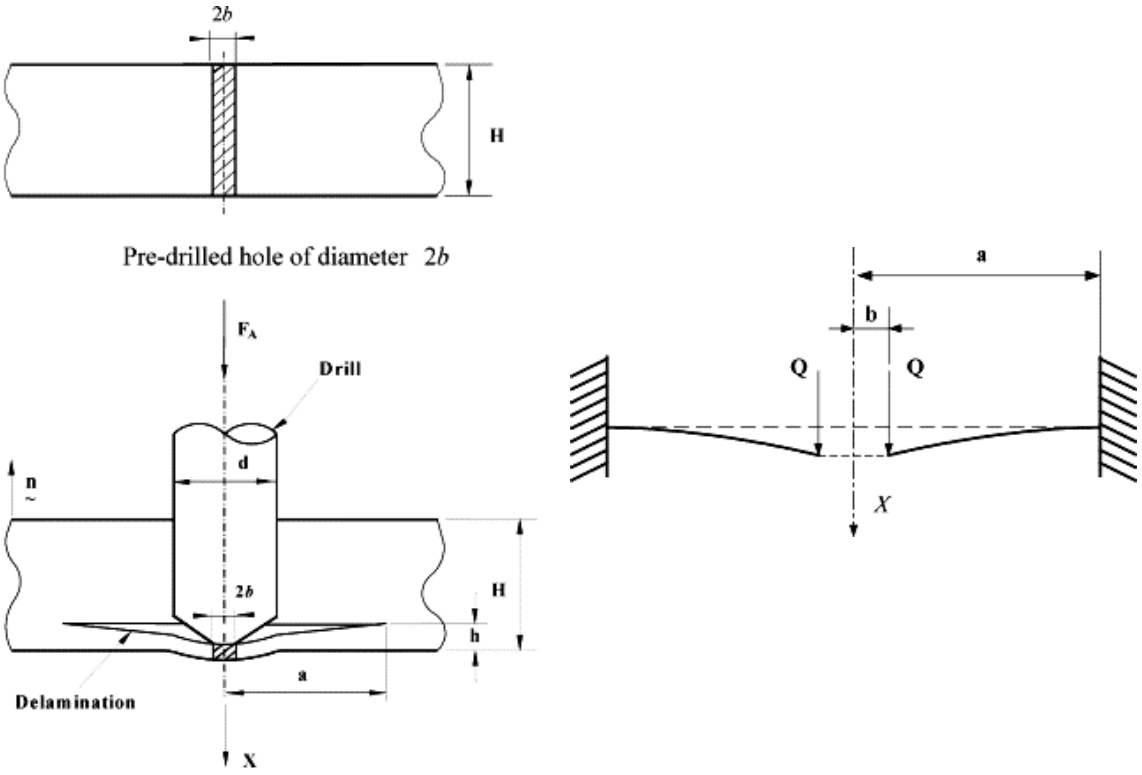

Figure 2.20 – Delamination model for pre-drilled holes [65].

This value is a function of Poisson's ratio v. When v = 0.3, ζ is found equal to 0.1176. The higher the value of v, the larger is the ζ* (fig 2.21).

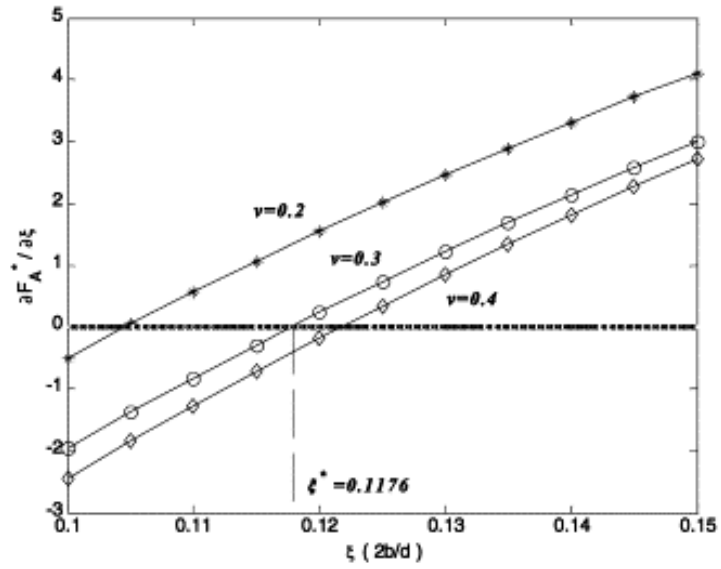

Figure 2.21– Critical ratio of chisel edge length to drill diameter with various Poisson's ratio [65].

2.5 MONITORING AND DAMAGE ANALYSIS TECHNIQUES

As was referred in precedent sections, it is important that data collection is possible during and after drilling of composite laminates. With the help of these data, it is possible to establish comparisons between different tool geometries, cutting parameters or even its effect according to ply orientation. In this section, a brief review of these techniques and their applicability will be presented. In a first approach, we can distinguish two kinds of techniques: those that can be used during drilling and those that can only be applied after drilling is completed. The first type will include forces and torque monitoring, acoustic emission and temperature measurement. The second type incorporates microscopy, radiography, computerized tomography, ultrasonic scanning, optical methods and surface roughness of machined parts.

2.5.1 MONITORING OF THRUST FORCES AND TORQUE

This technique is widely used in a large number of papers cited in precedent sections as well as during the experimental work here presented. Typical assembly consists in the use of a piezoelectric dynamometer clamped to the machine tool plate and to where the part to be machined is clamped. Kistler dynamometers are the most used. Signal from dynamometer is amplified and passed through signal conditioning equipment. The results are delivered to a PC through an A/D converter and data can be stored in a spreadsheet file (fig. 2.22).

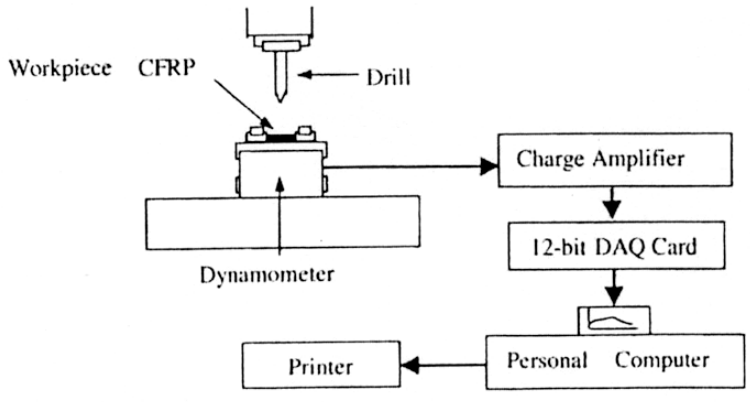

Figure 2.22 – Schematic diagram of the experimental set-up [60].

2.5.2 ACOUSTIC EMISSION

When an irreversible dynamic process occurs in or on the surface of a tensioned material, some of the energy, which is rapidly released, generates elastic stress waves that are equivalent to a vibration within the material. These stress waves propagate through the material and eventually reach the surface, so producing small temporary surface displacements. This phenomenon can be detected at the surface using sensitive transducers that detect and amplify the very small surface displacements. Generally the “noise” does not fall within the audible range as the stress waves are of low amplitude and high frequency, with some known exceptions like the cracking of ice [94]. Acoustic emission is based in the detection of the occurrence of energy generated within the material, so being called as a dynamic method.

In order to detect the acoustic emission at the material surface, the most commonly used transducers are the piezo-electric, which convert the surface displacement into an electric signal. That electrical signal is subsequently amplified, filtered and adequately registered.

The simplest method to obtain an indication of acoustic emission activity is to count the number of amplified pulses which exceed an arbitrary threshold voltage V_t. This is called the ring-down counting. This method, however, does not allow the determination of the operative damage mechanisms that are possible sources of emissions in composites, including fracture of fibres or matrix, fibre-matrix debonding, fibre pull-out, interlaminar defects and other. For such detailed investigations other features of the amplified acoustic signal must be monitored like peak amplitude, measured in dB, and that is characteristic of each failure mode [94].

Acoustic emission has been used during component testing and in service monitoring, as composites are noisy under load, particularly during quasi-static tension testing.

2.5.3 TEMPERATURE MEASUREMENT

According to Abrate [27] heat generated during drilling of composite materials is distributed differently than when drilling metal parts. For a carbon/epoxy laminate, approximately 50% of the energy is absorbed by the tool and the remainder is absorbed almost equally by the workpiece and the chips.

Temperatures generated during composites machining are affected by cutting speed, feed rate and depth of cut. An increase in speed and depth of cut tend to rise higher temperatures as well as lower feeds. Composites abrasiveness, increasing friction between tool and workpiece, is also responsible for thermal stress on the tools. If tool diameter is low, this problem becomes greater, as the heat must be absorbed by the tool and composites have low thermal conductivity. Temperature rise on the workpiece should be limited, in order to avoid thermal damages in the matrix. Generally, matrix materials have a softening temperature around 80ºC.

Sreejith et al. [36] have measured the temperatures at the tool-workpiece interface with a non-contact optical pyrometer. They have concluded that the minimum temperature was observed at a speed where force components are minimal.

Another temperature measurement method, infrared thermography, is used by Burkes et al. [95] to evaluate tool temperature during drilling of metal matrix composites.

Lee et al. [30] measured the temperature rise during cut-off grinding of carbon/epoxy composites. For that purpose they have placed a very thin thermocouple of 0.05 mm diameter at the centre of the middle ply, during pre-preg stacking. Comparing dry and wet grinding, the authors concluded that during dry grinding, material properties may be degraded due to higher temperature rise.

2.5.4 MICROSCOPY

Microscope analysis allows a simple evaluation of the machined edges of the workpiece. This method only needs a microscope with adequate amplification and a scale. It is important that the microscope is equipped with a camera for image registry in order to obtain images that can be compared later. When inspecting translucent materials, the use of a strong light source located on the back can be used [84]. Some examples of microscopy use are found in Davim et al. [70] for damage measurement, in Wang and Zhang [31] for observation of the morphology of the machined surface and in Zhang et al. [87] for delamination micrographs along the hole.

If more specific analysis is needed, scanning electronic microscopy – SEM - can be used. This method requires a set-up of the parts to be analyzed, so it should be considered as a destructive technique, as it is necessary to remove a portion of the material to study. The advantage of this method is the ability to show micro structural

behaviour of composite components (fibre and/or matrix). SEM analyses are found in several papers like [31, 47, 96, 97] in examination of machined surfaces morphology.

2.5.5 RADIOGRAPHY

Radiography is a well recognized and documented method that is applied in industry for assessment of the soundness of materials and components. The technique is based on different absorption of penetrating radiation by the object being inspected. Because of differences in density and variation of thickness of the part or in absorption characteristics caused by variations in composition, different portions of a test piece absorb different amounts of penetrating radiation. Unabsorbed radiation passing through the part can be recorded on a film or photosensitive paper [98].

In conventional radiography, an object is bombarded by a beam of X-rays and the portion of the radiation that is not absorbed by the object impinges on a sheet of film. The unabsorbed radiation exposes the film emulsion in a manner similar to the way that light exposes film in photography. Development of the film produces an image that is a two dimensional “shadow picture” of the object. Variation in the intensity of unabsorbed radiation appears as variations in shades of grey in the developed film [98].

A good deal of information about composite quality can be obtained with radiographic inspection. The linear absorption coefficient of glass is about 20 times that of most resins. Defects related with fibre distribution, quality of weave and presence of laminating defects are revealed by X-rays. The sensitivity of radiography can be improved by impregnating the composite with a radio-opaque material such as zinc iodide [99]. Delaminations are not detected by radiography unless a penetrating fluid is used and the damage is extended to the surface or machined surface of the part. Besides zinc iodide other image-enhancing fluids used are tetrabromoethane, di-iodobutane and di-iodomethane. Since is highly toxic to humans, tetrabromoethane should be avoided [100]. Detection of defects is possible using radio-opaque penetrating fluids, soft X-rays and high contrast techniques. In this case, the method provides an excellent mean for the detection of overlapping delaminations, provided the ingress of penetrating fluid is possible [101].

The use of radiography in composites has some limitations. Small dimension defects or damages with orientation parallel to radiation beam will not be detected.

Defects that are oriented perpendicularly to the beam are more probable to be detected. If parts of great thickness are used, exposure time can result greater than convenient. Human health hazards that come from radiation exposure should not be forgotten.

2.5.6 COMPUTERIZED TOMOGRAPHY

The purpose in the use of this technique is to achieve a three-dimensional image of the part that is subjected to radiographic analysis. To get this image it is necessary that the part is rotated or that the image detector and the X-ray source rotate. For practical reasons the first option has been more used. Radiation beam is narrow and crosses a small slice of material, causing some attenuation, as described in 2.5.5. This attenuation is a function of the density and thickness of the material as well as its composition and beam energy. Data gathered by the exposition of the part to different orientations are combined with the help of a computer algorithm and a cross-section image of the part is accomplished without the need to actually cut it. Initial development of this technique was aimed to medical use – generally known as CT (computerized tomography) or TAC ("tomografia axial computorizada"), in Portuguese. This technique can also be used in composites reinforced with glass or carbon fibres, even with medical equipment with slight modifications, as human body tissues, like bones, have densities near to carbon or glass.

Persson et al. [43, 44] use this technique in the analysis of carbon/epoxy plates with quasi-isotropic lay-up, with a rotation of 0.185º between two consecutive images (fig.2.23).

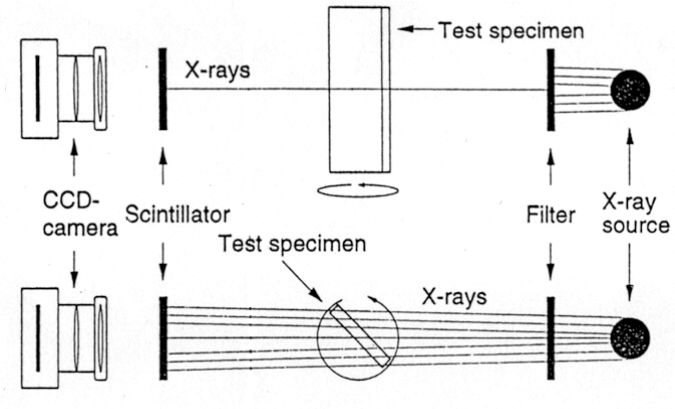

Figure 2.23 – Computerized tomography set-up [44].

Cornelis et al. [102] use the same technique in the characterization of metal matrix composites reinforced with carbon fibres. Metals used as matrix material, light metals like aluminium or magnesium, shall be sufficiently transparent to X-rays of the available energy.

2.5.7 ULTRASONIC SCAN

Ultrasonic techniques are most frequently used for non-destructive inspection of composites. In ultrasonic inspection a sound wave whose frequency is above the upper limit of audibility (20 kHz), most often in the range of 1 to 50 MHz is employed. The sound wave propagates through the material at a certain speed, which is typical of the material and depends on its density and elasticity. Sound waves are modified during their propagation by the boundaries encountered, by the material itself and the presence of defects [103]. Ultrasound inspection technique is based on the analysis of the changes that happen in the sound wave caused by material discontinuities [104].

The presence of a defect will cause a localized change in the acoustic impedance of the material when compared with the surrounding area and it will cause reflection of sound. This reflection can be detected by adequate equipment. Delaminations, because they are orientated at right angles to an ultrasonic wave propagated at normal incidence into a laminate, are ideally aligned for detection by ultrasonic. Because delaminations are good reflectors of ultrasound their presence can be revealed by detecting the sound they reflect or the corresponding loss of transmitted energy [103]. The measurement using the “time-of-flight” parameter can give fair information about defect depth.

In general, ultrasonic energy is both transmitted through the part and reflected from it. The transmitted energy may be detected by a separate transducer located on the far side of the specimen, in which case the procedure is called *through-transmission*. Alternatively, the reflected energy may be detected by the same transducer acting as both transmitter and receiver and in this case the procedure is called *pulse-echo*. In either case the received acoustic energy is converted into electrical energy by the receiving transducer and is amplified and displayed by the test-set [103]. If the part is immersed into a liquid, usually water, the procedure is called *by immersion*. The immersion in water increases the sensibility to defect detection. The selection of the

transducer frequency depends on the material to be inspected and is a compromise between the need for a high detection probability – low frequencies – and the accuracy in locating and dimensioning of the defect – high frequencies – [104].

The A-Scan technique is the simplest method of presenting ultrasonic information. The equipment needed is a transducer to generate sound and to receive and amplify the signals and to display the resulting information on an oscilloscope screen (fig. 2.24).

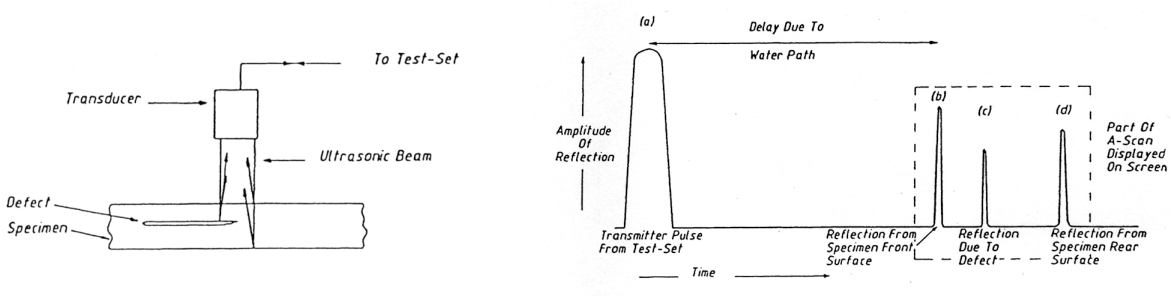

Figure 2.24 – The A-Scan presentation [103].

If the transducer used for recording the A-Scans is moved linearly in a plane parallel to that of the specimen a number of A-Scans can be recorded corresponding to different positions across the specimen. This method is called B-Scan.

The third type of ultrasonic technique that might be employed is the C-Scan. In this type of presentation a more complex scanning system is used such that the transducer is scanned in a plane parallel to the sample [103]. With this technique an image of the part, or of the inspected area, is plotted in a grey scale or colour presentation. The output will be proportional to the parameter that is chosen, like “time-of-flight”. The image will have different grey levels or colours, according to the defect depth. If no defect is detected, an image corresponding to the bottom of the part will be the result, allowing the measurement of part thickness.

Another technique using air-coupled ultrasonic C-scan was applied by Imielinska et al. [101] in impact response testing of composites. The measurements with this technique proved to be adequate to assess impact damage area in carbon/ epoxy composites.

2.5.8 OPTICAL METHODS

The existence of localized damage in a part leads to a distortion in their vibratory mode. Holographic techniques use this principle, causing a certain vibration in the part which in turn causes a planar or out-of-plane displacement. In order to detect these displacements the object shall be illuminated by a beam of coherent light and a CCD camera is used for image recording. Object stimulation, thermal or other, gives a second image, whose changes have a correspondence to variations in object surface [105].

The assembly needed to perform this analysis turns it into very limited applications. This method is more suitable for the detection of superficial damages in the parts. Internal defects, because they are not able to propagate their displacement field to the part surface, are virtually undetectable, even in cases where a simple visual inspection can give a positive indication of their existence.

2.5.9 SURFACE TOPOGRAPHY

Surface generation by material removal processes often change the surface layer properties of the material. The extent of surface layer microgeometric variations caused by a manufacturing process is usually quantified by surface roughness parameters. Surface roughness is influenced by tool geometry, cutting parameters, machine stiffness and chip formation mechanisms. Surface roughness and tolerances are closely interrelated, as it is generally necessary to specify a smooth finish to maintain a fine tolerance in production. Surface characterization parameters provide a basis for assessing the surfaces produced by a machining process. There are numerous parameters to describe surface texture that can be divided in three categories: average roughness heights, statistical methods and random process methods. In [106], Ramulu makes a description of these parameters, as well as their advantages and disadvantages. The most commonly used roughness parameter is the *average surface roughness* - R_a, which is defined as the arithmetic average of the absolute values of the deviations of the surface profile height – z – from the mean line – $\bar{z}$ - within the sampling length, l, [106]:

$$R_a = \frac{1}{l}\int_0^l \left| z - \bar{z} \right| dx \qquad (2.50).$$

Unlike metals, the microgeometry of machined composites surfaces is less regular and is usually rougher as the material is more inhomogeneous [106].

The measurement of surface roughness can be done using contact profilometers. These instruments use a diamond probe to give a profile of the surface to be measured. These are the most common instruments used for roughness measurement. Other methods are optical profilometry that use a laser spot of 1μm diameter, electronical methods that can be useful when evaluating surfaces changes and pneumatic methods with compressed air [107].

Roughness influence in mechanical properties of composites machined parts have been studied by several authors. Ramulu [106] has analyzed the roughness effect on tensile, compressive and flexure resistance, concluding that no significant effect was noted. In another study, Ramulu and Arola [108] studied the effect of surface roughness in the flexure strength of a graphite/epoxy laminate, concluding that surface quality of machined surfaces is process dependent and that flexural strength and modulus were essentially independent of machining method with insignificant variations. Eriksen [109] concluded that it is possible to set up guidelines for cutting parameters like feed rate, cutting speed tool radius and fibre orientation, but these relations will differ from the theoretical ones applicable to metal cutting. Eriksen and Hansen [110] compared profilometry results obtained by stylus instruments and optical profilometers. They have found that the roughness values were dependent on the instrument used. So, only results from equipment with the same setting of variable parameters are comparable. They have also found that the occurrence of local areas of higher roughness, as well as the difference in hardness of matrix and reinforcement material, contributes to large scattering of the results. Finally, they rise some questions about the possibility of direct comparison of the roughness values as in metals and if stylus instruments are reliable on all kind of materials.

CHAPTER 3 – EXPERIMENTAL WORK

3.1 MATERIALS SELECTION

The scope of this research work is the study of drilling conditions for composite materials. The term composite stands for a wide range of different materials and materials systems, so a more accurate definition of the scope is needed. From the numerous composites available, the focus is given to fibre reinforced plastics. This type of materials had seen their use widespread in recent years, as price goes down and reliability goes up. The most used materials are carbon reinforced plastics and glass reinforced plastics.

Carbon fibres are used in high technology sectors like aerospace and nuclear engineering, but also car racing and general engineering and transportation sector including several components like bearings, gears, cams, fan blades, automobile bodies, etc. [111]. There are several examples that can be referred about the crescent use of carbon fibres, the most recent of them is the new Airbus A-380 where the use of composites has reached a total of 16% of the total structure weight, part of it in CFRP, that is used in the wing box, tail section, and other parts of the structure. Composites offer several advantages besides weight reduction, when used in airplanes, like durability, reduced maintenance, parts consolidation and the possibility of self-monitoring using embedded sensors and 'smart' fibres. But that is not the only usage field where carbon fibres arise as a new material. Regional aircrafts are expected to raise their composite extent soon. Sporting goods, from golf cubs to bike frames and sports cars, are already using carbon composites. The next step can be the use of carbon composites in production cars, in order to be able to meet high fuel efficiency and low emissions. The use of CFRP to preserve historic buildings and civil engineering structures like bridges is also a present reality. Last but not the least, the wind energy industry, that normally uses fibre glass as reinforcement material, is turning to carbon as the market demands for bigger and more powerful turbines. The

increase demand for carbon is expected to grow at 7-8% for the next years. Toray Industries Inc., is expanding their production capacity of carbon fibres for about 20% in the next years.

The next figures show some of the applications of carbon fibre reinforced plastics in daily use products.

Figure 3.1 – The Airbus A380 – about 26 tons of carbon composite in each aircraft. Source: Reinforced Plastics.

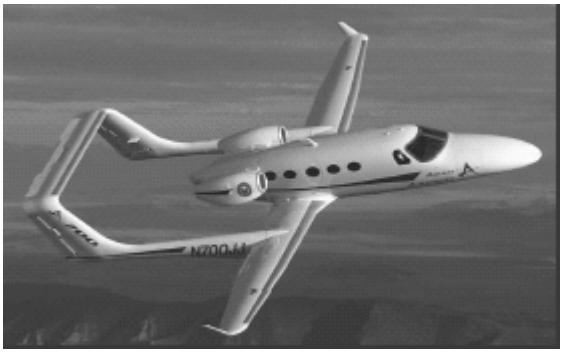

Figure 3.2 – Adam A700 all-composite personal jet. Source: Reinforced Plastics.

Figure 3.3 - Chevrolet Corvette Z06 has a carbon fibre bonnet. Source: Reinforced Plastics.

Figure 3.4 - Composite road bike ridden to victory in Tour de France by Lance Armstrong. Source: Reinforced Plastics.

The use of glass fibre is far more extensive, but less associated to high tech products. Glass fibre has a strength that is less than those of carbon. Besides their use in naval industries, domestic appliances, but also in sports and production cars, the usage of GFRP in wind turbines must be mentioned.

The wind turbine industry has developed from the blades in glass fibre to hybrids – carbon/glass – or carbon as the blades size has become greater. Here, the use of

carbon is selective and with the intention to solve the stiffness problem that becomes more important as the blade size is greater. The use of carbon in blades, whose stiffness is three times greater than glass, allows the use of less material producing slimmer and lighter blades. This is a promising evolution in the design of such turbines.

Figure 3.5 - Carbon fibres will be employed in wind turbine blades over 50m long. Source: Reinforced Plastics.

Hybrids are not likely to be used in aerospace and aeronautical structures, but they can be a fair option considering the balance between final cost against stiffness and reduced weight. Any part where glass fibre is the only reinforcement used and more stiffness and/or lower weight is required is a case that can be analysed for the use of carbon/glass hybrids. Cost will give a contribution to the decision. Imielinska et al. [101] compared the impact response and impact tolerance of carbon with carbon/glass, Kevlar®/carbon and Kevlar®/glass hybrids. They concluded that the introduction of internal layers of glass fibre instead of expensive carbon did not change the impact area for a given energy range. Hybrids can be used to meet diverse and competing design requirements in a most cost-effective way than either conventional or advanced composites [2]. This was the reason why the final choice was made to study, for the present thesis, the drilling of hybrid materials with two types of reinforcement – carbon and glass – fibres in an epoxy matrix. However, and due to the rising use of carbon fibre reinforced plastics, the drilling of carbon/epoxy plates deserved also a particular attention.

The development of the study was divided in three steps. In a first step, fibre reinforced plastics were evaluated and preliminary experiments performed. This first step was done using the materials that were easily available. So, it includes the drilling

of glass fibre in an epoxy matrix and also some plates of Kevlar®. The second step was preceded by the choice of material lay-up and fabrication method. The lay-up was decided to be quasi-isotropic. It also gives the opportunity to evaluate the possible periodic changes during drilling due to different ply orientation. Three types of glass fibre reinforced epoxy fabrication technologies were compared at this step, hand lay-up, prepreg and RTM, as well as carbon reinforced epoxy from prepreg. From the results obtained in this step, it was possible to decide the hybrid system that has been the third and final step on this thesis.

3.1.1 REINFORCEMENT FIBRES

The role of the reinforcement in a composite material is to increase the mechanical properties of the resin system. As the different fibres that can be used have different properties, they also affect the composite properties in different ways. The mechanical properties of a fibre/resin composite are dominated by the contribution of the fibre to the composite. There are four main factors that govern the fibre contribution:

- the mechanical properties of the fibre itself;
- the surface interaction of the fibre and resin;
- the amount of fibre in the composite;
- the orientation of the fibres in the composite.

The following figure (fig. 3.6) shows a comparison of the main fibre types when used in a typical high-performance unidirectional epoxy prepreg. These graphs show the strengths and maximum strains of the different composites at failure. It is interesting to note that some fibres, like aramid, display very different properties when loaded in compression or in tension.

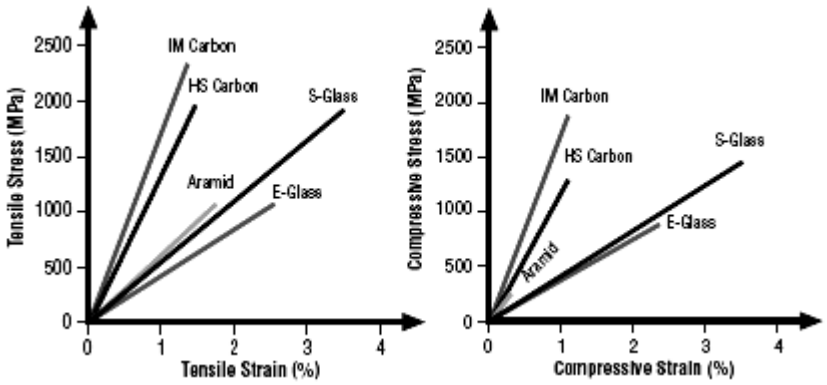

a) b)

Figure 3.6 – Properties of unidirectional prepreg laminate: a) tensile; b) compressive (Source: SP Systems).

Impact damage can pose particular problems when using high stiffness fibres, like carbon, in very thin laminates. When used in impact-critical applications, carbon is often found in combination with other fibres, in the form of a hybrid fabric where another fibre type is used.

The following table show some of the properties of the three types of fibres considered.

Table 3.1 – Characteristics of E-glass, aramid and HS carbon fibres.

Fibre	Advantages	Disadvantages	Remarks
E-glass	Good tensile and compressive strength and stiffness, good electrical properties, low cost	Poor impact resistance	Most commonly used
Aramid	High strength, low density, good resistance to impact	Low compressive strength	Used for ballistic, bullet-proof jackets
Carbon HS	Highest specific stiffness of any fibre, very high strength in tension and compression, high resistance to corrosion, creep and fatigue	Impact strength is lower than either glass or aramid; brittle, low break extension	Price is likely to decrease with increased production

3.1.2 COMPOSITES LAY-UP SEQUENCE

Hole generation is a major activity in the manufacture of structural assemblies, and its purpose is to enable joint fastening. Quality of those holes is critical for the life of the

joints [29]. Independently of the type of fastener used – pins, screws, rivets or bolts - joints will be loaded and stressed. When considering the stresses around a loaded hole, it is expected that a joint in a unidirectional laminate will fail at a very low load, if the load direction is parallel to the fibre orientation, by shear-out. When fibre orientation is perpendicular to the load it is expected that failure will be in tension at the net section. Even though their behaviour is more complex, multi-directional laminates are more practical, and their failure will depend on the proportions of fibres in the various directions. If the plies of a laminate are homogeneously mixed, with fibre direction changing from layer to layer, the stacking sequence has little effect on the bearing strength of bolted joints. As shown in figure 3.7, a near quasi-isotropic lay-up will give the best performance for a tightened bolt [60]. As a general rule, there should never be less than 1/8 nor more than 3/8 of the fibres in any one of the basic directions 0º, +45º, -45º and 90º. If highly orthotropic lay-ups are preferred, for instance, to satisfy a stiffness requirement, a reinforcement of the joints will be needed to achieve the required load transfer, causing the part to be extremely heavy and difficult to repair. Grouping of plies of the same orientation, known as ‘blocking’ can significantly reduce the bearing strength of a bolted joint when compared with the ‘homogeneous’ ply distribution [60].

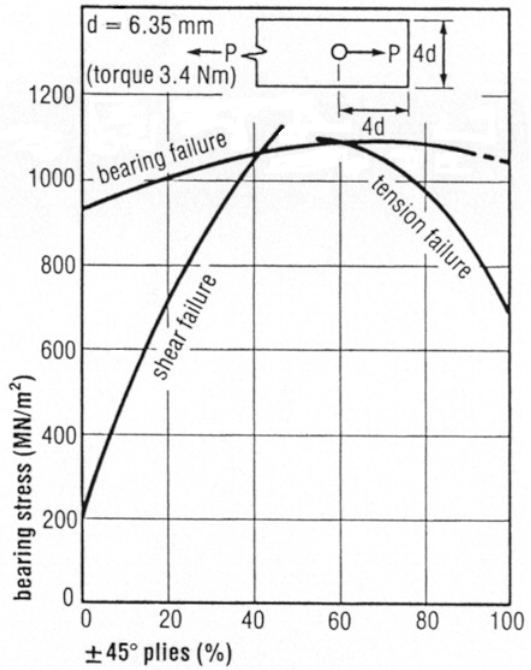

Figure 3.7 – Influence of fibre orientation on failure mode of bolted joints in 0/±45º CFRP [60].

A general rule to describe a quasi-isotropic laminate state that the angles between plies are equal to π/N, where N is an integer greater than or equal to 3, and the number of plies at each orientation is identical, in a symmetric laminate [6]. Because of the infinite variability of the angular orientation of the individual lamina, presumably a laminate can be constructed having a stiffness which behaves isotropically in the plane of the laminate by using a large number of plies having small, equal differences in their orientation.

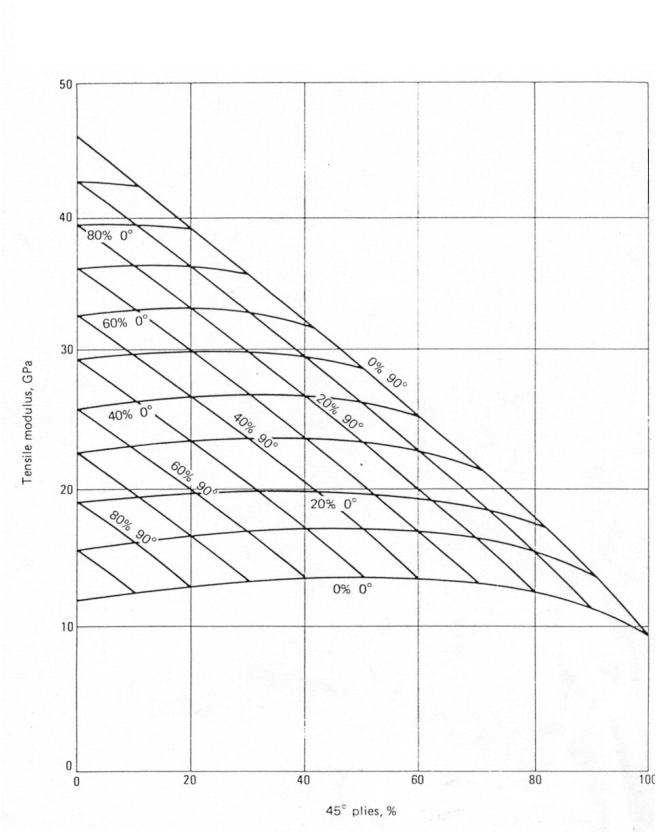

Figure 3.8 – Carpet plot example for a laminate [112].

Prediction of laminate properties is dependent on the lay-up sequence used. One option is the use of specific software that can enable some predictions useful for design engineers. If software is not available, and given specific angle orientations as a restriction, laminate data can be represented by carpet plots, which are maps of a laminate property versus the percentage of one of the lamina orientations. These maps consider a restriction to the use of 0º, ±45º and 90º lamina orientations [112]. Their advantage lies on their simple use. Figure 3.8 shows a carpet plot for the tensile modulus of a laminate. First, select the appropriate plot for the design application. Find

the percentage of ± 45º plies and then follow the value vertically until it intercepts the correct percentage of 0º or 90º plies, both at the same point. The ordinate value for the desired property can be read.

3.1.3 GLASS/ EPOXY COMPOSITES

Composites with fibre glass reinforcement in an epoxy matrix were fabricated by three different techniques.

One set was made from prepreg TEXIPREG® ET443 supplied by SEAL. Glass fibre is an E type, article EE190. Some of the cured material properties, available in supplier's data sheet, are shown in table 3.2.

Table 3.2 – Cured material properties of EE190 ET443 glass prepreg – Source SEAL.

Properties	Unit	Typical value	Standard method
Cured ply thickness	mm	0.15	
Tensile strength	MPa	415	ASTM D 3039
Tensile modulus	GPa	25	ASTM D 3039
Poisson ratio	----	0.18	ASTM D 3518
Shear modulus	GPa	35	ASTM D 3518
Flexural strength	MPa	520	ASTM D 790
Flexural modulus	GPa	28	ASTM D 790
ILSS	MPa	59	ASTM D 2344

Lay-up sequence is shown in table 3.3. Then the laminate was cured in a hot plate press with a 3 daN/cm^2 pressure (3 bar) for one hour at 130ºC, and then cooled. Final material thickness was 5.1 mm.

A second set was manufactured by hand lay-up of FIBERTEX® woven symmetrical tissue with a density of 500 g/m^2 with an isoftalic polyester resin 272 THV from Reichhold. Stacking sequence is shown in table 3.3. Laminate was cured at ambient temperature and the final thickness was 4.7 mm.

The third set was a RTM produced part. Reinforcement material was a mat from ROVICORE and the resin used was a low viscosity, AROPOL FS799 from Ashland. In this case fibre was in mat form. Filling pressure was 0.5 daN/cm^2, vacuum was -0.82 daN/cm^2, and plates were injected with a room temperature of 17ºC. Mould filling time

was 4 minutes. After filled, parts were left to cure inside the mould for 24 hours, at room temperature. Final thickness was 5 mm.

Table 3.3 – Glass/epoxy lay-up and thickness.

Material type	Lay-up sequence	Final thickness [mm]
Prepreg	$[(0/-45/90/45)]_{5s}$	5.1
Hand lay-up	$[0/45/0/45]_s$	4.7
RTM	mat, 2 plies	5.0

All materials were tested in order to evaluate some of their properties. The results and standard method used are indicated in table 3.4.

Table 3.4 – Glass/epoxy plates measured properties.

Properties	Unit	Values			Standard method
		Prepreg	Manual	RTM	
Density		1.9	1.7	1.3	
Tensile strength	MPa	394	223	85	EN ISO 527-4
Tensile modulus	GPa	21.8	11.8	5.6	EN ISO 527-4
Poisson ratio		0.53	0.79	0.64	EN ISO 527-4
Fibre weight	%	77	46	25	NP 2216
Glass transition temperature	ºC	116	78	64	ASTM D 4065

3.1.4 CARBON/ EPOXY COMPOSITES

Composites with carbon fibre reinforcement were done exclusively from prepreg material. The prepreg used, supplied by SEAL, was TEXIPREG® HS 160 REM, a high strength unidirectional carbon with REM epoxy resin. Main characteristics, given by the supplier, are shown in table 3.5.

Table 3.5 – Cured material properties of HS160REM carbon prepreg – Source SEAL.

Properties	Unit	Typical value	Standard method
Tensile strength	MPa	1700	ASTM D 3039
Tensile modulus	GPa	150	ASTM D 3039
Breaking strain	%	1.3	ASTM D 3039
Flexural strength	MPa	1400	ASTM D 790 (L/d=16)
Flexural modulus	GPa	130	ASTM D 790 (L/d=16)
ILSS	MPa	60	ASTM D 2344

Lay-up sequence for parts used in drilling tests is shown in table 3.6. Several thicknesses were used along the work. In all cases, the laminate was cured in a hot plate press with a 3 daN/cm^2 pressure (3 bar) for one and a half hour at 140ºC, and then cooled. Measured material properties are shown below.

Table 3.6 – Carbon/ epoxy lay-up and thickness.

Material type	Lay-up sequence	Final thickness [mm]
Prepreg	$[(0/-45/90/45)]_{4s}$	4.1

All materials were tested in order to evaluate some of their properties. The results and standard method used are indicated in table 3.7.

Table 3.7 – Carbon/epoxy measured properties.

Properties	Unit	Value	Standard method
Density		1.53	
Tensile strength	MPa	771	EN ISO 527-4
Tensile modulus	GPa	49.9	EN ISO 527-4
Poisson ratio		0.56	EN ISO 527-4
Fibre weight	%	65	NP 2216
Glass transition temperature	ºC	115	ASTM D 4065

3.1.5 HYBRID COMPOSITES

The term hybrid refers to a fabric that has more than one type of structural fibre in its construction. The initial concept was to optimize properties by using more than one type of fibre. The driving force is economic and the use of a small amount of carbon fibre, which is expensive, in a laminate composed mainly of a cheap fibre such as E-glass, is attractive [5]. Hybrid composites greatly expand the range of properties that can be achieved with advanced composites. Such laminates can have strengths higher than the predictions from the rule of mixtures, showing an apparent synergistic improvement. This effect is known as the hybrid effect.

The rule of mixtures can be put in a simple way, by considering a composite laminate consisting of alternate unidirectional plies of glass and carbon fibres in an epoxy resin. Under tension, parallel to the fibre direction, the stiffness of the laminate may be accurately predicted from the relative proportions of the two types of fibre [5]:

$$E_H = E_1 V_1 + E_2 V_2 \qquad (3.1),$$

where E_H is the modulus of the hybrid laminate and E_1, E_2, V_1 and V_2 are the respective modulus and fractions of each component of the hybrid laminate. Experimental measurements are found to fall very close to this prediction, meaning that there is no hybrid effect for stiffness. Other properties, like tensile strength, are not so simple to predict by this rule.

Although the most common hybrids are those containing two or more types of fibre, other forms of hybridization are also possible including hybrid matrix and metal/composite laminates such as Arall®, an aramid reinforced aluminium, and Glare®, a glass reinforced aluminium, from Azko [5].

When two fibres are combined with one matrix material, the most usual combinations are carbon/aramid, aramid/glass and carbon/glass. The final choice of hybrid went to a carbon/ glass system. In this hybrid, carbon fibre contributes with high tensile and compressive strength and stiffness and reduces density, while glass reduces the cost. Glass is less expensive, but has lower modulus. The other systems referred also have their pros and cons. Carbon/aramid combines the high impact resistance and tensile strength of the aramid with the high compressive and tensile

strength of carbon. The result is a light but expensive material. Aramid/glass hybrid combines the low density, high impact resistance and tensile strength of aramid with good compressive and tensile strength of glass. As glass is a less expensive fibre, the final cost is smaller than the carbon/aramid hybrid.

Finally, it was necessary to define the percentage of carbon plies in the laminate and lay-up sequence. For that purpose, ESACOMP 2.1 software was used to simulate hybrid laminate properties and try to establish a cost effective material with enhanced properties. As the lay-up was supposed to be quasi-isotropic, the number of plies and carbon proportion was limited to 25 and 33%, in order to keep the laminate cost as low as possible. Several properties were considered, like tensile strength, tensile modulus and flexure modulus. The results obtained from ESACOMP for quasi-isotropic lay-up are shown in figure 3.9.

It is easy to verify that flexure modulus is dependent on carbon plies distribution, as this has an influence on the final value. That effect is not verified on the other two properties shown in figure 3.9.

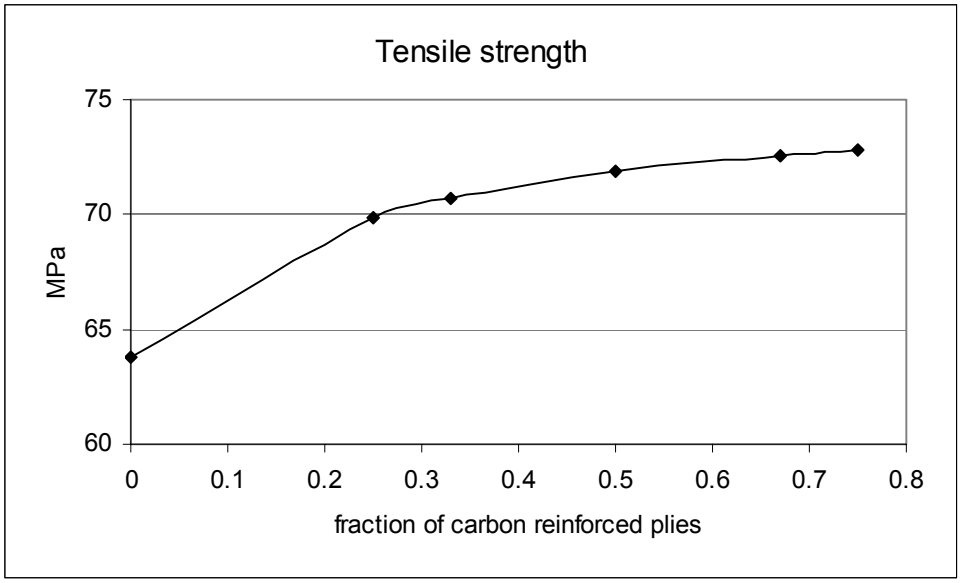

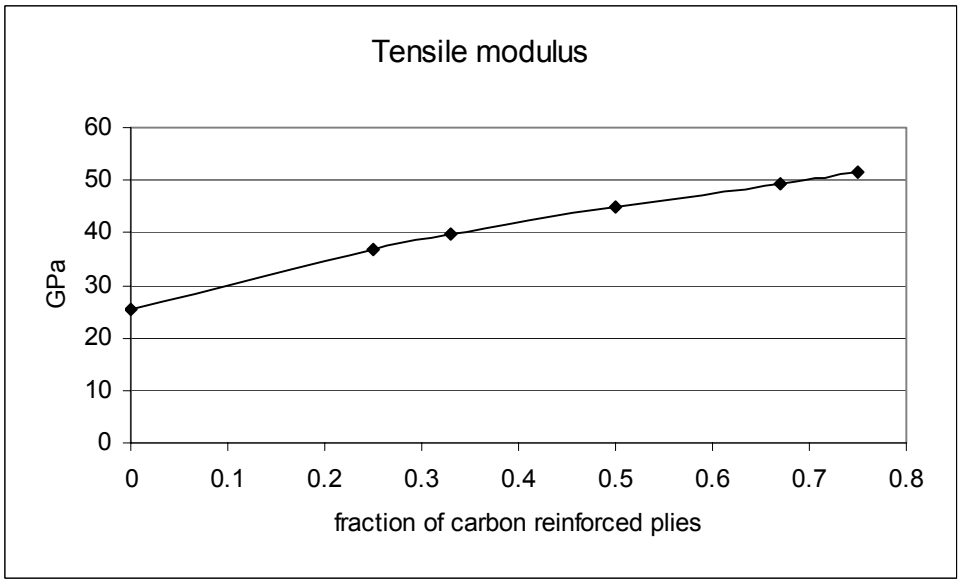

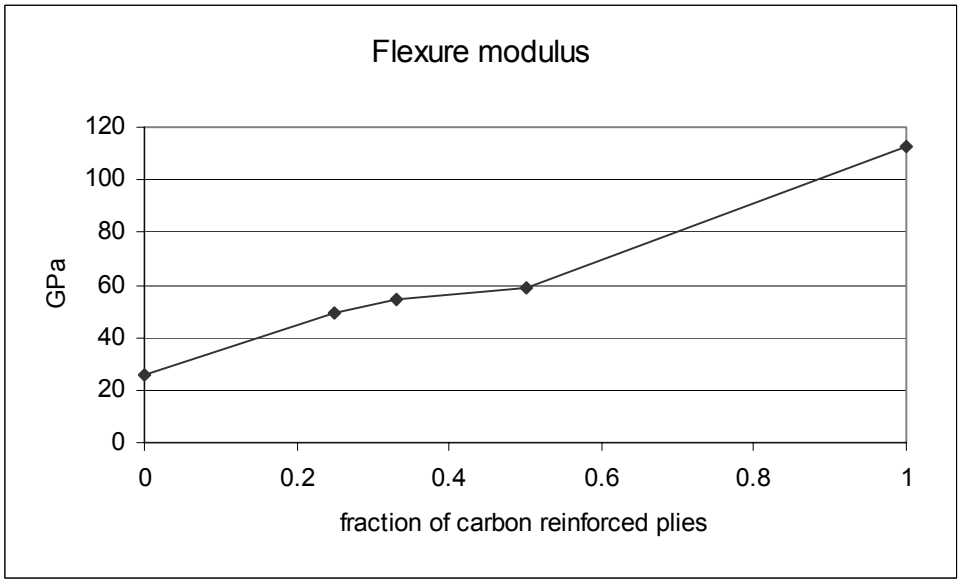

Figure 3.9 – Hybrid carbon+glass/epoxy properties from ESACOMP.

Final decision was to study a laminate with 25% carbon fibre plies, and two different stacking sequences, with carbon plies at the middle (HIBG) and carbon plies in the outer plies (HIBC). Flexure modulus comparison can be seen in figure 3.10 for the four different options available.

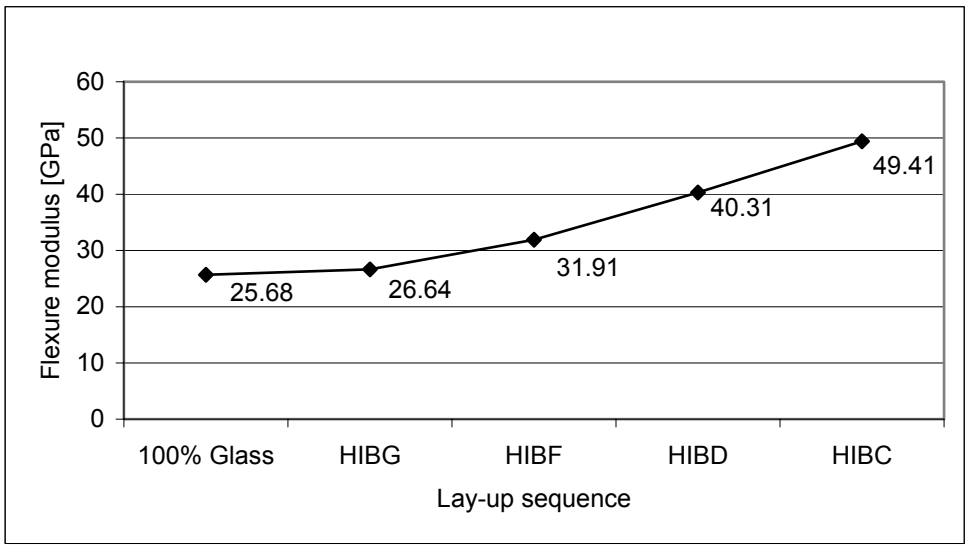

Figure 3.10 – Flexure modulus values for different hybrid lay-ups from ESACOMP.

It is clear that the lay-up with carbon plies at the middle does not represent an advantage in flexure modulus when compared with plain glass at the left of the graph. The upper right value, corresponding to carbon at outer plies, shows an increase of nearly 85% on flexure modulus, with the same amount of carbon but with a different lay-up sequence, so at the same final cost. Therefore, the correct choice of stacking sequence is also important when hybrids are considered, and should be made in accordance with the expected solicitations for the material when in service. The other properties considered, tensile strength and modulus, are not dependent on carbon plies distribution. A percentage of 25% of carbon fibres represents an expected increase of 10% in tensile strength and 45% in tensile modulus, when compared with plain glass/epoxy laminates.

Finally, it must be pointed out that an hybrid with carbon at the outer plies will show the same difficulties associated with peel-up and push-out delamination that are present when studying carbon/epoxy plates drilling, due to the most fragile nature of carbon fibre.

Hybrid composites were done using the prepreg already used and mentioned above, TEXIPREG® ET443 E-glass EE190 and TEXIPREG® HS 160 REM high strength unidirectional carbon both from SEAL. Lay-up sequences are shown in table 3.8. Then the laminate was cured in a hot plate press with a 3 daN/cm^2 pressure (3 bar) for one hour and thirty minutes at 140ºC, and then cooled. Final material thickness was 4 mm.

Table 3.8 – Hybrid carbon+glass/epoxy lay-up and thickness.

Material type	Lay-up sequence	Final thickness [mm]
HIBC	$[(0/-45/90/45)_C/((0/-45/90/45)_G)_3]_s$	4
HIBD	$[(0/-45/90/45)_G/(0/-45/90/45)_C((0/-45/90/45)_G)_2]_s$	not made
HIBF	$[((0/-45/90/45)_G)_2/(0/-45/90/45)_C\ (0/-45/90/45)_G]_s$	not made
HIBG	$[((0/-45/90/45)_G)_3/(0/-45/90/45)_C]_s$	4

All materials were tested in order to evaluate some of their properties. The results and standard method used are indicated in table 3.9.

Table 3.9 – Hybrid carbon+glass/epoxy measured properties.

Properties	Unit	Value	Standard method
Density		1.81	
Tensile strength	MPa	455	EN ISO 527-4
Tensile modulus	GPa	27.8	EN ISO 527-4
Poisson ratio		0.49	EN ISO 527-4
Flexure modulus HIBG	GPa	24.1	EN ISO 14125
Flexure modulus HIBC	GPa	43.2	EN ISO 14125
Fibre weight	%	73	NP 2216
T_g HIBG	ºC	118	ASTM D 4065
T_g HIBC	ºC	138	ASTM D 4065

Although tensile tests were executed to the two options considered for hybrids, results were equivalent. The only exception was the flexure modulus, and the two values are shown. In flexural tests a span of 160 mm was used.

Increments from tensile strength and modulus when compared with plates with glass fibre only were respectively 15% and 28%. The difference in the flexural modulus when considering the carbon placing at the outer plies of the laminate, instead of in the middle plies was remarkable, as expected from simulation results.

3.2 SELECTION OF TOOLS AND DRILLING CONDITIONS

Most composite structures are fabricated to near-net shape. So, machining of fibre reinforced composites is normally limited to finishing processes. Drilling is the most common machining operation as separate parts need to be fastened. Besides drilling, other processing techniques that are normally used are milling, water jet and laser beam. Tool wear caused by the reinforcing fibres is an important factor when costing the machining process. Extensive research has been conducted to determine the proper combination of tool design and operating conditions needed to produce quality holes [27]. The reference to the research work was the aim of chapter 2.

When fastening of parts is considered, fastener selection is also an issue. Although outside the purpose of this work, a reference to necessary considerations about fastener material is here considered useful. Graphite is a very efficient cathode and very noble in the galvanic series. Composites reinforced with carbon fibres are quite cathodic when used with aluminium or cadmium. Steel alloys are not compatible with carbon reinforced plates, as they are normally cadmium plated. Titanium and its alloys appear to be the most compatible fastener material with carbon fibres [113]. Tucker et al. [114] conducted an experimental work coupling a graphite/polymer composite with bare and hard anodized aluminium, titanium, stainless steel and monel. All the samples were immersed in natural seawater. Only titanium did not show any sign of corrosion and no degradation in the composite. The anodized aluminium only suffers corrosion after the removal of the coating, and then a rapid corrosion was observed both in the metal and in the composite. Titanium alloys are the most common materials used for carbon composites fastening. Fortunately, they also have the most desirable strength to weight ratio.

When selecting the type of fastener, rivets and bolts are the most used types. Screws, because they can be easily pulled out of the laminate, offer low efficiency and are not recommended for load-carrying joints. Rivets are suitable for joining laminates up to 3 mm thick. Bolts allow better control of the clamp force, reducing test results scattering [111].

Bonding is an alternative joining technique to fastening. Different joining techniques can be considered, involving joint preparation work, like tapering to reduce the peel stresses. Stepped lap or scarf joints configurations give the strongest bonded joints.

Double-lap and single-lap joints have similar strength provided the latter is restrained against rotation. Generally, ductile adhesives are preferred to brittle adhesives [111].

3.2.1 TOOL DESIGN

The machining process used in fibre reinforced plastics is more related with the fibre used as reinforcement than with the matrix material. Also the machine tool plays an important role to ensure a constant standard of process quality.

The first selection of tool for drilling composites is a conventional tool, generally used for metals machining. Comparison of tool material and fibre hardness can give us some information about suitable materials to cut the fibres (fig. 3.11). Particularly in the case of carbon /epoxy the possibility of shocks has to be considered, so tools should be tough and wear resistant.

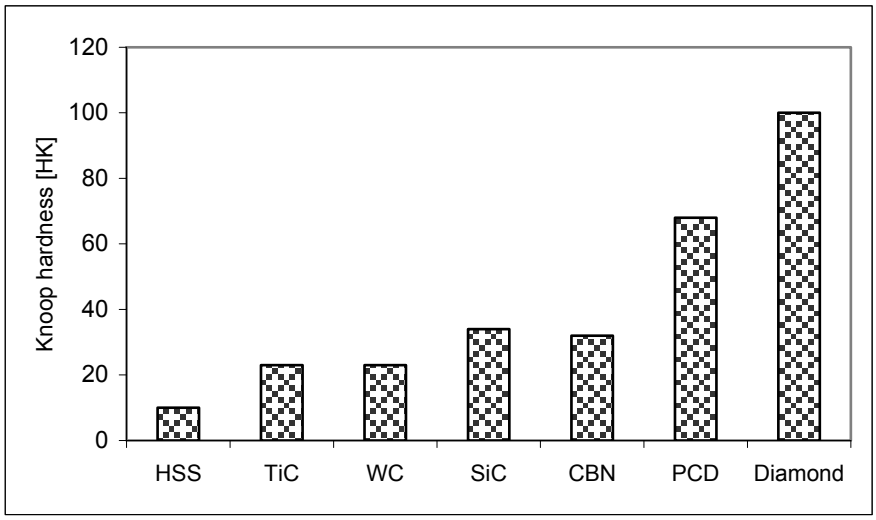

Figure 3.11 – Knoop hardness of some tool materials [33].

Tools made from high-speed steel (HSS) are not appropriate for composites drilling as tool life becomes extremely short. Solid carbide tools tend to be well-suited for this operation. Carbide grade selection depends on the toughness and resistance to wear required. For carbon/epoxy plates the K20 rating is a good choice as the tool must be both tough and wear resistant [48]. The use of coated carbides, unlike in the machining of metals, does not improve tool life because of the need for the cutting edge to be very

sharp when machining composites [33]. Murphy et al. [60] conducted a study on the performance of coated tungsten carbide drills when machining carbon/epoxy composites with a quasi-isotropic stacking sequence. Coatings tested were titanium-nitride (TiN) and diamond like carbon (DLC). In the end, the authors concluded that the use of coatings did not show any benefit when machining carbon-epoxy composites, because of the roundness of the cutting edge.

Diamond, or more usually polycrystalline diamond (PCD) tools are the best choice for fibre reinforced composites machining, in terms of tool wear, resulting in longer tool life and generating surfaces of better characteristics. PCD is superior to all the cutting materials and it has properties close to those of natural diamond, which is the harder material known. On the other hand PCD tools are expensive, although productivity is increased. PCD tools have high thermal conductivity, thus removing the heat from the cutting edge, and have high resistance to shock and vibration, being very effective during interrupted cuts [33].

Other materials that are used for tools are ceramics and cubic boron nitride (CBN). Ceramic cutting tools are not suitable because of their poor thermal conductivity. CBN tools can operate only under narrower bands of hardness and wear resistance [33]. Based on economical considerations, the present study has considered the use of a “micrograin” rate tungsten carbide K20, having good toughness and wear resistance.

Forces that are developed during drilling should be considered. Both thrust and torque depend on the cutting speed and the feed rate. Thrust force F_x during drilling has been found to increase with the diameter d and the feed rate f and can be given by an empirical relation [27]

$$F_x = 0.136 H_B d^m f^n \qquad (3.2),$$

where H_B is the Brinnell hardness of the material, m and n are constants that depend on the material to be drilled, stacking sequence and drill used. The thrust introduced by a twist drill is divided in three parts: primary cutting at the two lips, secondary cutting at the outer parts of the chisel edge and indentation at the centre of the chisel. The third part contributes up to 40-60% of the total force. Experimental data show that thrust force increases linearly with the chisel edge length. Tool wear can increase the machining forces up to ten times over their initial value. However, forces during

composites machining are always lower, about one-third to one-fourth than the forces normally involved in steel drilling [27].

Torque increases rapidly until the cutting edges of the tool are completely engaged. Then, it increases linearly until a maximum and drops after hole completion. The permanent torque at the end is due to the friction between the tool and workpiece [27].

Heat generated during drilling has a typical distribution, for carbon/epoxy, of 50% of the energy absorbed by the tool, 25% by the workpiece and the remainder by the chips. Therefore, a larger fraction of the energy dissipated is absorbed by the workpiece and tool, when comparing with metals machining.

Tool geometry plays an important role in damage prevention. When defining a drill, several parameters can be considered, like point angle, rake angle, clearance angle, lip relief angle, helix angle, web thickness and number of cutting edges. Piquet et al. [48], define some of the characteristics of a specific tungsten carbide K20 tool for composite drilling. A small rake angle of 6º, to prevent peel-up delamination, a greater number of cutting edges to increase tool/part contact, a point angle of 118º and a clearance angle of 6º. The value of the point angle is confirmed by Enemuoh et al. [66]. The helix angle is not so important because the chips are in powder. A small chisel angle improves penetration rate [27]. The use of a pilot-hole can reduce thrust force, thus reducing the risk of push-out delamination [64].

3.2.2 TOOL SELECTION

In order to accomplish the experimental work proposed for this study, it was necessary to select the tools to be used. The planning of destructive tests to be done later had led to the decision about the diameter to drill. As it was found that it will be interesting to carry out bearing tests (ASTM D5961-01) to compare the influence of drilling damage on the strength of the parts, a final diameter of 6 mm was decided. On the other hand, this diameter is within the range of the holes normally executed in composite plates. Tools of this diameter are too small to use inserts and robust enough to be able to withstand the necessary efforts without unwanted ruptures.

The drills used along this work are available in the market, from tool suppliers. The selection criteria used was the conformity of the geometry with the characteristics that were referred before and also the advice from the suppliers about the recommended

tool among the several options available. Not all tool suppliers have special drills dedicated to fibre reinforced materials as it was easily confirmed by consulting their catalogues.

As was already referred before, the drill material selected was tungsten carbide K20, but some other options were experimented. Carbide K20 drills used have a grain size inferior to 0.7 μm and are especially adequate to the machining of abrasive materials like fibre reinforced composites. Besides carbide drills, two other materials were used. One was high speed steel (HSS) drills, because of their availability and common use in every workshop, so representing a situation that is likely to happen when a very small number of drills or a time shortage situation is present. HSS drills represent the standard tool situation that is most usually found due to its very low cost. Another tool material was a TiAlN coated carbide drill, which has all the advantages of TiN, TiAlN and TiCN coatings with high thermal resistance and high toughness. Also, it was interesting to compare with uncoated drills, with the same geometry and from the same supplier. The main characteristics of the three drill materials are shown in table 3.10.

Table 3.10 – Typical tool material properties.

	HSS	**WC**	**WC with TiAlN**
Hardness (HV30)	700-900	1500-1700	3300
Composition	18%W; 4%Cr	90.5%WC; 8%Co	90.5%WC; 8%Co plus coating
Heat transfer rate (W/mK)	15-48	20-80	20-80

After selecting tool materials and size, the final step was the option for the drill geometries. After an analysis of the geometry options available in the market, the selected geometries were of five different types. The first one was the twist drill (fig. 3.12). It has a normal geometry with a point angle of 118º, and it was tested with three tool materials, HSS, tungsten carbide and coated carbide.

Figure 3.12 – Twist drill.

The second geometry is a drill adapted for the cutting of fibre reinforced plastics. The main characteristic of this drill is the scythe shape of the cutting edges, causing the fibres to be tensioned before being cut. The result is a clean cut and a smooth machined surface. The point of the drill is similar to a “C”, reason for why it will be referred as C-shape drill from this point on (fig. 3.13). This drill is available in tungsten carbide K20.

Figure 3.13 – Scythe shape or C-shape drill.

The third drill geometry was the *Dagger* drill. Advantages and disadvantages of this drill have already been discussed in chapter 2.1. This drill has a very sharp point angle of 30º and, due to its particular geometry, need to have enough space at the exit side of the plate. That can limit its application in field work. This drill is also available in tungsten carbide (fig. 3.14).

Figure 3.14 – *Dagger* drill.

The remaining two geometries that were tested in this work were drills that are not planned to drill fibre reinforced plastics, but they represent the possible solution to a two-step hole drilling of composite parts in one operation only. These drills have two diameters and are normally used to drill a hole with two diameters, one smaller for screw passing and a greater one for screw head lodging. According to standardized screw geometry two kind of bi-diametric drills are available, one with an angle of 90º in the diameter transition zone and another with a 180º diameter transition zone (fig. 3.15 and 3.16). These drills will be referred as StepD90 and StepD180, respectively. Both

drills are in tungsten carbide. For comparison purpose a drill of the StepD90 geometry in HSS was also tested.

Figure 3.15 – StepD90 drill.

Figure 3.16 – StepD180 drill.

As there was evident limitations on the available diameters for the StepD geometry, and it was found interesting to explore the advantages of the step geometry, it has been decided to add a sixth drill geometry, but using two successive drills – pilot hole plus final hole -, although not being a correct representation of a step geometry, represented the available option in order to evaluate the effect of such kind of drills. The tools used for the pilot hole drill were twist drills and three diameters were evaluated, 1.1 mm, 2.3 mm and 3.5 mm. The first pilot hole diameter was a result of the conclusions pointed out in [65] that a ratio between the pilot hole and the final diameter should be around 0.18, to withdraw the effect of the chisel edge of the final hole. The larger diameter was influenced by the step drills available, and tried to establish a reference point for result comparison. The intermediate diameter is located at the middle point of the two others. Another advantage of this method for two step drilling is that it can be tested with all the other drill geometries. In the following table a shrot description of the tools used is shown (table 3.11).

Table 3.11 – Main geometrical characteristics of drills.

Designation	Materials	Point angle	Chisel edge length	Tip height	Tip diameter
Twist drill	HSS, WC, WC+TiAlN	118º	1.08 mm	1.8 mm	----------
C-shape drill	WC	-------	----------	0.5 mm	----------
Dagger drill	WC	30º	0.1 mm	11.2 mm	----------
StepD90	HSS, WC	118º	0.65 mm	1.02 mm	3.2 mm
StepD180	WC	118º	0.65 mm	1.35 mm	3.4 mm
Pilot hole drill	HSS, WC	118º	----------	----------	----------

3.2.3 SELECTION OF DRILLING PARAMETERS

For every drill used, it was necessary to look for a selection of parameters that minimize the thrust force during drilling. This effect has to be balanced with the need to avoid excessive heating during machining operation. As was already referred, excessive heating of the part can cause matrix degradation. For each pair drill type/ composite material, an optimization of drill speed and feed has to be carried out. The first orientation for drilling parameters was based in suppliers' information, but other sources were considered. Several authors have studied the effect of parameters in hole machining. Although these papers were already referred, a short reference is now recalled. Bongiorno et al. [50] said that low feed rates improve behaviour under stress conditions. Chen [68] showed that cutting speed has a minor effect on thrust force and torque while feed rate has a strong influence on these forces. So, feed rate needs to be as low as possible, mainly at the last plies near the exit side of the plate, independently of the material considered. Caprino and Tagliaferri [84] concluded that the type of damage in a composite material during drilling is strongly dependent on the feed rate. Tagliaferri et al. [49] state that the damage extent is strictly dependent on the feed rate adopted during drilling. Higher feeds lead to poorer quality. They also pointed that an optimum feed rate seems to exist, resulting in maximum bearing strength. Mehta et al. [72] recommend a cutting speed of 156 m/min and a feed rate of 0.05 mm/rev in the drilling of PMR-15/Gr laminate with solid carbide dagger drills. Hocheng et al. [62] introduced the idea of an optimal operation domain based on quality and productivity considerations. Choice of conservative feed and speed is found to be adequate considering delamination, burr, surface roughness and tool wear. Davim et al. [70] concluded that the increase of feed rate and cutting speed have the effect to increase delamination, although feed has a greater influence than cutting speed. Won and Dharan [63] conducted drilling tests on aramid and carbon fibre reinforced composite laminates obtained an allowable maximum feed for delamination-free drilling. For a 6.35 mm diameter drill maximum feed is 0.145 mm/rev for carbon/epoxy and 0.045 mm/rev for aramid/epoxy. Enemuoh et al. [66] determined the optimum cutting conditions for a 118º point angle drill. Results were a cutting speed in the range of 45 to 51m/min with a feed rate of 0.022 mm/rev [115]. Davim et al. [54] studied the drilling of glass fibre reinforced laminates manufactured by hand lay-up concluding that thrust force increases with feed rate, which is the cutting parameter that has a stronger influence. He also showed that the damage increases when higher cutting speeds and

feeds are used, and that cutting speed has a greater influence on the damage in this material.

All the drilling experiments were performed in an OKUMA MC-40VA machining centre. Data collection was possible by the installation of a Kistler 4782 dynamometer on the machine table, for force and torque monitoring. The workpiece was clamped to the dynamometer prior to drilling. The dynamometer signal was transmitted to a Kistler 5019B multichannel charge amplifier. This equipment converted the piezoelectric signal from the dynamometer into proportional voltages. Finally, voltage signals were converted to digital domain by an A/D converter card and transmitted to a computer. The computer was equipped with Labview software that carried out the conversion of this signal in storable data. That data was then converted into a Microsoft Excel spreadsheet. The experimental set-up is schematically shown in fig. 3.17.

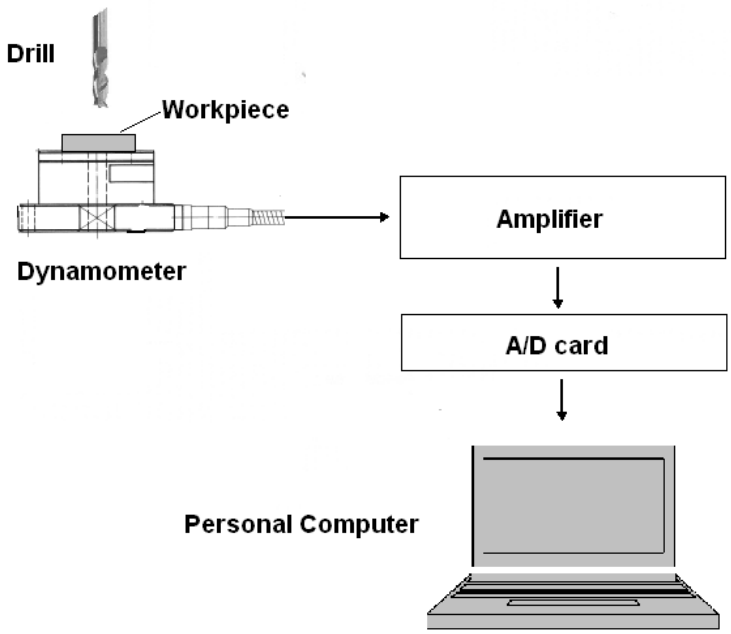

Figure 3.17 – Experimental set-up.

All results in this chapter represent the average result of five tests under the same conditions. As there is a signal variation during one drill rotation due to the mechanics of the process itself, the thrust force was always averaged over one spindle revolution. The results of this average will be referred as thrust force.

In order to be able to analyse the effects of the several parameters used along the multiple tests performed, the use of Taguchi orthogonal arrays was found necessary.

The orthogonal arrays and the respective analysis of variance (ANOVA) can be found in the literature [116, 117, 118]. The orthogonal arrays employed in this study are L4 (2^2), L8 (2^3) and L9 (3^2) as well as condensed L9 for experiments where only one factor has three levels. These tables can be found below. Some more information on the Taguchi method is given in Appendix A.

L4 Standard array

Run	Exper. factor		
	A	B	C
R1	1	1	1
R2	1	2	2
R3	2	1	2
R4	2	2	1

L8 Standard array

Run	Experimental factor						
	A	B	C	D	E	F	G
R1	1	1	1	1	1	1	1
R2	1	1	1	2	2	2	2
R3	1	2	2	1	1	2	2
R4	1	2	2	2	2	1	1
R5	2	1	2	1	2	1	2
R6	2	1	2	2	1	2	1
R7	2	2	1	1	2	2	1
R8	2	2	1	2	1	1	2

L9 Standard array

Run	Experimental factor			
	A	B	C	D
R1	1	1	1	1
R2	1	2	2	2
R3	1	3	3	3
R4	2	1	2	3
R5	2	2	3	1
R6	2	3	1	2
R7	3	1	3	2
R8	3	2	1	3
R9	3	3	2	1

L9 Condensed array

Run	Experimental factor						
	A	B	C	D	E	F	G
R1	1	These columns should not be used when considering condensed array		1	1	1	1
R2	1			2	2	2	2
R3	2			1	1	2	2
R4	2			2	2	1	1
R5	3			1	2	1	2
R6	3			2	1	2	1
R7	optional			1	2	2	1
R8	optional			2	1	1	2

1, 2, 3 - experimental levels for each factor

Figure 3.18 – Orthogonal arrays [118].

All the ANOVA studies were done using the quality characteristic smaller-the-better signal-to-noise (S/N) ratio, considering that the target was to minimize forces and, therefore, delamination around the drilled hole. This strategy was found as adequate for the problem to be studied. In this case, S/N ratio is given by the mathematical expression

$$S/N = -10\log\left(\frac{1}{n}\sum_{i=1}^{n} y_i^2\right) \quad (3.3),$$

where n is the number of replications and y_i are the experiment results. S/N ratio is a characteristic value that represents better the process quality, and, in this case, it was found appropriate because the quality characteristic (thrust force or delamination) for parameter optimization was to minimize. When the value of S/N ratio is maximized, it indicates the best set of parameters, that is to say, the combination that has less error variance. According to [118], the value of S/N ratio that leads to the "optimum project" shall always be used no matter how small is the difference to the second.

3.2.4 DRILLING OF GLASS/EPOXY PLATES

The drilling experiences occurred in parallel for the three materials considered, but here they will be related as separate experimental steps, in order to have a better understanding of the results. The first results related are those from the drilling of glass/epoxy plates. These plates were used in the preliminary tests that lead to the experimental steps described in this and next two sections.

The preliminary tests were done with glass/epoxy plates drilled with HSS drills, and the only purpose was to have a visual evaluation of the drilled hole and surrounding area, as well as some understanding of the parameter influence.

Although their disadvantages in the drilling of composites, already referred before, it was found useful to have a basic understanding of the drilling mechanisms using HSS drills. It also has the purpose to establish a "worst possible case" in terms of forces and damage on the drilled plates. Several options regarding parameters were considered and compared. In every case, a comparison between the use of a pilot hole and the direct drilling without it were performed.

The twist drill was used more extensively with glass/epoxy plates. Four cutting speeds – 19, 26, 37 and 53 m/min – and two feeds – 0.1 and 0.15 mm/rev were used. Later, a reduction of the lower feed was done from 0.1 to 0.09 mm/rev.

A StepD180 drill in high speed steel was only used in glass/epoxy plates with three cutting speeds – 19, 26 and 37 m/min – and the same two feeds used for twist drills.

In a first set of experiences, the effect of a pilot hole, feed and speed was evaluated. For this set, cutting speed of 37 m/min was not used. Results from that

experience show that the use of a pilot hole can reduce substantially the thrust force during drilling.

Table 3.12 – Maximum thrust force during drilling of glass/epoxy with HSS drills.

Cutting speed (m/min)	Feed (mm/rev)	Pilot hole	Maximum thrust force (N)		
			Prepreg	Hand lay-up	RTM
19	0.1	YES	63.9	58.8	36.1
	0.15	NO	130.9	118.0	94.9
26	0.1	NO	138.1	111.5	84.8
	0.15	YES	30.9	34.5	26.9
53	0.1	YES	52.4	35.5	43.1
	0.15	NO	185.9	132.8	126.7

When analysing the results from the above table, it is clear that the use of a pilot hole with 3.5 mm diameter is responsible for an average reduction of 64% in the results. The other two factors analysed, speed and feed, also have some effect on the reduction of thrust force. The option for the lower feed can reduce force in 10% and a speed of 26 m/min represents an average thrust reduction of 9%.

An analysis of variance was done with the data obtained during this experience. The influence of the pilot hole was always very significant, both physical and statistically. This strong influence has possibly hide the relative importance of feed and speed in thrust force reduction.

After analysing these results, a second set of experiences was planned, using pilot hole as a constant parameter present in all the drillings. Then, it was easier to analyse the influence of feed and speed in the thrust force. Also the higher speed was abandoned and replaced by a lower speed of 37 m/min, above the best result of 26 m/min found during the first set. Lower speed has suffered a 10% reduction from 0.10 mm/rev to 0.09 mm/rev, with the intention to enlarge the difference between low and high feed. As the results have shown similar tendencies between the three materials used, only prepreg glass/epoxy plates were used in this set.

Table 3.13 – Levels of drilling tests factors for glass/epoxy plates.

Control factor	Units	Level 1	Level 2	Level 3
Cutting speed	m/min	19	26	37
Feed	mm/rev	0.09	0.15	-----

Results from maximum force are shown in table 3.14. For the step drill two results are shown, corresponding to the two steps of drilling. In addition, the table shows the results for the pilot hole that were done under the same parameters as those used for step drill, during the step corresponding to the minor diameter.

Table 3.14 – Maximum thrust force during drilling of glass/epoxy with twist and step drills.

Cutting speed (m/min)	Feed (mm/rev)	Maximum thrust force (N)			
		Twist drill		Step D180 drill	
		Pilot hole	Final hole	Pilot hole	Final hole
19	0.09	73.1	14.8	52.9	24.5
	0.15	132.3	35.1	65.1	15.3
26	0.09	78.6	23.3	51.0	16.0
	0.15	125.3	25.6	97.3	40.0
37	0.09	86.1	35.5	65.1	33.6
	0.15	91.1	24.6	87.0	49.9

Comparing the results from the two types of drills, it can be said that results have different variations according to the geometry used. An analysis of variance was applied to both drills separately. Results are shown in the next tables, based on Taguchi's L8 condensed array, but ignoring the last two trials that, according to [117] are optional. More details are presented in Appendix B.

Table 3.15 – ANOVA for thrust force of HSS twist drill.

Factor	Level S/N			SS	DF	V	% P	F
	1	2	3					
Speed	-27.2	-27.8	-29.4	5.5	2	2.7	14.2	0.2
Feed	-27.3	-29.0		4.3	1	4.3	11.2	0.3
Error				28.7	2	14.4	74.6	
TOTAL				38.5	5		100	

SS – sum of squares; DF – degree of freedom; V – variance; %P – percentage of contribution; F- result of F-test.

Table 3.16 – ANOVA for thrust force of HSS step drill.

Factor	Level S/N			SS	DF	V	% P	F
	1	2	3					
Speed	-25.8	-28.1	-32.3	42.8	2	21.4	48.6	1.2
Feed	-27.5	-29.9		8.6	1	8.6	9.7	0.5
Error				36.6	2	18.3	41.7	
TOTAL				88.0	5		100	

SS – sum of squares; DF – degree of freedom; V – variance; %P – percentage of contribution; F- result of F-test.

The results obtained with these two tool geometries have converged in the best parameters to be used, when drilling glass fibre reinforced plastics. A cutting speed of 19 m/min (Cutting speed/Level 1) and a feed of 0.09 mm/rev (Feed/Level 1) were found as the best choice among the several options evaluated (table 3.13).

When looking at the ANOVA tables, it can be said that for twist drill there is a strong interaction between feed and speed, with a significant effect on the results. The use of a condensed array may have the effect of increasing error and noise in this experiment. In both cases, the percentage of contribution from parameters to variation is less significant than the error, as is clearly demonstrated by the results of F-test, shown in the last column of the tables, with results inferior to one, in almost all cases.

As the thrust force values were already low when compared with those obtained with carbon/epoxy plates, further drilling experiments of glass/epoxy plates with carbide drills were considerably less. The use of carbide drills in glass/epoxy plates was reduced to one single combination of speed and feed, just for reference. A cutting speed of 80 m/min and a feed of 0.05 mm/rev were used as global reference parameters to comparison between the different drill geometries evaluated along this work. The exception is the use of a Dagger drill, with a cutting speed of 38 m/min and a feed of 0.05 mm/rev. Results of maximum thrust force for these experiments are shown in table 3.17.

No search for thrust force minimization was done for the drilling of these plates, but it seems, based on the results for the other materials, that lower cutting speeds will lead to some reduction of the values.

Table 3.17 – Thrust force for different carbide drills on glass/epoxy plates drilling.

Drill	Maximum thrust force [N]
Twist with 1,1mm pilot hole	59.8
Twist with 3,5mm pilot hole	28.4
Twist without pilot hole	80.2
C-shape	69.5
Dagger	42.2
Step D90	13.6
Step D180	33.2

3.2.5 DRILLING OF CARBON/EPOXY PLATES

Drilling of carbon/epoxy plates was more extensive. At the beginning, HSS drills were used, then carbide drills and, at the end, some plates were drilled with the new drill prototype. Search for parameters optimization regarding thrust force was carried for carbide drills, among the values settled for the study. For that, plates were drilled according to different conditions, where tool geometry or drilling strategy was changed.

First holes were done with HSS twist drill without pilot hole, and a second set with pilot hole, and finally using HSS StepD180 drill. Maximum thrust force results are shown in table 3.18.

Table 3.18 – Thrust force values for carbon/epoxy drilling with HSS drills.

Drill	**Cutting speed [m/min]**	**Feed [mm/rev]**	**Maximum thrust force [N]**
Twist without pilot hole	53	0.1	417
Twist with pilot hole	53	0.1	154
StepD180	26	0.06	116

All the drilled holes presented a bad finish and rapid tool wear was observed. So, these values, which were not systematically experienced, did only serve as reference for the worst possible case. Holes obtained with StepD180 drills presented a very bad finishing, even when reducing both cutting speed and feed, and so no more drilling with this tool was done. No further experiments like parameter study and variation analysis were done with this tool material.

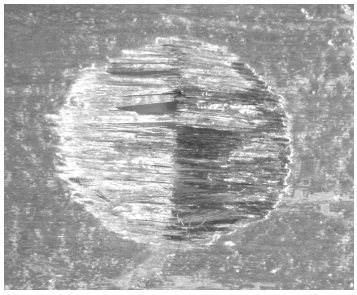

Figure 3.19 – Exit side of a carbon/epoxy plate drilled with HSS twist drill.

Experiments with carbide drills were more extensive considering the variety of geometries used for comparison. The first set of experiments had the purpose to evaluate the effect of the pilot hole and the possible advantages of coated carbides in the drilling of carbon/epoxy composite plates. It was easy to verify the advantages of the pilot hole, and this verification was only done for twist drill without TiAlN coating. It was also compared the effect of several pilot holes diameters, namely 1.1, 2.3 and 3.5 mm. In table 3.19 are presented the results from this set of experiments. All holes were drilled with a cutting speed of 80 m/min and a feed of 0.05 mm/rev.

Table 3.19 – Thrust forces with carbide twist drills in carbon/epoxy plates.

Drill	Pilot hole diameter [mm]	Maximum thrust force [N]	Thrust reduction
TiAlN coated	Without	160	------
TiAlN coated	3.5	84	48%
uncoated	Without	102	------
uncoated	3.5	24	76%
uncoated	2.3	49	52%
uncoated	1.1	73	28%

It is clear that the use of a coated drill did not show any advantage, as referred in [60]. Further experiments were done for comparison of coated and uncoated drills, varying cutting speed and feed rate, but the results were always significantly better for uncoated drills. Due to this fact, the uses of coated drills were abandoned and the work proceeded only with uncoated drills.

Another interesting fact is the evolution of thrust reduction according to the pilot hole diameter. This discussion will be presented in section 3.2.9.

After the choice of the coated or uncoated tool is settled, several sets of experiments had to be decided and executed. Based on available information from literature and some preliminary results and comparisons, three experiments were decided, using three different tool geometries – twist drill with pilot hole of 1.1 mm diameter, C-shape drill and Dagger drill.

In order to understand this decision, it is interesting to show the results obtained with the several options of tool geometry available, all with the same cutting speed and feed – 80 m/min and 0.05 mm/rev – except for Dagger drills where manufacturer recommendation was followed – 38 m/min, 0.05 mm/rev.

Table 3.20 – Thrust force comparison for different drill geometries in carbon/epoxy plates.

Drill	Pilot hole [mm]	Maximum thrust force [N]
Twist	1.1	72.7
Twist	3.5	24.2
Twist	------	102.4
C-shape	------	53.7
Dagger	------	61.6
StepD90	------	36.5
StepD180	------	45.0

Although thrust force values of Step90 drill was very interesting, when compared with the other geometries, the hole finishing was not very good with a considerable amount of fibre breakage. This can be explained by the purpose of this drill, not for step through drilling but for drill only in the conical region of the diameter transition. In our experiments, it was needed to drill a cylindrical hole. Another remark that has to be made is that the materials did not show the same order of results, when subjected to similar cutting conditions, except for the hybrids where it seems to have no difference whether type of stacking sequence was used. Holes made with C-shape drills have the best appearance. In figure 3.20 some of the exit sides of the holes are shown.

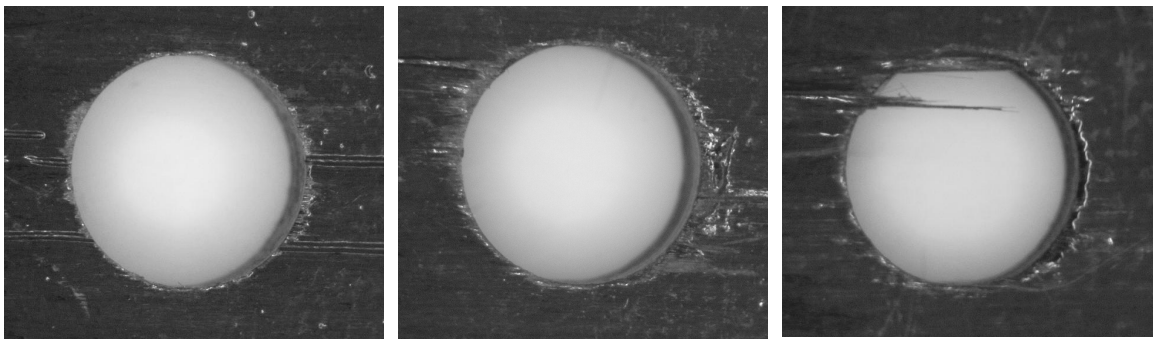

a) b) c)

Figure 3.20 – Plate exit side for several drills: a) twist drill; b) C-shape drill; c) stepD90 drill.

For twist drill, the set of experiments was established with two cutting speeds – 80 and 102 m/min – and two feeds – 0.025 and 0.05 mm/rev. These values are designated, respectively, as level 1 and level 2 in Taguchi L4's runs done for carbon/epoxy plates. The pilot hole has always 1.1 mm diameter.

Table 3.21 – Levels of drilling test factors for twist drill in carbon/epoxy plates.

Control factor	Units	Level 1	Level 2
Cutting speed	m/min	80	102
Feed	mm/rev	0.025	0.05

Results for this run and the linked analysis of variance (ANOVA) are shown in the following tables.

Table 3.22 – Thrust force for twist drill with 1.1mm pilot hole in carbon/epoxy plates.

Cutting speed [m/min]	Feed [mm/rev]	Maximum thrust force [N]
80	0.025	36.5
	0.05	72.7
102	0.025	44.3
	0.05	52.2

Table 3.23 – ANOVA for thrust force of twist drill with pilot hole in carbon/epoxy plates.

Factor	Level S/N		SS	DF	V	% P	F
	1	2					
Speed	-34.30	-33.68	0.38	1	0.38	2	0.03
Feed	-32.88	-35.10	4.93	1	4.93	26	0.37
Error			13.46	1	13.46	72	
TOTAL			18.77	3		100	

SS – sum of squares; DF – degree of freedom; V – variance; %P – percentage of contribution; F- result of F-test.

Observing the results, feed is the most relevant factor for thrust force with a greater percentage of contribution, but its significance is low when compared with experimental error, as is demonstrated by the result of the F-test. In this analysis, as well as in all the others, the effect of interactions was considered in the error. This may reduce the knowledge about the interaction between factors, even though the aim is not the search for optimum parameters. For this case, the best choice of parameters was found to be a cutting speed of 102 m/min (Level S/N 2) with a feed of 0.025 mm/rev (Level S/N 1).

For C-shape drill, a similar set of experiments was established, considering the same two cutting speeds – 80 and 102 m/min – but three feeds – 0.025, 0.05 and 0.1

mm/rev, in order to go further in feed effect. In this case, Taguchi L8 orthogonal array was used, both for parameter selection and ANOVA.

Table 3.24 – Levels of drilling test factors for C-shape drill in carbon/epoxy plates.

Control factor	Units	Level 1	Level 2	Level 3
Cutting speed	m/min	80	102	-----
Feed	mm/rev	0.025	0.05	0.1

In this test, the results pointed to a best choice of 80 m/min (Level S/N 1) and 0.025 mm/rev (Level S/N 1). The parameter that has a physical influence is feed, with an F-test value near 2, and the influence of cutting speed is lower than the experimental error. The following tables show the results of this experiment.

Table 3.25 – Thrust force for C-shape drill in carbon/epoxy plates.

Cutting speed [m/min]	Feed [mm/rev]	Maximum thrust force [N]
80	0.025	49.9
	0.05	64.1
	0.1	75.9
102	0.025	66.9
	0.05	61.7
	0.1	72.6

Table 3.26 – ANOVA for thrust force of C-shape drill in carbon/epoxy plates.

Factor	Level S/N			SS	DF	V	% P	F
	1	2	3					
Feed	-35.30	-36.06	-37.42	4.60	2	2.30	59	1.7
Speed	-36.00	-36.52		0.40	1	0.40	5	0.3
Error				2.78	2	1.39	36	
TOTAL				7.79	5		100	

SS – sum of squares; DF – degree of freedom; V – variance; %P – percentage of contribution; F- result of F-test.

The third set of experiments was made with *Dagger* drills. In this case, lower cutting speeds were used and the lowest feed was 0.05 mm/rev. The reason for this was the need to avoid vibrations during the drilling as the longer length of the drill can cause eccentricity, leading to poorer drill finishing. It was decided to stay only with two speeds – 30 and 38 m/min – and two feeds – 0.05 and 0.08 mm/rev – in order to analyse the

effect of cutting parameters in thrust force. The same analysis with a L4 Taguchi orthogonal array was made, and the best results considered.

Table 3.27 – Levels of drilling test factors for Dagger drill in carbon/epoxy plates.

Control factor	Units	Level 1	Level 2
Cutting speed	m/min	30	38
Feed	mm/rev	0.05	0.08

Table 3.28 – Thrust force for Dagger drill in carbon/epoxy plates.

Cutting speed [m/min]	Feed [mm/rev]	Maximum thrust force [N]
30	0.05	66.6
	0.08	68.0
38	0.05	61.6
	0.08	61.1

Besides the indication that is given by the thrust force values, there was also another relevant factor that was observed during these drilling tests. In drills executed with higher feed – 0.1 mm/rev - peel-up delamination was observed at the drill entrance side. This observation alone would be sufficient to lower feed rate values with this drill.

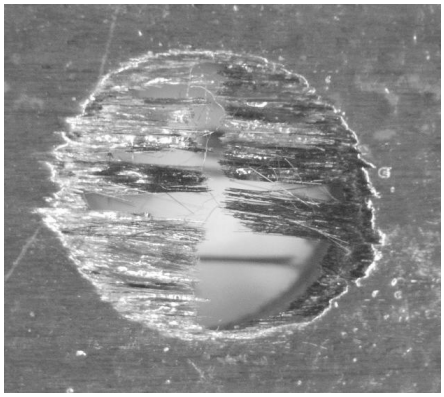

Figure 3.21 – Peel-up delamination in carbon/epoxy plate with a feed rate of 0.1 mm/rev.

Table 3.29 – ANOVA for thrust force of Dagger drill in carbon/epoxy plates.

Factor	Level S/N		SS	DF	V	% P	F
	1	2					
Speed	-36.59	-35.77	0.69	1	0.69	95	23.4
Feed	-36.13	-36.23	0.01	1	0.01	1	0.3
Error			0.03	1	0.03	4	
TOTAL			0.73	3		100	

SS – sum of squares; DF – degree of freedom; V – variance; %P – percentage of contribution; F- result of F-test.

The best parameters, according to ANOVA results, are 38 m/min as cutting speed (Level S/N 2) and 0.05 mm/rev as feed rate (Level S/N 1). The result of the feed influence on the thrust force is odd, showing minor influence on the result. This can be a consequence of the narrow variation of feeds considered in this experiment.

3.2.6 DRILLING OF HYBRID CARBON+GLASS/EPOXY PLATES

Hybrid plates, in both configurations, were also drilled with HSS drills. Two reasons can be pointed out to justify this recollection of values and results. One comes directly from the fact that both hybrids have 75% of glass/epoxy plies in their constitution, so there was the interest to be able to compare results with those referred before with glass reinforced plates. The other is the purpose to have a worst possible case. As the step drill showed poor hole finishing, only twist drill was used and the parameters chosen were those that had shown best results with glass/epoxy plates, a speed of 19 m/min and a feed of 0.09 mm/rev. According to the precedent section (table 3.8, page 105), hybrids are classified as HIBC when carbon plies are located outside the glass plies and as HIBG when they are in the middle of glass reinforced plies.

Table 3.30 – Thrust force values for hybrid plates drilling with HSS drills.

Drill	Maximum thrust force [N]	
	Hybrid HIBC	Hybrid HIBG
Twist without pilot hole	213	242
Twist with 3.5mm pilot hole	92	62

In all the results, it is important to note that the use of a pilot hole has always caused a strong reduction of the thrust force during drilling, superior to 50%.

The experimental set-ups used during thrust force evaluations were identical to those of carbon/epoxy plates, regarding tools and cutting parameters as well as control factor levels. The following tables show the results found in the several experiments as well as the respective analysis of variance (ANOVA), although this is only presented for HIBC plates.

Table 3.31 – Thrust force comparison for different carbide drill geometries in hybrid plates.

Drill	Pilot hole [mm]	Maximum thrust force [N]	
		Hybrid HIBC	Hybrid HIBG
Twist	1.1	66.4	68.3
Twist	3.5	19.3	19.5
Twist	------	94.8	88.7
C-shape drill	------	80.9	81.4
Dagger drill	------	47.5	44.6
StepD90	------	29	41.3
StepD180	------	42.1	43.3

Table 3.32 – Thrust force for twist drill with 1.1 mm pilot hole in hybrid plates.

Cutting speed [m/min]	Feed [mm/rev]	Maximum thrust force [N]	
		Hybrid HIBC	Hybrid HIBG
80	0.025	39.8	40.1
	0.05	66.4	68.3
102	0.025	44.7	52.6
	0.05	52.2	56.9

An ANOVA was performed for the two hybrid types, separately. Only the results for hybrid HIBC are shown here, as there are few and not significant differences between them in the results for F-test, showing a similar influence of the experimental factors in the results for both type of plates. On the other hand, this plate construction appeared more interesting in a cost-benefit basis, so the study was more focused on it.

Table 3.33 – ANOVA for thrust force of WC twist drill in HIBC plate.

Factor	Level S/N		SS	DF	V	% P	F
	1	2					
Speed	-34.24	-33.75	0.24	1	0.24	2	0.10
Feed	-32.57	-35.42	8.13	1	8.13	75	3.34
Error			2.43	1	2.43	23	
TOTAL			10.80	3		100	

SS – sum of squares; DF – degree of freedom; V – variance; %P – percentage of contribution; F- result of F-test.

Feed has physical significance in thrust force, under these experimental conditions.

Table 3.34 – Thrust force for C-shape drill in hybrid plates.

Cutting speed [m/min]	Feed [mm/rev]	Maximum thrust force [N]	
		Hybrid HIBC	Hybrid HIBG
80	0.025	45.8	45.8
	0.05	80.9	81.4
	0.1	102.9	110.2
102	0.025	66.3	77.0
	0.05	72.3	77.7
	0.1	93.6	95.9

Table 3.35 – ANOVA for thrust force of C-shape drill in HIBC plate.

Factor	Level S/N			SS	DF	V	% P	F
	1	2	3					
Feed	-34.85	-37.67	-39.84	25.02	2	12.51	81	4.65
Speed	-37.23	-37.68		0.41	1	1.33	1	0.15
Error				5.38	2	2.69	18	
TOTAL				30.81	5		100	

SS – sum of squares; DF – degree of freedom; V – variance; %P – percentage of contribution; F- result of F-test; Inter.-interaction effect.

Once again, feed has statistical and physical significance in the thrust force, with a result of the F-test greater than two. Cutting speed effect is less significant than the error, for the experimental conditions.

The third set of experiments was made with *Dagger* drills. In this case the effect of peel-up delamination with high feeds was only observed for HIBC plates, where carbon plies are first subjected to the mechanical action of the drill. When drilling plates with HIBG stacking sequence, with outer plies of glass/epoxy, this phenomenon was not observed.

Table 3.36 – Thrust force for Dagger drill in hybrid plates.

Cutting speed [m/min]	Feed [mm/rev]	Maximum thrust force [N]	
		Hybrid HIBC	Hybrid HIBG
30	0.05	55.6	54.9
	0.08	65.6	63.2
38	0.05	47.5	44.6
	0.08	65.8	58.8

Table 3.37 – ANOVA for thrust force of Dagger drill in HIBC plates.

Factor	Level S/N		SS	DF	V	% P	F
	1	2					
Speed	-35.62	-34.95	0.44	1	0.44	8	0.93
Feed	-34.22	-36.36	4.58	1	4.58	83	9.61
Error			0.48	1	0.48	9	
TOTAL			5.50	3		100	

SS – sum of squares; DF – degree of freedom; V – variance; %P – percentage of contribution; F- result of F-test.

ANOVA results showed again a physical significance of feed, with F-test result above two, and a very low effect of speed, inferior to the experimental error.

The other hybrid plate construction – HIBG – has some differences regarding maximum values of thrust force during drilling, as the alternate stacking sequence causes some differences in the plate resistance to flexion. The drill starts to cut in a glass/epoxy region and when it reaches the carbon/epoxy plies is close to be fully engaged. This improves tool guidance through the carbon/epoxy plates and prevents those plies from both delamination mechanisms, peel-up and push-out, as the glass/epoxy plies serve as sacrificial plates for the centre plies. Regardless of this differences, the results of ANOVA F-test showed similar values and the best parameters always agree.

3.2.7 THRUST FORCE ANALYSIS AND COMPARISON

Independently of the tool and parameters used or material to be drilled, the evolution of a drilling operation, according to Dharan and Won [61], can be divided in seven main stages:

1. Approach : the drill approaches the workpiece;
2. Contact : the drill tip makes contact;
3. Normal drilling : drilling without delamination;
4. Initiation of delamination: if the critical thrust force is exceeded, delamination starts;
5. Drill breakthrough : the drill tip exits the workpiece;
6. Completion : a hole is completed;
7. Withdrawing drill: the drill must be moved backward and withdrawn from the piece.

When a monitoring of thrust force and torque is being done, not all these steps are quite distinguishable. However, it is possible to identify some of them. Stage 1 happens before any force can be registered as there is no contact between the tool and the workpiece. Stage 2 is clearly related with a sudden increase in thrust force until full engagement of the drill, and the following curve represents stages 3 and 4. The problem of stage 4 is that it depends on the maximum force during drilling and when, or where in plate thickness, this point is reached. Stage 5 means the reduction of thrust force to zero, and stages 6 and 7 have no interest in the present study. However, they are responsible for a residual torque due to friction between the tool and the machined hole walls. Figures 3.22 and 3.24 show some typical curves of thrust force and torque during drilling of carbon/epoxy plates with different tools – twist, C-shape and Dagger drill.

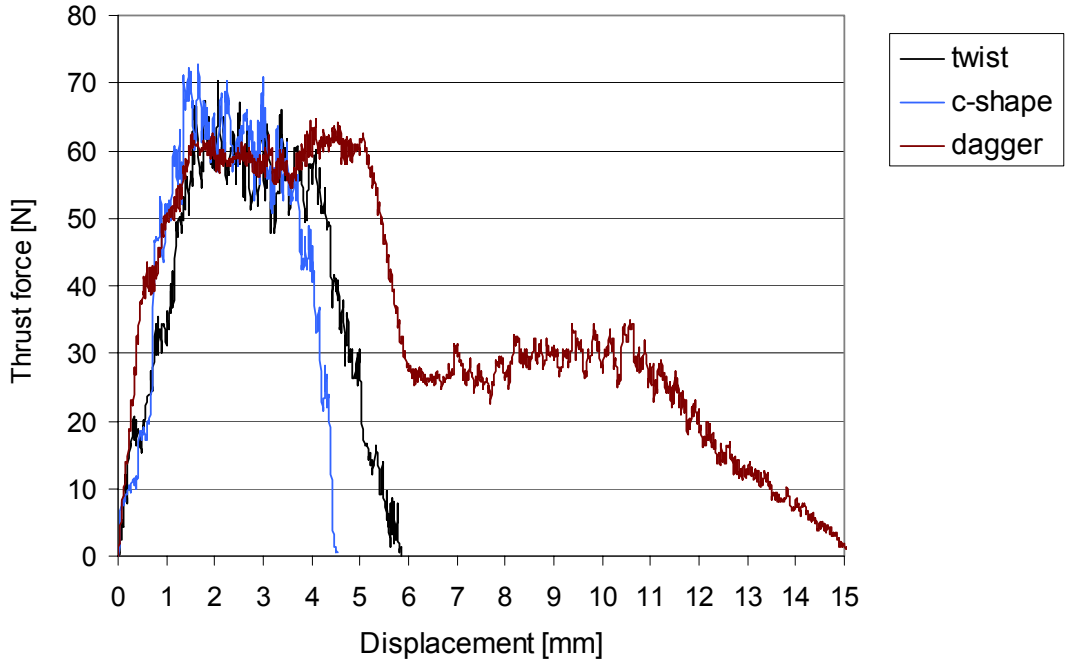

Figure 3.22 – Thrust force evolution for different drills.

The several results from the experiments can be easily compared to establish a hierarchy of best drilling geometries. For this, only the best results from each drill

geometry was considered and, whenever results were found better, only drills with pilot hole are considered.

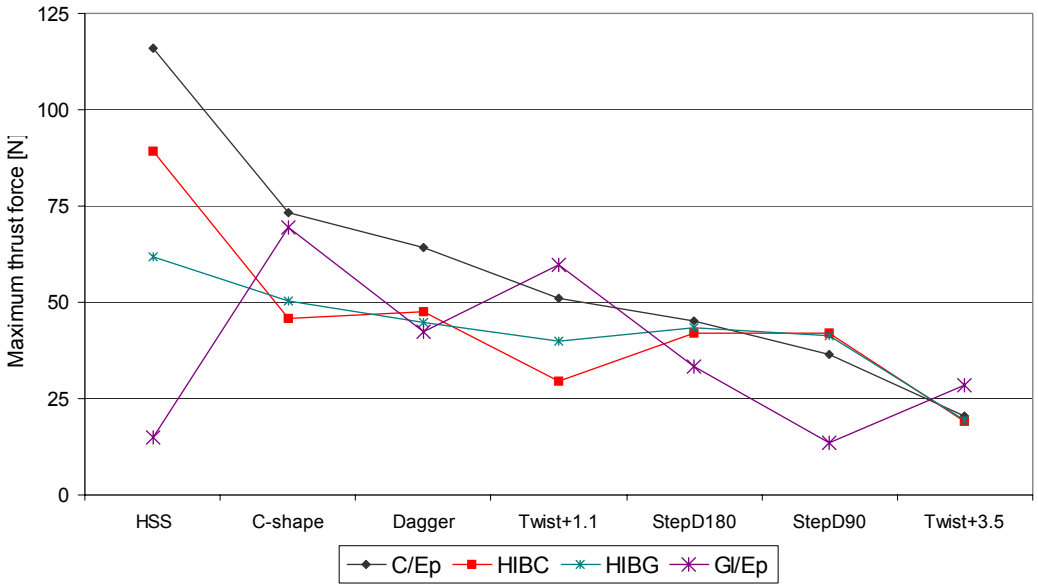

Figure 3.23 – Comparison of maximum thrust forces during drilling of composite plates.

From figure 3.23 the advantage of pilot hole drilling is evident, independently of the material considered.

Considering the results from the experiments with all the tool types, it was possible to reach to a conclusion about the preferable drilling parameters for thrust force minimization, among the conditions used in this phase. It is noteworthy that the parameters found as better for thrust force minimization, were the same for all the three materials, carbon/ epoxy and the two types of hybrid plates.

Table 3.38 – Best choice of parameters for carbide drills.

Drill designation	Cutting speed [m/min]	Feed [mm/rev]
Twist with 1.1 mm pilot hole	102	0.025
C-shape	80	0.025
Dagger	38	0.05

3.2.8 SPECIFIC CUTTING ENERGY

The value of torque measured during drilling experiments has the interest to enable the calculation of the specific cutting energy for each material considered – glass/epoxy, carbon/epoxy and hybrids plates. Specific cutting energy is defined as the total energy input rate divided by material removal rate and it is dependent on the material, chip cross section, tool geometry, position angle (χ) and tool wear. Shaw and Oxford [119] have shown that in ordinary two-dimensional orthogonal metal cutting, the specific cutting energy varies inversely with the product of feed rate and drill diameter to a certain power, and explained it as the size effect. Hocheng and Puw [47] plotted the specific cutting energy against the product of feed rate (f) and drill diameter (d) and found, for carbon/ABS a slope of -0.12, milder than that of metal cutting. They have also pointed that similar trends exist for current materials with different slopes and magnitudes. For carbon/epoxy a slope of -0.35 was found, meaning that the size effect was more significant.

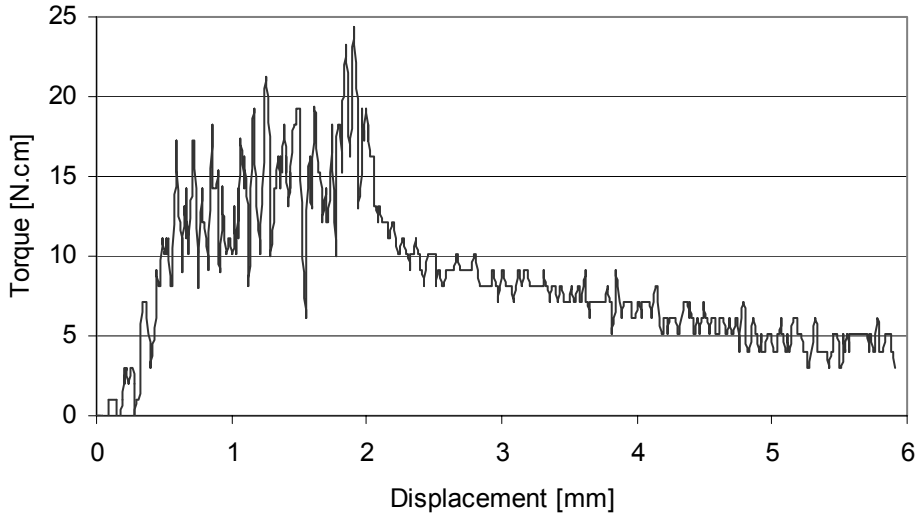

Figure 3.24 – Example of torque evolution during drilling with a twist drill.

For all the experiments that were executed, the value of specific cutting energy was calculated, and the data obtained for all tooling and drilling strategy was computed in a single plot. Then the slope was derived. One of these graphs is shown in figure 3.25, for carbon/epoxy plates with a slope of -0.13.

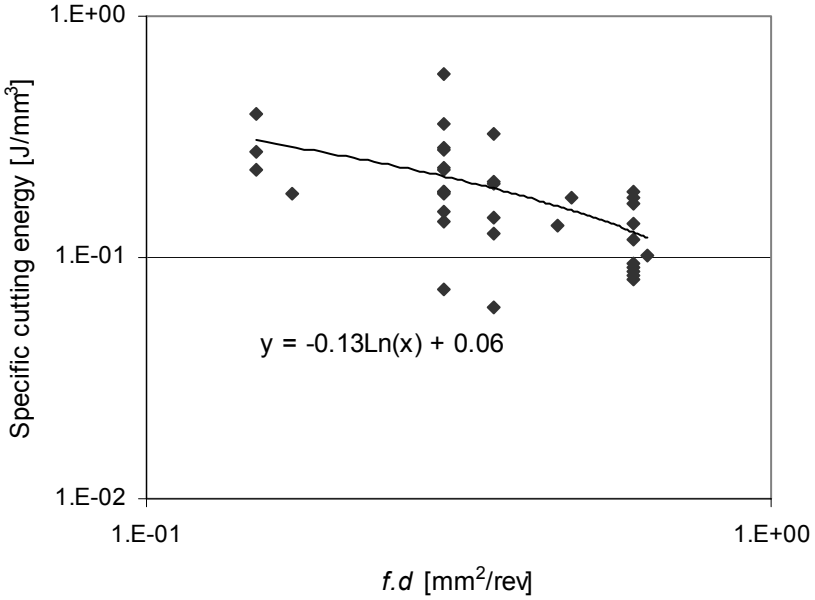

Figure 3.25 - Specific cutting energy in carbon/epoxy drilling.

Following the same procedure, the slopes for glass/epoxy and hybrids were respectively -0.13 and -0.17. So, it seems that size effect is more significant in hybrids than in the other materials. The value for glass/epoxy should be regarded with some caution, as the number of data points is considerably less, when compared with the remaining materials drilled. The milder slope found here for carbon/epoxy comes from the different orientation of the reinforcement fibres that have a quasi-isotropic stacking sequence which is not the case of the material used in [47], resulting in lower mechanical strength.

3.2.9 PILOT HOLE EFFECT

The influence of the pilot hole is mainly related with the reduction of thrust force during drilling. However, it must be noted that also the plate resistance to delamination is also reduced. So, the great reduction of thrust force that is achieved with the larger pilot hole used – 3.5 mm – has also a major risk of delamination. The balance between these two factors must be achieved, and related with non-destructive testing, in order to decide what is the best solution for the pilot hole diameter. Thrust force reduction is mainly a mechanical effect of lower material resistance due to the lack of material and

absence of fibre continuity in an area that corresponds to the pilot hole executed. All drills have been compared considering the thrust force with and without pilot hole. The reduction in thrust force by the use of pilot hole in C-shape drill is smaller than the effect observed with other drills.

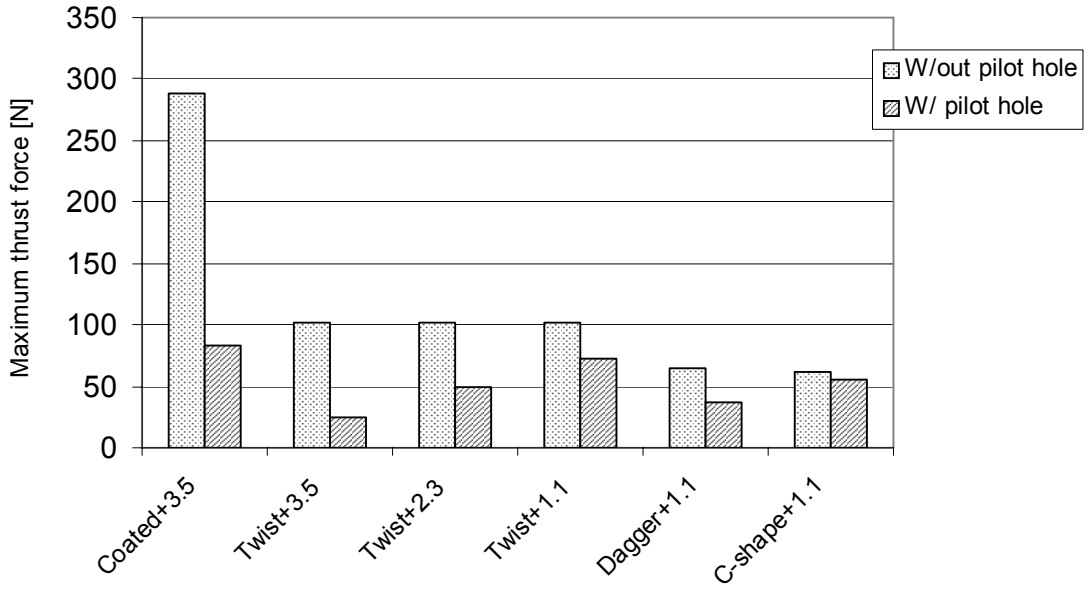

Figure 3.26 – Reduction of thrust force by the use of a pilot hole in carbon/epoxy plates.

For step drills, force comparison is made by the sum of the two forces observed during first and second step of the drilling. If the sum of the two thrust forces is considered – pilot hole plus final hole – the results can be interesting. The minimization of the total thrust force could mean that less pressure is applied to the area around the hole where delamination is keen to occur. So, considering this total force criteria, a new ordering of the drills with pilot hole can be presented. Here the best option for the use of a pilot hole is the twist drill. The only discussion that remains open is the diameter of the pilot hole, as the analysis must be complemented by the results from non-destructive testing, that are presented in next section.

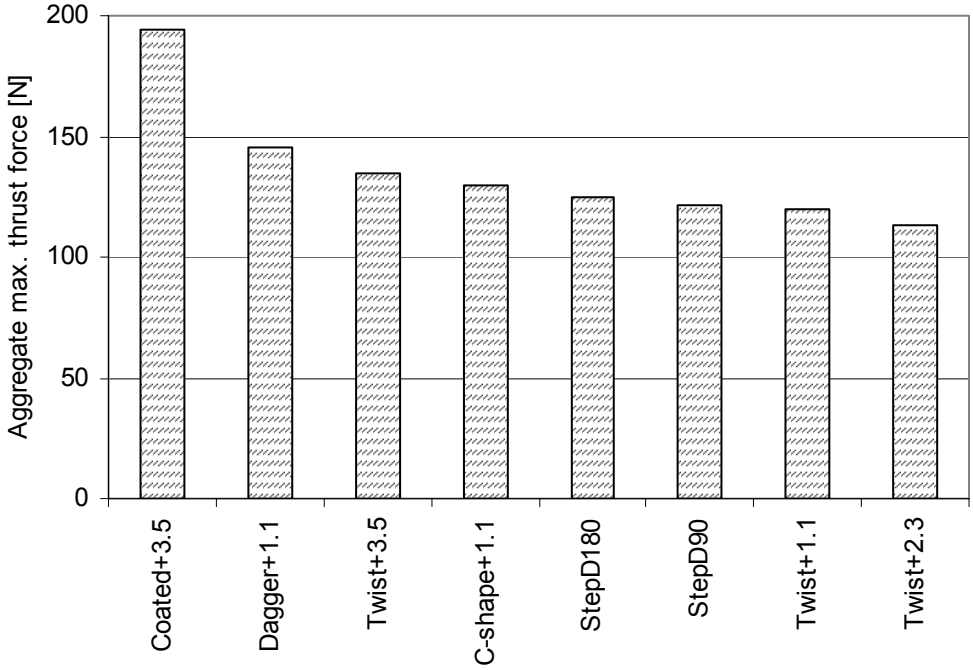

Figure 3.27 – Total thrust force in pilot hole drilling.

3.3 USE OF DAMAGE ANALYSIS TECHNIQUES

In the precedent section, drilling strategies used along the experimental work were described. Along with the drilling experiences, an extensive collection of data regarding thrust force and torque was done. This section refers to the damage evaluation techniques that are used during and after hole completion. As the grounds of each technique were described in Section 2.5, this section will be dedicated to the report of the setups used and results encountered.

3.3.1 ACOUSTIC EMISSIONS DURING DRILLING

Acoustic emission is a non-destructive technique that allows real-time monitoring of microscopic damage sequence mechanisms. These damages lead to the spreading of elastic deformation waves that can be detected at the material surface using piezoelectric transducers. Acoustic emission has been used successfully in the monitoring of composite parts in service, detection of impact damage and monitoring of curing process in fabrication.

During the drilling experiments, acoustic emission waves were detected with a resonant transducer μ30 from Physical Acoustics Corporation. Signals from the transducer were amplified by a pre-amplifier 1220 also from Physical Acoustics Corporation, with an adjusted gain of 40 dB. The acoustic emission system used was the AMSY5 from Vallen-System GmbH. Usually the signal acquisition is activated when the signal amplitude is greater than a predefined threshold value, normally equal to the environmental noise. In order to avoid that edge reflection is acquired and counted as signal, ‘blind’ time intervals are defined. During those periods, the system does not acquire the signal that comes from the transducer. The challenge of acoustic emission measurement comes from the fact that the drilling of fibre reinforced plates is a short time process with a great number of emissions.

The best option found to acoustic emission monitoring during drilling was the ‘continuous acquisition’ option. In this case, the signal acquisition is activated by a timer instead of a threshold value. When the predefined time expires, the data vector is closed and a new one opens. Each data vector has the same time frame

characteristics. The threshold value is only used for the event counting. Data vector has the following characteristics: initial time, event counting, energy, rise time.

The only option that seemed to give some satisfactory results was the hit counting of detected signals above certain amplitude. Figures 3.28 e 3.29 show some of the cases evaluated, in glass/epoxy and carbon/epoxy plates, respectively. The curves are plotted in a logarithmic scale. In all cases, there is a straight line that corresponds to the larger number of events, in the area between 30 and 70 dB. The difference is on the slope of the line segment when the transition from 70 to 90 dB is considered. This slope is known as the "*b factor*". For glass/epoxy plates only one slope can be considered while for carbon/epoxy two slopes are distinguishable. In general, each slope means a different damage mechanism, so it can be said that when drilling carbon/epoxy plates, two phases of damage can be considered.

For glass/epoxy plates there is a clear relation with the cutting speed, as greater speeds correspond to higher amplitude achieved. In lower amplitudes, the number of hits is smaller when higher speeds are considered.

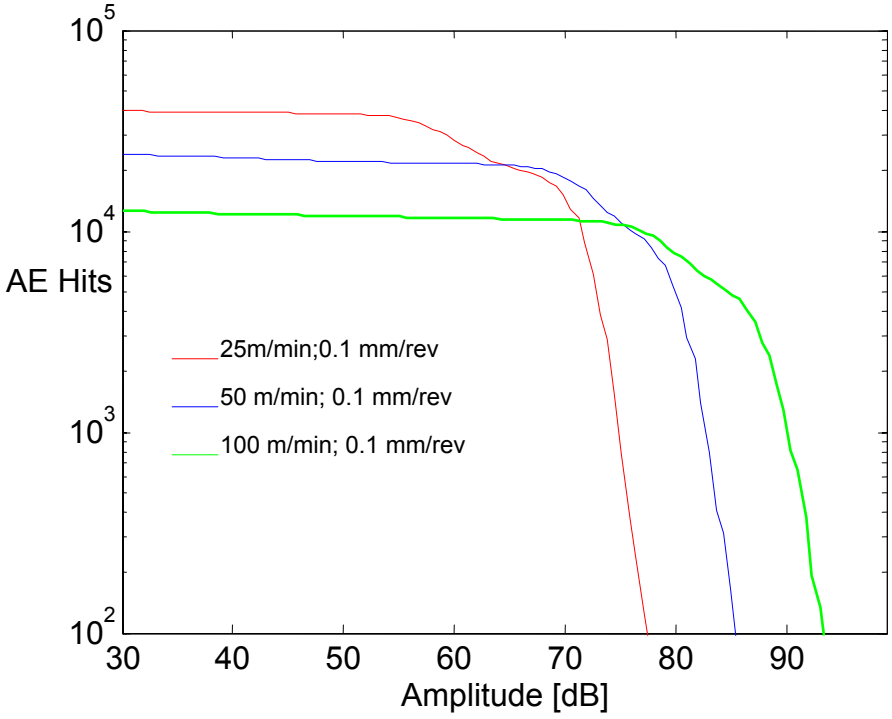

Figure 3.28 – Hit counting curves for glass/epoxy plates.

For carbon/epoxy plates, two different drill materials were considered: carbide and high speed steel drills. Higher signal amplitudes were always reached when drilling with carbide drills. The lowest amplitude was in the drilling with HSS drill at 100 m/min. Higher speed clearly have the effect to give less hits at low amplitudes. However, as further examination showed that HSS drills causes greater damage extent on the part, it comes difficult to relate acoustic emission with the damage observed after hole completion.

In a first conclusion, it is likely that the setup used for the AE experiments was not the most adequate for this kind of testing. For the moment, it appears as the acoustic emission observed could be more related with the drilling process itself, that is to say, the cutting action executed by the drill edges than with some other damage occurrence. This monitoring need to be deeply studied relating hits and counts with drill rotational speed and feed and only then it can be related with the onset of any damage. Also, the damage occurrence must be defined according to the depth of the acoustic emission origin. This facet of the analysis deserves a deeper study, relating AE expertise with drilling knowledge.

Hybrid plates were not included in these experiences.

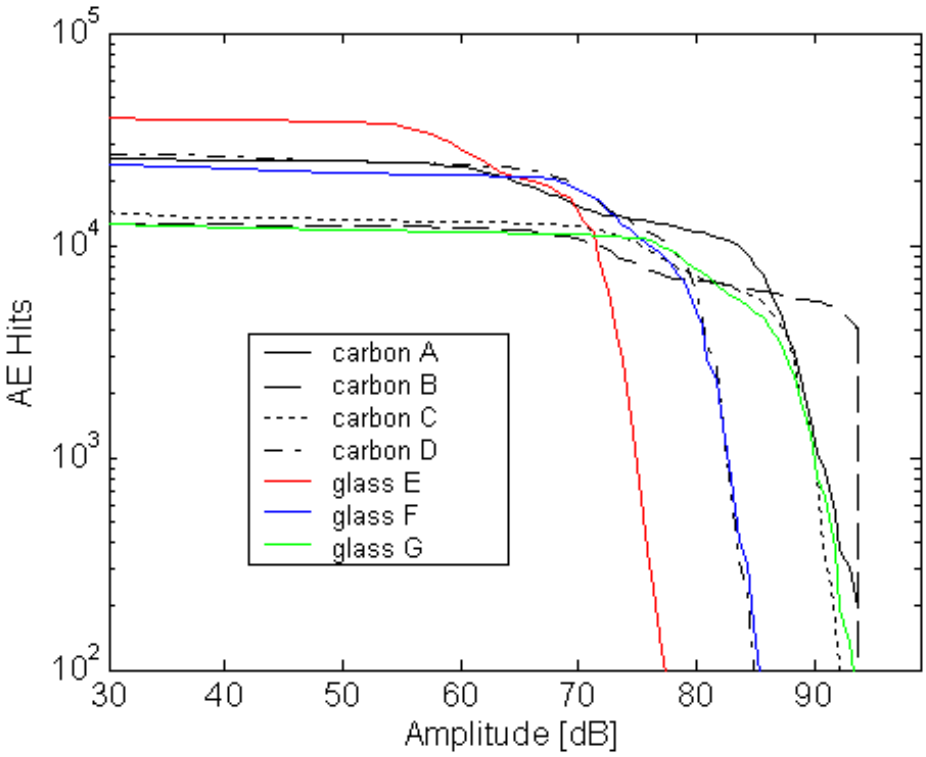

Figure 3.29 - Hit counting curves for carbon/epoxy and glass/epoxy plates:

	a	b	c	d	e	f	g	Unit
Feed	0.1	0.1	0.1	0.1	0.1	0.1	0.1	mm/rev
Speed	50	100	50	100	25	50	100	m/min
Tool	Carbide	Carbide	HSS	HSS	HSS	HSS	HSS	.

3.3.2 RADIOGRAPHY

One of the main objectives of this work was the evaluation of delaminated regions caused by the drilling of composite plates. With that purpose, an extensive use of radiography was made. For all the plates drilled and a large number of parameter settings and drill material, enhanced radiography was executed. As referred in 2.5.5, radiography is suitable for the detection of delaminations only if a contrasting fluid is used. With such purpose di-iodomethane – CH_2I_2, methylene iodide– from Merck was used. This product is a chemical reagent with a density of 3.32, radio-opaque, which is the important characteristic for the objective of its use.

To obtain a radiographic image, the following steps are needed:

- pour the contrasting fluid - di-iodomethane - into an appropriate container;
- immerse the plate or plate portion in the di-iodomethane;
- left the plates immersed for one and a half hour in a dark chamber;
- after time elapsed, clean the plates and the machined walls carefully, to remove all fluid stains, as drops of the fluid left at the plate surface or hole walls will be visible at the developed photographs;
- place the plate over a film and then the radiographic tube over the plate and shoot the picture, with an exposition time of 0.25 seconds;
- develop and reveal the film with a 2x magnification.

Developed films were used for the measurement of delaminations around the hole.

Some remarks are necessary about the enhanced radiography procedure. One is related with the contrasting fluid. This liquid is sensible to sunlight, air and moisture and should be stored in a dark and closed box. It must not be used with alkaline metals. During manipulation, care shall be taken as the contact with the skin can cause severe irritation. So, normal safety procedures with this product are the use of gloves, glasses and protective clothes. However, according to CE rules, this product is not classified as hazardous.

Another is concerned with immersion times. Some immersion times were experienced before, as there was not sufficient knowledge of the process. Shorter time of approximately one hour appears to be enough, but some conservative judgement

has enlarged this period for an extra thirty minutes. Longer periods up to six hours were also tried, but no difference was noted due to increased immersion time.

The equipment used was a SATELEC X-MIND SYSTEM with a Toshiba DG-073B tube of 60 mm diameter, a focal distance of 70 mm, a peak power of 70 kVp, an intensity of 8 mA and a power of 0.451 kVA. The exposition time was 0.25 seconds, as already mentioned. Shorter times will not reveal any contrast with all the area looking light grey and longer times will lead to the 'burning' of the film. In this case, the final photograph was too dark to get any contrast. The film used was a Kodak Ultra-speed DF-50.

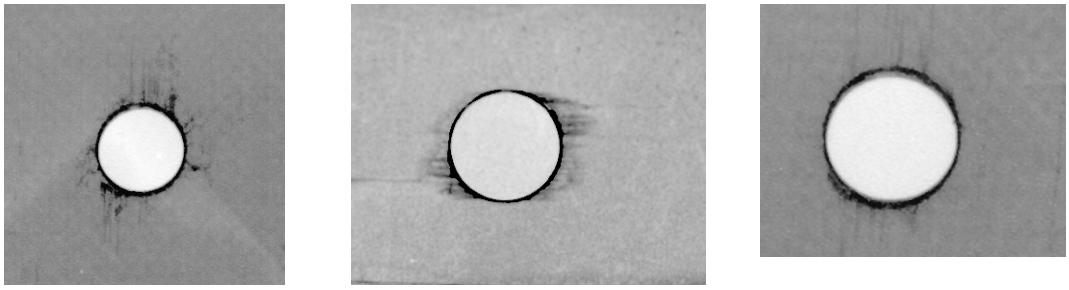

a) glass/epoxy b) carbon/epoxy c) hybrid

Figure 3.30 – Examples of developed radiographies.

Delamination measurement was made according to two different methods: use of a profile projector and computational vision. The last is more detailed in section 3.3.5.

The profile projector is a direct measurement method working in a dimmed light environment. Using an opposite source of light, it was possible to measure the revealed films, looking for the different degrees of transparency to establish the damaged diameter. The borders of those areas were easily identified at the monitor. Profile projector was a Mitutoyo PJN322 and a magnification of 20x was used. The use of an X-Y table connected to a PC to move the table turn it possible to compute the diameter from the measurement of three different points at the outer border of the damaged area, using GEOPAK software. In this method, three diameters were measured in every case. The final result considered was the maximum value of these three measurements. Results are shown and discussed below.

First delamination measurements were done for the comparison of results with three different glass/epoxy fabrication techniques – prepreg, manual and RTM. It was evident that RTM has, in all cases, the worst result of the three material types – figure

3.31. Remind that RTM is also the material with less fibre content. Use of pre-drilling reduced the delamination factor but less than expected. Delamination factor definition can be found in page 50, equation (2.4).

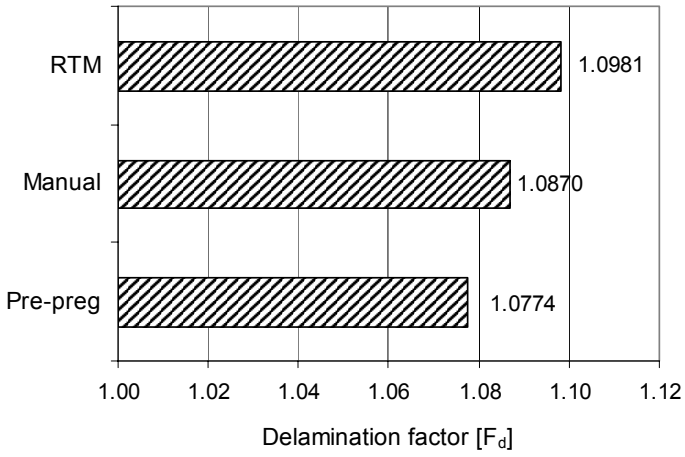

Figure 3.31 – Average delamination factor (F_d) for the three types of glass/epoxy plates.

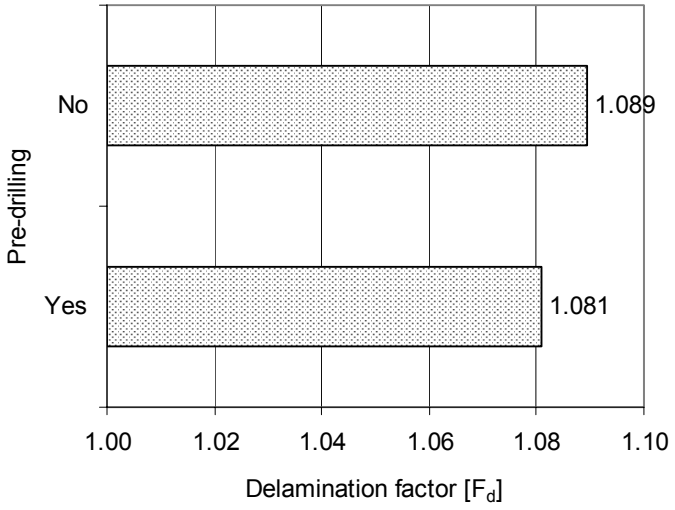

Figure 3.32 – Pre-drilling influence on delamination factor (F_d) of glass/epoxy plates.

It was clear from the results that the main factor in the delamination was the fabrication process. An ANOVA analysis about the results of the delamination factor showed that the experimental error is responsible for 50% of the variation. All the parameters analysed – speed, feed, pre-drilling – had lower contribution to the variation and the F-test results were in the range of one or less, so meaning that the effects

studied were not significant when compared to experimental error. Continuation of this work has focused in the drilling of glass/epoxy prepreg plates with HSS and carbide drills.

The next experiments on glass/epoxy drilling were made with HSS drills with pre-drilling and the step drill also in HSS. Carbide drills used were twist drill with 1.1 mm diameter pilot hole, C-shape drill, StepD90 and StepD180 drills. Results for the delamination factor can be found in figure 3.33.

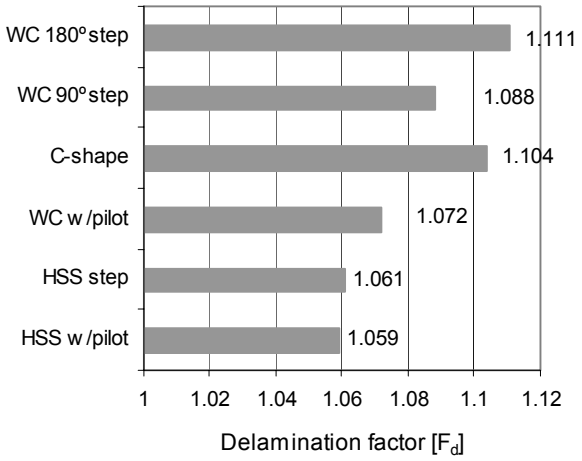

Figure 3.33 – Delamination factor for different drills in glass/epoxy plates.

As the results for the delamination factor were better than those found for carbon/epoxy plates, the focus was on the reduction of damage on these plates. The first results were higher from the experiments made with HSS and coated carbide drills as can be seen in table 3.39.

Table 3.39 – Delamination factor for some drilled carbon/epoxy plates.

Tool	Cutting speed [m/min]	Feed [mm/rev]	Delamination factor
HSS with pilot hole	53	0.1	1.556
HSS step	26	0.06	1.511
Coated WC	53	0.1	1.291
Coated WC with pilot hole	96	0.06	1.172

As it is evident from simple visual inspection – figure 3.34 - and the above table, HSS drills are not suitable for carbon/epoxy drilling, as the damaged area around the hole is too wide, covering a diameter that can almost double the drilled one.

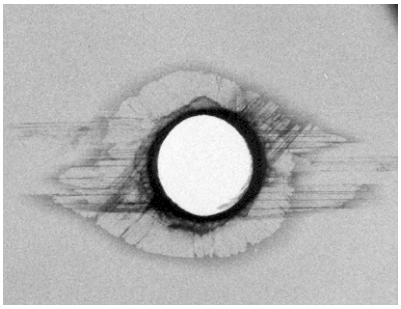

Figure 3.34 – Radiography of a carbon/epoxy plate drilled with HSS twist drill.

Further experiments on the drilling of carbon/epoxy plates have targeted a substantial reduction of the damage. For that, as described in the precedent chapter, several carbide drills were experimented, and the effect of speed and feed was evaluated. The results for the delamination factor showed some improvements, as under some cutting conditions, values below 1.20 were found. This was an indication that there was some space for improvement. Looking for such improved results was the task accomplished for the different carbide drills – twist drill with pilot hole, C-shape drill, step drill and *Dagger* drill. Naturally, this task was reduced to a small number of different levels of speed and feed to reduce the number of experiences performed. For twist drill with 1.1 mm pilot hole, C-shape drill and *Dagger* drill, an ANOVA analysis to measure the importance of the factors was done. In all these analysis, the best results were found using the lowest feed, 0.025 mm/rev for twist and C-shape and 0.05 mm/rev for *Dagger* drill. The *F-test* value, above two, for the feed showed that this is a significant factor in C-shape and *Dagger* drills and less important, in the range of one, for twist drill (Appendix A). This lower value could be explained by a smaller sensitivity of twist drill to feed variation because of the pilot hole. Previous experiments with higher feeds gave bad results in visual evaluation with the presence of peel-up delamination at the entrance side of the plate, already referred before, classified as non-acceptable and not included in further analysis. The influence of speed, evaluated by the F-test, was found to be small, in the range of two, indicating a moderate effect on the final result. Generally, the main factor for delamination is feed, which is in agreement with other studies described in chapter 2.

The importance of the pilot hole was evaluated for all drills. Only for twist drill some advantages were found, and the best result for the delamination factor was with the 1.1 mm pilot hole, as can be seen in figure 3.35, for a cutting speed of 80 m/min and a feed of 0.05 mm/rev.

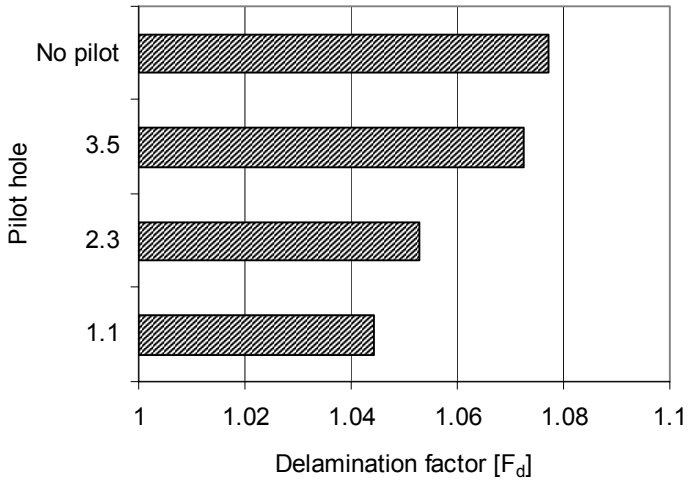

Figure 3.35 – Influence of pilot hole diameter on delamination factor (F_d).

Just for comparison, the delamination factor using a twist drill without pilot hole is also presented. The value found was superior to those obtained with any diameter of pilot hole as presented in figure 3.35, thus justifying its use.

It is possible to observe that when using a 3.5 mm pilot hole, the damage is near to that obtained with a full hole made in one step only. This can be explained considering that, after pilot hole completion, some delamination exists, meaning a damaged diameter near to the final hole diameter. In fact, in measurements done after pilot hole drilling, the average delamination factor was equal to 1.57. A simple calculation shows that, with a 3.5 mm pilot hole, the damaged diameter can reach, in some regions, 5.5 mm. That leads to a reduction of the material resistance to delamination when final drill is executed, and the increase of the damaged area. The interlaminar resistance of the laminate is reduced by the action of the thrust force exerted during pilot hole drilling. This mechanism is not so critical to material when smaller pilot hole diameters are used, as the damaged area is lesser.

The influence of speed and feed in delamination factor are shown in the following figures, where their effects are compared. These values were the most frequently used

in the several experiences done during this work and they are more representative of the overall effect and not of a specific drill.

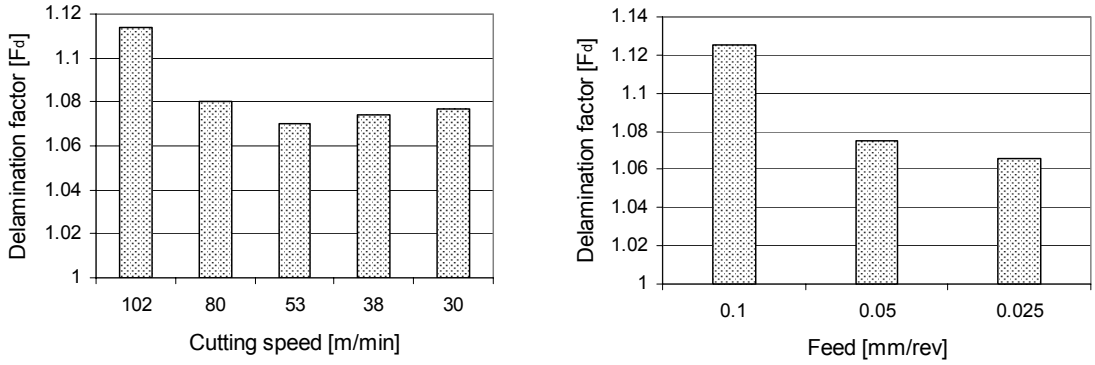

Figure 3.36 – Influence of cutting speed and feed on delamination factor (F_d).

Note that the best result for cutting speed was obtained for 53 m/min, although the best result of all experiences was achieved with a higher speed of 80 m/min, as it is shown in the next paragraph. An optimum cutting speed range seems to exist in the interval 53 to 80 m/min.

Next table shows some of the best results found after measurement of the damage around the holes executed with carbide drills. As the feed is the most significant factor and for carbide step drills the smaller feed of 0.025 mm/rev was not tried, a feed of 0.05 mm/rev was always considered for drill comparison purposes.

Table 3.40 – Delamination factor (F_d) results for carbon/epoxy plates.

Tool	Speed [m/min]	Feed [mm/rev]	Delamination factor
Twist with 1.1mm pilot	80	0.05	1.044
C-shape	80	0.05	1.064
Dagger	38	0.05	1.067
Step 90º	80	0.05	1.067
Step 180º	80	0.05	1.107

After reasonable knowledge of the damage extension was established, hybrid plates were subjected to the same cycle of drilling, radiography and damage measurement. At the beginning, only HIBC plates (table 3.8, page 105) were studied, because of the particular challenge that the drilling of the outer plies in carbon offers. It

was noted, during drilling experiments that the top plies of this hybrid were more sensitive to peel-up delamination, in the same way that occurred with carbon/epoxy plates. As some damage reduction was already achieved with the prior studies done to glass/epoxy and carbon/epoxy plates, the study of hybrid plates was simplified, that is to say, there was a selection of the drilling conditions that were fully analysed. So, only one set of drilling parameters was used.

Table 3.41 –Delamination factor (F_d) for different tools in hybrid HIBC plates.

Tool	Speed [m/min]	Feed [mm/rev]	Delamination factor
Carbide twist drill with pilot	80	0.05	1.071
C-shape drill	80	0.05	1.056
Dagger drill	38	0.05	1.077
Carbide step drill	80	0.05	1.097

It is clear that delamination extent is smaller than that obtained in the first experiences either with glass/epoxy or carbon/epoxy plates. This was considered as a confirmation of the improvements achieved previously. The second stage was to evaluate, only for the drills presenting best results, the effect of cutting speed and feed in delamination around the hole. With such purpose, simple experiments with two cutting speeds and two feeds were carried out for each drill. Results of these experiments are shown in the next figure.

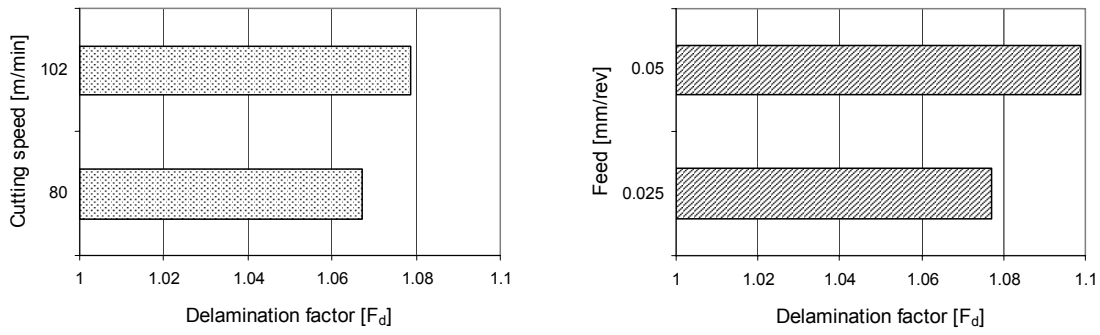

Figure 3.37 – Effect of cutting speed and feed in delamination factor (F_d) for hybrid plates.

The use of smaller feeds and lower speed gave best results regarding delamination, which is in accordance with the results found in carbon/epoxy plates.

Once again, for *Dagger* drills, lower cutting speeds were used, according to the conditions already referred for carbon/epoxy plates drilling. The best results for each drill are presented in table 3.42.

Table 3.42 – Delamination factor (F_d) best results for hybrid HIBC plates.

Tool	Speed [m/min]	Feed [mm/rev]	Delamination factor
Twist with 1.1mm pilot	80	0.05	1.058
C-shape	80	0.05	1.051
Dagger	30	0.05	1.066

These results are in the same range of those obtained for carbon/epoxy plates, although slightly superior. Some effect of the carbon-glass plies interface may be responsible for this worst result.

Before proceeding to the alternative hybrid plate, a reduced experience was made, in order to evaluate if there were significant differences in delamination results when comparing the two hybrid sequences. With such objective a L8 Taguchi orthogonal array (figure 3.18, page 115) was considered with the levels for each factor as described in table 3.43.

Table 3.43 – Taguchi L8 orthogonal array for hybrid comparison.

FACTOR	Units	Level 1	Level 2
Feed	mm/rev	0.025	0.05
Cutting speed	m/min	80	102
Interaction of feed and speed		1	2
Tool	-----	Twist with 1.1mm pilot	C-shape
Blank		-----	-----
Blank		-----	-----
Material	-----	Hybrid HIBG	Hybrid HIBC

Note that the selection of the blank lines was done according to a criterion of interaction minimization on the evaluation factors that were the main purpose of this experiment. Table 3.44 shows the results obtained (see also Appendix B).

Table 3.44 – ANOVA for delamination factor (F_d) of hybrid plates of two types (HIBG, HIBC).

Factor	Level S/N		SS	DF	V	% P	F
	1	2					
Feed	-0.66	-0.55	0.027	1	0.027	32	41
Speed	-0.59	-0.63	0.004	1	0.004	4	5
Interaction	-0.66	-0.56	0.019	1	0.019	23	29
Tool	-0.67	-0.54	0.031	1	0.031	37	47
Material	-0.62	-0.59	0.002	1	0.002	2	3
Error			0.001	2	0.0007	2	
TOTAL				7		100	

SS – sum of squares; DF – degree of freedom; V – variance; %P – percentage of contribution; F- result of F-test.

Based on these results, it was decided that there was no need to analyse the alternate hybrid HIBG, as the influence on final results is small, according to ANOVA results. From the same experiment, it was also possible to establish the significant influence, both physical and statistical, of feed and tool geometry, and the minor influence of cutting speed in delamination results. A strong interaction between feed and speed was noted. It means that the variation of one parameter can have some effect on the other. According to L8 array a feed of 0.025 mm/rev shall be combined with a cutting speed of 80 m/min in order to minimize delamination.

As a final note on the use of radiography, figure 3.38 compares the best results of delamination factor for the three materials and three main tools experimented.

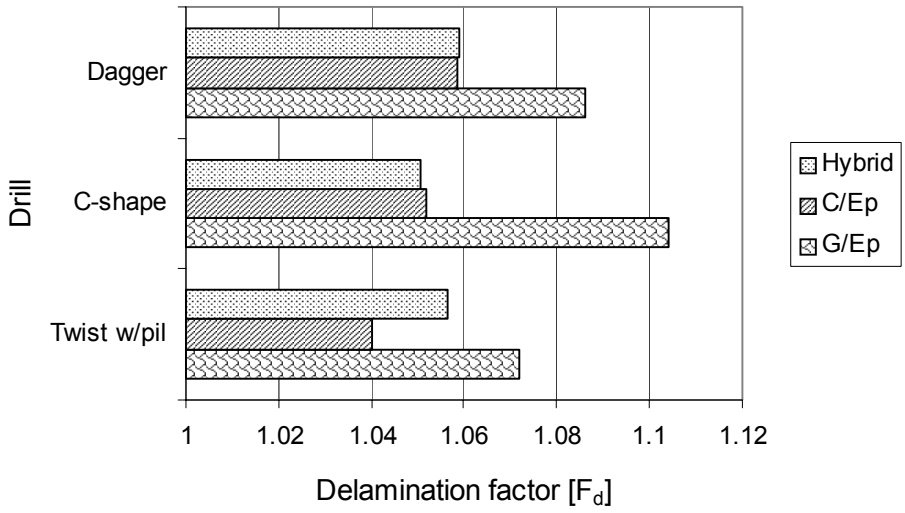

Figure 3.38 – Best results of delamination factor (F_d) for all materials and tool geometries.

From the above figure, it is evident that fair holes, with F_d <1.10, can be executed using carbide drills, as long as appropriate parameters are selected. Another possible conclusion is that these values can be achieved without the use of a sacrificial plate. This can be important as in some cases the use of such plate is not possible because of accessibility conditions.

Results for the three materials are not very different with the exception of twist drill in hybrid plates, where some delamination can be caused by the drill tip at the glass/ carbon interface, thus leading to poorer results in these materials.

3.3.3 ULTRASONIC SCANNING (C-SCAN)

As referred before, ultrasonic inspection is a good technique to detect delaminations, as they are perpendicular to the propagation direction of the wave and so reflecting them. In our work C-Scan method, ultrasonic inspection with sweeping commanded by a motorized X-Y table, was used. The ultrasonic scanning was made with Ultrapac II equipment and a 5 MHz transducer was used. Other frequencies available - 1 and 2.5 MHz - did not show good results in damage detection. The parameter used for the measurement of the echo was time-of-flight (TOF). The result, given in a colour scale, can be related with the depth from the transducer at which the wave hits an obstacle that causes its reflection. In the equipment used, the result was given in a colour scale. The top side of the plate also caused an echo that needs to be ignored by the system in order to detect the damage that exists inside the plate. This echo and the area considered are shown in figure 3.39. The area of greater signal amplitude is the echo due to the top of the plate and the region marked light blue is the analysis length that will give information to the equipment to be considered as analysis echoes.

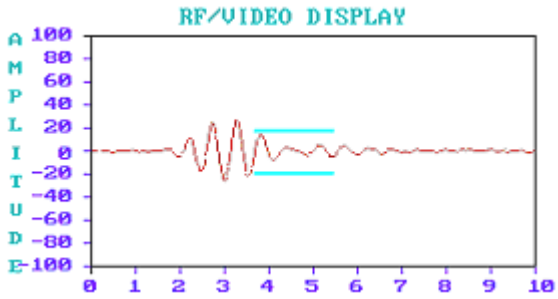

Figure 3.39 - Echo of the top side of the plate and area considered for analysis.

Final result of an ultrasonic analysis is shown in figure 3.40. The red area corresponds to the echo caused by the opposite end of the plate. The scale located at the left side shows that echoes caused by earlier reflections, which means the existence of damage located close to the top surface, will change colour from red to blue passing through green. The best results were achieved in the scanning of carbon/epoxy plates. For glass/epoxy plates a strong attenuation of the signal caused by the echo of the plate top side has the consequence of reducing the 'useful' width of the part and leading the equipment to be able to detect damages only in a small thickness of the part.

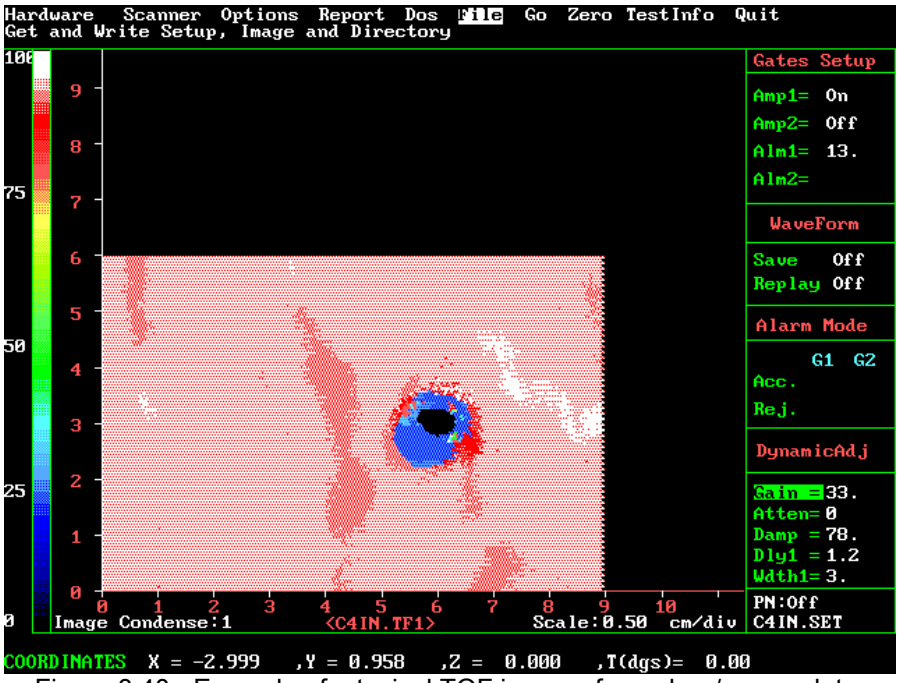

Figure 3.40 - Example of a typical TOF image of a carbon/epoxy plate.

Hybrid parts were even more difficult to analyse. The presence of successive layers of different materials, with different sound propagation speed, caused greater signal attenuations, narrowing so much the analysed width that it becomes useless in terms of damage evaluation. Next figures try to explain the problems encountered. Note the black region in the hybrid image, that can be interpreted as hole plus damaged area, although there is no certainty in this interpretation.

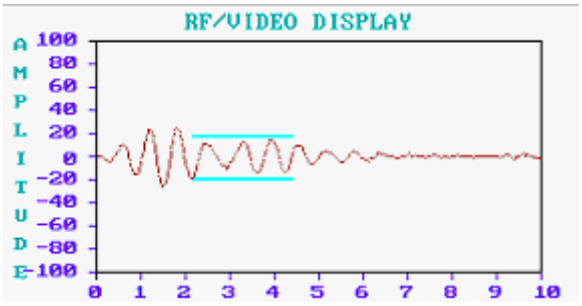

Figure 3.41 - Signal echo in a hybrid plate HIBC.

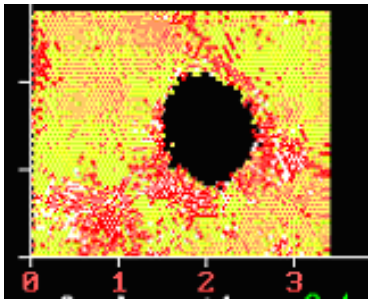

Figure 3.42 - TOF image of a hybrid plate.

The presence of such difficulties results in a less intensive use of this technique. Carbon/epoxy plates were C-scanned, but glass/epoxy and hybrid plates were left to radiography only. It should be also noted that there is a distortion of the shape of the hole in the scan images. That can be a consequence of the beam diameter – 6.35mm – as in some regions the transducer will 'read' the existence of the hole and also the surrounding plate. No way was found to avoid the system to give its view of those areas with the existing transducers. This leaves a region where the existence of damage may not be detected, due to possible erroneous lectures.

Experiments done by Tsao and Hocheng [69] with a transducer with a smaller beam diameter - 3.2 mm – resulted in images much more closer to the expected, specially regarding hole format.

This analysis method deserves more attention in future works, using adequate transducers, with diameters of 3.2 mm or smaller, and frequencies of 10 and 15 MHz in order to improve detection of damage shape and depth.

Images from ultrasonic C-Scan were used for the evaluation of damaged area around the hole, with the help of the computational vision that is described in 3.3.5. The digital nature of the images, in pixels, turns them ready to further measurement by the method described there.

3.3.4 SPECKLE INTERFEROMETRY

An attempt with the ESPI - Electronic Speckle Pattern Interferometry – technique was made to evaluate the detection of damages generated at the hole boundary due to the drilling process. This experiment was conducted by the LOME – Laboratory of Optics and Experimental Mechanics -, a laboratory integrated in INEGI – Instituto de Engenharia Mecânica e Gestão Industrial.

For that purpose, three test samples were executed, one of them in prepreg glass/epoxy, from manual lay-up and a third in prepreg carbon/epoxy. All the parts were drilled with HSS drills of 8 mm diameter with a cutting speed of 70 m/min and a feed of 0.15 mm/rev. These parameters were chosen in order to have a substantial damage around the holes. The photographs of the parts show their visual appearance.

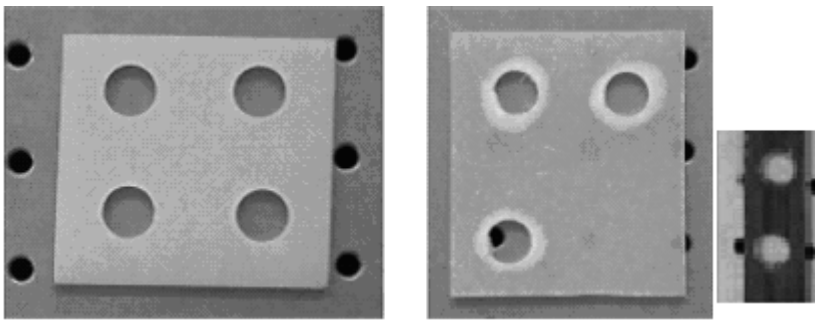

Figure 3.43 – Drilled plates for ESPI.

All the parts have shown, when visually inspected, an evident damage around the hole. The first deformation technique used was the slight heating of the plate. As it is shown in the pseudo 3D representation in figure 3.44, there was a global deformation of the plate. However, no localized temperature gradient was noted in hole surrounding area.

In this case, it can be said that, in spite of the evidence of damages in the plate, they do not have any influence on the displacement field at the surface. That led to the conclusion that this is not the most adequate technique to detect this kind of damage. Even after the calculation of the derivative of the displacement fields in the horizontal direction, no detection of the damaged or delaminated area was possible.

Figure 3.44 – Displacement field in the normal direction to heated plan of a glass/epoxy plate.

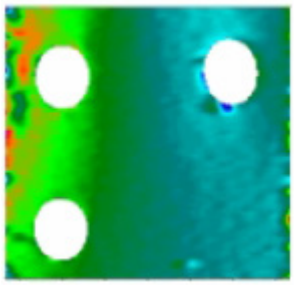

Figure 3.45 – Displacement field derivative in the horizontal direction of a glass/epoxy plate.

Identical procedures were used to the analysis of the carbon/epoxy plate – figure 3.46. Again, the results did not show any damage that can be detected by this technique.

As a conclusion from the use of ESPI, it seems that this is not an adequate technique to the detection of internal delaminations at the hole boundary and surrounding areas. ESPI have been described in the evaluation of surface damage, such as impact damage, with good results.

Figure 3.46 – Displacement field of the carbon/epoxy plate.

3.3.5 COMPUTATIONAL VISION

The use of Computational Vision has the purpose to reckon from the images obtained either by radiography or C-Scanning, information regarding damaged area or diameter. This process has the advantage of reducing operator dependence to measure the dimensions wanted, thus increasing results reliability. An existing processing and image analysis platform was used [120, 121]. This platform turned possible the use of some standard Computational Vision techniques [122, 123, 124] to accomplish the required values regarding damage measurement around the drilled hole.

According to the kind of image considered, different processing and analysis sequences need to be established. For radiographic images, the first step was the selection of the interest zone. This step was manually executed and has just the objective of reducing computational time involved in the following steps. The second step was the pre-processing of the sub image by a smoothing filter to reduce sudden changes of intensity thus reducing existing noise. Next step, on the smoothed image, was the segmentation of the interest areas. In many cases, this step results in a large number of segmented areas, so it is needed to eliminate those who were not relevant. Noise areas were eliminated by the application of erosion and dilation morphologic filters. After this processing step, each image is mainly the concern damaged area plus its background. In the final step, a region processing and analysis algorithm is applied to differentiate the several regions in each image, and for each region a certain number of measurements is presented. In figure 3.47, an example of the processing steps is shown for a radiographic image, with each step identified.

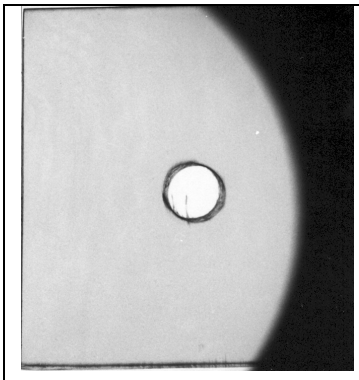

a) Original image (25% reduced).

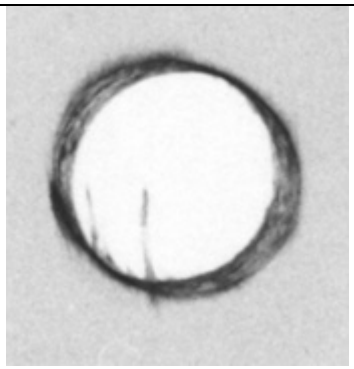

b) Interest zone (100%).

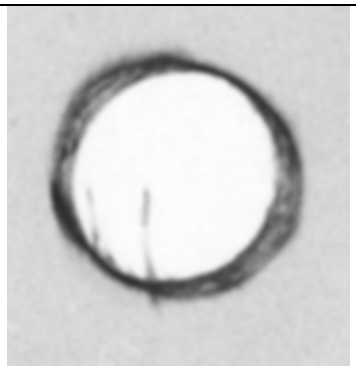

c) After smoothing

d) After segmentation.

e) After morphological filters applied

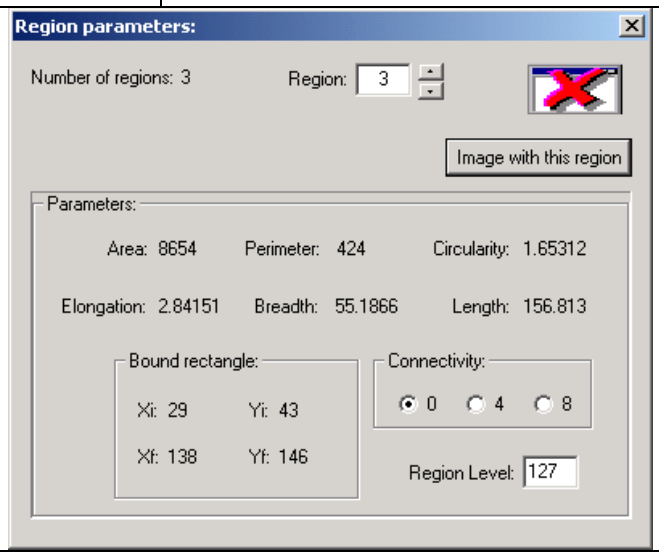

f) Area identification and measurement results

Figure 3.47 – Example of the determination of the necessary measurements in an image obtained by radiography using Computational Vision techniques.

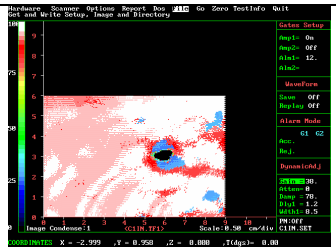

a) Original image (25% reduced).

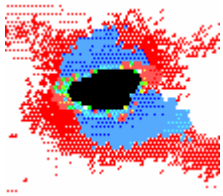

b) Interest zone (100%).

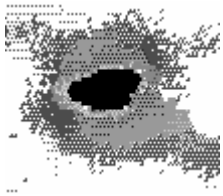

c) After smoothing.

d) After noise pixels removal.

e) After segmentation.

f) After morphological filters applied.

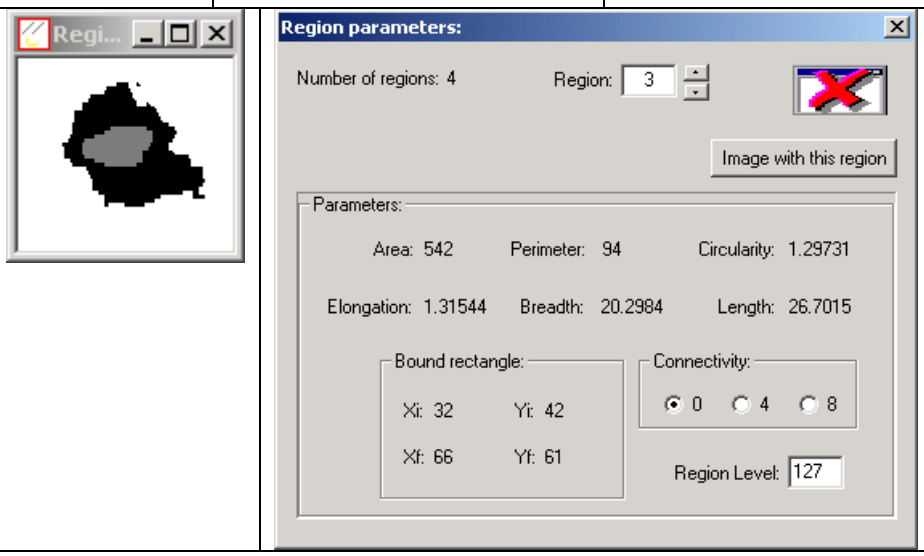

g) Area identification and some measurement results.

Figure 3.48 – Example of the determination of the necessary measurements in an image obtained by ultrasonic C-Scan using Computational Vision techniques.

For C-Scan images, the processing and analysis sequence was slightly different. The first step was, as before, the selection of the interest zone. Each colour image was then converted into grey levels. After this conversion was done, the pixels that were not included in the interest zones were removed. For this operation, a segmentation operation was used by selecting an adequate threshold level of grey. So, pixels below that level are classified as noise and removed. After this operation was completed, the images were binarized and subjected to the application of morphological filters to get

homogeneous regions. Final processing step is the same as for the radiography images, and consists in the application of the region processing and analysis algorithm to obtain the desired measurement. Figure 3.48 shows a sequence of the processing and analysis steps for the C-Scan images.

The results from these measurement procedures give the possibility to determine the values of the damaged area according to two different criteria, the delamination factor proposed by Chen [68] and the damage ratio proposed by Mehta et al. [72]. Considering the presence of irregular shape of the damage around the hole that can cause distortions between the two criteria, and the fact that delamination factor was largely used in 3.3.2, main focus in this section will be given to damage ratio – D_{RAT} – criteria (page 51, Eq. (2.5)). This criteria is based in a quotient between hole peripheral damage area and drilled hole nominal area, whose values are given by the Computational Vision methodology here described. As the measurement of damaged diameters is possible, even without the use of this method, as referred by other authors [54, 68, 69, 70], it is more interesting to demonstrate the advantages of the method going a little bit further in the damage assessment criteria used.

Some difficulties were encountered in the processing of radiographic images of glass/epoxy plates, due to the dispersion caused by the contrast of the glass fibres in the matrix. As this material was not the main target of the study, more attention in this work is paid to carbon/epoxy plates and, in the end, an analysis of hybrid plates was also done.

The first measurement was the evaluation of the pilot hole effect, confirming that the diameter of 1.1mm was the best option among those experimented. However, it is noteworthy that the results for a 2.3 mm pilot hole have results that are not very far, as was expected by the results of delamination factor presented in 3.3.2.

Table 3.45 – Damage ratio for pilot hole drilling of carbon/epoxy plates.

Tool	Pilot hole [mm]	Speed [m/min]	Feed [mm/rev]	Damage ratio D_{RAT}
Twist drill	1.1	80	0.05	1.212
	2.3	80	0.05	1.216
	3.5	80	0.05	1.261
	Without	80	0.05	1.271

Perhaps some more attention should have been given to this particular feature of the drill geometry, as the pilot hole diameter is an important variable in such definition.

However, and for the scope of this work, the present evaluation was judged to be sufficient. The assumption of the pilot hole diameter was made based in a study of a delamination model and subsequent experiences by Won and Dharan [64] and referred in section 2.4, pointing a ratio between pilot hole and final diameter of 0.18 for CRFP – carbon fibre reinforced plastic – with a Poisson ratio of 0.3. As the final hole has a diameter of 6 mm, that will lead to a pilot hole diameter of 1.08 mm, which was rounded up to 1.1 mm, for convenience.

Evaluation of the three different drill geometries was done using L4 Taguchi's orthogonal arrays, both for carbon/epoxy and hybrid plates. In order to justify the absence of a particular study for the two hybrid plates' sequence, another Taguchi orthogonal array was done considering the study of stacking sequence influence on hybrid plates.

In the following tables the several arrangements and results are presented.

Table 3.46 – Levels of drill test factors for carbon/epoxy and hybrid plates.

Tool	Feed rate [mm/rev]		Cutting speed [m/min]	
	Level 1	Level 2	Level 1	Level 2
Twist drill with 1.1mm pilot	0.025	0.05	80	102
C-shape				
Dagger	0.05	0.08	30	38

The results are shown separately, first for carbon/epoxy plates and for each drill (see Appendix B).

Table 3.47 – ANOVA for damage ratio of carbon/epoxy plates, using a twist drill with 1.1mm pilot hole.

Factor	Level S/N		SS	DF	V	% P	F
	1	2					
Feed	-0.80	-1.52	0.514	1	0.514	82	6.4
Speed	-1.24	-1.07	0.031	1	0.031	5	0.4
Error			0.080	1	0.080	13	
TOTAL			0.625	3		100	

SS – sum of squares; DF – degree of freedom; V – variance; %P – percentage of contribution; F- result of F-test.

Best parameters: feed rate of 0.025 mm/rev; cutting speed of 102 m/min.

Feed rate has physical significance on damage ratio. Speed has a minor significance on damage ratio.

Table 3.48 – ANOVA for damage ratio of carbon/epoxy plates using a C-shape drill.

Factor	Level S/N		SS	DF	V	% P	F
	1	2					
Feed	-1.52	-1.51	0.0001	1	0.0001	0	0.001
Speed	-1.06	-1.97	0.832	1	0.832	95	18
Error			0.046	1	0.046	5	
TOTAL			0.877	3		100	

SS – sum of squares; DF – degree of freedom; V – variance; %P – percentage of contribution; F- result of F-test.

Best parameters: feed rate of 0.025 mm/rev; cutting speed of 80 m/min.

Cutting speed has physical significance on damage ratio. This result comes in the opposite direction of all the others, including papers referred in chapter 2. This can be caused by the use of an excessive cutting speed – 102 m/min - for C-shape drill, when cutting carbon fibres.

Table 3.49 – ANOVA for damage ratio of carbon/epoxy plates using a *Dagger* drill.

Factor	Level S/N		SS	DF	V	% P	F
	1	2					
Feed	-4.38	-4.91	0.280	1	0.280	92.8	14
Speed	-4.63	-4.67	0.001	1	0.001	0.4	0.1
Error			0.020	1	0.020	6.8	
TOTAL			0.302	3		100	

SS – sum of squares; DF – degree of freedom; V – variance; %P – percentage of contribution; F- result of F-test.

Best parameters: feed rate of 0.05 mm/rev; cutting speed of 30 m/min.

Feed rate has physical and statistical significance on damage ratio.

The following tables show the results for hybrid plates, in HIBC configuration (table 3.8, page 105).

Table 3.50 – ANOVA for damage ratio of hybrid plates, using a twist drill with 1.1mm pilot hole.

Factor	Level S/N		SS	DF	V	% P	F
	1	2					
Feed	-3.68	-3.95	0.0730	1	0.0730	59.1	1.5
Speed	-3.82	-3.81	0.0001	1	0.0001	0.1	0
Error			0.0504	1	0.0504	40.8	
TOTAL			0.1235	3		100	

SS – sum of squares; DF – degree of freedom; V – variance; %P – percentage of contribution; F- result of F-test.

Best parameters: feed rate of 0.025 mm/rev; cutting speed of 102 m/min.

Feed rate has moderate significance on damage ratio.

Table 3.51 – ANOVA for damage ratio of hybrid plates using a C-shape drill.

Factor	Level S/N		SS	DF	V	% P	F
	1	2					
Feed	-1.13	-1.21	0.0075	1	0.0075	48	40
Speed	-1.22	-1.13	0.0081	1	0.0081	51	43
Error			0.0002	1	0.0002	1	
TOTAL			0.0158	3		100	

SS – sum of squares; DF – degree of freedom; V – variance; %P – percentage of contribution; F- result of F-test.

Best parameters: feed rate of 0.025 mm/rev; cutting speed of 102 m/min.

Both feed rate and speed have physical and statistical significance on damage ratio.

Table 3.52 – ANOVA for damage ratio of hybrid plates using a *Dagger* drill.

Factor	Level S/N		SS	DF	V	% P	F
	1	2					
Feed	-4.11	-4.16	0.002	1	0.002	1	0.02
Speed	-3.98	-4.28	0.091	1	0.091	35	0.5
Error			0.165	1	0.165	64	
TOTAL			0.258	3		100	

SS – sum of squares; DF – degree of freedom; V – variance; %P – percentage of contribution; F- result of F-test.

Best parameters: feed rate of 0.05 mm/rev; cutting speed of 30 m/min.

Both feed rate and speed have insignificant influence on damage ratio. A strong interaction between feed and speed is the cause of the low results found in F-test for factors feed and speed, below 1. That strong interaction is hidden by the error, with a percentage of contribution of 64% to the total variation.

The next table is the result of the experiment described in tables 3.43 and 3.44 for hybrid alternative comparison and the results lead to the conclusion that there was no need to proceed with further analysis on hybrid HIBG plates, as expected. Material influence on damage ratio is insignificant and lower than experimental error, as it can be seen by the results of the columns ‘percentage of contribution’ and ‘result of the F-test’ in table 3.53.

Table 3.53 – ANOVA for damage ratio of hybrid plates of two types (HIBC and HIBG).

Factor	Level S/N		SS	DF	V	% P	F
	1	2					
Feed	-3.71	-3.07	0.833	1	0.833	14	0.9
Speed	-3.81	-2.97	1.413	1	1.413	24	1.6
Interaction	-3.12	-3.66	0.596	1	0.596	10	0.7
Tool	-3.68	-3.10	0.694	1	0.694	12	0.8
Material	-3.6	-3.1	0.507	1	0.507	9	0.6
Error			1.776	2	0.888	31	
TOTAL			5.819	7		100	

SS – sum of squares; DF – degree of freedom; V – variance; %P – percentage of contribution; F- result of F-test.

From this experiment, an indication of best parameters to the drilling of hybrid plates are a feed of 0.025 mm/rev and a cutting speed of 102 m/min, using a carbide twist drill with 1.1mm pilot hole. Hybrid plates showed less sensitivity to the use of higher cutting speeds when compared with carbon/epoxy plates.

Finally, a more complete experiment was conducted for carbon/epoxy plates, joining two drill geometries in a L9 orthogonal array. Test factors and corresponding levels, as well as the results found are presented in the following tables.

Table 3.54 – Levels of L9 orthogonal array for carbon/epoxy evaluation of damage ratio.

Factor	Units	Level 1	Level 2	Level 3
Feed	mm/rev	0.1	0.05	0.025
Tool	-----	Twist with 1.1mm pilot	Twist with 3.5mm pilot	C-shape
Cutting speed	m/min	53	80	102

Table 3.55 – ANOVA for damage ratio of carbon/epoxy plates.

Factor	Level S/N			SS	DF	V	% P	F
	1	2	3					
Feed	-1.27	-1.62	-1.24	0.272	2	0.136	18	1.6
Tool	-1.16	-1.80	-1.17	0.807	2	0.403	55	4.9
Speed	-1.29	-1.49	-1.34	0.068	2	0.034	5	0.4
Error				0.333	2	0.166	22	
TOTAL				1.480	8		100	

SS – sum of squares; DF – degree of freedom; V – variance; %P – percentage of contribution; F- result of F-test.

From this experiment, a conclusion of the best choice for carbon/epoxy plates was the use of a twist drill with 1.1 mm pilot hole, with a feed of 0.025 mm/rev and a cutting speed of 53 m/min. These parameters are well inside the optimum range selected by

Enemuoh et al. [66], with a cutting speed between 40 and 60 m/min and a feed rate of 0.017 to 0.051 mm/rev, for twist drills with an optimum point angle of 118º.

When applying the predictive equation [118]

$$y_{predicted} = \bar{y} + (\bar{y}_A - \bar{y}_{\exp}) + (\bar{y}_B - \bar{y}_{\exp}) + (\bar{y}_C - \bar{y}_{\exp}) \quad (3.4),$$

the value for the damage ratio for twist drill with a 1.1 mm pilot hole, becomes **1.113**.

A similar experimental procedure was applied to hybrid HIBC plates in order to evaluate the effect of 53 m/min as cutting speed for this material. However, in order to reduce the number of experiments to be made, a L8 orthogonal array was selected, with only three factors at two levels each. Experimental condition was as shown in table 3.56.

Table 3.56 – Levels of L8 orthogonal array for hybrid (HIBC) evaluation of damage ratio.

Factor	Units	Level 1	Level 2
Feed	mm/rev	0.025	0.05
Cutting speed	m/min	53	102
Interaction of feed and speed		1	2
Tool		Twist with 1.1mm pilot	C-shape
Blank			
Blank			
Blank			

Results are presented below.

Table 3.57 – ANOVA for damage ratio of hybrid (HIBC) plates.

Factor	Level S/N		SS	DF	V	% P	F
	1	2					
Feed	-0.80	-1.04	0.116	1	0.116	17	2.6
Speed	-0.71	-1.13	0.348	1	0.348	51	7.7
Tool	-0.85	-0.99	0.041	1	0.041	6	0.9
Interaction	-0.85	-1.00	0.044	1	0.044	6	1.0
Error			0.136	3	0.045	20	
TOTAL			0.685	7		100	

SS – sum of squares; DF – degree of freedom; V – variance; %P – percentage of contribution; F- result of F-test.

Looking at the results obtained with this experimental evaluation, a conclusion about the best choice for tool and drilling parameters in HIBC plates, from those used, is possible. The recommended tool is a twist drill with a 1.1 mm pilot hole, with a feed of 0.025 mm/rev and a cutting speed of 53 m/min. It is worth mentioning that this conclusion is equal to the result obtained for carbon/epoxy plates.

It is possible to say that the main factor for drill and parameter choice is the reinforcement fibre used in the outer plies of the laminate. These plies will have a decisive influence on the damage caused and development of thrust forces during drilling. So, when hybrids laminates are to be machined, it is important to know what type of fibre is used in the upper ply, that will be the first to have contact with the tool, and the fibre in the bottom plies of the laminate, that will be responsible for the resistance to delamination onset.

3.3.6 ROUGHNESS MEASUREMENT

A conventional analysis of machined surface was carried after hole completion. This evaluation was done using a diamond stylus surface profilometer from Hommel, Tester 500 model, with a dedicated stylus holding part, which was able to fix in the machined hole. The roughness profile information obtained is analysed using specific software from Hommel, giving the parameters that characterize the surface. Normally, the low-frequency components of the signal that corresponds to shape and waviness are filtered out. Three main categories can be considered when giving roughness results: average roughness heights, statistical method and random process method. The results from the test are according to DIN 4777, with a cut-off length of 0.8 mm and a measurement length of 2.4 mm. In order to measure superficial roughness, a total length of 3.2 mm is needed using this setup. When plates with less than 4 mm thickness were used, measurement length was reduced to 1.6 mm and total length to 2.4 mm. Results given from the system are R_a – average surface roughness – R_z – ten-point average height – and R_m – maximum individual peak-to-valley height. Average surface roughness was presented in section 2.5.9. R_z and R_m were not considered in this work. The value that was always considered for roughness evaluation was the average surface roughness – R_a – and for each machining condition a minimum of 5 and a maximum of 8 measurements were made.

It should be noted that although each of the method provides unique information about the surface profile, adequate information about the surface can only be given using a combination of these parameters [106].

When metal machining is considered, there is a general understanding that greater speeds and lower feeds lead to smaller values of average surface roughness.

Results from the several roughness measurements done along this work, showed that there is a general trend to have lower values of R_a when feed rate lowers for every material. However, this trend is more pronounced in carbon/epoxy plates, and almost inexistent in glass/epoxy plates.

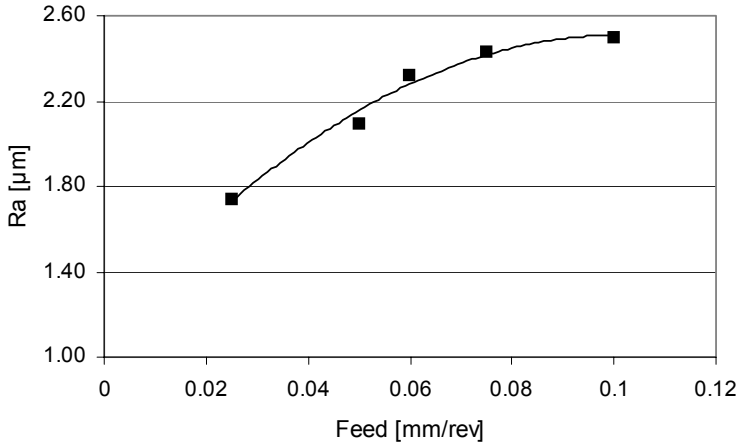

Figure 3.49 - Feed influence on roughness of carbon/epoxy plates.

The other factor, cutting speed, has different effects according to the plate material considered. When drilling carbon/epoxy plates, higher speeds reduced the average surface roughness. However, when correlating the data obtained from the roughness measurements, it seems that a 'critical cutting speed' can be considered, above which the roughness values will rise. From the data available, that speed could be in the range of 80 to 85 m/min. For glass/epoxy plates the trend is completely opposite with an increase of R_a values with the cutting speed. That give the curiosity to verify what the variation of the values of hybrid plates was, as those plates had 75% of glass plies in its construction. Results showed that the average roughness of hybrid plates increased with speed, however somehow not so pronounced as in glass/epoxy plates.

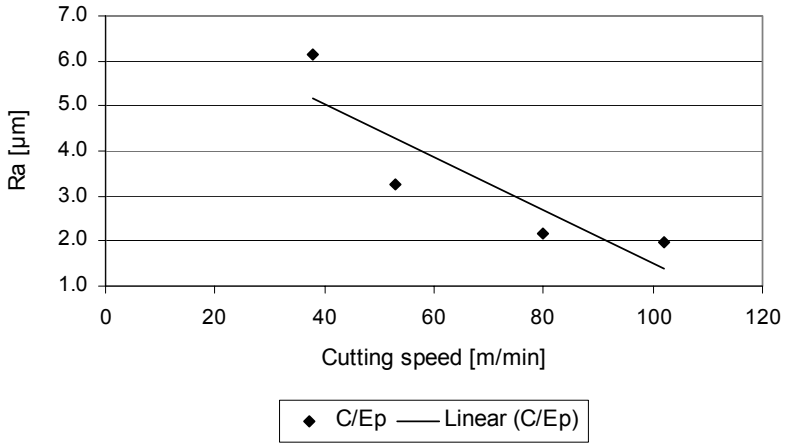

a)

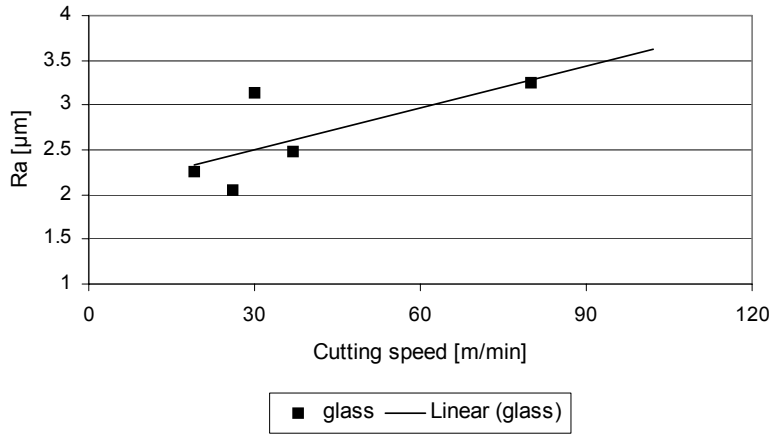

b)

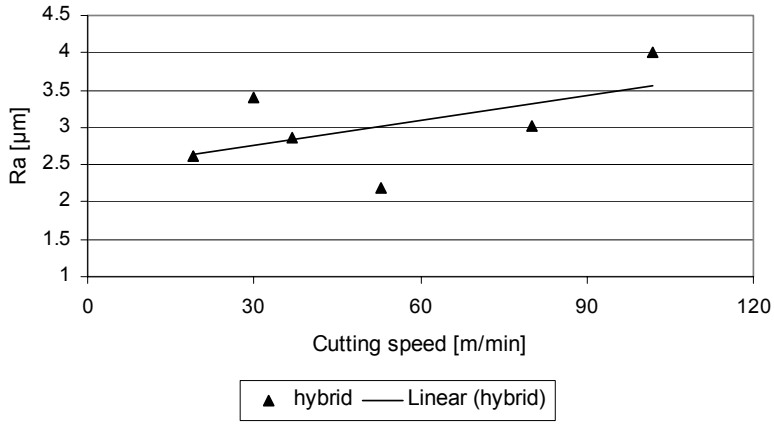

c)

Figure 3.50 – Cutting speed influence on surface roughness of: a) carbon/epoxy plates; b) glass/epoxy plates; c) hybrid (C+G)/epoxy plates.

A characteristic that was observed in all the materials was the large scattering of the results, showing that this roughness measurement method is sensible to the distribution of fibres and matrix material along the measurement length. In spite of that fact, some results can be given, as they can be of some interest when characterizing machined surfaces. Average of all results were different for the three materials considered in this work, although all in the same range, between 2.5 and 3 μm, with a large standard deviation.

Table 3.58 – Average roughness results of the three materials studied.

Material	Aver. R_a	Stand dev.	Max. R_a	Min. R_a
Carbon/epoxy	2.5	1.5	6.8	0.9
Glass/epoxy	3.1	1.6	6.8	1.6
Hybrids	2.9	1.3	4.4	1.1

When the effect for each tool and respective cutting parameter influence was analysed, there were some interesting results to note. Twist drills presented the best results for average surface roughness, except for carbon/epoxy plates where the values of R_a obtained with C-shape and *Dagger* drills were a little lower. With the other materials, roughness was greater with those drills. For *Dagger* drills, the values were higher, in the average, than those obtained with twist drills.

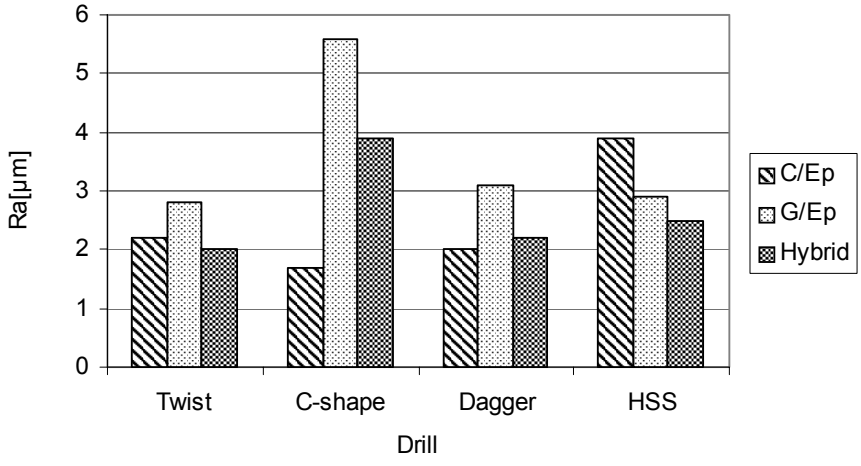

Figure 3.51 – Surface roughness results for the three materials used with four drill types.

These results can be interpreted as an indication of the appropriated drill to these materials. Based only on surface roughness, C-shape drills will not be recommended for the drilling of glass/epoxy plates, but will be adequate for carbon/epoxy plates. However, they also seem inappropriate for hybrid plates. So, the best selection will be the use of twist carbide drills for hybrid plates, as they represent the best average result of carbon and glass/epoxy plates.

When applying the ANOVA procedure to the several results measured, and following the same experimental selection already presented for thrust force and damage ratio analysis, it was found that, for average roughness, the effect of the parameters studied – feed rate and cutting speed – was low, with F-test under one, meaning that the experimental error was more significant than the parameter effect. This means that the parameters considered for cutting speed and feed rate had little significance to experimental results.

As a final note to roughness study, a paper of Ramulu is now recalled. In [106] he had said that although R_a is the most common mean of specification, is a poor indicator of surface damage, so composites need a combination of several parameters that describe and characterize the surface. Another statement comes from Hansen and Eriksen [110] when analysing surface profilometry by stylus instruments and optical profilometers. In the end they questioned if roughness values measured on FRP's could be compared to similar measurements on metals and about the reliability of stylus instruments. Both papers pointed for a need of a standardization of surface status for these materials.

The analysis made for this study lead to a similar conclusion about the poor significance of average surface roughness for damage assessment of composites machined surfaces.

3.3.7 BEARING TEST

The main purpose of making holes in any plate is to have the possibility to assemble it with other parts of a more complex structure. During service, parts will be subjected to efforts that will cause stress at the hole surrounding area, where a screw, bolt or rivet was placed. It is important for design engineers to know what the load carrying capacity of a connection is. A bearing test was utilized, ASTM D5961-01 [125], in order to analyse that capacity. This test determines the bearing response of multi-

directional polymer matrix composite laminates reinforced by high-modulus fibres. Two procedures are described in this standard. Procedure A – double-shear - was used. This procedure uses a single fastener, and is recommended for basic material evaluation and comparison. With this procedure, the target was to establish comparison between the several hole machining methods. According to section 6.5, damage due to hole preparation will affect strength results [125]. Procedure B is useful in evaluation of specific joint configuration, which is not the aim of this work. This test was executed with an INSTRON 4208, equipped with a data collection system. Tests were carried according to ASTM D5961-01, at a speed of 2 mm/min and data was collected by two separate systems, one connected to the test machine and a second one collecting data from the test machine and from the two LVDT used to dislocation measurement. Each test stops when a load maximum is reached and load has dropped about 30%.

The first set of tests according to this standard were done to three separate batches of glass/epoxy plates obtained by the three fabrication processes already described – hot plate press, manual and RTM – and a second set of carbon/epoxy plates. Different machining parameters were executed in the plates, in order to establish an ANOVA to every process. The objective was to evaluate the influence of feed rate, cutting speed and presence of pre-drilled hole in the final results – bearing stress – of these plates.

Generally the results showed that, in the range of parameters used and described in chapter 3.2, the experimental variation was superior to any effect measured. Considering the results, it looks as the main factor in this test is the material, and that it is necessary to have greater damage extent in order to get considerable differences in test results. The effect of the pre-drilling was an increase of the bearing stress by 2.6%, which has to be considered as positive. The average standard deviation is around 10%, meaning a dispersion of the results greater than the pre-drilling effect, and so conclusions are to be looked cautiously.

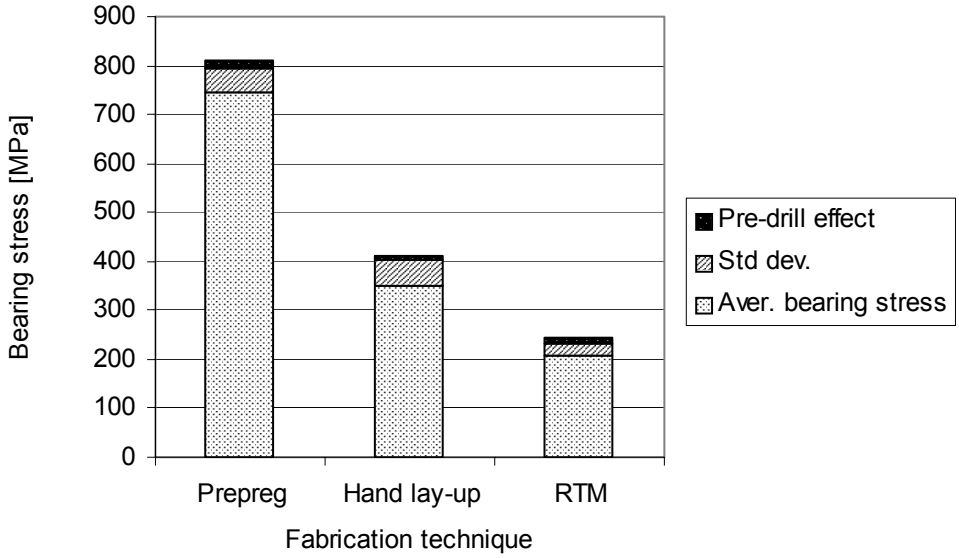

Figure 3.52 – Results from the bearing tests performed on glass/epoxy plates.

Similar experience was done to carbon/epoxy plates. Here, some relevance was found for the factors studied – pre-drilling, feed and speed. The contribution of each of these factors was approximate to the standard deviation, around 3%. It is interesting to note the lower value of the bearing stress for these plates, when compared with those of glass/epoxy plates from prepreg. That shows the greater importance of compression mechanisms in this test.

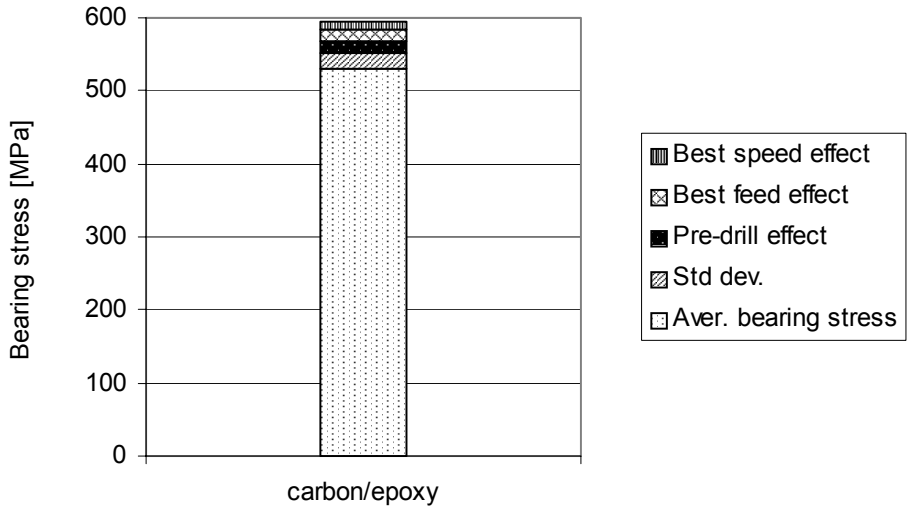

Figure 3.53 – Results from the bearing tests performed on carbon/epoxy plates.

Finally, a test was carried out for hybrid plates. For this material, the influence of pilot hole was not analysed and the only purpose was to have reference values. Tools used and drilling conditions are in table 3.59. The results of bearing stress are shown in the same table. A fact to observe is that the value of bearing stress of hybrid plates was almost equal to those of glass/epoxy plates and superior to what could come from the direct application of the rule of mixtures (equation 3.1 in page 101) – 700 MPa. This can be a good demonstration of the "hybrid effect", that is used to describe the phenomenon of an apparent synergistic improvement in the properties of a composite containing two or more types of fibre [5].

Table 3.59 – Results of the bearing test with hybrid plates.

Tool	Speed (m/min)	Feed (mm/rev)	Bearing Stress (MPa)	Std variation
Carbide twist with 1.1mm pilot hole	53	0.025	759	11
C-shape	53	0.025	737	15
Dagger	38	0.05	733	12
HSS twist	19	0.09	720	15
Overall average results			739	18

3.3.8 DOUBLE CANTILEVER BEAM (DCB) TEST

According to the models used to the determination of the critical thrust force for the onset of delamination [46, 64, 65, 85, 86, 87, 88, 89, 90, 91, 92, 93] and referred in chapter 2, the value of Mode I interlaminar fracture toughness – G_{IC} – is an important property. This value is the resistance to the initiation and propagation of a delamination crack in unidirectional fibre polymer matrix composite laminates under a load applied perpendicular to the plane of delamination [126]. These tests use the double cantilever beam specimen defined in ISO /DIS 15024. The mode I specimen - figure 3.54 - has two piano hinges bonded at one end of the laminate for the application of a load perpendicular to the interlaminar layer. Initiation of delamination along the intermediate layer is set by the insertion of a thin PTFE film during laminates fabrication. Following the standard indications, this film is inserted at the mid-thickness of all laminates that are to be tested.

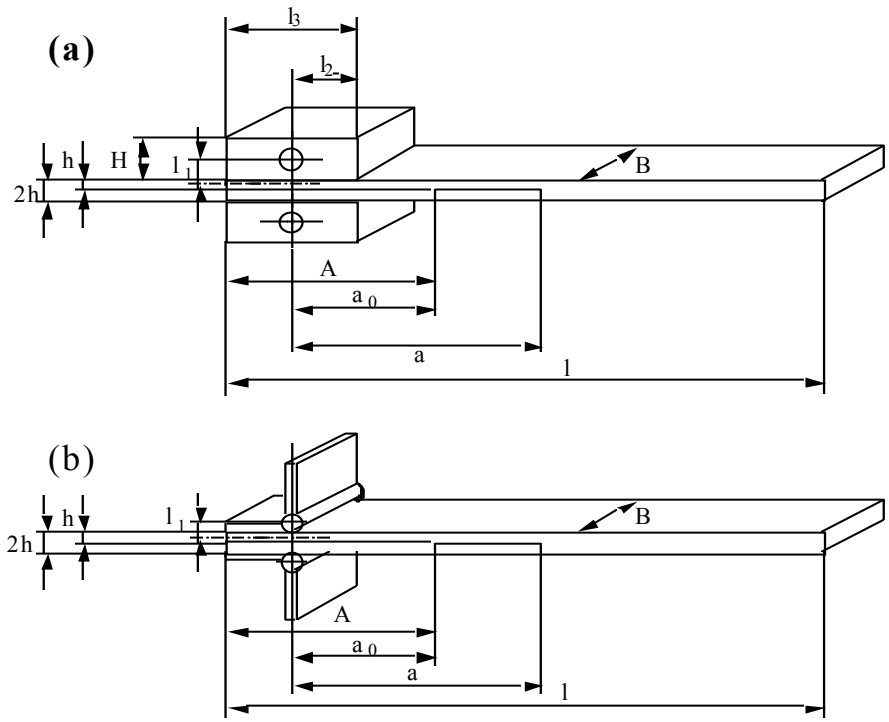

Figure 3.54 – Geometry for the DCB specimen: a) load-blocks; b) piano hinges [126].

Different values of G_{ic}, with some scattering, were found in the literature for carbon/epoxy plates. From the lower value in [128] – 90 J/m^2 – to the higher value in [24] – 304 J/m^2 – a number of intermediate values were also found in other published papers [63, 85, 87, 88, 127]. However, the largest number of values is in the range from 250 to 304. It seems that test result is highly material dependent and the results found are from the same kind of material, but from different suppliers.

For glass/epoxy only one result was found [128] – 525 J/m^2 – and no value was found regarding the hybrid plate's construction under evaluation.

Three batches of samples were executed, according to test standard. The plates stacking sequence was different from the one used for drilling experiments. The conditions defined in the standard indicate the use of unidirectional laminate plates, in order to avoid fibre bridging that is reported to occur when testing multidirectional laminates, and is not representative of the composite material tested. One batch was made only in carbon/epoxy, with a thickness of 3 mm and a second one only in glass/epoxy and 5 mm thickness. The third batch intended to determine the value of G_{IC} in hybrid plates. With that purpose, the plate was done with all the plies in carbon/epoxy except one in glass/epoxy. This odd ply was located at one side of the

starter film. Final thickness of the hybrid plate was 3 mm. With this setup the crack opening will occur along an interface between a carbon reinforced ply and a glass reinforced ply.

Tests were done in an INSTRON 4208 test machine, equipped with a data collection system, at a speed of 5 mm/min. The initial delamination was simulated by applying a pre-load until the first increment of delamination from the insert was detected. Then the specimen was unloaded, followed by re-loading. The crack length delamination increments were controlled visually with the help of a magnification glass and registered. Results for the three materials are presented in table 3.60.

Table 3.60 – Interlaminar fracture toughness values.

Material	Carbon/epoxy	Glass/epoxy	Carbon-glass (hybrid)
G_{Ic} (J/m^2)	290	568	299

These results show that, when delamination onset is considered, hybrid plates will have critical thrust force values that are almost equal to those considered for carbon/epoxy plates, at the hybrid interface.

Values of interlaminar fracture toughness will be used in the finite element model, described in chapter 4.

3.4. CONCLUSIONS FROM EXPERIMENTAL WORK

Drilling of holes in laminate plates was the main work carried out during the experimental stage. During and after hole completion data was gathered in order to be able to relate the damage encountered around the hole with the various parameters analysed. Main focus was given to the measurement of delamination caused by the drilling operation and the application of known criteria to evaluate and compare this damage under different conditions and even from dissimilar materials.

Materials used in this work were of three types: glass/epoxy plates, carbon/epoxy plates and hybrid (carbon+glass)/epoxy plates. The first type was divided in three different fabrication procedures, hot press plates, manual lay-up and RTM. Due to the nature of the study and the need to have comparable data for the three types, more attention was given to the prepreg materials, leaving manual lay-up and RTM behind. For all the materials used, a number of tests were performed in order to have basic information about material properties, like tensile and flexural tests, fibre weight determination, dynamic mechanical thermal analysis (DMTA) and double cantilever beam (DCB) – tables 3.4, 3.7, 3.9 and 3.60.

Tools materials used were HSS – high speed steel –, carbide and coated carbides. Diamond tools, in spite of their good performance when drilling fibre reinforced thermosets, were not employed as they have been considered as not cost effective when compared to carbide drills. Several geometries of carbide tools were used along the experimental work like twist drills, step drills, C-shape drills and *Dagger* drills. The advantages and disadvantages of each drill geometry was discussed and the results evaluated in terms of maximum thrust force during drilling and delamination around the hole.

The measurement of thrust force and torque was done using a dynamometer coupled to an amplifier and a personal computer.

Acoustic emission techniques are already used for the detection of delamination in quasi-stationary processes like tensile or fatigue testing with good results. The use of this technique during drilling will need a preliminary work of noise characterization before the application on the detection of damages that are located near the tool like delamination of others. Eventually, alternative setups have to be experimented.

The use of enhanced radiography was relatively easy to establish. Some know-how about the use of this technique as well as the necessary equipment was available. It

needed only to establish the procedure regarding dipping times in di-iodomethane, exposure time to radiation and film development. Once this procedure was established, radiographic work was able to give good results in terms of enabling images that could be used for delamination measurement. One of the greatest advantages in the use of this technique was the possibility to 'see' the delamination that occurs in opaque materials, as is the case of carbon/epoxy plates or hybrid plates with carbon reinforced plies at the surface. Some drawbacks can be pointed out when using radiography. The first is related with the nature of the process itself, as the image obtained is merely an orthogonal projection, not giving any information about the depth of the damage. The other is the need to immerse the plates in a hazardous and expensive liquid, that need to be carefully handled and used only in well ventilated areas. Enhanced radiography was able to supply a good amount of information regarding delaminated areas, mainly for carbon/epoxy plates where the contrast was more evident. When used in plates containing glass/epoxy plies, the image was not so clear because of the visibility of glass fibres in radiography. This was more evident in RTM and manual lay-up plates as is shown in figure 3.55.

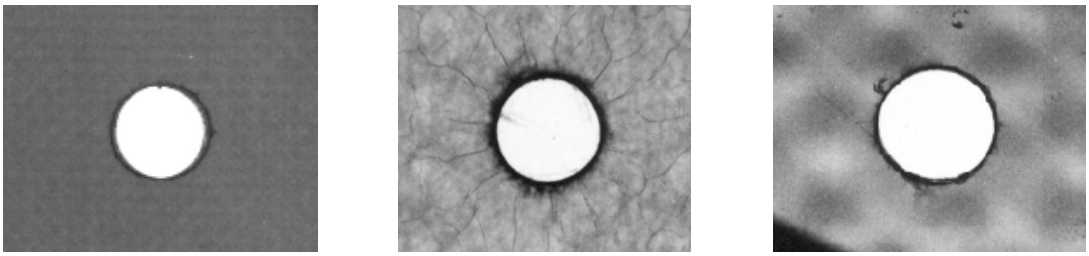

a) b) c)

Figure 3.55 – Radiographies of glass/epoxy plates: a) prepreg; b) RTM; c) hand lay-up.

Images obtained by radiography were used for the determination of delamination factor - F_d -, with the help of a profile projector for the measurement of delaminated diameter.

The images thus obtained were also used, after scanning, to a process of area reckoning and measurement by the use of Computational Vision techniques. This technique was able to give information about the maximum delaminated diameter and also the peripheral damaged area around the hole. With that information, it was possible to use other damage assessment criteria, the damage ratio – D_{RAT}. Both criteria were applied to the evaluation of the several drill geometries and parameter evaluation regarding feed rate and cutting speeds used. The use of Computational

Vision was possible by the use of an existing processing and image analysis platform, giving the possibility to measure accurately the dimensions needed. Once the sequence of image treatment was established, it was possible to apply it to a great number of images, thus obtaining a great number of results. The advantage of this processing method is that, once a threshold of damage pixel is established, it can be used successively to a group of images keeping the classification criteria constant. This technique can be applied, with necessary adaptations, to any other image evaluation needed, independently of the material. The use of this technique with glass/epoxy plates radiographs was not possible due to the difficulty in area isolation. Some improvements can be considered, regarding image capture techniques, in order to assist Computational Vision technique.

Another imaging technique used along this work was the ultrasonic C-scanning. The use of ultrasonic waves is a good technique to detect delaminations, as they are perpendicular to the wave direction, thus facilitating its detection by reflection. From the two parameters available at the equipment used, time-of-flight and amplitude, the former was found to be more useful. The advantage of the ultrasonic scanning is the possibility to have information regarding the depth of a given damage. That information is given by a colour or grey level scale where a correspondence exists between a given colour and the depth of the echo.

Although the process is reliable and able to supply useful information, some drawbacks need to be pointed out. The existence of a ‘shadow’ extent caused by the need to signal stabilization after the wave hits the top surface of the plate causes a narrowing of the scanned thickness of the plate. There will be an initial length where eventual damages will not be detected. This length can represent a large portion of the plate in the case of thin parts. This problem can be solved if a second scan is made turning the part upside down, but increasing inspection time. When scanning hybrid plates, this problem become more relevant. In those plates there were three ‘shadow’ zones along a 4mm thickness plate. These ‘shadows’ were caused by the top of the plate and the two transitions from carbon to glass and from glass to carbon reinforced plies. Because of this great extent of ‘shadow’ zone, the scanning of hybrids was abandoned. Another problem found when scanning carbon reinforced plates was the need to use transducers of smaller diameter than the one used – 6.35 mm –. It would be interesting to experiment the process with higher frequency transducers, like 10 or 15 MHz. These experiences will have to be programmed in a near future.

Another imaging technique that should deserve more attention is the use of computerized tomography – CT (TAC). A single experience was carried out, using medical equipment that was available at a certain moment. The images obtained in a carbon/epoxy plate were encouraging about the possibilities of the method. Regrettably, it was not possible to carry on with the experiments, as it was not allowed to change equipment settings. The use of CT technique has been reported by Persson et al. [43] and Cornelis et al. [102] in damage assessment of carbon reinforced composites.

An interferometry technique – ESPI, Electronic Speckle Pattern Interferometry - was attempted to damage detection in drilled plates. The conclusion from that experience was that this technique, although able to detect superficial damage, was not adequate when detecting internal delaminations at the hole boundary and surrounding areas.

Roughness measurement was done by profilometry. The equipment used was able to give results regarding the surface profile like average surface roughness - R_a -, ten-point average height – R_z - and maximum individual peak-to-valley height – R_m -. Only R_a values were considered in the analysis.

The results showed large scattering that can be explained by the existence, along the measured surface, of zones rich in fibre and other rich in resin. The former will have higher roughness due to the presence of pulled-out and bent fibres. The latter will be a zone of lower roughness due to the smoothness of a resin surface. The final result will be largely influenced by the proportion of these zones along the stylus path. In order to try to reduce this scattering every holes were measured more than once, with a 90º rotation of the part between two measurements. Even so, the scattering was substantial. This can be explained by the fact that along a hole surface, the stylus passes through the plate plies with fibres oriented differently and where the tool has exerted a cutting mechanism that is a function of the angle between the tool cutting edge and the fibre in each ply. Considering the existence of such variation in values, the roughness was only considered in average results.

3.4.1 INFLUENCE OF FEED RATE

For all the materials that were drilled in this work and for all the tools, a clear trend was found regarding the effect of feed rate. When comparisons of two or more feed

rates were considered, the best results were always found with the lower feed rate. During the experimental work, the lowest feed rate used was 0.025 mm/rev. The reduction of feed rate causes a reduction of the indentation force that is exerted on the uncut plies of a laminate, thus keeping thrust force value below the critical force for delamination onset. Although some authors have referred the use of lower feeds [1, 58, 62, 66, 69, 74] in the range of 0.015 to 0.02 mm/rev, further reductions have to be balanced with heating of the material surrounding the hole, as the possibility of softening matrix material increases when feed decreases. This feature calls for the application of thermograph techniques that were not used during drilling experiences, in order to have data considering heat distribution and temperature rise.

As a general conclusion, it can be said that when drilling fibre reinforced composites, feed rate should be as low as possible, in a range centred at 0.025 mm/rev. The use of CNC machines with a variable feed rate, as referred in [1], is a good option to consider, becoming possible to reduce feed rate as the drill reaches the bottom plies of the plate, and reducing thermal stresses on the matrix material by the use of higher feeds when the tool is at the top plates of a laminate.

Figure 3.56 shows feed influence on thrust force in the drilling of carbon/epoxy and hybrid plates. When data is correlated by a 2nd-polinomial curve, a minimum is identified at a feed rate of 0.022 mm/rev for carbon plates and 0.046 mm/rev for hybrid plates. If data is correlated linearly a positive slope is returned for both materials.

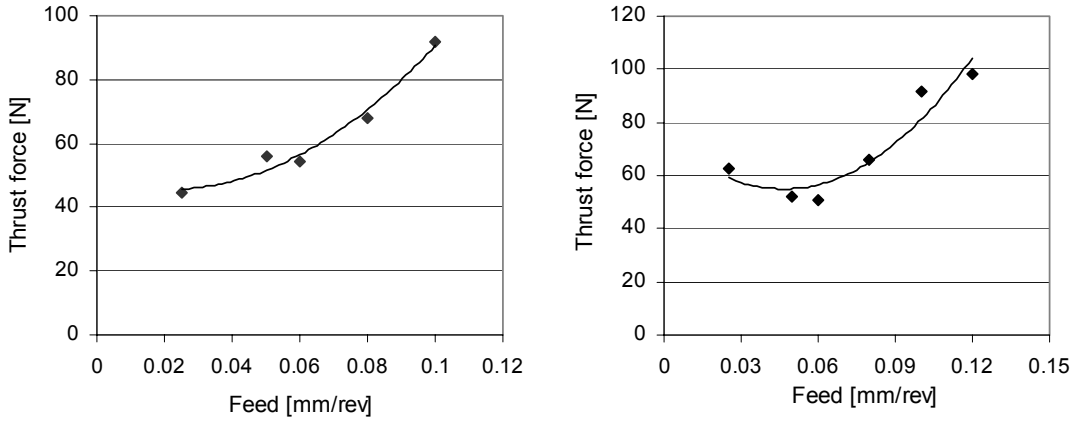

Figure 3.56 – Feed rate influence in thrust force: a) carbon plates; b) hybrid plates.

Figure 3.57 shows feed influence in delamination factor for the same plates. There is a clear trend to the reduction of the delamination factor when feed rate is lower.

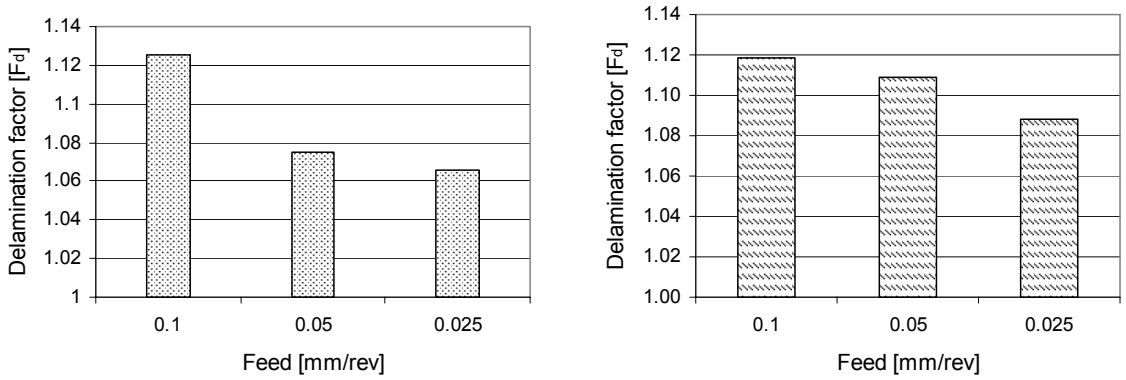

a) b)

Figure 3.57 – Feed rate influence in delamination factor: a) carbon plates; b) hybrid plates.

Feed influence on average surface roughness of carbon/epoxy and hybrid plates has the same trend with lower values when feed rate is 0.025 mm/rev, similar to what is normal when machining metallic materials.

When ANOVA analysis was used, feed had shown to have more significance than cutting speed both in thrust force and delamination around the hole.

Based on the available information from experimental work and references quoted in chapter 2, it is possible to conclude that, when drilling fibre reinforced plates, the recommended feed rate should be **0.025 mm/rev**, as long as the matrix material does not reach softening temperature.

3.4.2 INFLUENCE OF CUTTING SPEED

The results from the various experiences carried for this work give the possibility to draw some conclusions regarding the cutting speed range that should be recommendable when drilling plates from the materials used.

Although cutting speeds in the range of 80 to 100 m/min, based in tool supplier's information, were used for a long period of the experimental work, in the end it becomes evident that these speeds were too high in order to reduce plate damage.

Thus, final experiments have considered a speed of 53 m/min, corresponding to a rotation speed of 2800 rpm that is a common regulation value in vertical drilling machines. Results showed here incorporate values from that final experiment. The cutting speed of 53 m/min has been used at the first experiments, but then left for higher speeds, which is a good option for productivity, but not so good when damage reduction is the primary target.

Cutting speed has shown to be less significant than feed rate in both effects analysed, thrust force and damage around the hole. For this reason, it was considered that the experimental data was enough for the intended scope.

The influence of cutting speed in thrust force for carbon/epoxy and hybrid plates is shown in figure 3.58. When data is correlated by a 2nd-polinomial curve, a minimum is identified at a cutting speed rate of 62 m/min for carbon plates and 65 m/min for hybrid plates. It is interesting to note the proximity of the two values. For a 6 mm diameter drill, this cutting speed corresponds to a rotational speed of 3300 to 3500 rpm.

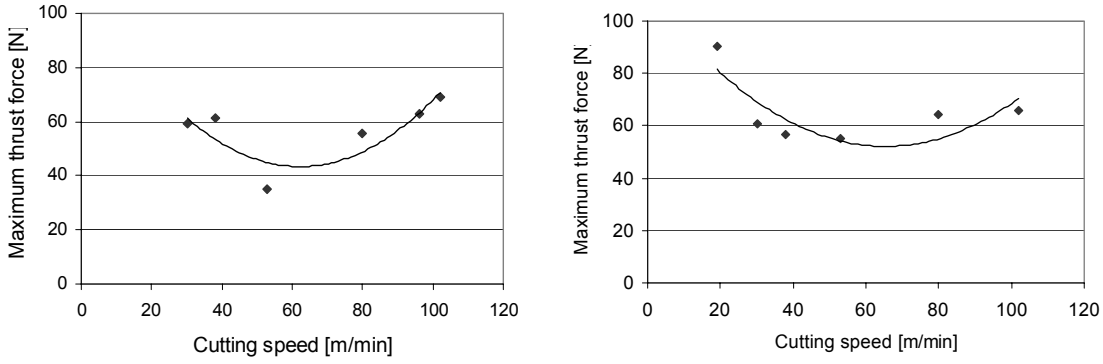

a) b)

Figure 3.58 – Cutting speed influence in thrust force: a) carbon plates; b) hybrid plates.

It must be remembered that glass/epoxy plates turned out to be more restrictive when cutting speeds are considered. Though a smaller number of results were considered, it appears that thrust force when drilling these plates lowers when reducing cutting speed. So, for glass/epoxy plates drilling, speed should be in the smaller values experimented, from 19 to 26 m/min.

Figure 3.59 shows cutting speed influence in delamination factor for the same plates. Once again correlation of data by a 2nd polynomial curve reveals a minimum for damage in the range of 50 to 60 m/min for carbon/epoxy and around 70 m/min for

hybrid plates. A 'critical cutting speed' may be considered for the drilling of carbon/epoxy and hybrid plates used. Speeds above and below will cause an increase in thrust force values as well as in delamination around the hole.

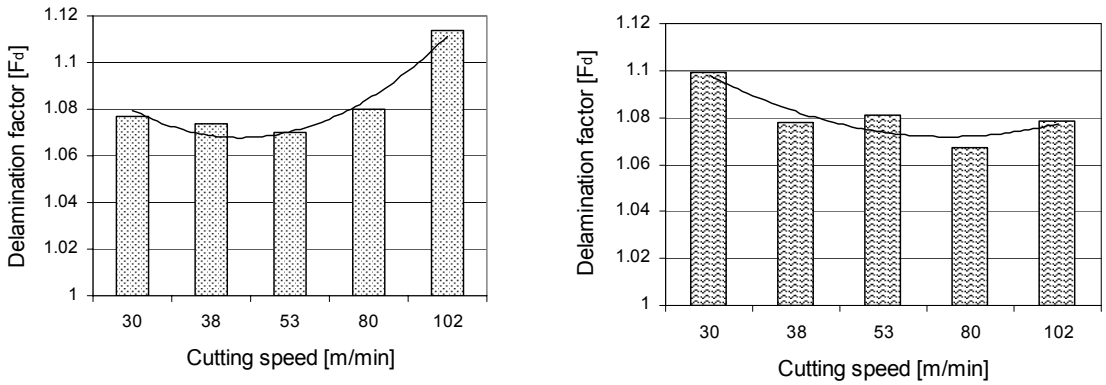

Figure 3.59 – Cutting speed influence in delamination factor: a) carbon plates; b) hybrid plates.

When considering the influence of cutting speed in average surface roughness, the conclusion is once more similar to what would be expected when metallic materials are machined. The values of superficial roughness show a trend to reduce when higher cutting speeds are used.

Based on the experimental work, it is possible to conclude that, when drilling carbon fibre reinforced or hybrid plates, the recommended cutting speed shall be in the range of **50 to 60 m/min**.

3.4.3 INFLUENCE OF TOOL MATERIAL AND GEOMETRY

As previously discussed, the material that is more adequate for the cutting of fibre reinforced plates is carbide, because of its good performance regarding toughness and resistance to abrasive contact with fibres combined with moderate cost. From the several grades available, K20 seems to be the most suitable considering the abrasive nature of the material to be machined. High speed steel is a material not recommended for the cutting of fibre reinforced materials because of rapid wear. Diamond tools, or PCD tools, although very resistant to abrasion are also very expensive.

Tool geometry also is important when considering thrust force and delamination around the hole. The main mechanism in the onset of delamination is the indentation force caused by the drill chisel-edge. That force is responsible for 40 to 60% of the total thrust force exerted on the plate plies. When thrust force exceeds a critical value, delamination occurs. Several geometries – twist, C-shape and *Dagger* drill – were compared. Each one has its advantages in the goal to achieve good quality holes with minimum damage caused by drilling operation.

Twist drill is the most common tool geometry. It is the type of drill that is possible to find in every tool supplier. It is possible to be used in all materials to be cut, even hybrids of metal/composite type as long as cutting parameters are settled. When combined with a pre-drilling stage, the values for the thrust force are sufficiently low to have reduced delamination around the hole as demonstrated by the results presented in the precedent sections. If parameter selection is adequate, or CNC machines with variable feed are used, it may be possible to drill without reaching the critical thrust force for delamination onset. Roughness values are positioned in the lower half of the range established by average plus and minus standard deviation.

C-shape drill is a tool available at some suppliers in order to increase hole quality when composite plates are considered. It is more dedicated to the machining of fibres like aramid that are better cut if pre-tensioned. Results when cutting carbon fibres, brittle by nature, are also good and a clean cut can be observed. The peculiar shape of the drill bit turns it possible to start the cutting of the material at the start of part/tool contact, thus eliminating the indentation effect of twist drills. For that same reason, no advantage was identified when a pre-drill was executed. Thrust forces during drilling are near to those of twist drills with pilot hole, and delamination around the hole was always reduced. The most puzzling result was the average roughness. For carbon/epoxy plates the roughness value was one of the lowest, but for glass/epoxy and hybrid plates the situation was completely reversed, and the result found was significantly higher than the average. This could mean some inadequacy of this tool geometry for the cutting of fibre reinforced plates or even plates containing plies with this type of fibre as reinforcement.

Dagger drills have the great advantage of having no indentation effect at all as the tip of the drill is sharpened, starting immediately to cut the material when it touches the part. This can, however, be the cause of some increased pressure exerted on the uncut plies as a similar force is applied in a reduced area, causing fibre bending instead of cut. Another drawback is the need to have space available for a long drill exit

by the opposite side of the plate. If that was not an obstacle for the experimental work, it can be the ground for some problems in tool shop or repair work. Cutting speeds used were lower than those of the other drill types, as this tool, due to its length, was more sensible to vibrations. Thrust force measured was lower than with other drills, but delamination was more extended when compared with the same drills. Roughness results were also higher than with other drills considered.

The next figures compare the three drill geometries – twist with pilot hole, C-shape and *Dagger* – regarding thrust force and delamination factor for the three materials analysed – carbon/epoxy, glass/epoxy and hybrid plates.

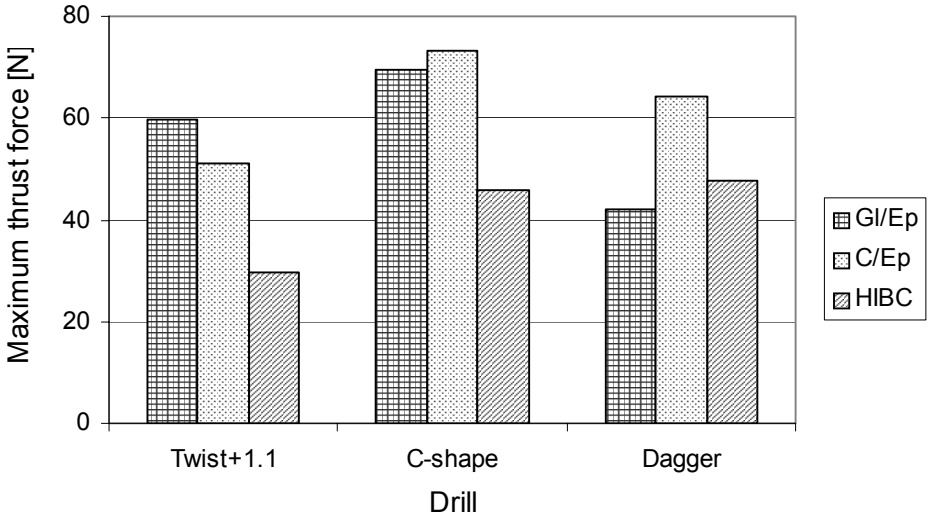

Figure 3.60 – Tool geometry effect in thrust force.

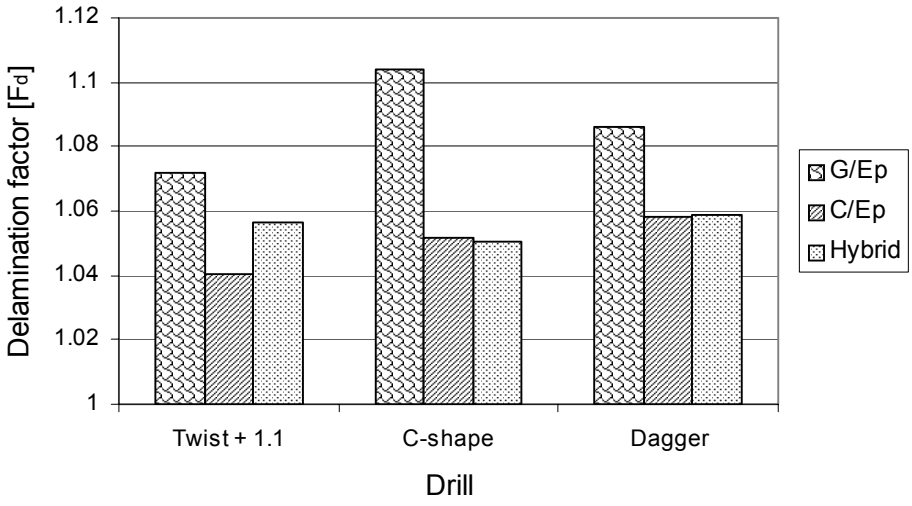

Figure 3.61 – Tool geometry effect on delamination factor (F_d).

3.4.4 CONCLUSIONS FROM BEARING AND DCB TESTS

The bearing test described in precedent section does not seem to be the most helpful mean to evaluate the damage caused by drilling. The results of the three experimental sets showed that the material of the plate was the most relevant factor in the final result of the test.

Double cantilever beam test results can be used to determine the critical thrust force for the onset of delamination. Using Hocheng and Dharan model [46], the value of this force for the three materials considered in this work can be calculated. The conditions considered for this calculation is the situation of a plate with an uncut thickness of 0.5 mm, corresponding to 4 plies. That is the situation of the HIBC hybrid plates at the carbon-glass interface. Values from elastic modulus and Poisson ratio of carbon and glass/epoxy cured material were from material supplier's information and for hybrid plates those values were calculated with ESACOMP® 2.1. According to the referred model, the values of these constants used consider unidirectional material.

Table 3.61 – Critical thrust force values for delamination: carbon, glass and hybrid/epoxy plates.

Material	G_{Ic} (J/m^2)	E (GPa)	ν	F_{crit} (N)
Carbon/epoxy	290	150	0.25	391
Glass/epoxy	568	25	0.18	220
Hybrid	299	52.5	0.20	231

For the same uncut thickness, the critical thrust force for the onset of delamination is greater in carbon/epoxy plates, even though the G_{Ic} value is lower. This is easily explained by the superior value of the elastic modulus of carbon reinforced plates. The other two interlaminar forces considered – glass and hybrid plates – are almost equal. For these two materials it can be said that no 'hybrid effect' is observed.

3.4.5 CONCLUDING REMARKS

Three types of composite laminates were selected for the experimental work. This work consisted in the evaluation of drilling parameters and tool geometries. Some analysis techniques were experimented in order to evaluate those more applicable to the analysis of delamination damage caused by drilling.

For carbon/epoxy and hybrid laminates the selected drilling conditions from those experimented were:

- feed rate equal to 0.025 mm/rev;
- cutting speed equal to 53 m/min;
- carbide as tool material, in a cost effective perspective;
- twist drill geometry, as long as a pilot hole of 1.1 mm diameter is done.

From the several analysis techniques used, the most promising were radiography and ultrasonic C-scan. These techniques can be associated with Computational Vision techniques in order to assess damage in composite plates and the determination of delamination factor – F_d – or bearing ratio – D_{RAT}.

Other analysis techniques used, like acoustic emission during drilling and computerized tomography, deserve further study to improve the setup, in order to achieve satisfactory results.

Results from Bearing test showed that the material was the main factor, covering the possible effect of drilling strategies in the test values.

From Double Cantilever Beam test is possible to say that the ‘hybrid effect’ is not present in interlaminar fracture toughness.

CHAPTER 4 - DEVELOPMENT OF A NEW TOOL DESIGN

4.1 TOOL MODEL DESCRIPTION

In this thesis, a study of the drilling conditions for plates made of plastic reinforced fibres was performed. Three different materials were considered – glass/epoxy, carbon/epoxy and hybrid plates with carbon/epoxy and glass/epoxy plies. Several tools were experimented, starting from the cheapest HSS drills to the middle price carbide drills. As carbide drills are pointed out to be cost-competitive for high-production workshops when compared with diamond drills, this latter material was not studied.

The main objectives of the present work were the understanding of the delamination phenomena during drilling, the use and development of analysis techniques and the proposal of an alternative design for a tool which enables the drilling of such materials without delamination or other damages, minimizing them as far as possible.

The grounds for this tool are in the work presented previously by other authors. The most important papers were the conclusions of Piquet et al. [48], Enemuoh et al. [66] and the recollection presented by Abrate [27] regarding tool material and geometry. The importance of a proposal for an alternative geometry was first established by Won and Dharan [64], as well as Tsao and Hocheng [65]. In a lecture at INEGI – Porto in 2000, H. Dharan [129] had suggested such geometry. In the following paragraphs a synopsis of the most important conclusions from the above mentioned authors is recalled.

Piquet et al. [48] said that machining of carbon/epoxy plates requires the use of a “micrograin” tungsten carbide tool of the K20 grade, which is tougher than ordinary carbides, but equally hard. Tools made from this material are tough and wear resistant,

two important properties when composites machining is considered. In order to reduce the peel-up defect that occurs at the tool entrance side, a rake angle not greater than 6º is recommended. The existence of more than one cutting edge increases the length of tool/part contact and facilitates the removal of the heat produced during machining, as lubricants are not used. The edge angle shall be around 70º to not weaken the tool and a point angle of 118º, usual for twist drills, should not be exceeded. Finally, the onset of delamination is related mainly with the chisel edge dimensions, so reducing those becomes necessary when it is important to avoid delamination of the last plies.

Enemuoh et al. [66], with the same objective of having damage-free holes in carbon reinforced composites, have reached to the conclusion that, among the point angles analysed – 75º, 95º, 118º, 140º and 160º - for the drill tip, the best value was 118º. This conclusion was the result of an experiment with different factors, speed, feed and geometry where the objective was the minimization of thrust force. An ANOVA analysis was done and S/N main effects on thrust force calculated. The result of the F-test presented for tool tip geometry was 74, the highest of the three factors involved. Other conclusion from their work is more related with cutting parameters, than with tool geometry. Just to remember the best parameters found were a cutting speed in the range of 50 m/min with a feed rate of 0.020 to 0.022 mm/rev.

Abrate [27] made a recollection of the available knowledge about the drilling of composite materials, referring that the drill chisel edge is responsible for 40 to 60% of the total thrust force increasing linearly with the chisel edge length. So a small chisel edge is an element to consider when optimizing tool geometry to decrease the importance of the chisel edge force and improve penetration rate. Rake angle shall be positive in order to avoid heat generation during cutting, but sufficiently small to avoid the weakening of the cutting edge. The helix angle is not so important in the drilling of these materials because the chips are in powder and normally a suction system is installed. If composites are bonded to metal parts, recommendation goes to the use of two drills, one to composite drilling and another to metal part. The alternative to this duplication of operations can be achieved by drill design or by changing operating conditions when the transition between materials is reached.

The other papers are more related with the effect of chisel edge and delamination. Won and Dharan [64] have started to study the effect of the chisel edge experimentally. They have concluded that for specimens with pilot holes thrust force can be reduced from one-half to one-fifth of those measured in holes without pilot hole. The delamination model presented for predicting the critical thrust force in specimens with

pilot hole was described in chapter 2. In the same paper, the authors refer a decrease of the critical force of 9% when pilot hole has a dimension of 0.18 of the final diameter. This value is interesting to note as is the relation between chisel edge length and nominal diameter in standard twist drills. Finally, the conclusions were that the potential for delamination damage can be reduced considerably by drilling in two stages, the first stage being a pilot hole whose diameter is about 18% of the final diameter and then drilling the final hole diameter. Hence total thrust force is divided in two stages and the maximum value is lower.

Tsao and Hocheng [65] presented a model where the pilot hole diameter is equal to the chisel length of the drill, just as the precedent quoted work. The model allowed the calculation of formulas that give the critical thrust force at the onset of crack propagation with pre-drilled pilot hole as well as the ratio between pilot hole and final hole that minimizes critical thrust force. Such optimum ratio was found to be 0.1176 for a material with a Poisson ratio of 0.3. The dimensionless chisel length should be designed between 0.09 and 0.2 of the final diameter, because as it was also pointed out, the thrust force in final drilling will be substantially reduced if contact between the piece and the chisel edge of the final drill is avoided.

Along the present work, the importance of a pilot hole was demonstrated by the results presented in chapter 3. The most relevant are now remembered. In first place, the use of a pilot hole has the positive effect of a strong reduction on thrust force during drilling. A reduction of 25 to 75% was observed during the experimental work, depending on the dimension of the pilot hole. Although the value of the critical thrust force for delamination onset decreases [64], the final balance is favourable to the use of a pilot hole. Laminates with carbon as reinforcement fibre seem to be more sensitive to this effect.

On the other hand, damage around the hole, evaluated by delamination factor also showed a reduction of damaged area in the order of 10% for carbon/epoxy plates. This reduction was not so relevant for the other materials studied. Results from damage assessment are in agreement with expectations of getting lower damaged areas around the hole when using pilot hole strategy. The effect on machined surface roughness was not taken into account. Next table summarizes the positive effects of a pilot hole, measured during experiences.

Table 4.1 – Pilot hole positive effects on thrust force and delamination reduction.

Effect	Material	Pilot hole diameter		
		1.1 mm	2.3 mm	3.5 mm
Thrust force reduction	C/Ep	26%	47%	74%
	Gl/Ep	25%	-----	
	Hybrid (C+G)	32%	-----	
Delamination reduction	C/Ep	10%	10%	7%
	Gl/Ep	1.5%	-----	
	Hybrid (C+G)	0.6%	-----	

The exact geometry of a drill is a complex process. The complete definition of a tool for drilling must consider several design items, like the helix angle, rake angle, point angle, lip relief angle, web thickness, number of cutting edges and others and their combination can have different effects in the cutting quality. This is a matter of some proprietary information from the manufacturers. Each manufacturer's exact cutting edge geometry is regarded as confidential information and it is patented, in most cases.

During cutting, both point geometry and cutting speed vary along the cutting lips. Chisel edge, although normally disregarded in drill geometry studies, plays an important role in the development of thrust force during drilling and in controlling hole size and accuracy. Some attention has been paid in the optimization of drill point design to minimize thrust and torque. Some examples can be found in [130, 131, 132]. However they are dedicated to the study of metal drilling which normally is not applicable to composites as referred before. A recent paper from Langella et al. [42] had focused on the development of a prediction model for drilling composite materials. The authors pointed the fact that composite and metal drilling requires different process parameter optimization approaches. The drilling process was divided in:

- chisel edge action where the material is not cut but extruded;
- lip region where orthogonal cut with negative rake angle is produced;
- main cutting region, where tool is fully engaged and rake angle becomes positive.

The contribution of the chisel edge on the total thrust force was found to be 50 to 70% of the total thrust force.

Based on the available information and the conclusions withdrawn from the experimental work, an alternative design can now be proposed for a tool dedicated to the drilling of fibre reinforced materials. The application of such tool is intended to drill

glass/epoxy, carbon/epoxy and carbon+ glass/epoxy (hybrid) plates. Other hybrids, like metal/fibre reinforced materials can possibly be integrated within the scope of this tool. However, that type of hybrid materials was not evaluated along the present study. The main factors influencing the tool design were the reduction of the thrust force during drilling and the reduction of damage around the machined hole.

The basic shape for that tool is the step drill in order to divide the thrust force in two stages, thus lowering maximum thrust during drilling by reducing the chisel edge effect. A point angle of 118º is used. The main difference of this tool is the presence of two conical regions, one corresponding to the chisel edge extension or pilot hole and other for the transition area between the pilot and final diameters. The drill tip was designed in a way to promote the initiation of cutting action immediately after touching the part, thus reducing the indentation effect, like in a *Dagger* drill. Drill engagement is divided in two steps, one for each diameter, increasing the length of the drill that fully contacts the plate, so increasing drill guidance during plate machining.

The complexity of the study of the drilling in the angular regions was not accomplished in this work. The variable speed and feed typical of the lip edge region is here repeated at the diameter transition zone. The importance of the cutting mechanisms that exists in angular regions is not to be ignored and should be carefully studied both theoretically and experimentally.

The use of a step drill like the one proposed also has the advantage of reducing machining time as the drilling can be executed in one operation only, instead of two operations separated by a tool change cycle. The diameter and extent of the pilot hole results from a compromise between the need to have a durable tool and the need to reduce pilot hole in the range of 10 to 20% of the final diameter. Smaller pilot hole diameters will cause the tool to be fragile and greater pilot hole diameter will increase the risk of delamination. Therefore, a balance is needed. Another important parameter to be considered when designing such tool is the need to be adequate to the plate that is going to be machined. The pilot hole extent shall not be inferior to the plate thickness. Otherwise, contact between the second conical region and the plate will be initiated before the pilot hole is completed causing an increase in thrust force by the addition of both effects. This can increase the risk of delamination onset. No experiments were done in order to evaluate this effect. On the other side, greater extent will cause an increase in machining time and a greater risk of tool breakage due to compressive efforts on the pilot drill. A rake angle of 6º is recommended, as it was seen before. In the tool prototype, the rake angle is zero (0º), as the drill has two

straight blades. Considering that chips produced during drilling are in powder, the importance of the helix angle is small. So, a straight vertical shape is proposed instead of a helix. Powder chips are evacuated from the cutting region and the tool is more stable dimensionally. Representation and photographs of this tool are shown in figure 4.1 and 4.2.

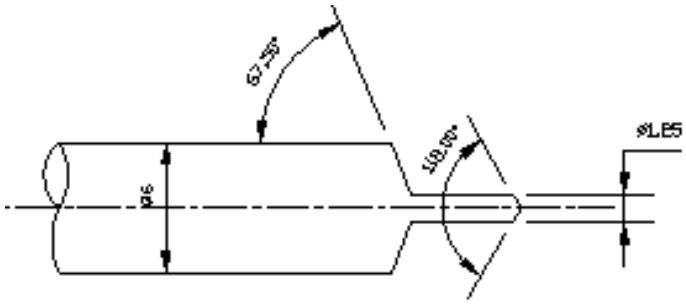

Figure 4.1 – Proposed tool geometry.

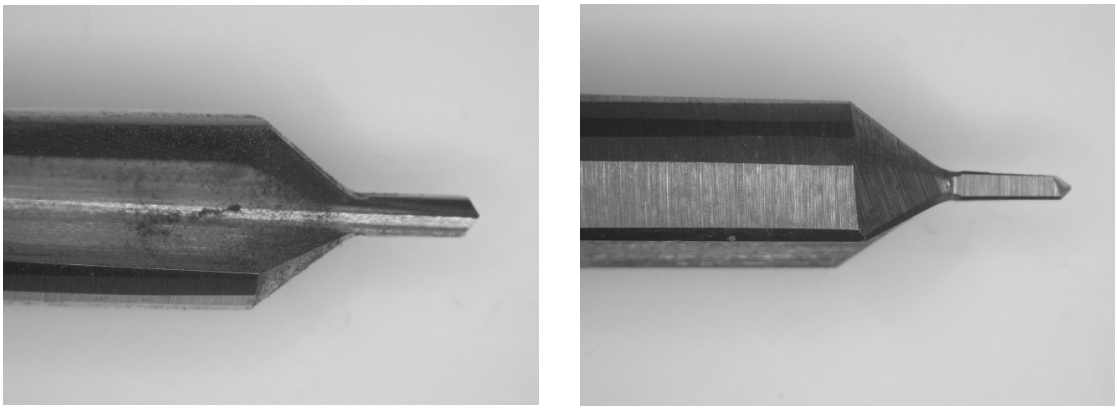

Figure 4.2 – Photographs of proposed tool.

According to the previous conclusions and notes, a prototype of a K20 tungsten carbide drill with the geometry as in figure 4.1, considering a pilot hole of 1.25 mm diameter and a pilot extent of 5 mm was made. Dimension of the pilot hole was constrained by material elastic properties which limits diameter reduction. Ratio between pilot and final diameter is 21%. This prototype has the intention to drill fibre reinforced plastics of the three types here studied. Experiments were only made with

carbon/epoxy and hybrid plates. From the experimental work, it has become clear that carbon/epoxy is the most challenging material from the three, due to the fragile nature of carbon fibres.

Tests with the new tool were reduced to only one cutting speed and two feeds, in agreement with the results from the cutting parameter analysis described in Chapter 3. The main objective of this experiment was to validate the possible advantages predicted for this drill and establish a comparison between the results obtained with this tool and those obtained under the same cutting conditions with the tools used in experimental work.

An experimental sequence was then established to evaluate this prototype tool and compare results with the best results from experimental work, as described in the following table. At the same time, and only for HIBC hybrid, an extra batch of plates was drilled using sacrificial plates and a twist drill with 1.1mm pilot hole, creating an 'optimum' standard for comparison purposes. Some objectives were intended for the expected results that were to be measured during this sequence. Such objectives are presented in table 4.2.

Table 4.2 – Experimental conditions for the new tool evaluation and comparison.

Experience description	Experimental parameters		Objective
	Speed	Feed	
Drilling	53 m/min	0.025 mm/rev	Max thrust force < 45 N
		0.05 mm/rev	Max thrust force < 70 N
Roughness measurement	----		Ra < 2 µm
Delamination measurement	----		F_d < 1.10 D_{rat} < 1.13
Bearing test	----		σ_{bear} > 750 MPa

The settings of the experience, as well as the equipment used, were the same as described before for the experimental work. The results obtained in this experiment are given and discussed in the next section.

4.2 RESULTS WITH NEW TOOL MODEL

The experimental sequence consisted of five consecutive drills for each feed condition on carbon/epoxy plates and then, after tool changing, on hybrid plates. Each drill has executed a total of 10 holes or a cutting length equal to 40 mm.

The force-displacement curve has a different shape when compared with those obtained with twist or C-shape drills. The reason for the difference comes from drill geometry joining the two steps – pilot and final hole – in one action only. The two phases of the drilling are well distinguishable in the graph. After a rise of the force when the drill touches the plate, the stabilization occurs at a lower level of force, below 20 N, corresponding to the first diameter full engagement. When the drill tip reaches the bottom of the plate, thrust force starts to descend but not reaching zero. That is the moment when the second conical region of the drill starts to contact the top of the plate causing the force to increase again, but avoiding a sum of the two effects, by the correct selection of the drill tip length, slightly superior to the plate thickness. The second part of the thrust-displacement curve is more similar to those observed when using twist drill. In figure 4.3 a typical thrust-displacement curve can be seen.

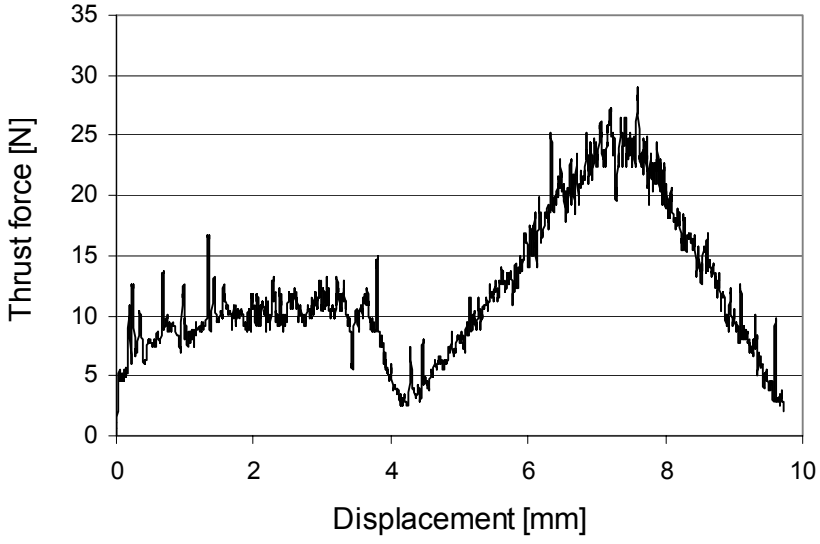

Figure 4.3 – Thrust-displacement curve with new tool in carbon/epoxy plates.

Experimental results regarding thrust force, specific cutting energy and surface roughness are presented in table 4.3 for carbon/epoxy plates. For comparison purposes, values for twist and C-shape drills are also shown.

Table 4.3 – Results with new tool for carbon/epoxy plates (v=53 m/min; f=0.025mm/rev).

Result	Unit	New tool	Twist drill with 1.1mm pilot	C-shape drill
Maximum thrust force	N	42.1	36.5	56.3
Specific cutting energy	J/mm^3	0.61	0.62	0.42
Surface roughness	µm	1.46	1.00	4.68

Thrust force values for a feed of 0.025 mm/rev are within the objectives for the new tool, although they are higher than those of the twist drill. A similar situation is observed for surface roughness, where the results for twist drill are good even though the result for the new tool is well below the objective initially proposed. In figure 4.4, a comparison of results for a cutting speed of 53 m/min and two different feeds – 0.025 and 0.05 mm/rev – when drilling carbon/epoxy plates is presented. The increase in feed from 0.025 to 0.05 mm/rev had an effect on the maximum thrust force for the new tool that is well within the gap observed for other drills in chapter 3. When C-shape drill is used, the gap is minor, as can be seen by the data represented in figure 4.4.

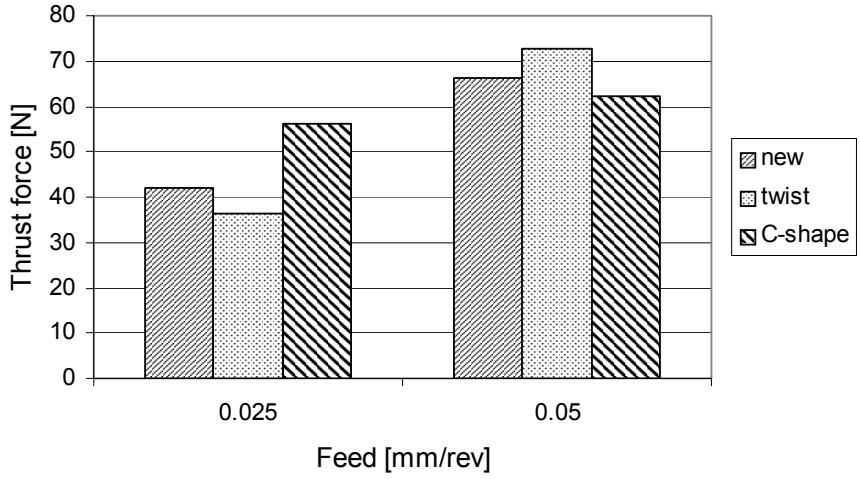

Figure 4.4 – Comparison of maximum thrust forces for carbon/epoxy plates.

One of the criteria used when discussing the pilot hole diameter selection was the result of the sum of the two maximum forces achieved during the two steps of the

drilling. In this case, such comparison is also possible. Results in table 4.4 show that the use of the new tool is more favourable than the use of a twist drill with pilot hole in terms of total thrust force. For both feeds used, the reduction is in the order of 13% with the new tool.

Table 4.4 – Total force for new tool and twist drill with pilot hole in carbon/epoxy plates.

Feed	Tool	Pilot hole (F_1)	Final hole (F_2)	TOTAL ($F_t=F_1+F_2$)	Reduction
0.025 mm/rev	New tool	19.4 N	42.1 N	61.5 N	13.4 %
	Twist drill with 1.1 mm pilot hole	34.5 N	36.5 N	71.0 N	-----
0.05 mm/rev	New tool	26.6 N	66.1 N	92.7 N	12.7 %
	Twist drill with 1.1 mm pilot hole	33.5 N	72.7 N	106.2 N	

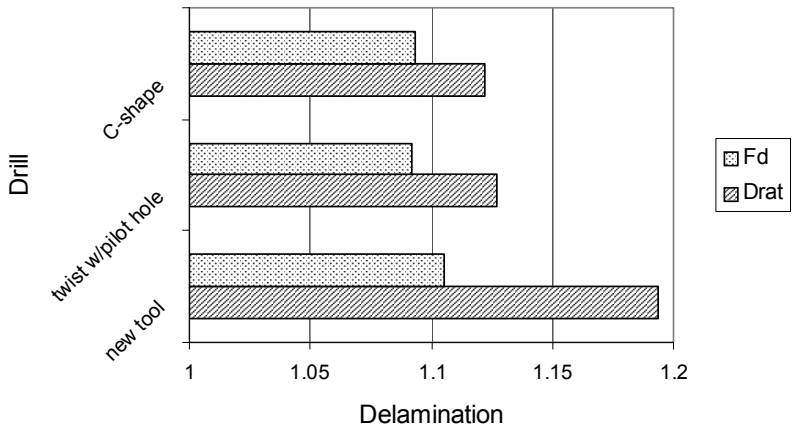

Figure 4.5 – Delamination factor (F_d) and damage ratio (D_{rat}) comparison in carbon/epoxy plates.

The measurement of the damage around the hole caused by the new tool is not as good as the objectives settled. The values of both evaluation criteria are above those obtained for twist or C-shape drills and the objectives described in table 4.2. This fact could be related with the straight blade design adopted for the tool, for both cutting diameters. This cutting edge geometry has to be changed in order to be possible to have a 'clean cut' of the fibres in the final diameter. In order to have a clean cut, some changes in tool geometry will be needed, like giving a helix angle in the final diameter region. It must be noted that no parameter optimization was carried out with this tool.

The comparison is made with one single cutting speed and two feeds. After reaching an improved design for the tool, a search for optimal cutting conditions will be needed.

Table 4.5 shows the experimental results regarding thrust force, specific cutting energy and surface roughness for hybrid HIBC plates. Values for twist and C-shape drills are again shown in the same table.

Table 4.5 – Results with new tool for hybrid plates (v = 53 m/min; f = 0.025 mm/rev).

Result	Unit	New tool	Twist drill with 1.1mm pilot	C-shape drill
Maximum thrust force	N	42.7	41.3	42.1
Specific cutting energy	J/mm^3	0.72	0.93	0.77
Surface roughness	μm	2.18	1.18	2.87

In figure 4.6 a comparison of results for a cutting speed of 53 m/min and two different feeds – 0.025 and 0.05 mm/rev – when drilling hybrid plates is presented.

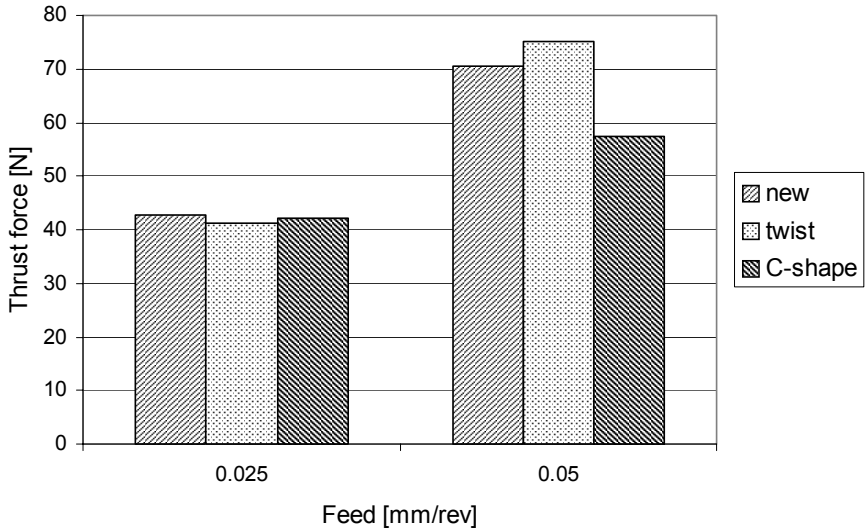

Figure 4.6 - Comparison of maximum thrust forces for hybrid plates.

Once again the results for the new tool are inside the objectives established, even tough just in the limit for a feed rate of 0.05 mm/rev. It must be referred that the values found for twist drill are again very good, being almost identical for thrust force, better for surface roughness and only superior for specific cutting energy, meaning a greater effort for the cut of the plates with this drill.

When cutting of hybrid plates is concerned, the results for the new tool are more satisfactory than those with carbon/epoxy plates. The values for delamination factor and damage ratio are closer to the objectives proposed. Figure 4.7 shows the results obtained for both damage criteria with the new tool and also with other tools, in order to establish a comparison.

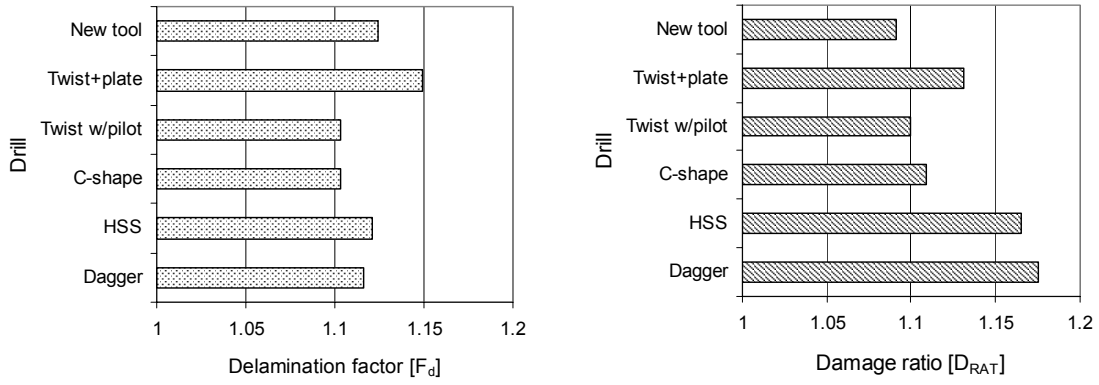

Figure 4.7 – Delamination factor and damage ratio for hybrid plates with several tools.

The value of delamination factor is in the range of what was measured for *Dagger* drill. For damage ratio, the new tool has the best result of all drills compared. Further progress in tool design, as referred above, will certainly have a positive effect, improving these values.

Finally, a set of test probes for bearing test was done in order to compare the results when using the new tool, a twist drill with pilot hole without and with a sacrificial plate. Summary of results is presented in table 4.6. Objectives proposed in table 4.2 are now repeated in order to establish a relationship between targets and results.

Table 4.6 – Comparison of results with hybrid plates under three different drilling conditions.

Test	Units	New tool	Twist drill with 1.1mm pilot hole	Twist drill w/ sacrificial plate	Objective
Max thrust force - F_x	N	42.9	29.8	56.4	< 45
Aver. surface roughness - R_a	µm	2.2	1.4	4.3	< 2.0
Delamination factor - F_d	---	1.12	1.10	1.15	< 1.10
Damage ratio - D_{RAT}	---	1.09	1.10	1.13	< 1.13
Bearing stress - σ_{bear}	MPa	764	759	761	> 750

From table 4.6 it is possible to observe that for thrust force, damage ratio and bearing stress the results are better than the target. It is encouraging that the bearing stress value for the new tool is the highest of all values, together with the fact that the damage ratio is the lowest. The values for delamination factor and surface roughness are close to the objectives, which make it possible to achieve them in next developments of the tool.

Figure 4.8 shows a complete comparison of bearing test results for some tools experimented for this work, use of a sacrificial plate and new tool. The values for the new tool and twist drill with pilot hole drilling are very close. The distance to the values for the other tools make it believe that some influence on the drilling strategies is present. This can explain the different bearing values whose ordering is similar to the results of damage ratio, except when sacrificial plate is used. So, a relation between the delamination area, measured by the damage ratio, and the bearing stress of a laminate plate is possible to be established, as shown in figure 4.9. As observed by the results, holes with greater damage ratios will tend to have lower values of bearing stress. Data correlation was found to be acceptable. In order to establish this relationship, data regarding holes with sacrificial plate was not considered.

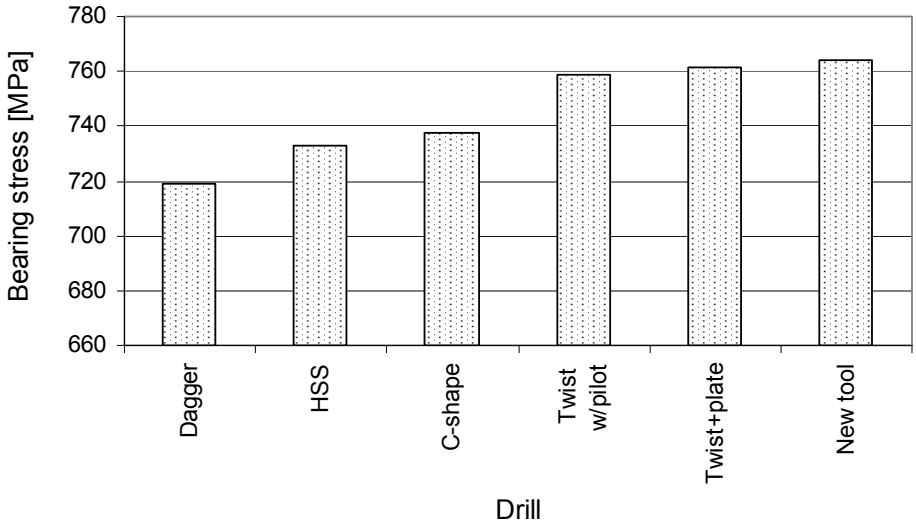

Figure 4.8 – Comparison of bearing test results for hybrid HIBC plates.

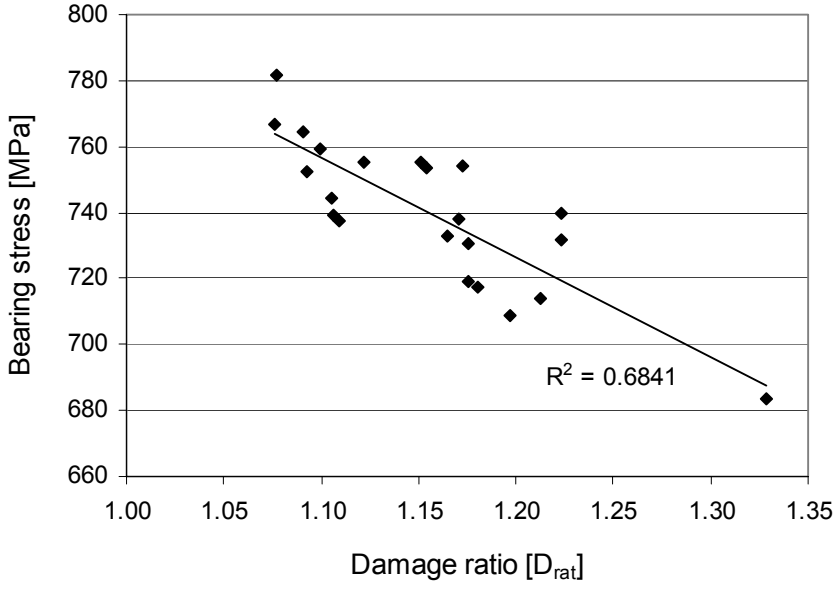

Figure 4.9 – Correlation between bearing stress and damage ratio in hybrid plates.

4.3 FINITE ELEMENT MODEL

The application of the Finite Element Model to the study of materials machining has known a growing interest, especially in orthogonal cut modelling. The relevant information that the author had gathered has been presented in section 1.4. That work has been facilitated by a literature alert elaborated by J. Mackerle [11], where a total of 372 references covering finite element analysis and simulation on machining were listed. In spite of this extended list, only a few papers dealt with the problem of resin reinforced composites drilling. There is still a large extent of research work to be carried out in this specific area. None of those drilling models used three-dimensional elements.

The objective considered in the present work was the development of a Numerical Model that was able to simulate a drilling process. The software package ABAQUS® with three-dimensional elements and interface elements were used to perform this simulation. The model considers the use of two different types of prismatic elements available from ABAQUS® library: 6-node triangular prisms for the central region of the plate; and 8-node linear bricks for the remainder of the modelled plate. These two element types used are presented in figure 4.10.

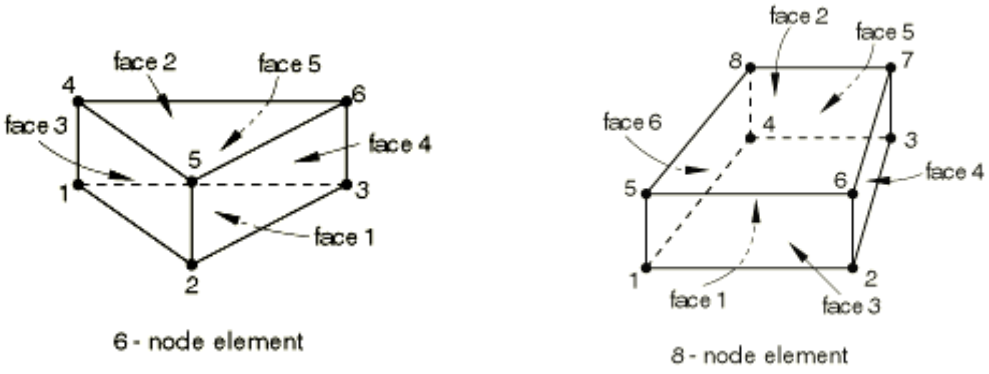

Figure 4.10 – 6-node and 8-node prismatic elements.

Together with those, the model uses 8-node interface finite elements, compatible with 8-node prismatic elements, previously developed for the prediction of delamination onset. The interface elements are placed at the interfaces between differently oriented layers where delamination is likely to occur and their formulation is based on the penalty function method - figure 4.11. The choice of the penalty value must be

cautious. If small values are used, physically unacceptable interpenetrations are induced and large values bring numerical problems. For the present model, and based in previous experience [133, 134] a value of 10^7 N/mm^2, has proved to be adequate.

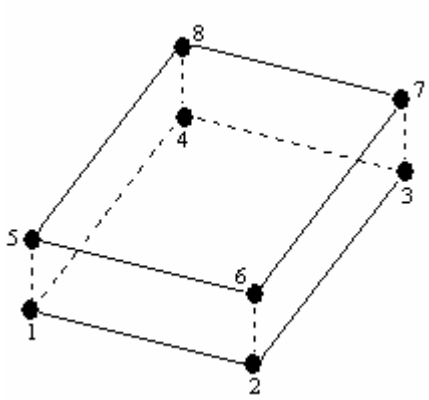

Figure 4.11 – Eight-node interface element.

The stresses at the interface element between differently oriented layers are calculated from the relative displacements between those layers from equation

$$\boldsymbol{\sigma} = \mathbf{D}\boldsymbol{\delta} \qquad (4.1),$$

where δ is the relative displacement vector between homologous points and D a diagonal matrix containing the penalty parameter d_i ($i = s, t, n$)

$$D = \begin{bmatrix} d_s & 0 & 0 \\ 0 & d_t & 0 \\ 0 & 0 & d_n \end{bmatrix} \qquad (4.2),$$

where d_s and d_t are the shear and d_n the normal interface stiffness.

The interface element incorporates a damage model to simulate crack initiation and growth. The damage model combines aspects of strength-based analysis and fracture mechanics. It is based on a softening process between stresses and interfacial relative displacements and includes a mixed-mode formulation. To avoid singularity at the

crack tip and its effects, a gradual rather than a sudden degradation, which would result in mesh degradation, is introduced. It is assumed that failure occurs gradually as energy is dissipated in a cohesive zone behind the crack tip. This is equivalent to the consideration of a "*Fracture Process Zone*" (FPZ), defined as the region in which the material undergoes softening damage by different ways, e.g., micro-cracking and inelastic processes. Numerically, this is implemented by including a damage parameter whose values vary from zero to unity as the material deteriorates. For pure mode (I, II or III) loading, a linear softening process starts when the interfacial stress reaches the respective strength $\sigma_{u,i.}$ The softening relationship can be written as

$$\boldsymbol{\sigma} = (\mathbf{I} - \mathbf{E})\mathbf{D}\boldsymbol{\delta} \tag{4.3},$$

where $\mathbf{I}$ is the identity matrix and $\mathbf{E}$ is a diagonal matrix containing on the *i*-position the damage parameter,

$$e_i = \frac{\delta_{u,i}(\delta_i - \delta_{o,i})}{\delta_i(\delta_{u,i} - \delta_{o,i})} \tag{4.4},$$

which represents the damage accumulated at the interface. This parameter is zero for the undamaged state and reaches one when the material is fully damaged. Due to the irreversibility of the damage process, the damage parameter e_i for a material point at a given increment *n*, is determined using the following equation

$$e_i = \max(e_i^n, e_i^{n-1}) \tag{4.5},$$

which avoids a healing phenomenon. The maximum relative displacement $\delta_{u,i}$, for which complete failure occurred, is obtained by equating the area under the softening curve to the respective critical fracture energy

$$G_{ic} = \frac{1}{2}\sigma_{u,i}\delta_{u,i} \tag{4.6}$$

During drilling, a complex stress state is present and damage propagation would occur under mixed-mode loading (modes I, II and III). Therefore, a formulation for interface elements should include a mixed-mode damage model which, in this case, is an extension of the pure mode model described above.

Damage initiation is predicted by using a quadratic stress criterion

$$\begin{aligned} &\left(\frac{\sigma_{\mathrm{I}}}{\sigma_{u,\mathrm{I}}}\right)^2 + \left(\frac{\sigma_{\mathrm{II}}}{\sigma_{u,\mathrm{II}}}\right)^2 + \left(\frac{\sigma_{\mathrm{III}}}{\sigma_{u,\mathrm{III}}}\right)^2 = 1 \quad \text{if} \quad \sigma_{\mathrm{I}} \geq 0 \\ &\left(\frac{\sigma_{\mathrm{II}}}{\sigma_{u,\mathrm{II}}}\right)^2 + \left(\frac{\sigma_{\mathrm{III}}}{\sigma_{u,\mathrm{III}}}\right)^2 = 1 \qquad \text{if} \quad \sigma_{\mathrm{I}} \leq 0 \end{aligned} \tag{4.7}$$

assuming that normal compressive stresses do not promote damage.

The mixed-mode damage propagation is studied considering the linear energetic criterion

$$\frac{G_{\mathrm{I}}}{G_{\mathrm{I}c}} + \frac{G_{\mathrm{II}}}{G_{\mathrm{II}c}} + \frac{G_{\mathrm{III}}}{G_{\mathrm{III}c}} = 1 \tag{4.8}$$

The released energy in each mode at complete failure can be obtained from the area of the minor triangle of figure 4.12.

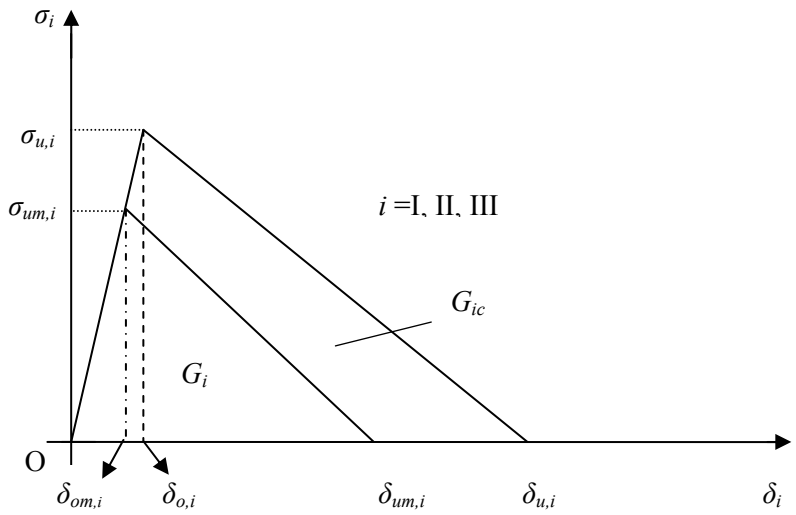

Figure 4.12 – Softening stress/relative displacements relationship for pure modes ($\mathrm{I}, \mathrm{II}, \mathrm{III}$).

$$G_i = \frac{1}{2}\sigma_{um,i}\delta_{um,i} \tag{4.9}$$

The energies in equations (4.6), (4.9) can be written as a function of relative displacements.

The final shape of the modelled plate is a cylinder with 16 mm diameter using a mesh with a total of 2541 brick elements. These elements are distributed along the 14 layers considered in a quasi-isotropic stacking sequence, resulting in a total plate thickness of 4 mm. The thicknesses of the layers are a consequence of the pre impregnated material used in experimental work, 0.125 mm. So, the first 8 layers which are going to be drilled at its centre had a thickness of 0.0625 mm, corresponding to half of a material ply. When the development of the model started, only 4 layers with 0.125 mm were considered in the region to be drilled. Later, these layers were divided in two, in order to have results closer to experimental curves of thrust force during drilling. This division has intended to approach the numerical discrete process to the continuous experimental process. It's similar to the approach of a curve by linear segments. If the numerical process was divided in smaller steps, the curve would be even closer to experimental. The present division seemed to be a good balance, considering the computing time involved and the shape obtained for the thrust force curve. Each two consecutive layers have the same orientation and no interface elements were

considered between them as delamination is an interlaminar damage. The layers 9 to 12 had a standard thickness of 0.125 mm. Layers 13 and 14, in order to reduce computational time, represent the aggregate of homogenization of 8 and 16 plies of a quasi-isotropic plate. In table 4.7 the main characteristics of the layers are presented.

Table 4.7 – Main characteristics of modelled layers.

Layer number	Thickness	Orientation	Interface elements
1, 2	0.0625 mm	0º	No
3, 4	0.0625 mm	45º	between plies 2 and 3
5, 6	0.0625 mm	90º	between plies 4 and 5
7, 8	0.0625 mm	- 45º	between plies 6 and 7
9	0.125 mm	0º	between plies 8 and 9
10	0.125 mm	45º	No
11	0.125 mm	90º	No
12	0.125 mm	- 45º	No
13	1 mm	aggregate 8 material plies	
14	2 mm	aggregate 16 material plies	

The modelled plate corresponds to a fabricated composite plate with 32 plies in a quasi-isotropic stacking sequence, as those used in experimental work. Mechanical properties considered in the finite element model are the result of experimental tests previously performed.

Table 4.8 – Properties of carbon/epoxy plates considered in FEM.

Property	Unit	Value
E_1	MPa	100 400
E_2	MPa	7 700
E_3	MPa	7 700
$G_{12}=G_{13}$	MPa	2 800
G_{23}	MPa	1 000
$\nu_{12}= \nu_{13}$	-----	0.25
G_{Ic}	J/m^2	290
G_{IIc}	J/m^2	632
G_{IIIc}	J/m^2	817
σ_u	MPa	40
τ_u	MPa	44

Double Cantilever Beam (DCB) experimental test was used for the determination of interlaminar fracture toughness of fibre reinforced laminates, according to ISO/DIS 15024. In spite of the quasi-isotropic lay-up of the plates, the test specimens were unidirectional, with the inclusion of a thin, non-adhesive starter film embedded at the

mid-plane, which is used to simulate an initial delamination. The test procedure was explained in section 3.3. Values from G_{IIc} and G_{IIIc} were taken from de Morais et al. [23] who used a similar material. The recommendation for the use of unidirectional instead of multidirectional laminates comes from the nature of the test itself. The data obtained on the test represents a minimum value of G_{Ic}. If multidirectional laminates are tested, the crack tends to jump and move along ply interfaces above and below the laminate midplane, creating nonlinear self-similar crack growth and mixed-mode response. As a consequence, values of G_{Ic} results higher than those obtained with a unidirectional specimen. The effect of fibre bridging on the results of DCB test have been the object of different studies [24, 25]. Generally, values of G_{Ic} are higher than those of unidirectional laminates, especially the propagation values. De Morais et al. [24] conducted an experimental work of DCB tests on unidirectional and cross-ply laminates. The values for the cross-ply laminates were in the order of 70% higher for crack initiation and 3 times higher for crack propagation. De Moura et al. [154] conducted similar experiences and observed extensive fibre bridging at the 0º/90º interface – figure 4.13. According to the authors, the higher propagation G_{Ic} values for cross-plies interfaces must be attributed to extensive fibre bridging observed. Initiation values of G_{Ic} are identical in unidirectional and cross-ply laminates, because there is no fibre bridging at the delamination onset. This fibre bridging is a phenomenon inherent of the DCB test and is not representative of the composite material tested. It is not reported to happen in field situations.

a) b)

Figure 4.13 – Picture of a) 0º/0º and b) 0º/90º specimens after testing [154].

The drilling simulation process is only considered in plies 1 to 8, so only these plies have elements in its central region, that are to be removed as the simulation undergoes. The remaining plies are hollow. Figure 4.14 shows the modelled plate.

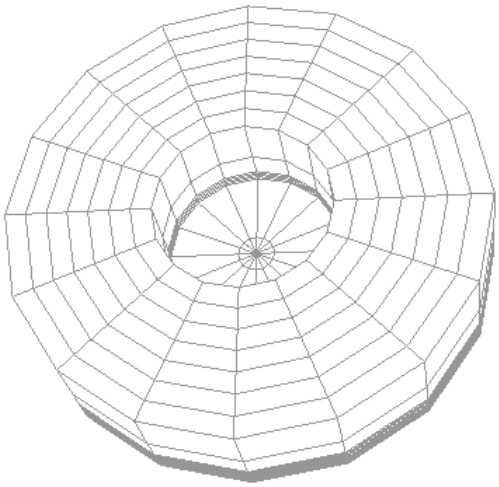

Figure 4.14 – Modelled plate.

A tool is needed to act as a drill in the simulation process. With such purpose, the 'rigid body' option available from ABAQUS® was used. A rigid body is a collection of nodes, elements, and/or surfaces whose motion is governed by the motion of a single node, called the rigid body reference node. The relative positions of the nodes and elements that are part of the rigid body remain constant throughout a simulation. Therefore, the constituent elements do not deform. Drill generation using this option was easy as it was only needed to create a contour line. The reference node is located at the drill tip. In order to create the different profiles for the simulation process, drills were measured. Consequently a contour as close as possible to the real drill geometry was created.

The drill – rigid body - acts over the uncut thickness of the modelled plate – deformable body - as the analytical damage models presented in section 2.4. The simulation is very similar to the experimental process described by Lachaud et al. [85, 86]. Model similarities can be observed looking at figure 4.15a) and figure 4.15b) where the finite element model with tool is presented.

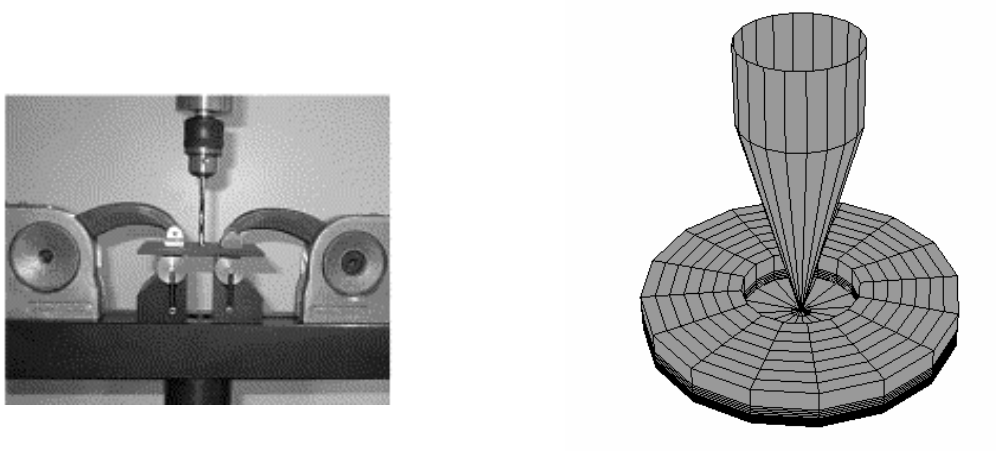

a) b)

Figure 4.15 – Delamination model: a) analytical [85]; b) finite elements.

The simulation of the drilling process is mainly confined to the indentation effect of the drill chisel edge when it contacts each ply of the plate. Displacement of the reference node of the rigid body causes the application of a force on the region of the plate that is going to be drilled. The contact region between the drill chisel edge and the part located under the drill has a correspondence with the chisel edge length of each drill. If the displacement of the reference node was completed in one step only, that is to say a course length of 0.5 mm, the simulation will be more likely to an extrusion. Hence, the model has to carry this displacement using an incremental method. When the reference node displacement reaches a predetermined value, function of modelled layer thickness – 0.0625 mm - and node deformation, a step of the process is ended. This value is related with the model described before and is the thickness of each layer of the model where the drilling simulation is applied. Then a layer is removed and another step starts with the contact between drill and uncut part being exerted on the new top of the part. This step-by-step process is repeated until the bottom of the plate is reached. This process is only possible with the use of an adequate instruction from ABAQUS®, the “MODEL CHANGE, REMOVE” option. Just prior to the removal step, ABAQUS® stores the forces that the region to be removed is exerting on the remaining part of the model at the nodes on the boundary between them. These forces are ramped down to zero during the removal step, therefore, the effect of the removed region on the rest of the model is completely absent only at the end of the removal step. The forces are ramped down gradually to ensure that element removal has a smooth effect on the model. This incremental process requires the measurement of node displacements caused by the drill on the different plies in order to keep the rigid

body always in contact with the part. Thus, the development of a simulation is a kind of an iterative process.

The model here presented does not consider the rotating movement of the tool, so there is no action of the tool cutting lips. It does not take into account the possible effect, experimentally verified, of feed rate variation in thrust force and delamination. Some attempts were done in order to incorporate feed effect in the program, but the increase of computational effort causes the software to look for a minimum 'feed', by dislocating the tool 0.1% of total displacement in each computational increment, whatever the initial feed would be. These two aspects of the simulation will need to be addressed in future developments of the model.

The present status of the model is more focused on the indentation process that occurs by the action of the chisel edge. For that reason, the influence of pilot hole was not evaluated, as the main purpose of such hole is the reduction or elimination of the chisel edge effect.

The drilling simulations that were run only considered the case of carbon/epoxy plates. The model is able to simulate the drilling of glass/epoxy or hybrid plates like those used in the experimental work, simply by changing the mechanical properties of the modelled plate. With regard to the dimensions of tool, modelled geometry of the drills here considered was based on chisel edge length and point angle. The modelled drills were in accordance with the three drill types used in experimental work – twist, C-shape and dagger – and the new drill prototype that was presented at sections 4.1 and 4.2. Modelled drills are shown in figure 4.16.

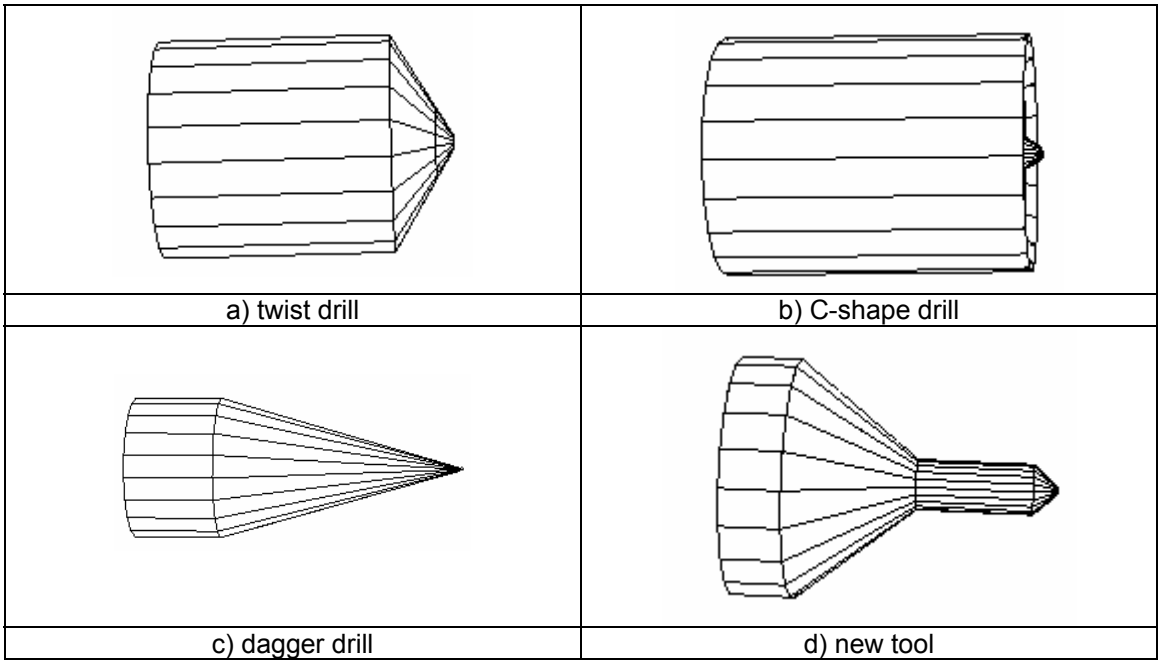

Figure 4.16 – Modelled drills: a) twist; b) C-shape; c) dagger; d) new tool.

Figure 4.17 shows some different images of the simulation process. In order to keep the image easy to understand, the top plies – from 10 to 14 – were removed from the picture.

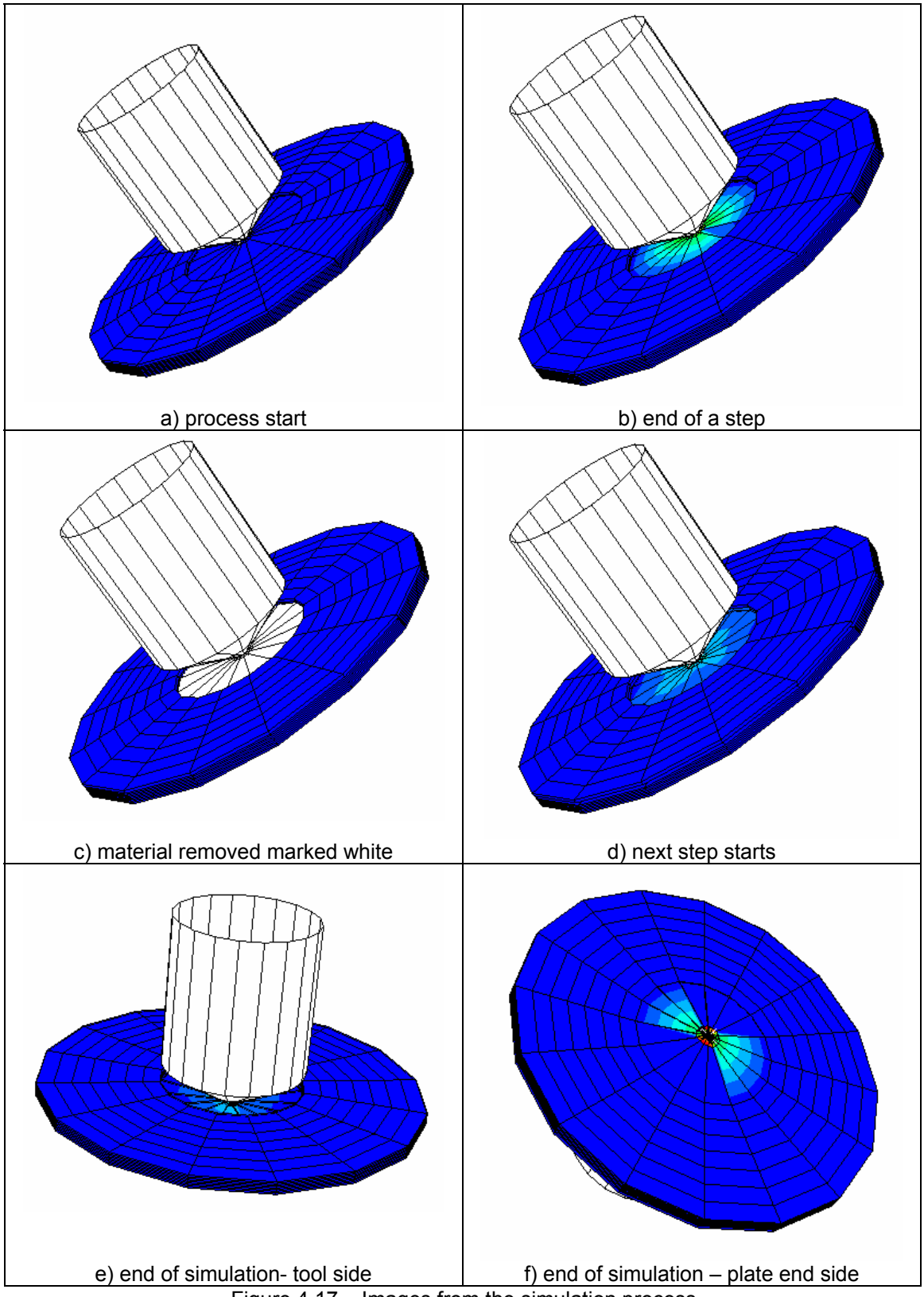

a) process start

b) end of a step

c) material removed marked white

d) next step starts

e) end of simulation- tool side

f) end of simulation – plate end side

Figure 4.17 – Images from the simulation process.

Results that are considered relevant during a simulation correspond to two events:

- delamination, when stress in a certain point drops to 0, due to non-continuity;
- maximum thrust force.

For the first case it is possible to identify the nodes where these phenomena occur and plot them in an *X*-*Y* graph. The second result is a consequence of the thrust-displacement curve that can be traced from simulation results.

Table 4.9 presents the results of delamination onset for the four different tool geometries considered. These results can be compared with the predicted value given by the Hocheng- Dharan analytical model [46], whose value is given in the last column of the table, for the same uncut plate thickness.

Table 4.9 – Delamination results from FE model and analytical model.

	Delamination onset		**Critical force Hocheng-Dharan**
Drill	**Value [N]**	**Layer nr**	**[N]**
Twist	59.1	4	78.1
C-shape	59.9	4	79.4
Dagger	59.6	4	80.4
New tool	77.5	4	97.0

Figure 4.18 makes a comparison of the experimental thrust-displacement curves for the four drills and respective curves of the FE models. From this figure, it is clear that the force-displacement curve generated by the model has a shape that corresponds to the experimental curve established for drills with standard helix geometry, where the indentation effect before actual cutting and removing of material is more pronounced. Particularly for the C-shape drill the fitting of the modelled curve is very good.

If different cutting parameters are used, the shape of the experimental curve will be the same, but the maximum value will be different, higher or lower according to the changes discussed in chapter 3. This dependence of the force values with cutting parameters is not possible in the model yet.

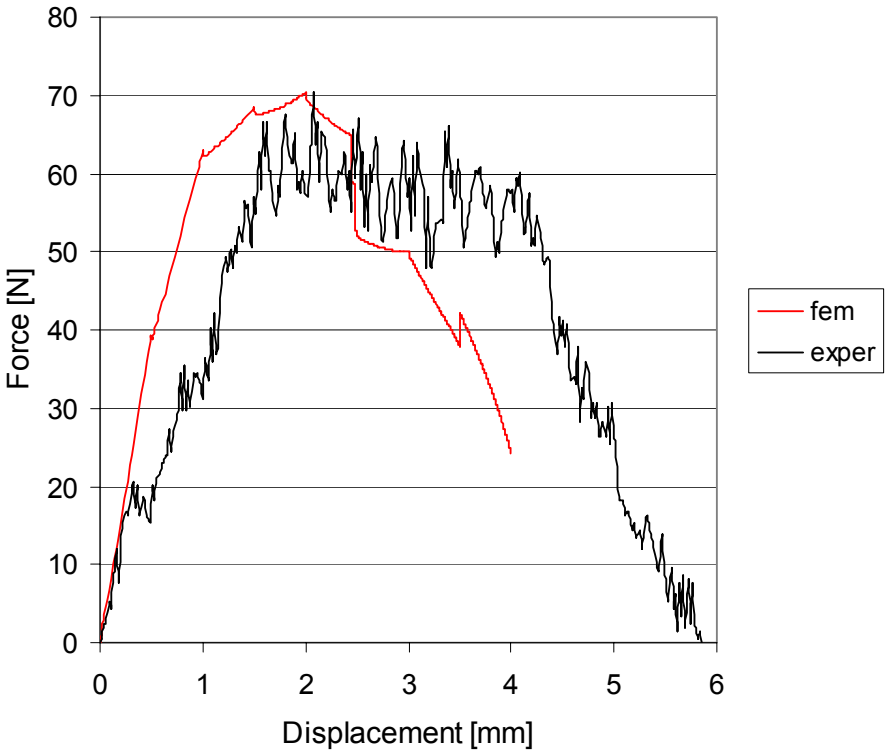

a) Twist drill

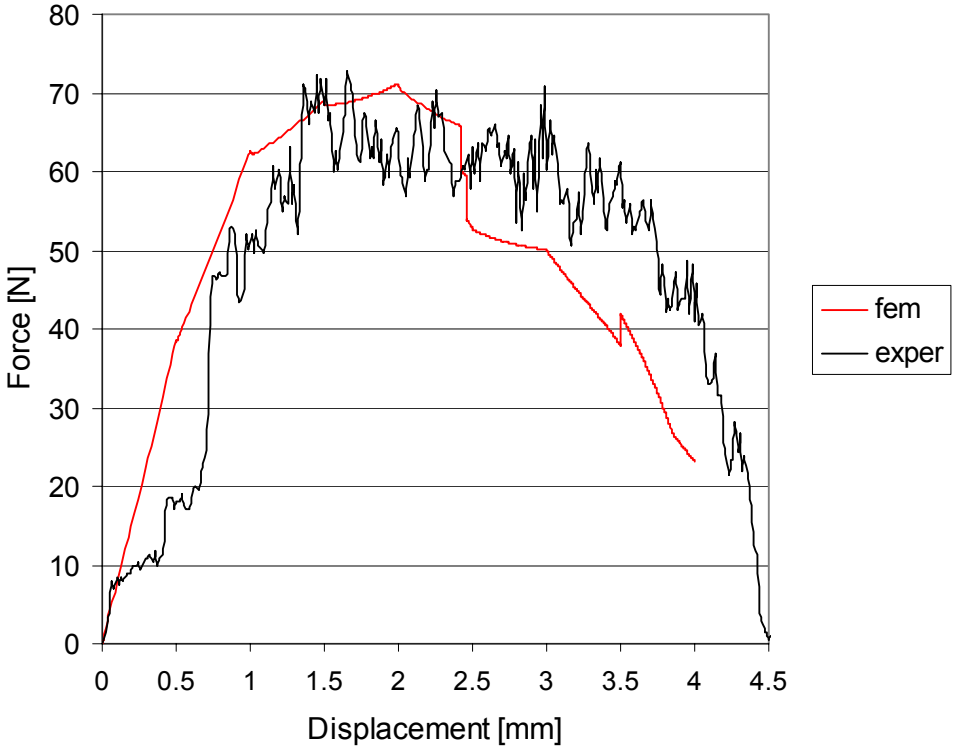

b) C-shape drill

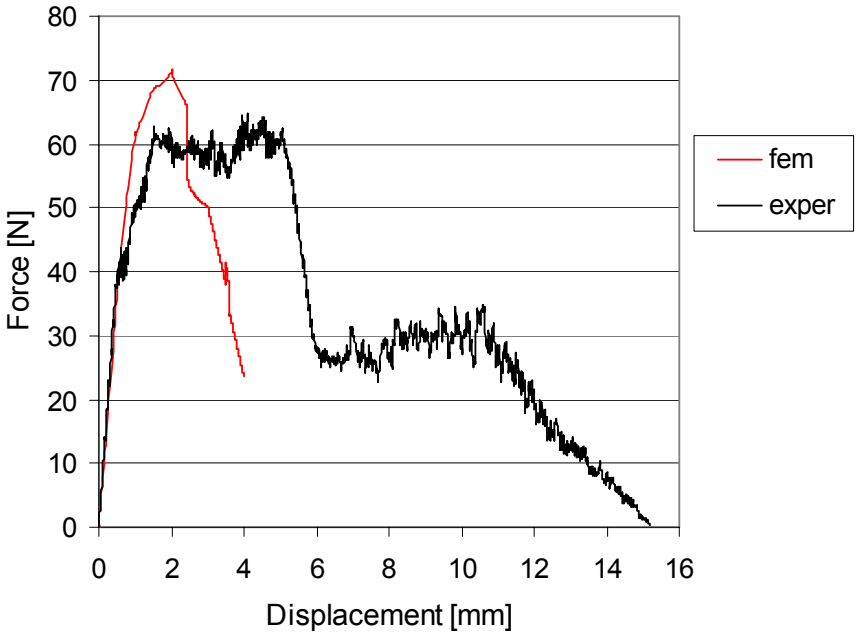

c) *Dagger* drill

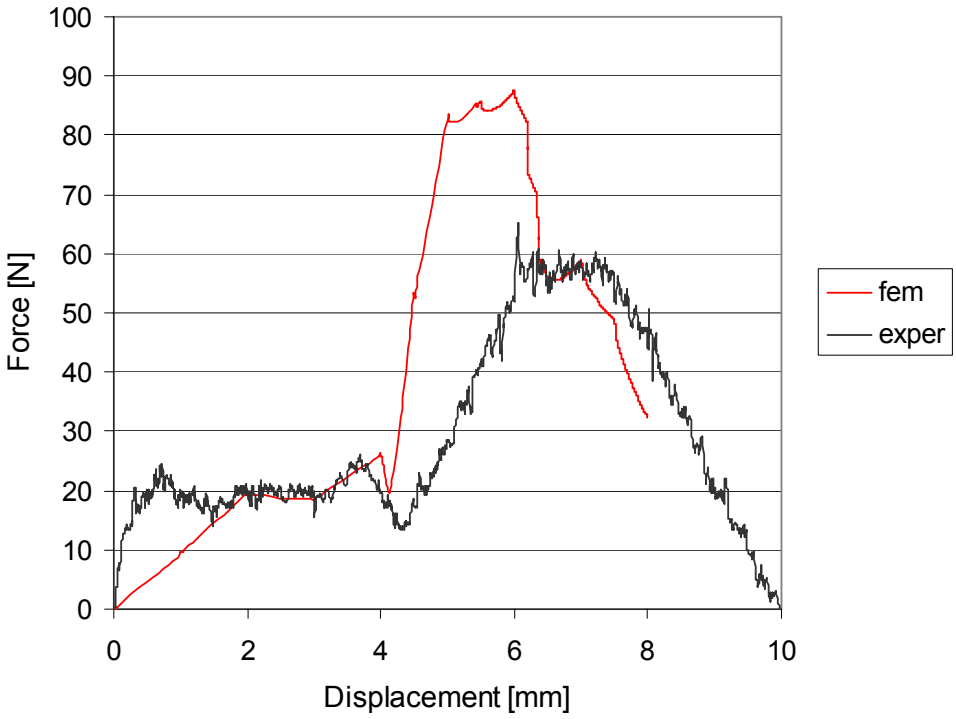

d) New tool

Figure 4.18 – Comparison of the thrust-displacement curves for the four drills considered.

For the other two drills – *Dagger and new tool* – whose geometry has the objective to reduce the indentation effect by start material cutting right after the tip contact, the experimental curve follows a different shape. For *Dagger* drill, the initial rise of the force is not perfectly reflected in the present state of FE model, as there is a material removal after a discrete displacement is given to the tool, making an indentation of the part instead of a cut right after tool-part contact. For *new tool* the step shape of the curve, corresponding to the different actions performed by the drill pilot and the drill main body was not possible to be modelled accurately. The quick start of cutting action by the lip edges is not taken into account at the FE model, which can explain the differences found. In table 4.10 the maximum thrust forces, experimental and FE, are compared.

Table 4.10 – Maximum thrust forces in N: FE model and experimental values.

DRILL	FE model [N]	Experimental [N]	Speed [m/min]	Feed [mm/rev]
Twist	70.4	70.3	80	0.05
C-shape	71.1	72.7	80	0.05
Dagger	70.5	64.8	38	0.05
New tool	87.4	65.2	53	0.05

Finally, in figure 4.19, the delaminated region is represented and compared with an image obtained by radiography. The figure shows the result of delaminated points given by application of the finite element model. The dark grey region represented results from the linking of the several points where delamination had occurred.

a) b)

Figure 4.19 – Delamination area of a twist drill hole: a) radiography; b) finite element model.

It can be observed that the main direction of delamination is an angle that corresponds to a direction with no fibre aligned – 22.5º. This direction is in the middle of the fibre orientations defined for the two remaining plies at the time of damage occurrence.

The three-dimensional finite element model here presented has the objective of studying the drilling process in fibre reinforced composite plates. The use of interface elements gives the possibility to the determination of delamination onset and propagation.

Forces in modelled drilling are a little greater than real values used for comparison. Experimental forces change due to feed rate or cutting speed variation which does not happen with the model. However, thrust-displacement curve has a similar shape independently of the drill considered. One of the present limitations of the model is the fact that only the drill point contact is actually considered in the development of forces during a simulation. Opposite to what is verified in experimental drilling, the cutting and breaking of fibres is not possible to address in the FE model. That is why the effect of cutting parameters was not possible to evaluate. This aspect will be included in future developments of the model. The values for delamination onset and its orientation can be of some interest for the designing of laminate plates and tools to achieve holes without delamination.

CHAPTER 5 - CONCLUSIONS AND RECOMMENDATIONS FOR FUTURE WORK

5.1 CONCLUSIONS

The machining study of fibre reinforced plastics – FRP's - was the main objective of this work.

The FRP systems considered were of three types: glass/epoxy composites, carbon/epoxy composites and interply hybrid composites with glass and carbon fibre as reinforcement in an epoxy matrix. Glass/epoxy composites were divided in three categories according to the fabrication procedure: manual lay-up, RTM and prepreg stacking with hot platen press curing. Carbon/epoxy and hybrid laminates were only fabricated using prepreg and hot platen press curing. Interply hybrids had 25% of plies in carbon/epoxy and 75% in glass/epoxy. The hybrid stacking sequence that was found to be more interesting was that with carbon fibre reinforcement in the outer plies of the hybrid laminate. All the plates in this study had a quasi-isotropic stacking sequence, with the objective of obtaining mechanical properties almost independent of the direction considered.

Among the several machining processes, drilling was selected for a deeper study, including tool geometry and cutting parameters. Main tool material used was carbide, as it is considered to be more cost effective. Some holes were drilled with HSS tools for comparison. The main drill geometry used was twist drill. Besides that, other drills were used like C-shape, a drill adequate to the cutting of Kevlar® reinforced plastics, and *Dagger*, a drill dedicated to carbon/epoxy plates drilling. The importance of a pilot hole as a first step before full drilling was evaluated and its advantages documented. In some experiences, a sacrificial plate, whose advantages are well documented, was

used. The cutting speed and feed influence was also evaluated in order to obtain a range of selected cutting parameters.

This work had the intention to relate the drilling parameters, cutting speed and feed, with damage around the hole that is normally caused by the machining process. With that purpose, some damage analysis techniques were used. From those that were available, radiography and ultrasonic C-scan deserved more attention and a great number of results were collected using these techniques. During plate machining, continuous monitoring of thrust force and torque was carried out in order to collect relevant data. Detection of delamination onset during drilling by acoustic emission techniques was equally experimented. Finally, bearing test was used to establish a relationship between hole damage and mechanical properties of the machined plate, when used in an assembled structure.

The use of established criteria for delamination assessment was done with the development and utilization of Computational Vision techniques, based in an existing image and processing platform. This technique enabled the measurement of the maximum delaminated diameter and damaged area around the hole after binarization of the images from radiography or C-scan. Results for both criteria – delamination factor and damage ratio – were extensively presented in chapter 3. Also, results from the measurement with the use of a profile projector were given in the same chapter.

Based on the information given by the different analysis techniques used, an optimum range of parameters was established, considering drill geometries and scope of cutting speeds and feeds experimented.

In the end, a proposal for a new tool design was presented and a prototype was prepared. With this prototype, of which only the first version was executed, an experimental set was completed and results for thrust force, torque, delamination, surface roughness and bearing test were presented in chapter 4 and compared with the results obtained with the other tools.

Also in chapter 4, a finite element model for the simulation of composite plates drilling was presented. The composite plate was modelled by successive layers, allowing the usage of different stacking sequences. The tool was modelled as a ‘rigid body’, and different tool geometries were compared, including the new tool geometry, as well as axial thrust forces and delamination onset. The model simulations considered non-linear three-dimensional analysis and included the use of previously

formulated interface finite elements incorporating a damage model based in Fracture Mechanics. Results were compared with experimental data.

In the present chapter, a summary of the conclusions are presented and briefly discussed.

There were three objectives established in this work:

- optimization of drilling strategies based in available damage models;
- proposal of a drill design for composites machining;
- presentation of a finite element model.

Some conclusions were possible to establish at the completion of this work.

- Machining of fibre reinforced plastics is highly dependent on the reinforcement used. Each composite material had a different reaction to the variation of drilling parameters.

- When plates with the same type of reinforcement are compared, the fibre content was a determining factor in the plate mechanical properties and extension of delaminated area.

- The main damages that can occur during the drilling of composite laminates are delamination, fibre pull-out and burrs. Push-out delamination is the damage that is more difficult to avoid, as it is a consequence of the indentation force executed by the drill chisel-edge over the last plies of the laminate. In that region, the chisel thrust force exceeds the interlaminar fracture toughness of the laminate and a separation of the plies can be observed. Push-out delamination is also the most serious damage as it reduces the load carrying capacity of the plate.

- Another type of delamination, peel-up, is easier to avoid by reducing the feed, as it was observed during experimental work.

- Although few published information about composites drilling is available, the scattering of cutting speeds and feeds referred is remarkable, making the establishment of a starting point to the development of parameter analysis and optimization more difficult. For that reason, the initial parameters were those indicated by tool suppliers.

- An optimized range of cutting speeds and feeds seem to exist as the most appropriate choice for cutting parameters. The recommended parameters for composite plates with carbon reinforcement in all or some of the plies shall be:
  - Cutting speed : from 50 to 65 m/min;
  - Feed : around 0.025 mm/rev.
- If glass reinforced composites are to be drilled, the range of suggested parameters are:
  - Cutting speed : 19 to 25 m/min;
  - Feed : around 0.05 mm/rev

  These values are only suggested as the search for optimized parameters was not so thoroughly carried out for this reinforcement material.
- Drilling of carbon reinforced composites, due to the brittle nature of carbon fibres, is more challenging than the drilling of glass reinforced composites and delamination is more likely to occur when carbon fibres are used as reinforcement.
- Thrust force exerted by the drill chisel-edge during drilling is the main factor in delamination onset. Several accepted and published models were referred in this work. Reduction of thrust force during drilling can lower delamination risk.
- The use of a pilot hole, dividing the drilling thrust force in two steps, is a good strategy to reduce delamination, as it was confirmed experimentally.
- Some non-traditional machining techniques can become promising as they turn out to be cost effective. It must be noted that these processes are not suitable for all materials.
- The use of acoustic emission for real-time monitoring of damage mechanisms during drilling was tried in the ‘continuous acquisition’ option. The experimental setup seemed to be more adequate for the monitoring of damage for composite parts in service or in low speed processes like tensile or fatigue testing. Some differences were found in the hit counting curves according to the cutting speed used. A relation between acoustic emission and damage caused by drilling could not be established.

- Enhanced radiography of drilled plates, immersing parts in a contrasting fluid, was extensively used along the experimental work. Images obtained represent an orthogonal projection of existing delamination in the ply interfaces of the laminate. The depth of such defects is not possible to be measured with radiography. It is a technique that can be easily used in test probes, but its use in manufactured parts can raise some problems. Enhanced radiography of FRP's should be seen more as a laboratorial technique than as a field analysis method.

- Ultrasonic C-scanning of drilled parts was also performed. This is a good technique for delamination detection, as this kind of damage is located at a plan that is perpendicular to the propagation direction of the wave. Depth of the damage can be estimated by a colour or grey level scale of the echoes which are related with the plate thickness. This technique showed good results when used in carbon/epoxy plates. For glass/epoxy and hybrid plates, the strong attenuation of the signal largely reduces the damage detection length.

- Two existing criteria were used for the evaluation and comparison of drilled plates – delamination factor (F_d) and damage ratio (D_{RAT}) -. The main advantages of both criteria is the fact that they can be applied in images of the drilled parts after hole completion obtained by radiography, ultrasonic C-scan or other imaging method that is used. The two criteria were able to give useful information for the comparison of tool geometries and drilling strategies.

- Standard Computational Vision techniques using an existing processing and image platform had the purpose to accomplish the measurement of damaged areas or damaged diameter around the hole. As two types of images were considered – radiographic and C-scan – different processing and analysis sequences were established. From the information that was acquired regarding areas and diameters of delaminated areas, it was possible to calculate the values for the two damage evaluation criteria adopted in this work. This technique was applied to images from carbon/epoxy and hybrid plates and it can be used to other materials. Some difficulties were found in their use for glass/epoxy plates images due to lack of contrasting areas.

- Evaluation of machined surface quality by roughness measurement was experimented. Large scattering of the values was observed, due to the

presence of two distinguishable zones, one with high content in fibre and other rich in resin. Another possible reason for the scattering observed is the different orientation of the fibres in the stacking sequence, causing the cutting mechanism to change along the hole wall.

- Bearing test has the intention of analysing the load bearing capacity of a composite part when subjected to efforts causing a certain stress level at the hole surrounding area. Tests executed tried to establish a relation between damage around the hole and bearing test values. Some correlation was found confirming this trend, particularly in hybrid plates. For the other plates, correlation was not high, but the number of tests performed was also smaller.

- Interply hybrid with 25% plies in carbon and the remaining in glass was used in part of the experimental work. The use of hybrids of this type is driven by economical issues. The staking sequence that appeared as more interesting was that with carbon reinforcement in the outer plies of the plate. With this configuration the so called 'hybrid effect' was evident in flexure modulus and bearing stress, but almost inexistent in the interlaminar fracture toughness in mode I.

- A new tool design, dedicated to the drilling of composite parts, was proposed and a prototype executed and tested. This tool had a pilot diameter of 1.25 mm and a pilot extension of 5 mm. Tests were reduced to only one cutting speed and two feeds in carbon/epoxy and hybrid plates.

- The results from the experience with the new tool were:
  - thrust force during drilling could be minimized within the objectives planned;
  - damage around the hole was in the same range as the optimized results obtained with twist or C-shape drill, which is promising when compared with the initial experimental results with other drill geometries;
  - the bearing stress of plates drilled with the new tool was the highest.

- The new tool geometry seems to be a good starting point and future developments will be necessary.

- A finite element model was developed to simulate a drilling process. Interface elements were placed at ply interfaces where delamination is likely to occur.

Tool was modelled as a 'rigid body'. The drilling simulation, considering the removal of material as the tool is displaced against the modelled plate, is a kind of an iterative process. The simulation need to be divided in a certain number of steps. Only carbon/epoxy plates were considered for the simulation study, although the model is able to simulate the drilling of glass/epoxy or hybrid plates.

- Results from finite element model were:
  - the force-displacement curve generated by the model has a shape that corresponds to the experimental curve for thrust force;
  - delamination onset forces are inferior to those that result from the application of existing analytical models;
  - main direction of delamination onset points is 22.5º, corresponding to a direction with no fibre aligned in a quasi-isotropic plate, and showing some similarities with some radiographies of drilled plates.

5.2 RECOMMENDATIONS FOR FUTURE WORK

Based on the existing work, some suggestions can be pointed for future developments. These suggestions can be divided in three areas:

- drilling tools and parameters; use of analysis techniques; finite element method.

A. DRILLING TOOLS AND PARAMETERS

- The pilot hole diameter has some influence on the final delamination observed, that need to be more thoroughly studied, using a larger number of pilot hole diameters.
- The diameter used in all the holes along this work was 6 mm. Other diameters shall be experimented and results compared.

- The new tool design needs to be optimized, in the tip area, with different profiles for the lip region and the changing of vertical blades to helix construction in the final diameter region.
- Also, an optimization of parameters for the new tool is needed.
- High-speed machining effect on composites needs to be investigated.
- Temperature distribution on part and tool during machining is another aspect that should deserve some attention in the near future.
- The study here presented should be extended to other kind of hybrids whose use is rising, like composite/metal hybrids.

B. USE OF ANALYSIS TECHNIQUES

- Ultrasonic C-scan need to be experimented in carbon/epoxy plates with different transducers, of smaller diameter and higher frequencies than those used (10 or 15 MHz).
- Computerized tomography (CT) should be tried in a dedicated installation to be able to change the setup according to the specific needs of damage detection in composite plates.
- Acoustic emission technique should be tested with alternative setups or combined with optical fibres (smart composites) embedded in the plates, in a way that will be possible to relate delamination onset during drilling with a particular acoustic emission phenomenon.
- Mechanical tests in drilled plates, like fatigue or open-hole test, shall be experimented to verify the effect of delamination on results.
- New non-destructive techniques, like tera-rays technology, should be evaluated in the damage detection of composite laminates, monolithic or hybrids.

C. FINITE ELEMENT METHOD

- The drilling simulation has to be extended to glass/epoxy and hybrid laminates that were also used in the experimental work of this thesis.
- The model shall incorporate the parameter effect, incorporating the change of rotation speed and feed.

REFERENCES

[1]- Stone, R., Krishnamurthy, K., "*A Neural Network Thrust Force Controller to Minimize Delamination During Drilling of Graphite-Epoxy Composites*", Int. J. Machine Tools and Manufacture, 36, pp. 985-1003, 1996;

[2]- Schwartz, M. M., "*Composite Materials Handbook*", McGraw Hill, 1988;

[3]- Delmonte, J., "*Historical perspectives of composites*", International Encyclopaedia of Composites, Vol. 2, pp. 335-340, 1991;

[4]- Gay, D., "*Matériaux Composites*", 3rd edition, Ed. Hermés, Paris, 1991;

[5]- Bader, M. G., "*Hybrid effect*", Handbook of Polymer-fibre Composites, Longman Scientific Technical, pp. 225-230, 1994;

[6]- Edward, A. H., Rosen, B. W., "*Properties analysis of laminates*", Engineered materials handbook, ASM International Handbook Committee, Vol.1, pp. 222-224, 1987;

[7]- Van Otterloo, D. L., Dayal, V. – "*How isotropic are quasi-isotropic laminates*", Composites A, 34, pp. 93-103, 2003;

[8]- Boothroyd, G., Knight, W. A., "*Fundamentals of machining and machine tools*", 2nd edition, Marcel Dekker Inc., New York, pp. 205-224, 1989;

[9]- Groover, M. P., "*Fundamentals of Modern Manufacturing : Materials, processes, and systems*", Prentice Hall, New York, pp. 543-611; 1996;

[10]- Ferraresi, D., "*Fundamentos da Usinagem dos metais*"; 1st ed., Ed. Blucher, São Paulo, pp. 17-65, 1970;

[11]- Mackerle, J. "*Finite element analysis and simulation of machining: an addendum. A bibliography (1996-2002)*", Int. J. of Machine Tools and Manufacture, 43, pp. 103-114, 2003;

[12]- Mahdi, M., Zhang, L., "*An adaptive three-dimensional finite element algorithm for the orthogonal cutting of composite materials*", J. Materials Processing Technology, 113, pp. 368-372, 2001;

[13]- Mahdi, M., Zhang, L., "*A finite element model for the orthogonal cutting of fiber-reinforced composite materials*", J. Materials Processing Technology, 113, pp. 373-377, 2001;

[14]- Ramesh, M. V., Seetharamu, K. N., Ganesan, N., Sivakumar, M. S., "*Analysis of machining of FRPs using FEM*", Int. J. of Machine Tools and Manufacture, 38, pp. 1531-1549, 1998;

[15]- Arola, D., Sultan, M. B., Ramulu M., "*Finite element Modelling of edge trimming fiber reinforced plastics*", J. of Manufacturing Science and Engineering, 124, pp. 32-41, 2002;

[16]- Zitoune, R., Collombet, F., Lachaud, F., Piquet, R., Pasquet, P., "*Experiment-calculation comparison of the cutting conditions representative of the long fibre composite during drilling phase*", Composites Science and Technology, 65, pp. 455-466, 2005;

[17]- Budan, D. A., Vijayarangan, S., "*Quality assessment and delamination force evaluation in drilling glass fiber-reinforced plastic laminates – a finite element analysis and linear elastic fracture mechanics approach*", Proc Instn Mech Engrs, 216 Part B, J. Engineering Manufacture, pp. 173-182, 2002;

[18]- Sicot, O., Gong, X. L., Cherouat, A., Lu, J., "*Determination of residual stress in composite laminates using the incremental hole-drilling method*", J. of Composite Materials, 37, pp. 831-844, 2003;

[19]- Strenkowski, J. S., Hsieh, C. C., Shih, A. J., "*An analytical finite element technique for predicting thrust force and torque in drilling*", Int. J. Int. J. of Machine Tools and Manufacture, 44, pp. 1413-1421, 2004;

[20]- Camanho, P. P., Matthews, F. L., "*Delamination Onset Prediction in Mechanically Fastened Joints in Composite Laminates*" J. of Composite Materials, 33, pp. 906-927, 1999;

[21]- Camanho, P. P., Matthews, F. L., "*A Progressive Damage Model for Mechanically Fastened Joints in Composite Laminates*", J. of Composite Materials, 33, pp. 2248-2280, 1999;

[22]- Nori, C. V., Mantena, P. R., McCarty, T. A., "*Experimental and finite element analysis of pultruded glass/graphite/ Epoxy hybrids in axial and flexural modes of vibration*", J. of Composite Materials, 30, pp. 1996-2018, 1996;

[23]- de Morais, A. B., de Moura, M. F., Gonçalves, J. P. M., Camanho, P. P:, "*Analysis of crack propagation in double cantilever beam tests of multidirectional laminates*", Mechanics of Materials, 35, pp. 641-652, 2003;

[24]- de Morais, A. B., de Moura, M. F., Marques, A. T., de Castro, P. T., "*Mode-I interlaminar fracture of carbon/ epoxy cross-ply composites*", Composites Science and Technology, 62, pp. 697-686, 2002;

[25]- de Moura, M. F., Pereira, A. B., de Morais, A. B., *"Influence of intralaminar cracking on the apparent interlaminar mode I fracture toughness of cross-ply laminates*", Fatigue Fract Engng, Mater Structures, pp. 1-8, 2004;

[26]- Jimenez, M. A., Miravete, A., "*Application of the Finite Element method to predict the onset of delamination growth*", J. of Composite Materials, 38, pp. 1309-1335, 2004;

[27]- S. Abrate, S., "*Machining of Composite Materials*", Composites Engineering Handbook, P. K. Mallick, Marcel Dekker, New York, pp. 777-809, 1997;

[28]- Wern, C. W.; Ramulu, M. and Shukla, A., "*Investigation of Stresses in the Orthogonal Cutting of Fibre-Reinforced Plastics*", Experimental Mechanics, pp. 33 – 41, 1994;

[29]- Boldt, J. A., Chanani, J. P., "*Solid-tool machining and drilling*", Engineered materials handbook, ASM Intern. Handbook Committee, Vol.1, pp. 667-672, 1987;

[30]- Koplev, A., Lystrup, Aa., Vorm, T., "*The cutting process, chips, and cutting forces in machining CFRP*", Composites, 14, pp. 371-376, 1983;

[31]- Wang, X. M., Zhang, L. C., "*An experimental investigation into the orthogonal cutting of unidirectional fibre reinforced plastics*", Int. J. of Machine Tools and Manufacture, 43, pp. 1015-1022, 2003;

[32]- Klocke, F., Koenig, W., Rummenhoeller, S., Wuertz, C., "*Milling of Advanced Composites*", Machining of Ceramics and Composites, Ed. Marcel Dekker, New York, pp. 249-266, 1998;

[33]- M. Ramulu, Cutting-Edge Wear of Polycrystalline Diamond Inserts in Machining of Fibrous Composite Material, Machining of Ceramics and Composites, Ed. Marcel Dekker, pp. 357-410, 1998;

[34]- Ramulu, M., Faridnia, M., Garbini, J. L., Jorgensen, J. E., "*Machining of graphite/epoxy materials with polycrystalline diamond tools*", Machining characteristics of advanced materials, Winter Annual Meeting of ASME, pp. 33-39, 1989;

[35]- Krishnamurthy, R., Santhanakrishnan, G., Malhotra, S. K., "*Machining of polymeric composites*", Proc. of the Machining Composite Materials Symposium, ASM Materials Week, pp. 139-148, 1992;

[36]- Sreejith, P. S., Krishnamurthy, R., Narayanasamy, K., Malhothra, S. K., "*Machining characteristics of carbon/ phenolic ablative composites*", ECCM-8, Naples, Italy, Vol. II, pp. 503-507, June 1998;

[37]- Klocke, F., Wurtz, C., "*Comparision of techniques for the machining of thermoplastic fibre reinforced plastics*", ECCM-8, Naples, Italy, Vol. II, pp. 729-735, June 1998;

[38]- Klocke, F., Wurtz, C., "*The use of PCD tools for machining fibre reinforced materials*", ECCM-8, Naples, Italy, Vol. II, pp. 509-515, June 1998;

[39]- Hu, N., Zhang, L., "*Grindability of unidirectional carbon fibre-reinforced plastics*", ICCM-13, Beijing, China, 2001;

[40]- Tonshoff, H. K., Lierse, T., Inasaki, I., "*Grinding of advanced ceramics*", Machining of Ceramics and Composites, Ed. Marcel Dekker, New York, pp. 85-118, 1998;

[41]- Chandrasekharan, V., Kapoor, S. G., DeVor, R. E., "*A mechanistic approach to predicting the cutting forces in drilling: with application to fibre-reinforced composite materials*" J. of Engineering for Industry, 117, pp. 559-570, 1995;

[42]- Langella, A., Nele, L., Maio, A., "*A torque and thrust prediction model for drilling of composite materials*", Composites A, 36, pp. 83-93, 2005;

[43]- Persson, E., Eriksson, I., Zackrisson, L., "*Effects of hole machining defects on strength and fatigue life of composite laminates*", Composites A, 28, pp. 141-151, 1997;

[44]- Persson, E., Eriksson, I., Hammersberg, P., "*Propagation of hole machining defects in pin-loaded composite laminates*", J. of Composite Materials, 31, 4, pp. 383-408, 1997;

[45]- Hamdoun, Z., Guillaumat, L., Lataillade, J. L., "*Influence of the drilling on the fatigue behaviour of carbon epoxy laminates*", ECCM 11, Rhodes, Greece, May 2004;

[46]- Hocheng, H., Dharan, C. K. H., "*Delamination during drilling in composite laminates*" J. of Engineering for Industry, 112, pp. 236-239, 1990;

[47]- Hocheng, H., Puw, H. Y., "*On drilling characteristics of fibre-reinforced thermosets and thermoplastics*", Int. J. of Machine Tools and Manufacture, 32, pp. 583-592, 1992;

[48]- Piquet, R., Ferret, B., Lachaud, F., Swider, P., "*Experimental analysis of drilling damage in thin carbon/epoxy plate using special drills*", Composites A, 31, pp. 1107-1115, 2000;

[49]- Tagliaferri, V., Caprino, G., Ditterlizzi, A. "*Effect of drilling parameters on the finish and mechanical properties of GFRP composites*", Int. J. of Machine Tools and Manufacture, 30, pp. 77-84, 1990;

[50]- Bongiorno, A., Capello, E., Copani, G., Tagliaferri, V. "*Drilled hole damage and residual fatigue behaviour of GFRP*", ECCM-8, Naples, Italy Vol. II, pp. 525-532, June 1998;

[51]- Khashaba, U. A., "*Notched and pin bearing strength of GFRP composite laminates*", J. of Composite Materials, 30, pp. 2042-2055, 1996;

[52]- Khashaba, U. A., "*Delamination in drilling GFR-thermoset composites*", Composite Structures, 63, pp. 313-327, 2004;

[53]- El-Sonbaty, I., Khashaba, U. A., Machaly, T., "*Factors affecting the machinability of GFR/epoxy composites*", Composite Structures, 63, pp. 329-338, 2004;

[54]- Davim, J. P., Reis, P., António, C. C., "*Experimental study of drilling fibre reinforced plastics (GFRP) manufactured by hand lay-up*", Composites Science and Technology, 64, pp. 289-297, 2004;

[55]- Velayudham, A., Krishnamurthy, R., Soundarapandian, T., "*Evaluation of drilling characteristics of high volume fraction fibre glass reinforced polymeric composite*", Int. J. of Machine Tools and Manufacture, 45, pp. 399-496, 2005;

[56]- Lin, S-C., Shen, J-M., "*Drilling Unidirectional Glass Fibre-Reinforced Composite Materials at HighSpeed*", J. of Composite Materials, 33, pp. 827-851, 1999;

[57]- Ramkumar, J., Malhotra, S. K., Krishnamurthy, R., "*Effect of workpiece vibration on drilling of GFRP composites*", J. of Materials Processing Technology, 152, pp. 329-332, 2004;

[58]- Aoyama, E., Nobe, H., Hirogaki, T., "*Drilled hole damage of small diameter drilling in printed wiring board*", J. Materials Processing Technology, 118, pp. 436-441, 2001;

[59]- Park, K. Y., Choi, J. H., Lee, D. G., "*Delamination-free and high efficiency drilling of carbon fibre reinforced plastics*", J. of Composite Materials, 29, pp. 1988-2002, 1995;

[60]- Murphy, C., Byrne, G., Gilchrist, M. D., "*The performance of coated tungsten carbide drills when machining carbon fibre-reinforced epoxy composite materials*", Proc Instn Mech Engrs, 216 Part B, pp. 143-152, 2001;

[61]- Dharan, C. H. K., Won, M. S., "*Machining parameters for an intelligent machining system for composite laminates*", Int. J. of Machine Tools and Manufacture, 39, pp. 415-426, 2000;

[62]- Hocheng, H., Puw, H. Y., Yao, K. C., "*Experimental aspects of drilling of some fibre-reinforced plastics*", Proc. of the Machining Composite Materials Symposium, ASM Materials Week, pp. 127-138, 1992;

[63]- Won, M. S., Dharan, C. H. K., "*Drilling of aramid and carbon fibre polymer composites*", Trans. of ASME J. of Manufacturing Science and Engineering, 124, pp. 778-783, 2002;

[64]- Won, M. S., Dharan, C. H. K., "*Chisel edge and pilot hole effects in drilling composite laminates*", Trans. of ASME J. of Manufacturing Science and Engineering, 124, pp. 242-247, 2002;

[65]- Tsao, C. C., Hocheng, H., "*The effect of chisel length and associated pilot hole on delamination when drilling composite materials*", Int. J. of Machine Tools and Manufacture, 43, pp. 1087-1092, 2003;

[66]- Enemuoh, E. U., El-Gizawy, A. S., Okafor, A. C., "*An approach for development of damage-free drilling of carbon-fibre reinforced thermosets*", Int. J. of Machine Tools and Manufacture, 41, pp. 1795-1814, 2001;

[67]- Linbo, Z., Lijiang, W., Xin, W., "*Study on vibration drilling of fibre reinforced plastics with hybrid variation parameters method*", Composites A, 34, pp. 237-244, 2003;

[68]- Chen, W. C., "*Some experimental investigations in the drilling of carbon fibre-reinforced plastic (CFRP) composite laminates*", Int. J. of Machine Tools and Manufacture, 37, pp. 1097-1108, 1997;

[69]- Tsao, C. C., Hocheng, H., "*Taguchi analysis of delamination associated with various drill bits in drilling of composite material*", Int. J. of Machine Tools and Manufacture, 44, 1085-1090, 2004;

[70]- Davim, J. P., Reis, P., António, C. C., "*Furação de laminados reforçados a fibras de carbono obtidas por autoclave – Influência dos parâmetros processuais na delaminagem*" VII Congr. de Mecânica Aplicada e Computacional, Évora, pp. 475-483, 2003;

[71]- Davim, J. P., Reis, P., "*Furação de laminados epóxidos reforçados a fibras de carbono (CFRP): relação entre as forças de corte e o factor de delaminagem*", VI Congr. Ibero-Americano de Engenharia Mecânica, Coimbra, pp. 1079-1084, 2003;

[72]- Mehta, M., Reinhart, T. J., Soni, A. H., "*Effect of fastener hole drilling anomalies on structural integrity of PMR-15/Gr composite laminates*", Proc. of the Machining Composite Materials Symposium, ASM Materials Week, pp. 113-126, 1992;

[73]- Durão, L. M. P., Tavares, J. M. R. S., Magalhães, A. G., Marques, A. T., Freitas, M., "*Caracterização de danos de maquinagem em placas compósitas*", VIII Congr. de Mecânica Aplicada e Computacional, Lisboa, 2004;

[74]- Di Ilio, A., Tagliaferri, V., Veniali, F., "*Cutting Mechanisms in Drilling of Aramid Composites*", Int. J. of Machine Tools and Manufacture, 31, pp. 155-165, 1991;

[75]- Di Ilio, A., Tagliaferri, V., Veniali, F., "*Progress in drilling of composite materials*", Proc. of the Machining Composite Materials Symposium, ASM Materials Week, pp. 199-203, 1992;

[76]- Rahman, M., Ramakrishna, S., Prakash, J. R. S., Tan, D. C. G., "*Machinability study of carbon fibre reinforced composite*", J. of Materials Processing Technology, 89-90, pp. 292-297, 1999;

[77]- Caprino, G., De Iorio, I., Nele, L., Santo, L., "*Effect of tool wear on cutting forces in the orthogonal cutting of unidirectional glass fibre-reinforced plastics*", Composites A, 27, pp. 409-415, 1996;

[78]- Sadat, A. B., "*Machining of composites*", International Encyclopaedia of Composites, Vol. 3, pp. 95-102, 1991;

[79]- Korican, J., "*Water-jet and abrasive water-jet cutting*", 2a - Engineered materials handbook, ASM International Handbook Committee, Vol.1, pp. 673-675, 1987;

[80]- Ramulu, M., Arola, D. "*Water jet and abrasive water jet cutting of unidirectional graphite/ epoxy composite*", Composites, 24, pp. 299-308, 1993;

[81]- Hocheng, H., Tsai, H. Y., Shiue, J. J., Wang, B., "*Feasibility study of abrasive water-jet milling of fibre-reinforced plastics*", Trans. of ASME J. of Manufacturing Science and Engineering, 119, pp. 133-141, 1997;

[82]- Hocheng, H., Tai, N. H., Liu, C. S., "*Assessment of ultrasonic drilling of C/SiC composite material*", Composites A, 31, pp. 133-142, 2000;

[83]- Strong, A. B., "*Damage Control*", International Encyclopaedia of Composites, Vol. 2, pp. 1-6, 1991;

[84]- Caprino, G., Tagliaferri, V., "*Damage development in drilling glass fiber reinforced plastics*", Int. J. of Machine Tools and Manufacture, 35, pp. 817-829, 1995;

[85]- Lachaud, F., Piquet, R., Collombet, F., Surcin, L., "*Drilling of composite structures*", Composite Structures, 52, pp. 511-516, 2001;

[86]- Piquet, R., Lachaud, F., Ferret, B., Swider, P., "*Étude analytique et expérimentale du perçage de plaques minces en carbone/époxy*", Mec. Ind. 1, pp. 105-111, 2000;

[87]- Zhang, L-B., Wang, L-J., Liu, X-Y., "*A mechanical model for predicting critical thrust forces in drilling composite laminates*", Proc Instn Mech Engrs, 215 Part B, pp. 135-146, 2001;

[88]- Tsao, C. C., Chen, W. C., "*Prediction of the location of delamination in the drilling of composite laminates*", J. of Materials Processing Technology, 70, pp. 185-189, 1997;

[89]- Jain, S., Yang, D. C. H., "*Effects of feed rate and chisel edge on delamination in composites drilling*", J. of Engineering for Industry, 115, pp. 398-405, 1993;

[90]- Kim, D. W., "*Machining and drilling of hybrid composite materials*", PhD thesis, Univ. of Washington, 2002;

[91]- Jung, J. P., Kim, G. W., Lee, K. Y., "*Critical thrust force at delamination propagation during drilling of angle-ply laminates*", Composite Structures, 68, pp. 391-397, 2005;

[92]- Tsao, C. C., Hocheng, H., "*Effect of eccentricity of twist drill and candle stick drill on delamination in drilling composite materials*", Int. J. of Machine Tools and Manufacture, 45, pp. 125-130, 2005;

[93]- Kim, G. W., Lee, K. Y., "*Critical thrust force at propagation of delamination zone due to drilling of FRP/metallic strips*", Composite Structures, 69, pp. 137-141, 2005;

[94]- Rawlings, R. D., "*Acoustic emission and acousto-ultrasonics*", Non-destructive testing of composite materials, Imperial College, London, pp. 3/1-3/15, January 1996;

[95]- Burkes, J. M., Lesher, M. R., Lowe. M. A., "*The use of infrared thermography for drill tool evaluation*", Proc. of the Machining Composite Materials Symposium, ASM Materials Week, pp. 105-112, 1992;

[96]- Wang, D. H., Ramulu, M., Arola, D., "*Orthogonal cutting mechanisms of graphite/ epoxy composite. Part II: multi-directional laminate*", Int. J. of Machine Tools and Manufacture, 35, pp. 1639-1648, 1995;

[97]- Wang, D. H., Ramulu, M., Arola, D., "*Orthogonal cutting mechanisms of graphite/ epoxy composite. Part I: unidirectional laminate*", Int. J. of Machine Tools and Manufacturing, 35, pp. 1623-1638, 1995;

[98]- Evans, N. "*The applicability of radiography to the inspection of composites*", Non-destructive testing of composite materials, Imperial College, London, pp. 5/1-5/8, January 1996;

[99]- Harris, B., "*Non-destructive evaluation of composites*", Handbook of Polymer-fibre Composites, Longman Scientific Technical, pp. 351-356, 1994;

[100]- Henneke, E. G., "*Destructive and nondestructive tests*", Engineered materials handbook, ASM International Handbook Committee, Vol.1, pp. 774-777, 1987;

[101]- Imielinska, K., Castaings, M., Wojtyra, R., Haras, J., Le Clezio, E., Hosten, B., "*Air-coupled ultrasonic C-scan technique in impact response testing of carbon fibre and hybrid: glass, carbon and Kevlar/epoxy composites*", J. of Materials Processing technology, 157-158, pp. 513-522, 2004;

[102]- Cornelis, E., Kottar, A., Mohammed, A., Degischer, H. P., "*X-Ray computed tomography characterizing carbon fibre reinforced composites*", ICCM14, San Diego, California, USA, July 2003;

[103]- Smith, R. A., "*An introduction to the ultrasonic inspection of composites*", Non-destructive testing of composite materials, Imperial College, London, pp. 1/1-1/21, January 1996;

[104]- Fernandes, A. J. A., "*Técnicas de Controlo Não Destrutivo dos Materiais Compósitos*", Tese de Mestrado, FEUP, 1987;

[105]- Amaro, A. M., Cirne, J. S., Rilo, N. F., Vaz, M., Monteiro, J., "*Análise de defeitos em compósitos laminados com técnicas de interferometria holográfica*", VI Congr. Ibero-Americano de Engenharia Mecânica, Coimbra, pp. 889-8984, 2003;

[106]- Ramulu, M., "*Characterization of Surface Quality in Machining of Composites*", Machining of Ceramics and Composites, Ed. Marcel Dekker, pp. 575-648, 1998;

[107]- Baptista, A. M., Ferreira, L. A., "*O estado geométrico das superfícies técnicas*", Tecnometal, 46, September-October 1986;

[108]- Arola, D., Ramulu, M., "*Machining-induced surface texture effects on the flexural properties of a graphite/epoxy laminate*", Composites, 25, pp. 822-834, 1994;

[109]- Eriksen, E., "*Influence from production parameters on the surface roughness of a machined short fibre reinforced thermoplastic*", Int. J. of Machine Tools and Manufacture, 39, pp. 1611-1618, 1999;

[110]- Eriksen, E., Hansen, H. N., "*Surface topography of machined fibre reinforced plastics obtained by stylus instruments and optical profilometers*", Proc Instn Mech Engrs, 212 B, pp. 479-488, 1998;

[111]- Phillips, L. N., "*Joining of Composites*", Design with Advanced Composite Materials, Springer Verlag, London, pp. 129-144, 1989;

[112]- Tohlen, M. E., "*Generation of design allowables*", Engineered materials handbook, ASM International Handbook Committee, Vol. 1, pp. 308-312, 1987;

[113]- Parker, R. T., "*Mechanical Fastener Selection*", Engineered materials handbook, ASM International Handbook Committee, Vol. 1, pp. 706-708, 1987;

[114]- Tucker, W. C., Brown, R., Russell, L., "*Corrosion between a graphite/polymer composite and metals*", J. of Composite Materials, 24, pp. 93-102, 1990;

[115]- Enemuoh, E. U., "*Smart drilling of advanced fibre reinforced composite materials*", PhD thesis, Univ. of Missouri-Columbia, 2000;

[116]- Ross, P. J., "*Taguchi techniques for quality engineering: loss function, orthogonal experiments, parameter and tolerance design*", McGraw-Hill, New York, 1996;

[117]- Fowlkes, W. Y., Creveling, C. M., "*Engineering Methods for Robust Product Design*", Addison Wesley, New York, 1997;

[118]- Taguchi, G., "*Introduction to quality engineering: designing quality into products and processes*", Asian Productivity Organization, 1990;

[119]- Shaw, M. C., Oxford Jr., J. C., "On the drilling of metals Part II: the torque and thrust in drilling", Trans. ASME, 79, pp. 139-148, 1957;

[120]- Tavares, J. M. R. S., Tese de Doutoramento: "*Análise de Movimento de Corpos Deformáveis usando Visão Computacional*", FEUP, 2000;

[121]- Tavares, J. M. R. S., Barbosa, J. G., Padilha, A. J., "*Apresentação de um Banco de Desenvolvimento e Ensaio para Objectos Deformáveis*", RESI - Revista Electrónica de Sistemas de Informação, vol. 1, 2002;

[122]- Awcock, G. W., Thomas, R., "*Applied image processing*", McGRAW-HILL International Editions, New York, 1995;

[123]- Jain, R., Kasturi, R., Schunck, B. G., ”*Machine Vision*”, McGRAW-HILL International Editions, New York, 1995;

[124]- Schalkoff, R. J., “*Digital image processing and computer vision*”, John Willey & Sons, Inc., 1989;

[125]- ASTM D5961-01, “*Standard Test Method for bearing response of polymer matrix composite laminates*”, ASTM International, 2001;

[126]- ISO/DIS 15024, “*Fibre-Reinforced Plastic Composites – Determination of Mode I interlaminar fracture toughness, Gic, for unidirectionally reinforced materials*”, ISO, Geneva, 1999;

[127]- Rebelo, C. A. C. C., “*Avaliação da tenacidade à fractura interlaminar de materiais compósitos*”, Ciência e Tecnologia dos Materiais, 3/4, pp. 5-13, 1989;

[128]- Saghizadeh, H., Dharan, C. K. H., “*Delamination Fracture Toughness of Graphite and Aramid Epoxy Composites*” J. of Engineering Materials and Technology, 108, pp. 290-295, 1986;

[129]- Dharan, C. K. H., Conferência sobre maquinagem de materiais compósitos, INEGI, 2000;

[130]- Chen, W-C., Fuh, K-H., Wu, C-F., Chang, B-R., “*Design optimization of a split-point drill by force analysis*”, J. of Materials Processing Technology, 58, pp. 314-322, 1996;

[131]- Paul, A., Kapoor, S. G., DeVor, R. E., “*Chisel edge and cutting lip shape optimization for improved twist drill point design*”, Int. J. of Machine Tools and Manufacture, 45, pp. 421-431, 2005;

[132]- List, G., Nouari, M., Girot, F., “*On the optimisation of machining parameters for dry drilling of aeronautic aluminium alloy*”, J. Phys. IV France 110, pp. 471-476, 2003;

[133]- de Moura, M.F.S.F., Gonçalves, J.P.M., Marques, A.T., Castro, P.M.S.T., “*Modelling compression failure after low velocity impact on laminated composite using interface elements”*, J. of Composite Materials, 31, pp. 1462-1479, 1997;

[134]- de Moura, M.F.S.F, Gonçalves, J.P.M, Marques, A. T., Castro, P.M.S.T., “*Prediction of compressive strength of carbon-epoxy laminates containing delamination by using a mixed-mode damage model*”, Composite Structures, 50, pp. 151-157, 2000;

BIBLIOGRAPHY

- Berthelot, J. M., “Matériaux Composites”, Ed. TECH & DOC, Paris, 1999;
- Davim, J. P., “Princípios da maquinagem” Livraria Almedina, Coimbra, 1995;
- Holroyd, T., “The Acoustic Emission & Ultrasonics Monitoring Handbook”, Coxmoor Publishing Company, Oxford, 2000;
- Montgomery, D. C., “Design and analysis of experiments”, J. Wiley Sons, New York, 2001;
- MIL-HDBK-17-E, 3 vols., Department of Defense Handbook, USA, 1997;
- Tavares, C. M. L., “Efeito da utilização de insertos metálicos nas características de juntas aparafusadas em compósitos”, Tese de Mestrado, FEUP, 2003;
- Modern Metal Cutting – a practical handbook–SANDVIK Coromant, 1994;
- Summerscales, J., “Non destructive testing of fibre reinforced plastics composites”, Elsevier Applied Science Publishers Ltd, Essex, 1987;
- Materiaux composites – Introduction à l’usage des ingénieurs et technicians, Ed TEKNEA, Marseille, 1989;
- Carlsoon, L. A., Pipes, R. B., Experimental characterization of advanced composite materials, Technomic, Lancaster, Pennsylvania, 1997;
- Ochoa, O. O., Reddy, J. N., Finite Element Analysis of Composite Laminates, Ed. Kluwer, 1992;
- SP Systems Composite Engineering Materials, RefNet^{TM} CD-ROM, Version 7.1, 2002.

APPENDIX A

Experimental design – Orthogonal arrays

Experiments are used to study the effects of parameters as they are set at various levels. The following four approaches are possible to study a specific experimental design:

1. Build-test-fix
2. One-factor-at-a-time experiments
3. Full factorial experiments
4. Orthogonal array experiments

Build-test-fix is an ineffective and inefficient method.

One-factor-at-a-time, although interesting in developing a scientific understanding of the effect of a parameter, is slow.

Full factorial experiment investigates all possible combinations of all factor levels. The total number of experiments can be too high, so they are only used when small number of factors and levels are used.

The orthogonal array is a method of setting up experiments that only requires a fraction of the full factorial combinations. The treatment combinations are chosen to provide sufficient information to determine the factor effects using the analysis of mean. The orthogonal array imposes an order on the way the experiment is carried out. Orthogonal refers to the balance of the various combinations of factors so that no one factor is given more or less weight in the experiment than the other factors. Orthogonal also refers to the fact that the effect of each factor can be mathematically assessed independently of the effects of the other factors.

Along the experimental work, the orthogonal arrays used are two-level and three-level. The convention for naming the fractional orthogonal array is

$$La\left(b^c\right) \qquad \text{(A.1)},$$

where *a* is the number of experimental runs, *b* is the number of levels for each factor and *c* is the number of columns in each array.

The two-level orthogonal arrays used are L4 (2^3) and L8 (2^7). The L4 can handle three factors at two levels. The L8 can handle seven factors at two levels.

The three-level orthogonal arrays used are L9(3^4) and condensed L9. The L9 can handle four factors at three levels. The condensed L9 is derived from L9, but allowing the use of three levels in one factor, the remaining factors having two levels only.

The orthogonal arrays referred are shown below.

L4 Standard array

	Exper. factor		
Run	A	B	C
R1	1	1	1
R2	1	2	2
R3	2	1	2
R4	2	2	1

L8 Standard array

	Experimental factor						
Run	A	B	C	D	E	F	G
R1	1	1	1	1	1	1	1
R2	1	1	1	2	2	2	2
R3	1	2	2	1	1	2	2
R4	1	2	2	2	2	1	1
R5	2	1	2	1	2	1	2
R6	2	1	2	2	1	2	1
R7	2	2	1	1	2	2	1
R8	2	2	1	2	1	1	2

L9 Standard array

	Experimental factor			
Run	A	B	C	D
R1	1	1	1	1
R2	1	2	2	2
R3	1	3	3	3
R4	2	1	2	3
R5	2	2	3	1
R6	2	3	1	2
R7	3	1	3	2
R8	3	2	1	3
R9	3	3	2	1

L9 Condensed array

	Experimental factor						
Run	A	B	C	D	E	F	G
R1	1	These columns should not be used when considering condensed array		1	1	1	1
R2	1			2	2	2	2
R3	2			1	1	2	2
R4	2			2	2	1	1
R5	3			1	2	1	2
R6	3			2	1	2	1
R7	optional			1	2	2	1
R8	optional			2	1	1	2

1, 2, 3 - experimental levels for each factor

Figure A.1 – Orthogonal arrays: L4(2^3), L8(2^7), L9(3^4) and condensed L9.

Degrees of freedom is a concept that is useful to describe how big an experiment must be and how much information can be extracted from the experiment. The number of degrees of freedom of an experiment is one less than the number of runs in the experiment:

$$DOF_{\exp} = \#\,\text{runs} - 1 \qquad \text{(A.2)}$$

The degrees of freedom needed to describe a factor effect is one less the number of levels tested for that factor:

$$DOF_f = \#\text{levels} - 1 \quad \text{(A.3)}$$

Variance is the expected value of the square of the difference between the random variable and the mean of the population.

The percentage of contribution reflects the portion of the total variation observed in an experiment attributed to each significant factor. It is a function of the sum of squares for each significant item.

The *F test* is a statistical tool which provides a decision at some confidence level as to whether these estimates are significantly different. The test was named after Sir Ronald Fischer, a British statistician, who invented the ANOVA method. This ratio is used to test the significance of factor effects. To determine if an *F* ratio is statistically large enough, one should consider a confidence level and the degrees of freedom (α) associated with the sample variance of the numerator (v_1) and the denominator (v_2). The format for determining its value is $F_{\alpha, v1, v2}$. Tables that list the required *F* ratio to achieve a certain confidence level can be found in [116].

In [117] a ranking for *F*-ratio values is suggested:

- *F*<1 : the experimental error outweighs the control factor effect; the control factor is insignificant and indistinguishable from the experimental error;
- *F*≈ 2 : the control factor has only a moderate effect compared to experimental error;
- *F*>4 : the control factor is strong compared to experimental error and is clearly significant.

There are, however, some limitations in the *F* test. In ANOVA, the sums of the squares for all estimates of error are pooled together and divided by the total degrees of freedom for error. A basic assumption of ANOVA is that error variance is equal for all treatment conditions. This may not be true. In *F* test, only the *alpha risk* is addressed, which is the risk of saying that a factor affects the average performance when in fact it doesn't. The opposite side of the same coin, known as the *beta risk*, is not assessed. *Beta risk* is the risk of saying that a factor has no effect on the average performance when in fact it does.

Repetition is a multiple test observation within a trial in an orthogonal matrix.

A smaller-is-better characteristic is one that does not take on negative values and has a target of zero. It is the characteristic used along the experimental work.

Two more characteristics can be selected. A larger-is-better characteristic is one that does not take on negative values and for which the most desirable value is infinity. The other characteristic is nominal-is-better.

The S/N – signal-to-noise – ratio, developed by G. Taguchi, is a transformation of the repetition data to another value which is a measure of the variation present. This ratio consolidates several repetitions into one value that reflects the amount of variation present. The S/N ratio is the reciprocal of the variance of the measurement error, so it is maximal for the combination of parameter levels that has the minimum error variance. This is the optimum design. The combination that gives the better S/N ratio should be selected, even when the difference is slight.

There are several S/N ratios available, depending on the type of characteristic: smaller-is-better, larger-is-better and nominal-is-better. The S/N ratio, which condenses the multiple data points within a trial, depends on the type of characteristic being evaluated. The equations for calculating the S/N ratios characteristics are:

- smaller-is-better:

$$S/N = -10\log\left(\frac{1}{n}\sum_{i=1}^{n} y_i^2\right) \qquad \text{(A.4);}$$

- larger-is-better:

$$S/N = -10\log\left(\frac{1}{n}\sum_{i=1}^{n} \frac{1}{y_i^2}\right) \qquad \text{(A.5);}$$

- nominal-is-better:

$$S/N = -10\log V_e \quad \text{(variance only)} \qquad \text{(A.6),}$$

$$S/N = +10\log\left(\frac{V_m - V_e}{rV_e}\right) \quad \text{(mean and variance)} \qquad \text{(A.7),}$$

where y_i is the individual value, n is the number of repetitions, V_e is the variance due to the error and V_m is the variance due to the mean.

APPENDIX B

Analysis of variance (ANOVA) tables

TAGUCHI CONDENSED L8 ORTHOGONAL ARRAY - ANOVA FOR THRUST FORCE OF HSS TWIST DRILL

		Level 1	Level 2	Level 3	Level 4
Factor1	Vc	19	26	38	optional
Factor2	Factor2	1	2	do not use	
Factor3	Factor3	1	2	condensed columns	
Factor4	Feed	0.09	0.15		

Run Nº	Vc	Factor2	Factor3	Feed	Results nº repet.	R1	R2	R3	R4	Configured to smaller-is-better SUM	AVERAGE	S/N RATIO
1	19	1	1	0.09	4	13.36	13.47	14.76	17.56	59.15	14.79	-23.45
2	19	1	1	0.15	4	35.89	35.41	35.89	33.02	140.21	35.05	-30.90
3	26	2	2	0.09	4	22.25	21.96	24.55	24.55	93.30	23.33	-27.37
4	26	2	2	0.15	4	25.84	26.99	24.98	24.55	102.35	25.59	-28.17
5	38	1	2	0.09	4	34.93	36.85	35.89	34.45	142.12	35.53	-31.01
6	38	1	2	0.15	4	22.49	24.40	24.40	27.28	98.57	24.64	-27.85
7	optional	2	1	0.09	0					0.00		
8	optional	2	1	0.15	0					0.00		
										Total sum	Average	Average
										635.70	26.49	-28.13
										S/N ratio results	Vc	Feed
										Level 1	-27.2	-27.3
										Level 2	-27.8	-29.0
										Level 3	-29.4	

ANOVA with S/N ratio

		DoF	Variance	% contrib.	F test
GTSS	4785.1				
SS mean	4746.6				
Total SS	38.5	5			
SS fact A	5.5	2.0	2.7	14.2	0.2
SS fact B	4.3	1.0	4.3	11.2	0.3
Error	28.7	2.0	14.4	74.6	

$$GTSS = \sum_{i=1}^{8} (S/N)_i^2$$

$$SSmean = n \times \left(\overline{S/N}\right)^2_i$$

$$n = n^o \text{experiments}$$

$$TotalSS = GTSS - SSmean = \sum_{i=1}^{89} ((S/N)_i - (\overline{S/N}))^2$$

$$SS_{fact} = \sum_{i=1}^{k} (\#\text{exp})((\overline{S/n})_i - (\overline{S/N}))^2$$

$$Error = TotalSS - \sum SS_{fact}$$

$$DoF = n_i - 1$$

$$Variance = SS_{fact} / DoF$$

$$\%contribution = SS_{fact} / SS_{mean}$$

$$F_{test} = Variance_{fact} / Variance_{error}$$

Ranking for F-test values	
F<1	experimental error>factor effect; factor is insignificant
F=2aprx.	factor has a moderate effect compared to error
F>4	factor effect is strong and is significant

TAGUCHI L8 ORTHOGONAL ARRAY - ANOVA FOR DELAMINATION FACTOR OF HYBRID PLATES OF TWO TYPES

		Level 1	Level 2
Factor1	Feed	0.025	0.05
Factor2	Speed	80	100
Factor3	Interaction	1	2
Factor4	Tool	Tw+1.1pilot	C-shape
Factor5	Factor	1	2
Factor6	Factor	1	2
Factor7	Material	HIBG	HIBC

Run Nº	Feed	Speed	Interaction	Tool	Factor	Factor	Material	Results nº repet.	R1	R2	R3	R4	R5	Configured to smaller-is-better SUM	AVERAGE	S/N RATIO
1	0.025	80	1	Tw+1.1pilot	1	1	HIBG	3	1.095	1.093	1.092			3.28	1.09	-0.78
2	0.025	80	1	C-shape	2	2	HIBC	3	1.080	1.069	1.070			3.22	1.07	-0.61
3	0.025	100	2	Tw+1.1pilot	1	2	HIBC	3	1.094	1.090	1.068			3.25	1.08	-0.70
4	0.025	100	2	C-shape	2	1	HIBG	3	1.066	1.069	1.070			3.20	1.07	-0.57
5	0.05	80	2	Tw+1.1pilot	2	1	HIBC	3	1.058	1.061	1.063			3.18	1.06	-0.51
6	0.05	80	2	C-shape	1	2	HIBG	3	1.052	1.056	1.051			3.16	1.05	-0.45
7	0.05	100	1	Tw+1.1pilot	2	2	HIBG	3	1.091	1.084	1.074			3.25	1.08	-0.69
8	0.05	100	1	C-shape	1	1	HIBC	3	1.069	1.059	1.066			3.19	1.06	-0.54
														Total sum	Average	Average
														25.74	1.07	-0.61

S/N ratio results	Feed	Speed	Interaction	Tool	Factor	Factor	Material
	-0.66	-0.59	-0.66	-0.67			-0.622
	-0.55	-0.63	-0.56	-0.54			-0.591

ANOVA with S/N ratio	SQ	DoF	Variance	% contrib	F test
GTSS	3.0265				
SS mean	2.9421				
total	0.0843	7			
Feed	0.0271	1	0.0271	32.2	41.0
Speed	0.0035	1	0.0035	4.2	5.3
Interaction	0.0190	1	0.0190	22.5	28.7
Tool	0.0314	1	0.0314	37.2	47.4
Factor					
Factor					
Material	0.0020	1	0.0020	2.3	3.0
error	0.0013	2	0.0007	1.6	

Ranking for F-test values	
F<1	experimental error>factor effect; factor is insignificant
F=2aprx.	factor has a moderate effect compared to error
F>4	factor effect is strong and is significant

TAGUCHI L4 ORTHOGONAL ARRAY - ANOVA FOR DAMAGE RATIO OF CARBON/EPOXY PLATES USING A TWIST DRILL WITH 1.1 MM PILOT HOLE

		Level 1	Level 2
Factor1	Feed	0.025	0.05
Factor2	Speed	80	102
Factor3	Factor3	N1	N2

Run Nº	Feed	Speed	Factor3	Results nº repet.	R1	Configured to smaller-is-better SUM	AVERAGE	S/N RATIO
1	0.025	80	N1	1	1.090	1.09	1.09	-0.74
2	0.025	102	N2	1	1.103	1.10	1.10	-0.85
3	0.05	80	N2	1	1.222	1.22	1.22	-1.74
4	0.05	102	N1	1	1.160	1.16	1.16	-1.29
						Total sum	Average	Average
						4.57	1.14	-1.16

S/N ratio results	Feed	Speed
	-0.80	-1.24
	-1.52	-1.07

ANOVA with results

	SQ	DoF	Variance	% contrib	F test
GTSS	5.2431				
SS mean	5.2320				
Total SS	0.0110	3			
SS feed	0.0090	1	0.0090	81.3	6.2
SS speed	0.0006	1	0.0006	5.5	0.4
SS fact 3	0	0			
Error	0.0015	1	0.0015	13.2	

ANOVA with S/N ratio

	SQ	DoF	Variance	% contrib	F test
GTSS	5.980				
SS mean	5.355				
Total SS	0.625	3			
Feed	0.514	1	0.514	82.3	6.4
Speed	0.031	1	0.031	4.9	0.4
Factor3	0.000	0			
Error	0.080	1	0.080	12.8	

Ranking for F-test values	
F<1	experimental error>factor effect; factor is insignificant
F=2aprx.	factor has a moderate effect compared to error
F>4	factor effect is strong and is significant

$$GTSS = \sum_{i=1}^{4} y_i^2$$

$$n = n^{o}\,\text{experiments}$$

$$SSduetomean = n \times \bar{y}^2$$

$$SS_{fact} = \sum_{i=1}^{2} (\#\exp_i)(\bar{y}_i - \bar{y})^2$$

$$TotalSS = GTSS - SSmean = \sum_{i=1}^{4} (y_i - \bar{y})^2$$

$$Error = TotalSS - \sum SS_{fact}$$